Dust emission from croplands in the Free State, South Africa

Dissertation
zur
Erlangung der Würde eines Doktors der Philosophie
vorgelegt der
Philosophisch-Naturwissenschaftlichen Fakultät
der Universität Basel
von

Heleen Cornelia Vos

2022

Genehmigt von der Philosophisch-Naturwissenschaftlichen Fakultät
auf Antrag von

Prof. Dr. Nikolaus J. Kuhn, Universität Basel
Dr. Wolfgang Fister, Universität Basel
Prof. Dr. Markus Kalberer, Universität Basel
Dr. Jacobus Johannes Le Roux, University of the Free State

Basel, den 22. Juni 2021

Prof. Dr. Marcel Mayor
Dekan der Philosophisch-Naturwissenschaftlichen Fakultät

Abstract

The global dust load showed a large increase during the last century due to climate change and the expansion of vulnerable land, both of which are caused by human modifications. The increase in vulnerable land, both in size as in intensity, is mainly attributed to the increase in agricultural areas and agricultural intensification. Dust emission has both an onsite effect due to the degradation of the emitting area, and an offsite effect on human health and climate. The degradation of land is especially relevant for agricultural areas where crop yield can strongly diminish due to the depletion of clay, silt, and nutrients from soils.

The semi-arid Free State province has been identified as the largest emitter of dust in South Africa, which is caused by the large-scale agriculture, climate, and soil type. Dust storms have the potential to reach the densely populated Gauteng province causing negative consequences on human health and well-being. Dust events in the Free State show a strong seasonality that is attributed to the agricultural practices that leave soils bare and vulnerable to erosion after harvesting. However, the large differences in dust events per year indicate that additional surface characteristics control the emissions from these harvested croplands. One of the primary potential controls that farmers have on the emissivity of the land is the management of soil crusts, but, the role of soil crusts on sandy soils is often not considered. Therefore, this thesis will address the possible role of soil crusts on the dust emission from the Free State croplands.

This thesis examines the formation of crusts by rainfall, the dust emissions from cropland soils, and the surface characteristics that control this erosion. The main instrument used to measure the erodibility of a surface is the Portable In-Situ Wind Erosion Laboratory (PI-SWERL). The comparability of this portable instrument was assessed by a cross-comparison with a traditional straight-line wind tunnel. The threshold friction velocity of sandy surfaces was similar for the two instruments, whereas the threshold friction velocity of loamy sand indicated that the PI-SWERL is a more precise instrument that is capable of detecting the initial, small PM_{10} emissions from a surface.

To determine the potential for crusts to form on the sandy cropland soils, rainfall experiments combined with shear strength measurements were performed on Free State soils. The results showed that significant crusts develop within 15 mm of rainfall, and shear strengths similar to those measured in the laboratory were observed in the field. PI-SWERL measurements showed that these experimental crusts can limit the PM_{10} emission flux from 10.53 and 3.87 mg m^{-2} s^{-1} Luvisol and Arenosol soils, respectively, to below 0.03 mg m^{-2} s^{-1} for both. The addition of abraders increased the emission from a crust to 0.43 and 0.31 mg m^{-2} s^{-1} for Luvisol and Arenosol, respectively.

The strong effect of crusts on emissions have been compared to field measurements, which showed a similar potential to minimize dust emissions, but also are complex interaction on the surface that defines this influence. The average emission of crusted surfaces was 0.476 mg m^{-2} s^{-1} (standard

deviation = 0.348, min = 0.004, max = 1.401 mg m^{-2} s^{-1}) at a friction velocity of 0.59 m s^{-1}, whereby the presence of abraders showed a power relationship to the emission from these surfaces. The emission from loose surfaces ranged between 1.646 mg m^{-2} s^{-1} (standard deviation 0.980, min = 0.291, max = 5.974 mg m^{-2} s^{-1}), with a linear relationship between the emission and the clay and silt content.

The initial sensitivity of an agricultural field to wind erosion needs to be considered when assessing the surface conditions under which crusts could play a minimizing role in the emission of dust. This is controlled by the soil cover, such as vegetation or degrading crop straw and stubble that is left after harvesting. Four fields, with a range of soil cover and crust characteristics, have been measured in the field. The soil cover has been quantified using Unmanned Aerial Vehicle (UAV) image analyses. The erodibility of the soils was characterised by the horizontal sediment flux and the saltation threshold. The soil cover differed from 11% for a harvested groundnut to 66% for a harvested maize field, the latter being the most common crop type in the Free State. This data shows the high initial importance of soil cover on the wind erosion from a field, whereby the sediment flux from the maize field was 11 and 187 times lower than that of fallow and groundnut fields. Considering the relatively high sediment flux from the fallow and low soil cover fields, crust and abrasion management should be considered on such surfaces

Some surfaces showed a depletion of clay and silt, which is evidence of land degradation caused by dust emission. This depletion could eventually lead to a lower yield and the need for more fertilizers. Furthermore, an enrichment in certain allergens and pathogens has been found in the suspended dust from Free State croplands. This shows the relevance of minimizing dust, both for the emitting region and the offsite areas that dust eventually reaches.

Future studies should investigate the relationship between the sediment flux and the PM_{10} flux since this relationship is not known and could differ per field and soil type. Furthermore, the influence of roughness needs to be assessed because roughness is generally known to decrease the emission from a surface. However, to create roughness, it is required to disturb existing crusts, making it uncertain if such activities could increase or decrease overall emissions. Lastly, the implications raised by this thesis are not only relevant for Free State but can also be considered for other cropland areas with strong seasonality in cover and moisture.

Acknowledgement

This thesis could not have been without the endless support I received from my colleagues, friends, and family. All this help I received inspired me and kept me going, and I am very grateful for all the kindness that I received throughout my PhD.

First of all, I would like to thank Nikolaus Kuhn, who offered me this project and who supported me greatly throughout it. His guidance and patience to have very long discussions with me were invaluable for this project, challenged me to think outside the box, and made me grow as a scientist. Secondly, I would like to thank Wolfgang Fister, who introduced me to the many methods of wind erosion research and who joined me in digging soil pits during fieldwork. His sharp mind and the many nice discussions we had were a big help and inspiration for me. Then there are the many colleagues in South Africa, who introduced me to the Free State and its dust, who accompanied me during the many fieldworks, and who were a great motivation. Frank Eckardt, Johanna von Holdt, Pedro Lebre, Tony Palmer, Sindy Ndara, and the others who joined us in South Africa, it was a real privilege to work with you, thank you all!

I am also furthermore very grateful to all the colleagues in Basel who helped me, advised me, or simply kept me company during the many breaks, lunches, and apéros. Ruth was very generous with her support and her knowledge in the laboratory was of great value. Also, the many coffee breaks I shared with her were always a great pleasure. I would furthermore like to acknowledge the work and help from Brigitte, both with the UAV analyses in the field and with all the tricky fieldwork logistics. Also, many thanks go to Phil, who proofread part of the thesis and who gave some insightful comments and suggestions. I would like to thank Hans Ruedi and Lukas, who contributed greatly to all the technical aspects of this project. Besides them, there are still many more wonderful colleagues to whom I am so thankful for their help, support, and kindness: Juliane, Colin, Ieva, Lu, Sandra, Lena, Martina, Sebastian, Tomaso, Seid, Gabriela, Alex, Joshua, and many more! I would also like to express my appreciation to the master's students, Claudio, Alexandra, Patrice, Cynthia, Kim, and Fabien, who accompanied me during fieldwork and this research in general.

During this PhD, I was lucky to receive so much love and encouragement from my friends and loved ones in Switzerland, the Netherlands, and anywhere else in the world. I would especially like to thank Nina, who played such an important role in welcoming me to Basel and making it feel like my new home. Furthermore, I would like to express my appreciation for my flatmates, the old and the new ones. It was great to always have a group of people that I could come home to, and all the brunches, dinners, evenings and hikes we shared were a real delight. I would also like to thank my old and very dear friends in the Netherlands: Gwen, Arzo, Nisa, Wendy, Loren, and Eva. I have known you all for a long time now, and I am so lucky to have such loving and supporting friends, despite my decision to move away from you. I am also very grateful for the unflinching support and encouragement from

my Arthur. I am so lucky that we found each other, and I am very happy that you were by my side during this PhD and that I could share this adventure with you.

Lastly, I would like to thank my parents, grandparents, Barbara, Bart and Jeroen. You supported me more than I could ever thank you for, you taught me so much, and you inspired me to become the person I am now. I would like to give a special thanks to my father. I wish you could have stayed with us much longer. Besides all the love and support you gave me, you inspired me to go out and discover the world, which brought me where I am today.

Table of contents

List of figures

List of tables

1.

Introduction

1.1 Global dust emission

1.1.1 Current global dust emission

Dust can be defined as small particles that are suspended in the air. These particles can originate from different sources, such as industry, volcanism, or fires, but the largest global dust load is linked with wind erosion (Ginoux et al., 2012; Tegen et al., 2004). Globally, 432.2 million ha of land is exposed to wind erosion (Middleton and Thomas, 1997), which is 2.9% of the global land surface. The global dust emission is estimated to range between 500 and 3320 Tg yr^{-1} (Shao et al., 2011). Generally, semi-arid to arid regions are identified as the main emitters of dust, with the Sahara being the most emissive area in the world (Figure 1-1).

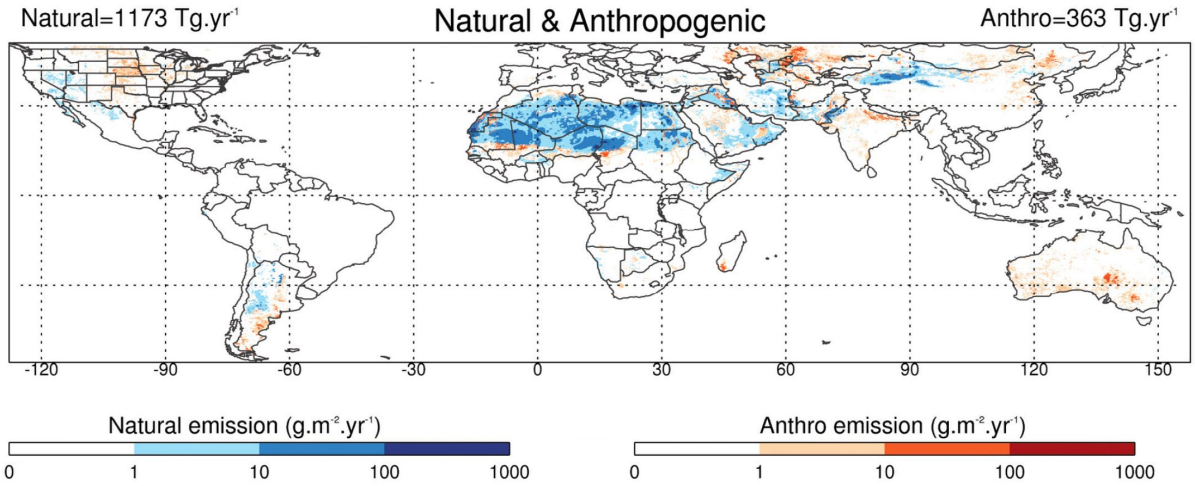

Figure 1-1. Figure from Ginoux et al. (2012) showing the natural and anthropogenic dust emission identified using MODIS data.

1.1.2 Anthropogenic sources

While most dust sources are natural sources, a significant amount of dust sources can be linked to human activities. Satellite observations suggest that the percentage of mineral dust with an anthropogenic origin could be 10% to 25% of the total dust load (Ginoux et al., 2012; Tegen et al., 2004), (Figure 1-1). The majority of the identified anthropogenic sources can be characterised as originating from agricultural areas, even though fires, roads, and industry and mining areas can also emit dust (Bali et al., 2017; Brotons et al., 2010; Csavina et al., 2012; Jiang et al., 2020; Koch et al., 2007; Li and Zhang, 2007; McKenna Neuman et al., 2009; Strode et al., 2009; Zielinski et al., 2016). Practices in agricultural areas that increase the vulnerability of a surface to erosion include overgrazing, wild fires, deforestation, tillage practices, sparse vegetation cover on agricultural land, and the removal of natural wind barriers (Geist and Lambin, 2004; Shepherd et al., 2016). The distribution of anthropogenic dust differs per region. Anthropogenic dust makes up 75% of the total dust emissions in Australia, whereas anthropogenic sources only account for 8% of total dust emissions in Northern Africa (Ginoux et al., 2012). The areas that are most sensitive to anthropogenic

dust emissions are, similar to natural emissions, semi-arid and arid drylands with sandy soils (Zobeck and Baddock, 2013).

An important event that demonstrated the disastrous consequences of dust emissions and wind erosion on agricultural land was the Dust Bowl in the Southern Great Plains in the United States, from 1931 to 1939. This was caused by a prolonged period of drought that corresponded with a high number of fallow fields due to the economic depression that followed a period of intense farming, intensive tillage and above-average precipitation (Lee and Gill, 2015). During the Dust Bowl, fertile soil was removed from 40 million hectares of land (Zobeck and Baddock, 2013) which led to the emission of between 4.1 to 5.5 billion tons of aerosols from the soil (Hansen and Libecap, 2004). This event also led to the formation of the Natural Resources Conservation Service (NRCS) in 1935, which sought to develop methods for wind erosion prevention and soil conservation (Zobeck and Baddock, 2013).

The use of water for agriculture or industry can also have a secondary effect on the emission of dust. The desiccation of lakes by diversion of water for croplands leaves dry lake beds that have highly erodible surfaces. Famous examples of such indirect anthropogenic dust sources are the Aral Sea in Central Asia and Owens Lake in California. Also, the decrease of surface-level water and groundwater can reduce the natural plant cover and increase the erodibility of land.

The influence of human activity on dust emissions can also be defined by the anthropogenic influence on climate (Zender et al., 2004). The change in climate can lead to stronger wind events (Pryor and Barthelmie, 2010; Seneviratne et al., 2012) which causes more wind erosion and higher emissions of dust. Furthermore, climate change can cause more droughts and an expansion of drier regions, which leads to larger areas that become more sensitive to wind erosion. The human influence on climate can impact both natural and anthropogenic dust sources.

1.1.3 Temporal change in anthropogenic dust

Over longer timescales, the global dust load has fluctuated with the ice ages, which can be linked to a decrease in plant cover and an increase in aridity (Mahowald et al., 1999). However, global agriculture has seen profound changes over the last few centuries and it is generally accepted that the emission of dust has increased over time due to human activities. The anthropogenic influences on climate and dust emissions can be tracked back to at least 5000 years ago (Neff et al., 2008; Ruddiman, 2003), but the largest increase in global dust load has been observed in the 20th century when the suspended dust load has doubled (Mahowald et al., 2010; McConnell et al., 2007). This can be partially linked to a change in climate and an increase in population and demand for food, which led to an intensification of agriculture and the expansion of croplands (Moulin and Chiapello, 2006; Mulitza et al., 2010; Stanelle et al., 2014; Zobeck and Baddock, 2013). Stanelle et al. (2014) estimate that 56% of the dust increase since the 19th century is caused by climate change and 44% by the anthropogenic influence on land cover. However, to what extent the increase in dust emission during the last century was precisely caused by human impact and to what extent by an increase in wind

erosivity or change in surface conditions such as sediment supply, roughness, and surface disturbance, is still debated (Cowie et al., 2013; Ridley et al., 2014). The precise increase or decrease of emissions during the last century differs for each region and depends on the level of desertification and the rate at which agricultural intensification increased, and the climate change, which can include a change in wind strength, precipitation, humidity, and temperature (Webb and Pierre, 2018).

Despite the current trend showing an increase in dust load, Mahowald and Luo (2003) demonstrate that the future dust load could decrease, assuming that the current anthropogenic land cover will remain static, an assumption that has also been more recently proposed by (Hurtt et al., 2011). Furthermore, the expected increase in atmospheric CO_2 could increase the plant cover in semi-arid and arid regions and could therefore minimize the erodibility of these surfaces (Stanelle et al., 2014). Exact predictions on the change in the global dust load are difficult since it depends on many variables, both on climate and change in land use. However, the tendency for a decrease in dust emissions should be considered for predictions of the impacts of the global dust load.

1.2 The on- and offsite effects of dust

1.2.1 Onsite effects of dust emission

In the IPCC 2019 report, dust emission is mentioned as a land degradation process with a global extent. However, dust emission is especially seen as the major process of soil degradation in semi-arid- and arid regions (Ravi et al., 2011). Despite the fact that saltation can result in the largest transport of particles (Sterk et al., 1996), this redistribution is only local, whereas suspended sediment can cause the removal of clay and silt from an area. Due to the removal of clay and silt from the soil, the emitting surface could become deficient in fines. Clay and silt often also carry significantly more nutrients due to their electrochemical nature, which causes dust emission also to result in a disproportionate removal of carbon (C) and nutrients such as phosphorus (P), nitrogen (N), potassium (K), iron (Fe), magnesium (Mg) (Van Pelt and Zobeck, 2007). The depletion of N, P, C, and other elements by wind erosion has been described for arid soils (Lawrence and Neff, 2009; Neff et al., 2005), agricultural soils (Sterk et al., 1996), and grazed grasslands (Neff et al., 2005). Visser and Sterk (2007) described the loss for N and P as up to 73% and 100%, respectively, of what is needed for crop production within one wind event. The recovery of degraded soil can be slow, especially in semi-arid to arid climates (Fernandez et al., 2008). This depletion of fines and nutrients from agricultural soils can have negative effects on crop yield. Zobeck and Bilbro (1999) described a decrease of 42% in grain yield from wind-eroded fields. Wind erosion can even change the soil type of an area due to the removal of the surface horizon and depletion of fines and organics (Buschiazzo et al., 1999). Furthermore, the removal of fines can also influence the infiltration and holding capacity of a soil (Lyles and Tatarko, 1986). Besides the removal of fines, wind erosion can also have a direct effect on the production and yield from agricultural fields. The abrasion from saltating crops can result in significant damage to plants (Sterk et al., 2001). Also, the covering of seeded fields by deposited sand can obstruct the growth of seedlings (Farmer, 1993).

1.2.2 Offsite effects of dust emission

1.2.2.1 Chemical flux

Dust particles have the potential to be transported around the globe within two weeks (Uno et al., 2009) which makes dust emission, transport, and deposition a significant process in the global chemical flux as described by, among others, Csavina et al. (2012), Derry and Chadwick (2007), Grantz et al. (2003), Jickells (1995), Lawrence and Neff (2009), and Mahowald et al. (2009). As discussed before, suspended particles are generally nutrient-rich due to the high content in clay, silt, and organic carbon (Ted M Zobeck and Fryrear, 1986). However, the exact chemical content of depositional dust shows great variance since it is also based on the surface texture and chemistry of the source material, the dust particle sizes, and the distance from the source (Dansie et al., 2017; Grantz et al., 2003; Lawrence and Neff, 2009; Visser and Sterk, 2007; Ted M Zobeck and Fryrear, 1986). Lawrence and Neff (2009) summarized the chemical content of depositional dust and showed especially a strong enrichment in N, lead (Pb), Ni, and Co, and a depletion in Na, Si, and Al compared to the composition of the upper continental crust.

One of the most important areas of dust deposition is the ocean. The Fe, N, and P in dust particles are one of the most important nutrients for ocean biochemistry since the storage of carbon by algae is dependent on the deposition of these elements (Falkowski et al., 1998; Mahowald et al., 2010; Moore et al., 2013; Okin et al., 2011). The deposition of Fe by aerosols can be responsible for 50% of the carbon uptake in the ocean, depending on the nutrient concentration and chlorophyll activity, which is generally the highest in higher latitudes (Okin et al., 2011). The effect of Fe deposits is also great in areas with coastal upwelling regimes, such as the coast of Namibia (Capone and Hutchins, 2013). Mahowald et al. (2010) described that the last century's trends in dust deposition increased ocean productivity by 6%, which represents a carbon uptake of roughly 4 ppm from the atmosphere.

Besides in the oceans, phosphorus is also often a limiting factor in forests and other ecological systems (Cleveland et al., 2002; Okin et al., 2011; Peterson et al., 1993; Wu et al., 2000). Swap et al. (1992) described the high quantity of Saharan dust that is being deposited in the Amazon and the increase in trace elements that this deposition brings to this nutrient-poor region (Swap et al., 1992). Also in South Africa, the deposition of dust brings nutrients such as K, Ca, and Zn to the nutrient-poor region of the fynbos ecosystems in the southwest of the country (Soderberg and Compton, 2007).

1.2.2.2 Regional and global climate

Dust suspension is one of the most important phenomena that generally has a cooling effect on earth's climate (Boucher et al., 2013). The influence of dust on climate can be split into the influence of directly emitted aerosols such as mineral dust, black carbon (BC), organic carbon (OC), and sea salt, and aerosols that form in the atmosphere due to the chemical reactions such as secondary organic aerosols (SOA) and sulphate (Myhre et al., 2013). Aerosols can have positive and negative radiative forcing (RF) and the effect on the RF can be divided into direct and indirect aerosol effects (Boucher et al., 2013). The direct aerosol effect consists of the interaction between aerosols and

radiation, which generally has a negative RF, and the impact that aerosols have on a surface albedo after deposition, which generally has a positive RF. The indirect effect represents the aerosol-cloud interaction since aerosols function as droplet nuclei that encourage cloud formation, which then has a cooling effect on the earth's climate (Forster et al., 2007). The effect of dust on climate introduces large uncertainties since it depends on the composition, size, altitude, and geographical location of the particle (Grantz et al., 2003; Mahowald et al., 2014). The RF values of aerosols, together with that of gases and other processes, are shown in Figure 1-2. This figure also shows the development of the total RF from aerosols over the last century, which shows an overall decrease in RF over time due to the increase in suspended aerosols. Mahowald et al. (2010) estimated that the increase in suspended dust between 1955 and 1989 could have resulted in a global temperature decrease of 0.11 °C. The removal of all current anthropogenic aerosols from the atmosphere could result in a global temperature increase of 0.5 °C (Samset et al., 2018).

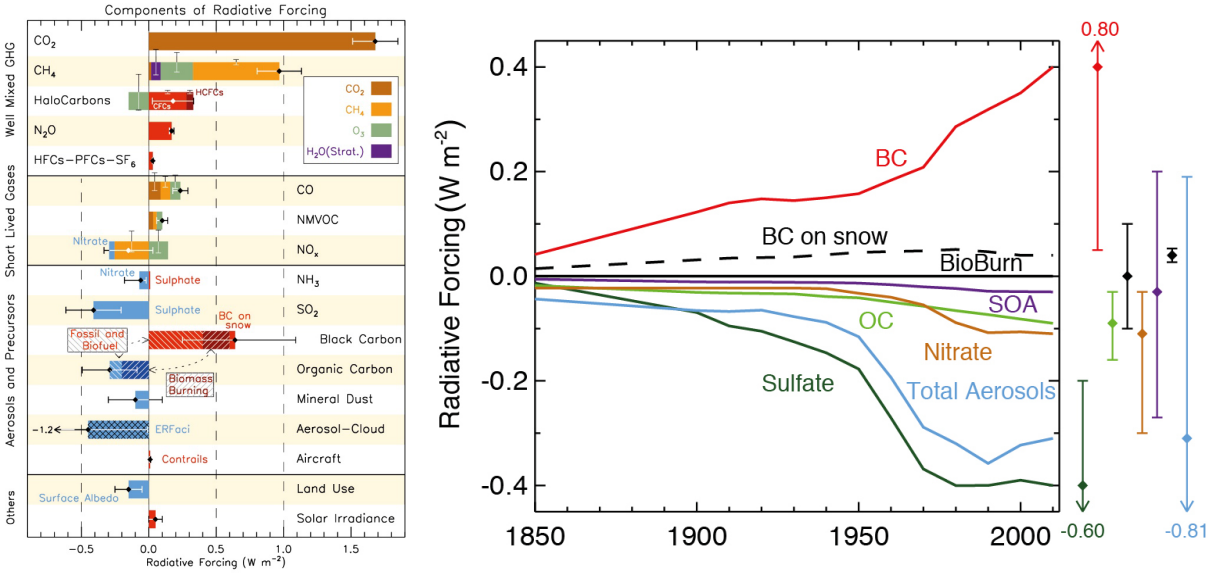

Figure 1-2. Figures from Myhre et al. (2013) showing the total RF from aerosols (left), and the increase in the RF of the different aerosols over the last 150 years (right).

1.2.2.3 Human health

According to the World Health Organisation (WHO), air pollution by aerosols has severe effects on human health. It is estimated that 2 million people are killed by air pollution each year (WHO, 2005). The severity of respiratory problems is often linked with the PM_{10} concentration since particles below 10 micrometres are small enough to reach the bronchioles, the deepest part of the lung (WHO, 2005). The World Health Organization describes a PM_{10} concentration of up to 20 µg m^{-3} as an acceptable annual mean, and 50 micrometres as an acceptable mean for a period of 24 hours. Particles at 2.5 micrometres can even pass through the lungs and affect other internal organs and cause cardiovascular problems, for example (Martinelli et al., 2013). Other risks that dust storms pose to human health depend on the presence the pesticides, heavy metals, fungi, bacteria, pathogens, pollen, and spores that dust can contain (Goudie, 2013). Little is known about the influence of the

origin of dust on the microbial communities in the dust, but it has been suggested that agricultural practices create a more significant content of allergens and pathogens in the dust than natural conditions (Corden et al., 2003; Friesen et al., 2001).

1.3 Physical processes and methods in wind erosion

1.3.1 Wind erosion controls

The intensity of wind erosion is controlled by a range of factors, as described in many wind erosion models such as the Wind Erosion Equation (WEQ) (Woodruff and Siddoway, 1965), the Revised Wind Erosion Equation (RWEQ) (Fryrear et al., 1998), the Wind Erosion Prediction System (WEPS) (Hagen, 1991), the Dust Production Model (DPM) (Marticorena and Bergametti, 1995), and the Wind Erosion Assessment Model (WEAM) (Shao et al., 1996). This intensity depends on both the erodibility of a surface and the erosivity of the wind. The erodibility of soil depends on several factors that can roughly be defined as (1) the factors that influence the cohesion of a surface, (2) the factors that influence the quantity of erodible particles, and (3) the factors that influence the interaction with the wind. The cohesion can be influenced by, among others, moisture, aggregation, the presence of a crust, soil texture, chemistry, and mineralogy. The quantity of erodible particles is mainly defined by the particle size distribution and organic content. Characteristics such as the cover of soil from plants and stubble, and roughness, which can originate from tillage, cultivation, and aggregation, can influence the interaction of a surface with the wind and increase or decrease erosion. These controls are summarised in Figure 1-3, together with the interactions of these controls on different scales. The impact of land management on dust emission mainly regards the removal of vegetation cover and the disturbance of soil cohesion (Ginoux et al., 2012).

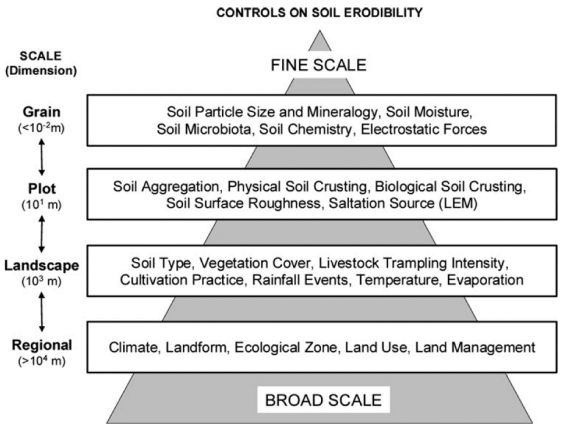

Figure 1-3. Figure adapted from Webb and Strong (2011) showing the factors that can influence the erodibility of a surface on different scales.

Soil cover, which originates from vegetation, plant residue or stubble, is generally seen as the initial main control of wind erosion since a high cover can almost completely prevent wind erosion (Chepil, 1944; Tibke, 1988; Woodruff and Siddoway, 1965). The decrease in vegetation cover by human interference can come from grazing, crop production, or groundwater decrease. The effect that soil

cover has on wind erosion has been summarised by Funk and Engel (2015) as the reduction of the wind velocity near the surface, the increase in roughness, the decrease in threshold velocity, the direct protection of a surface by the overlying cover, and the reduction of the horizontal sediment mass. Only with a low vegetation cover, do other surface erodibility controls, as summarised in Figure 1-3, become relevant.

A high cohesion is often the result of the formation of a soil crust, which can either be a biological or physical crust. Biological crusts consist of algae, lichens, cyanobacteria, and/or mosses that create a cohesive surface due to the formation of filaments that bind soil grains together (Belnap et al., 2008; McKenna Neuman et al., 1996). They are relevant surface characteristics for the stabilisation of the soil and prevention of wind erosion in many semi-arid and arid areas (Belnap, 2006; Eldridge and Leys, 2003; McKenna Neuman et al., 1996; McKenna Neuman and Maxwell, 1999). However, the formation of a biological crust after disturbance takes many years (Belnap, 2006, 2001; Belnap and Gillette, 1998), which makes these crusts not common in agricultural areas. Physical crusts, however, can form on much shorter timescales. Physical crusts form due to the disintegration of aggregates by slaking and raindrop impact, and the dispersion and movement of fine, often clay, particles (Bryan, 2000; Gal et al., 1984; Morin, 1993; Qiang-guo, 2001; Zejun et al., 2002). The formation of crusts depends on the clay, silt, and organic carbon content, the aggregate stability, and the rainfall characteristics, as summarised by Valentin and Bresson (1997). Crust formation is often regarded as a form of soil degradation due to its enhancement of interill erosion and the restraining effect on seedling emergence (Ries and Hirt, 2008; Valentin and Bresson, 1997, 1992; Zejun et al., 2002), but crusts can also minimize degradation by protecting the soil against wind erosion (Gillette et al., 2001, 1982, 1980; Goossens, 2004; Klose et al., 2019; Rice et al., 1996; Rice and McEwan, 2001; Sharratt and Vaddella, 2014; Sterk et al., 1999; Yan et al., 2015; Zobeck, 1991a). Even after disturbance, the crust clods that remain can limit erosion due to their roughness and cohesion, as described by (Gillette, 1988).

Besides the erodibility of a soil, wind erosivity, mainly defined by wind velocity and air density, determines the amount of wind erosion and dust emission. Wind erosion can happen by deflation, which is the process whereby wind lifts and transports loose, single particles. This can be combined with abrasion, whereby saltating sand particles hit a surface and launch other particles, after which finer particles can be picked up by the wind. Besides the big effect that abrading particles can have on dust emissions (Houser and Nickling, 2001a; Rice et al., 1996; Shao et al., 1993), abrasion is also one of the main processes that can degrade crusts and aggregates (Langston and McKenna Neuman, 2005; McKenna Neuman et al., 1996; Rajot et al., 2003). Regarding the influence of the wind velocity, it is generally assumed as a rough estimate that dust emission is proportional to the cube of the velocity (Gillette, 1977; Nickling and Gillies, 1989; Shao et al., 1993; Sweeney et al., 2008). However, the exact relationship is determined by the many characteristics of a soil surface and is strongly dependent on whether a surface is supply limited or supply unlimited.

1.3.2 Field monitoring methods

The most common way for measuring the emission of dust and wind erosion that is taking place in an area is by monitoring the process on a field scale. This most often relies on instruments that can quantify the eroding sediments in a point-scale measurement. The most commonly used instrument type is passive sediment samplers because of their low cost and long-term monitoring capabilities. Over time, different passive samplers have been developed that measure the horizontal sediment flux, such as the Big Spring Number Eight (BSNE, Fryrear, 1986), the Modified Wilson and Cook (MWAC, Wilson and Cooke, 1980), the Wedge Dust Flux Gauge (WDFG, Hall et al., 1993), the Suspended Sediment Trap (SUSTRA, Janssen and Tetzlaff, 1991), the Guelph-Trent Wedge trap (GTW, Nickling and McKenna Neuman, 1997), the International Centre for Eremology sampler (ICE, Cornelis and Gabriels, 2003), and the Basaran & Erpul Sediment Trap (BEST) (Basaran et al., 2011). The different efficiencies of these samplers and their dependency on wind velocity have been described by several studies (Basaran et al., 2011; Goossens and Offer, 2000; Mendez et al., 2011; Nickling and McKenna Neuman, 1997). Furthermore, passive samplers that measure vertical deposition such as the Marble Dust Collector (MDCO), dust deposition gauges (Hall et al., 1993), and other "frisbee-type" dust samplers (Wiggs and Holmes, 2011) are commonly used. More advanced field monitoring instruments include active dust samplers and saltation sensors. Saltation sensors, such as the Sensit (Stockton and Gillette, 1990), Saltation Flux Impact Responder (SAFIRE, Baas, 2004), and the saltiphone (Spaan and van den Abeele, 1991), are especially used to determine the saltation threshold velocity.

Field monitoring on wind erosion and dust emission are measurements that are often accompanied by meteorological measurements, from which especially high temporal wind velocity measurements are important, and characterisation of the field characteristics. Field characteristics can include descriptions of roughness, vegetation, cohesion, and soil characteristics. The latter can be described by the grainsize distribution, aggregate stability, soil density, and soil content, such as the organic carbon content. The field and soil characteristics can be described by many more variables, but will generally all fit in one of the surface characteristics as described in paragraph 1.3.1.

1.3.3 Experimental measurements

To determine the erodibility of soil in an experimental way, a wind tunnel is the most commonly used method. The basic principle of a wind tunnel is using an artificial wind stream with a logarithmic wind profile to mimic natural wind conditions. This logarithmic wind profile is necessary to create turbulence that is responsible for the uplift of particles from the surface (Raupach and Leys, 1990). Even though a wind tunnel is one of the best ways to mimic wind erosion, the big disadvantage is that most wind tunnels cannot be used in the field, and even portable wind tunnels require big efforts to employ, which limits the amount of measurement that can be done.

Another instrument that can be used for soil erodibility measurements is the in 2007 presented Portable In-Situ Wind Erosion Laboratory (PI-SWERL) (Etyemezian et al., 2007). The PI-SWERL uses

a circular blade to create shear stress on a surface, after which it measures the dust concentration that is emitted from the soil. The PI-SWERL is much smaller than a traditional wind tunnel, which makes it practical for field measurement, making a larger number of measurements and replicates possible. However, in contrast to most wind tunnels, the PI-SWERL does not create an artificial wind profile. The comparability between the emission from the PI-SWERL and the straight-line wind tunnel has been made by Sweeney et al. (2008), but whether the threshold friction velocity measured by the PI-SWERL is comparable to that of a wind tunnel has yet to be determined

1.3.4 Satellite imagery

The applicability of satellite data has given large insights into the global dust sources, from which the Total Ozone Mapping Spectrometer (TOMS), Meteosat Second generation - Spinning Enhanced Visible and Infrared Imager (MSG-SEVRI), Moderate Resolution Imaging Spectroradiometer (MODIS), and Landsat have been most widely used to assess dust source areas. The TOMS was the first method to identify the global dust distribution using the Aerosol Index (AI), which quantifies the absorption of UV, between 340 nm and 380 nm (Herman et al., 1997; Prospero et al., 2002). The TOMS has a daily data acquisition with a resolution of 13 by 24 km and is most suitable for detecting larger inland sources and is not suitable for detecting non-UV absorbing aerosols. The MSG-SEVIRI has a 15-minute sampling rate and a resolution of 4 by 4 km, from which the Infrared reflections (8.7, 10.8 and 12.0 micrometres wavelengths) are used to detect temperature differences between aerosols and land (Schepanski et al., 2007; Vickery et al., 2013). The MODIS samples twice per day with a resolution of 250 by 250 metres and uses visual to far-infrared bands (between 0.4 and 14.4 micrometres) (Miller, 2003; Vickery et al., 2013). Lastly, the Landsat has the highest spatial resolution (15 by 15 metres to 30 by 30 metres) but the lowest temporal resolution (16 days). The advantages of the different methods depend on the resolution, whereby higher resolutions can detect emissive landforms or even dust source points and lower resolutions can detect emissive regions. Furthermore, the sampling rate and the sensitivity to detect certain types of dust with different compositions, latitudes, and surface backgrounds are relevant for prioritizing satellite data.

1.3.5 Wind erosion models

To gain insight into the spatial and temporal variation of wind erosion and dust emission, and to enable predictions in these processes, wind erosion models have been developed. These models generally include one or multiple variables describing the influence of wind, climate (including precipitation and humidity), vegetation, roughness, soil texture and composition, and cohesion. These models are generally based on values that were empirically determined by field and experimental measurements (Zobeck et al. 2003). It should be noted that these wind erosion models describe the quantity of sediment eroded by wind, and are therefore not necessarily an indication of the amount of dust that is being suspended in the air.

A summary of the seven most common wind erosion models has been given by Zobeck et al. (2003), from which three take the presence of a crust into account: the wind erosion equation (WEQ,

Woodruff & Siddoway, 1965), the wind erosion prediction system WEPS (Hagen, 1991), and RWEQ (Fryrear et al., 1998). The quantification of the influence of crusts differs per wind erosion model. For the WEQ the presence of a crust is a sixth of the erodibility of loose soil. However, it is assumed that crusts can disintegrate over time and the authors state that when an average erodibility is considered the crust factor can be disregarded. The WEPS uses a more complex expression of the influence of crusts, which entails the crust fraction, crust thickness, loose particles on the crust, crust density, and crust stability (Hagen, 1991; Zobeck et al., 2003). For the RWEQ, a soil crust factor (SCF) expresses the resistance of crusts against abrasion and is calculated as follows:

$$SCF = \frac{1}{1 + 0.0066(Cl)^2 + 0.021(OM)^2} \quad (1)$$

Whereby Cl represents the clay content (%) and OM the organic matter content (%), both values accounted for a range of 5% to 39.3% and 0.32% to 4.74%, respectively. The formation of a crust has been assumed after a rainfall of 12 mm. Hereby it is taken into account that any tillage activities destroy a crust completely. However, no external factors such as abraders have been taken into account in this wind erosion model.

1.4 The Free State as a dust source

1.4.1 Southern African dust emission

The dust emission from Southern Africa is around 3.4% of the global dust emission (Tanaka and Chiba, 2006). Vickery et al. (2013) identified dust plume sources in Southern Africa from 2005 to 2008 using a combination of MODIS and MSG-SERVI data. This study found that the largest number of dust plume sources originated from the Etosha Pan and the Namib Coast in Namibia, and the Makgadikgadi Basin in Botswana. In South Africa, the Western Kalahari and the Free State showed a small quantity of dust plume sources. A study from Eckardt et al. (2020) used the MSG-SERVI data to identify the dust sources from 2006 to 2016 in South Africa. Their data showed that 71% of the identified sources were located in the Free State province (Figure 1-4). As mentioned before, the dust emission from this region has been identified by Vickery et al. (2013) and Ginoux et al. (2012). Furthermore, wind erosion in the Free State has been described by Holmes et al. (2008; 2012) and Wiggs and Holmes (2011). However, the Free State has not yet been recognized in the literature as the major dust source region in South Africa.

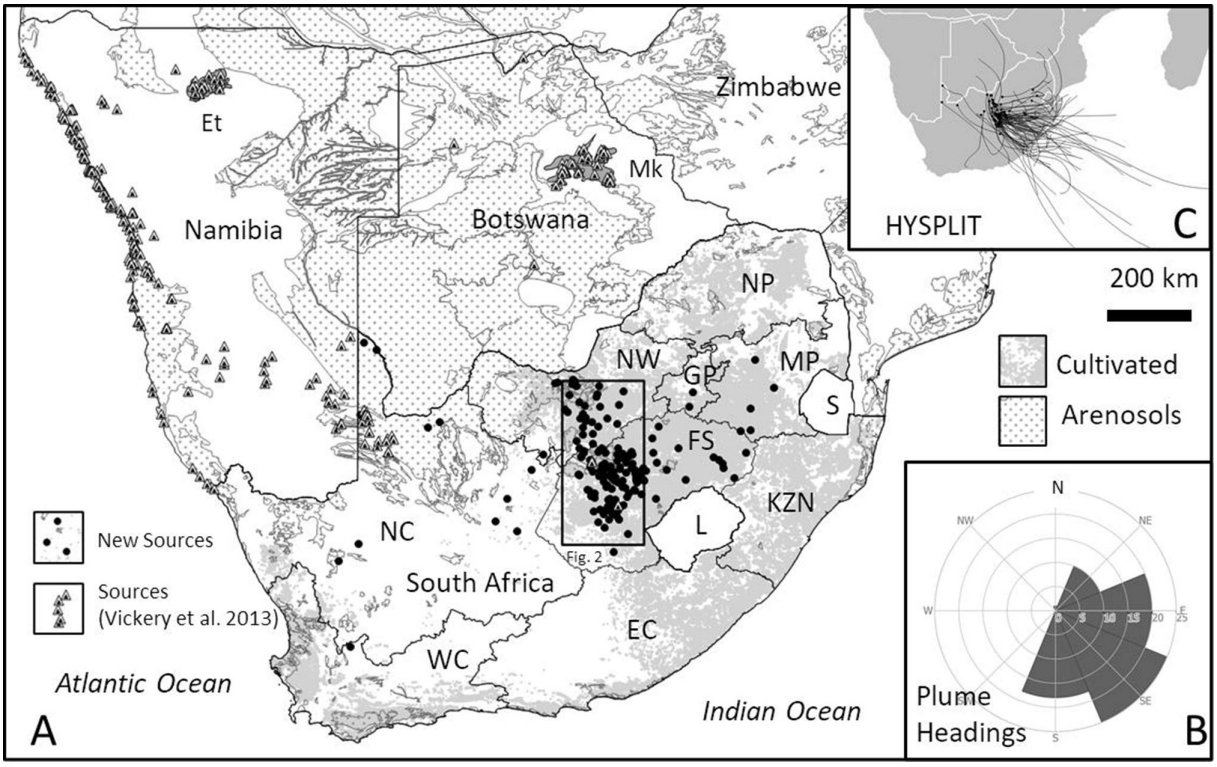

Figure 1-4. Figure from Eckardt et al. (2020) showing their identified dust source points and the source point from Vickery et al. (2013) (A), the direction of the plume headings (B), and the tracked route from the identified dust plumes (C).

The identified dust source points are mainly located in the centre to the northwestern part of the Free State, around the city of Bultfontein (Figure 1-5). The land cover of the 10 km buffer radius of the dust source points in the Free State accounts for 62% of natural land, and for 34% of agricultural land (Eckardt et al., 2020). Most of the dust source buffer areas are on Luvisols and Arenosols (30% and 21%, respectively), soils that are commonly under agricultural use in this region (Hensley et al., 2006). Other prominent soils are Lixisol, Cambisols, and Calcisoil (15%, 14%, and 10%, respectively)[1]. The dust season is between August and December but can start as early as June and extend to January (Figure 1-6). This temporal pattern can be linked with the cropping activities in this region, which leaves the agricultural fields harvested and often disturbed by tillage during this period.

[1] The classification used by this thesis and Eckardt et al. (2020) is from the World Reference Base (WRB). A national classification on the soil types and soil families in South Africa has been made by the Soil Classification Working Group (1991).

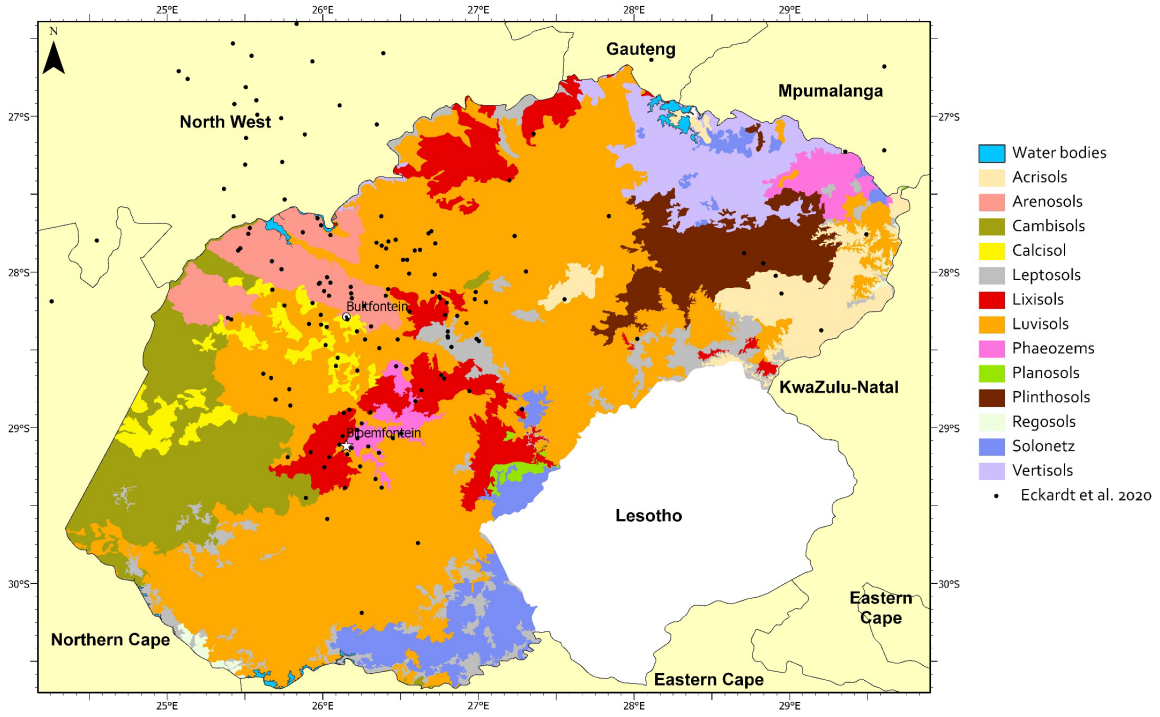

Figure 1-5. The soil map of the Free State showing the main soil types. The soil data comes from the Soil and Terrain Database (SOTER) for South Africa (FAO-ISRIC 2003).

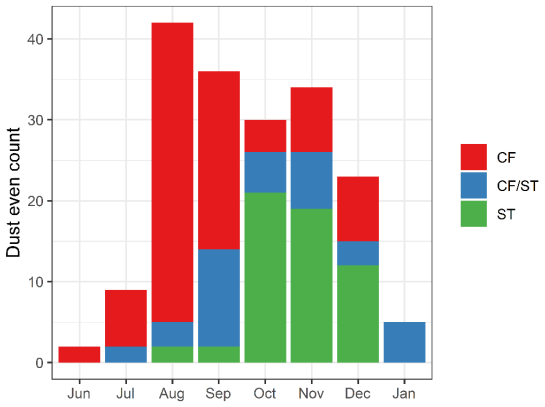

Figure 1-6. The dust event count per month from 2006 to 2016, and the number of Cold Fronts (CF) and Stationary Troughs (ST) that have been related to the dust events. The data comes from Eckardt et al. (2020).

1.4.2 Free State climate and weather

The Free State is located between the humid regions in the east, the arid Kalahari to the west, and the semi-arid Karoo in the south (Wiggs and Holmes, 2011). In general, the mean annual precipitation ranges from 400 mm in the southwestern part of the province to above 1000 mm in the outermost eastern part, (Figure 1-7). The Free State has a semi-arid climate, except for the arid climate in the southwest, with a precipitation /evaporation ratio (AI) of 0.2 to 0.5, (Hensley et al., 2006). The Free State has a summer rainy season, the onset of which starts in the east and moves to the west (Figure

1-7). However, the quantity and pattern of precipitation in this region are highly variable per year, as described by Moeletsi (2010) and shown in Figure 1-8.

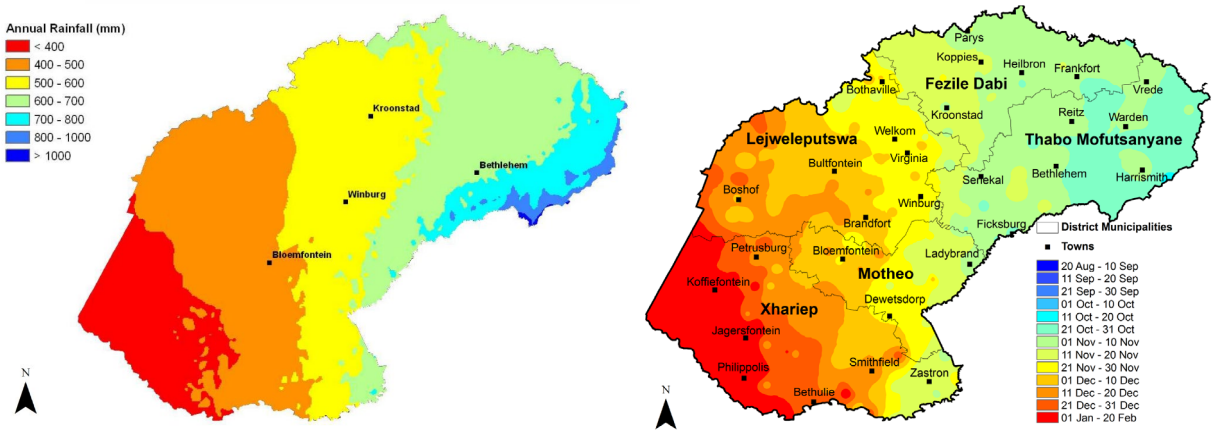

Figure 1-7. Figure adapted from Moeletsi (2010) showing the total annual precipitation pattern (left) and the onset of the rainy season with 80% non-exceeding probabilities (right).

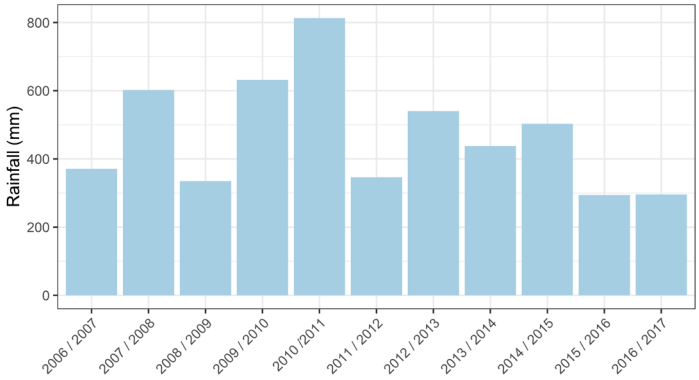

Figure 1-8. The yearly precipitation pattern in Bultfontein. The rainfall data comes from the weather station of the Agricultural Research Council (ARC) near Bultfontein.

The Free State experiences strong winds that reach the highest velocities in November, with the main wind direction being in NNE or SSW direction, but the strongest winds having a predominantly NW direction (Figure 1-9). The strong winds in the Free State are caused by thunderstorms from stationary troughs and cold fronts (Kruger et al., 2010). Eckardt et al. (2020) described that cold fronts tend to be the main cause of dust events from June to August, and stationary troughs tend to be the main cause of dust events later in the dust season (Figure 1-6). Cold fronts can result in strong northern to western winds (South African Weather Bureau, SAWB, from Eckardt et al. 2020) and are the result of eastward-moving frontal systems that cause steep pressure gradients (Kruger and Service, 2004). Stationary troughs produce prevailing winds from both southern and northern directions (Eckardt et al., 2020). The wind patterns are also visible in the wind rose from Bultfontein (Figure 1-9). Dust events themselves appear to be almost solely day events, mostly taking place between 09:30 to 12:30, with a wind velocity of 10 to 11 m s^{-1} (Eckardt et al., 2020).

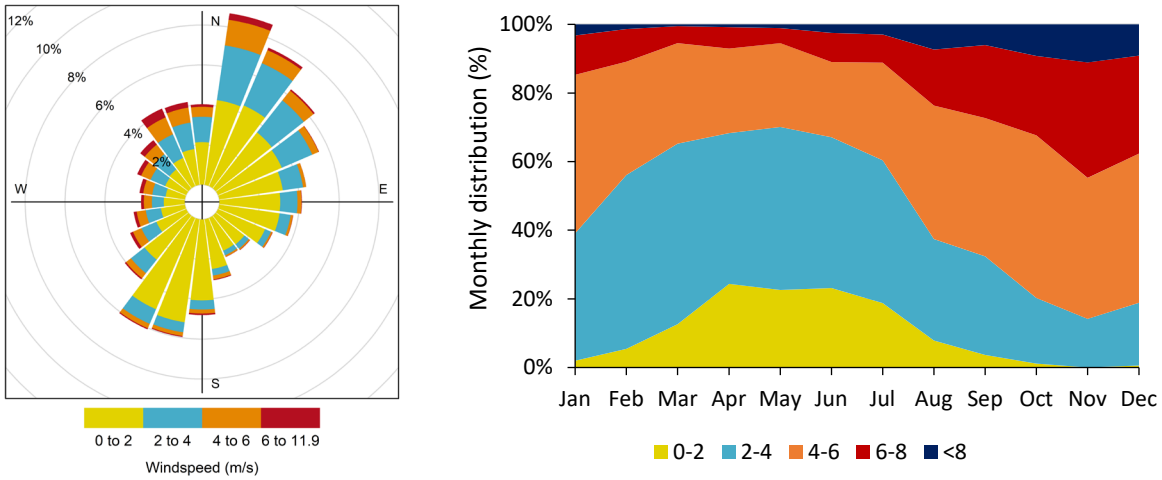

Figure 1-9. The wind rose (left) and daily maximum wind velocity per month from (right) from 2006 to 2018 in Bultfontein. The wind data comes from the weather station of the ARC near Bultfontein.

1.4.3 Geological background

The current geographical setting of the Free State is significantly influenced by its geology (Holmes and Barker, 2006). The Free State is partially located on the Highveld, an interior plateau in South Africa that has an elevation of between 1500 and 2100 metres above sea level (ASL). The geology of this region is mainly influenced by the tectonic activities during the time of the supercontinent Gondwana. The Free State geology is made up of the Karoo Supergroup, a stratigraphic unit that covers the largest part of South Africa (Figure 1-10), which was deposited between the Late Carboniferous and Jurassic periods. Below is a simplified description of the geological history of Southern Africa, which is based on descriptions from Catuneanu et al. (2005), Holmes and Barker, (2006), McCourt (2016), and Oriolo and Becker (2018).

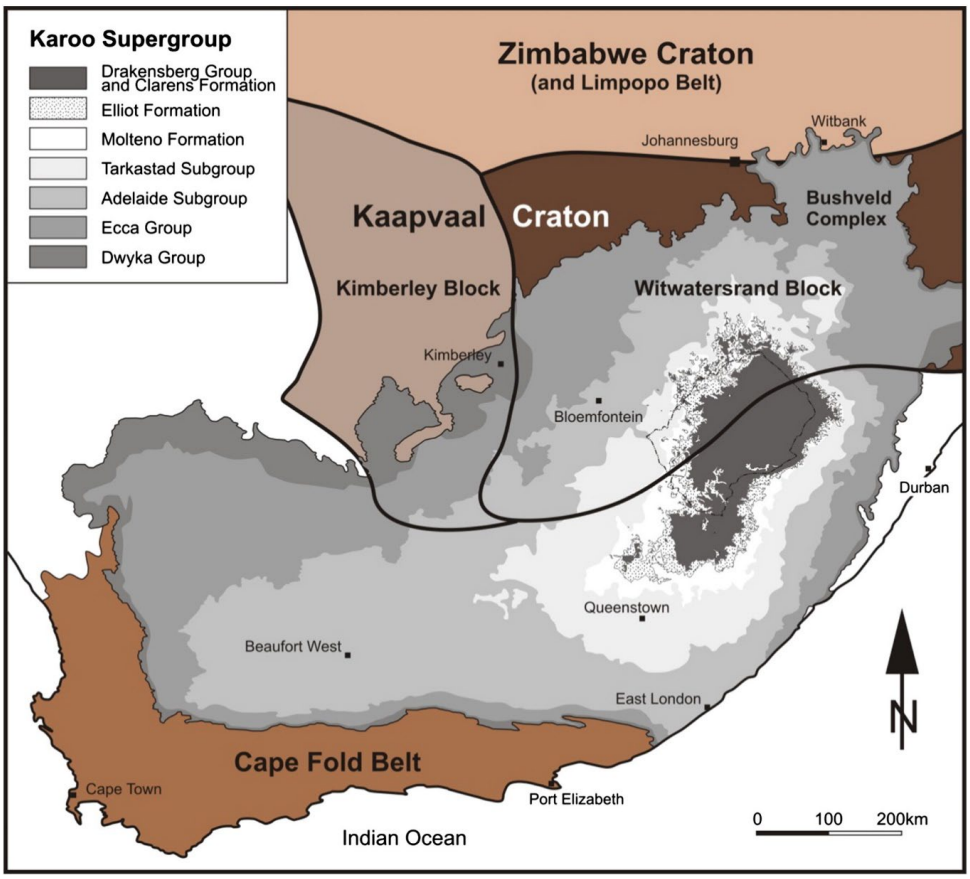

Figure 1-10. Geological map from Hancox and Götz (2014) showing the location of stratigraphic groups from the Karoo Supergroup. The Adelaide and Tarkastad Subgroup are part of the Beaufort group, and the Molteno and Elliot Formation are part of the Stormberg group.

The Archean-aged Kalahari Craton forms the base of the Southern African subcontinent. This craton is split into the Zimbabwe Craton to the north, and the Kaapvaal craton to the south by the Limpopo Belt, whereby the Kaapvaal craton is the continental base for the largest part of South Africa (Figure 1-10). This was followed by the formation of the Namaqua Belt south of the Kaapvaal Craton between 1400 and 1000 Ma during the assembly of the supercontinent Rodinia (Eglington, 2006). Around 600 Ma, the Pan-African orogeny led to the formation of the supercontinent Gondwana (Siegesmund et al., 2018). Following, around 500 Ma, the divergent movement of the Falkland Plateau caused a rift in the Southern part of Gondwana, which led to the accumulation of sediments in the rift valley, which formed the Cape Supergroup. This divergent movement changed to a convergent one around 330 Ma, which resulted in the closing of this rift valley, the folding of the Cape Supergroup, and the formation of the Cape Fold Mountains, which are still a prominent feature of the South African landscapes. The weight of this mountain range caused the lowering of the continental crust, which results in the formation of the Karoo Ocean. This sea is the base for the formation of the Karoo Supergroup.

At the end of the Carboniferous, around 300 Ma, the Karoo Ocean was located near the South Pole and was covered for large parts with thick ice sheets. When Gondwana moved in a northerly direction, these ice sheets melted and the deposits from this ice formed the Dwyka group. The

drainage towards the sea created deltas and vegetated regions. This became the sandstones and shales of the Ecca group. The vegetation resulted in the formation of coal which is mined in certain regions of the Highveld. Slowly the Karoo Sea was in-filled with sediments, and the region became a terrestrial environment dominated by rivers from the Cape Fold Mountains. These resulted in the deposition of the Beaufort Group which consisted of shale, mudstone, and sandstone and covers the central part of the Free State. During the late Triassic (around 237 Ma), the South African part of Gondwana became drier and more arid, and alluvial fans and rivers resulted in the deposition of sandstones from the Stormberg Group. These sandstones are found in the eastern part of the Free State, and also make up the famous yellow sand stone feature of the Golden Gates Highlands National Park. At the end of the Gondwana stage, rifting along the Pan-African welts preceded the break-up of Gondwana which started around 182 Ma. Rupture in the continental crust led to the outflow of basaltic lava which covered nearly the whole of Southern Africa and which forms the current Drakensberg group of rocks. Within 2 million years, 1600 metres of basaltic rocks were horizontally deposited. Also, the dolerite sills in the Karoo Supergroup formed. During this period, the continent also experienced uplift and the development of rift valleys along the current continental borders.

After the break-up of Gondwana, around 180 Ma, the Highveld region was a high-laying region and changed from a depositional to an erosional environment. This alluvial erosion moved from the higher-lying regions of Lesotho to the Atlantic Ocean, similar to the current drainage of the Orange River and the Vaal River in the Free State. The whole of the Drakensberg group was eroded in the Free State, and parts of the Stromberg, Beaufort and Ecca groups have been eroded. Only some of the dolerite sills from the Drakensberg group remain, protecting the underlying sedimentary rocks, which results in dolerite hills in the landscape of the Free State and the Highveld.

1.4.4 Geographical background

Currently, the Free State is the highest-laying province in South Africa, with almost the entire area laying above a 1000-metre altitude ASL. The majority of the province has a slope gradient of < 5% (Holmes and Barker, 2006). The Free State is bordered by the Orange River in the south and the Vaal River in the north. The Orange River is thought to have changed its drainage several times (Partridge, 1987). Several smaller rivers including the Modder River, Riet River, Vet River, Vlas River, and Wilge River drain westwards through the province. The Free State has almost completely a grassland biome, with some savannah and Nama Karoo areas in the west (Rutherford et al., 2006).

Free State soils are mainly of a sandy texture, from which Luvisol soils are the most prominent (Figure 1-5). These sandy soils are thought to have an aeolian origin due to their contrast with the fine-grained shale substrates and their rounded grain properties, whereby the Kalahari desert is likely the origin of these grains (Barker, 2002). The soils in the northwestern part of the Free State can be linked with blown-out sediment from the Vaal River specifically. Most of the Free State soils overlay the Beaufort and Ecca shales. These shales serve as parent material, whose influence is expected to be fairly uniform (Hensley et al., 2006). However, the occurrence of calcium carbonate in

soils, like in the Calcisols, can be attributed to nearby, higher-laying dolerite. The climate has a large impact on soil formation: in the arid and semi-arid south-western part of the province, the soil has a predominant red B horizon, which is more yellow-brown in the northeast due to the higher rainfall in this region (Hensley et al., 2006). Also, the lack of clay-rich Vertisols, Acrisols, and Plinthosols in arid regions can be attributed to the lack of chemical weathering (Hensley et al., 2006).

The Free State is characterised by a high concentration of pans which can be characterised as flat, closed depressions and are often associated with arid climates (Goudie, 1991; Holmes et al., 2008). There are roughly 8800 pans in the Free State, which cover 3% of the surface (Geldenhuys, 1982), whereby especially the northwestern region of the Free State holds a high concentration of pans (Roux and Le Roux, 1978). The presence of pans in the Free State has furthermore been linked with the Ecca shales (Goudie, 1991; Goudie and Wells, 1995). Pans are the result of drainage activities followed by wind erosion (Goudie, 1991). The often-observed crescent-shaped or lunette dunes downwind of pans confirm the relationship with wind erosion (Goudie and Thomas, 1986; Horowitz et al., 1978; Visser and Joubert, 1991). Pans are known for being major emitters of dust (Prospero et al., 2002; Vickery et al., 2013; von Holdt et al., 2017). Eckardt et al. (2020) described that the pans in the dust emission buffer area take up only 1% of the surface area, and are generally less than 2 ha. However, Eckardt et al. (2020) do call for a more extensive examination of smaller pans in the Free State due to the decrease in surface water (Pekel et al., 2016).

1.4.5 Cropland system

The Free State province is known for its large-scale commercial agriculture, which dates back to the 19th century. The following description of the agricultural history of the Free State is based on the information provided by Holmes et al. (2012). The grasslands of the Free State were used by the indigenous inhabitants for cattle grazing and hunting. The trekboers, which arrived in the Highveld at the end of the 18th century, performed similar practices of cattle grazing. The first European settlements likely occurred around 1850 (Nixon 1880), after the Great trek led to the mass migration of people into the interior of the country from the coastal Cape Colony. The settlers redistributed the land for private possession which was inherited within individual families and led to the birth of commercial agriculture. This was in contrast with the communal sharing of land by indigenous inhabitants (Holmes et al. 2012). Commercial farming was further stimulated by the building of the railway from Kimberley, a city in the Northern Cape on the border with the Free State, to Cape Town in 1985, as a consequence of the diamond mines located near Kimberley (Robert 1976). At present, more than 99% of arable land remains under commercial ownership (DAFF, 2018), and agriculture is practised on a large scale.

At the moment, the highest proportion of land in the Free State remains under agricultural usage, which is either for cattle grazing or crop production. Figure 1-11 shows the distribution of land use in the Free State, and the relative proportions of crops produced. Agriculture in this semi-arid region is supported by sandy and loamy soils that have a high infiltration rate and can function as a storage

for water (Hensley et al., 2006). The main crop that is grown in the Free State is maize (*Zea mays*), followed by soybeans (*Glycine max*), sunflowers (*Helianthus annuus*), wheat (*Triticum aestivum*), dry bean (*Phaseolus vulgaris*), sorghum (*Sorghum bicolor*), groundnut (*Arachis hypogaea*), and barley (*Hordeum vulgare*). On average, the Free State produces 5.8 million tonnes of food per year (DAFF, 2018). This high production is notable since 28% of the province has been identified as non-arable, with land currently under arable production having been classified as having a very low (6%), low (35%), or medium (31%) agricultural potential by Hensley et al. (2006). This classification has been based on the soil type and climate conditions. Precipitation above 450 mm has been regarded as necessary for any crop production, but higher precipitation increases the agricultural potential strongly (Hensley et al., 2006; Moeletsi, 2010). The land that has been identified as non-arable is located in the arid southwest and is used for cattle farming. Agriculture in the Free State is furthermore controlled by the onset of the rainy season, which starts on average in December and ends in April (Moeletsi and Walker, 2012). For the soil types, sandy loam or loamy sand soil is preferred since this offers easy infiltration and reduces incidences of run-off and soil erosion (Hensley et al., 2006; Tait and Zheng, 2003).

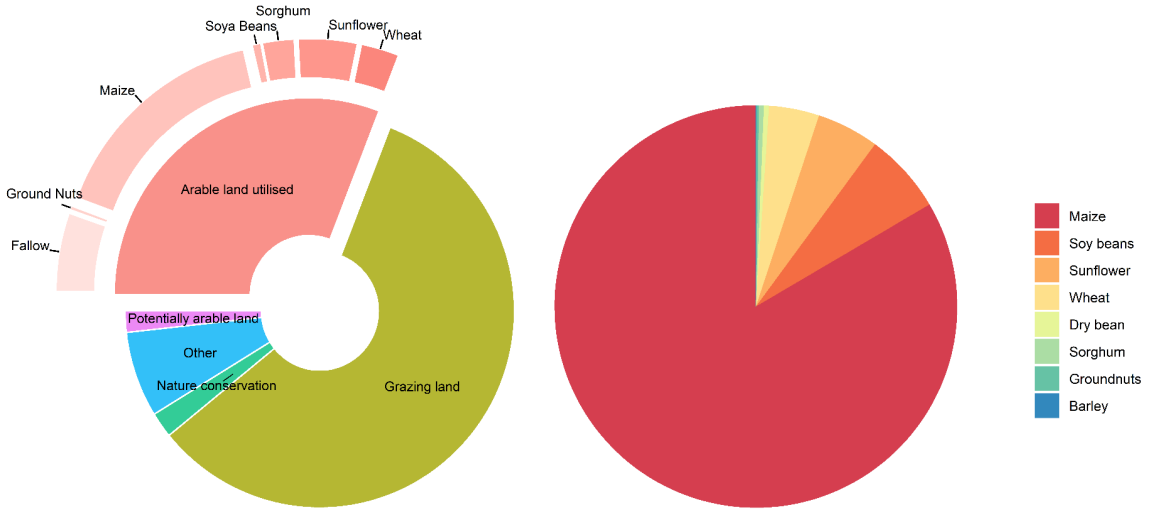

Figure 1-11. The land use distribution in the Free State from 2006 to 2017 relative to the total size (ha) (left). The data comes from the DAFF (2018).

Maize is the preferred crop for most farmers considering its high financial yield. However, farmers in the region of Bultfontein have stated that maize should be planted before the end of December to limit the risk of a failed harvest due to frost damage. This would only be possible, however, if sufficient rainfall has fallen, which again emphasizes the importance of the onset of the rainy season, as raised by Moeletsi (2010). The optimum planting window is later for sunflowers (personal communication). Winter wheat is the only crop that can be planted in winter due to its frost resistance (Tait and Zheng, 2003). However, the profit of wheat is low due to international competition and decreasing demand (Moeletsi, 2010). Lastly, on average 17% of the agricultural area consists of fallow land (Figure 1-11). This can be the result of a late onset of the rainy season, causing

farmers to miss the planting window. However, a fallow field can also be a purposeful decision to store more water in the soil for the planting season next year (Bennie and Hensley, 2001).

1.4.6 Climate sensitivity of Free State agriculture

Homes et al. (2012) identified the start of the mobilization of sediment in the Free State to be around the year 1880. However, as described by Eckardt et al. (2020), dust storms have been observed as early as 1861 (Widdicombe, 1891), which matches the beginning of commercial agriculture in this region. At the moment, almost all the arable land is utilised, with only 1.7% of the land area has been identified as uncultivated but potentially arable. This would indicate that the erodible area will not increase strongly and that any future changes in dust emission will likely be triggered by changes in agricultural practices or climate change.

The emission of dust at the global scale is expected to be influenced by climate change. To determine whether this would also be the case for croplands in the Free State, the specifics of the climate change in this region and its possible effect on agriculture need to be considered. For the whole of South Africa the maximum and minimum temperatures are expected to increase and decrease, respectively, combined with a general increase in temperature (DEA, 2013). Generally, an increase in rainfall is expected during the rainy season in spring and summer, and a decrease in autumn (DEA, 2013). The yearly change in rainfall is uncertain and depends on the climate scenario. In recent years, a delay in the start of the rainy season has been observed, but it cannot be confirmed whether this is statistically significant (AgMIP). Lastly, the wind erosivity in Southern Africa is expected to increase (Thomas et al., 2005). A link between the dust emission in the Free State and the remobilisation of Kalahari sand dunes due to climate change (Thomas et al., 2005) has also been reported by Baker and Holmes (2006).

Rainfall is the most important parameter controlling the crop yield in the Free State (Hensley et al. 2006; Moeletsi 2010), and both the onset and quantity are of importance. However, due to uncertainties in the climate models, it is not possible to make certain statements on the influence of climate change on crop growth. The expected increase in rainfall in the summer season would be advantageous for maize growth. However, this would require no delay on the onset of the rainy season, since a delayed rainy season would increase the number of fallow fields or the risk of frost damage. A decrease in rainfall is mainly expected in the autumn and winter, which would be strongly disadvantageous for the growth of winter wheat since it relies on rainfall during this season and the remaining moisture in the soil after the rainy season has ended (personal communication). Considering the importance of this crop for cover and protection against erosion during the dust season, a decrease in winter wheat could enhance the emission of dust.

An increase in temperature could have positive effects on crop yields since frost has been identified as one of the main risks for crop production in the Free State (Moeletsi 2010). However, the contrasting decrease in minimum temperatures might counterbalance the increase in temperature, or even exacerbate the effect of the frost damage. At the moment, temperature has not been raised

as a problematic phenomenon for crop yields. The development of heat-resistant crops has been suggested by Agricultural Model Intercomparison and Improvement Project (AgMIP), to prevent damage from high maximum temperatures. In conclusion, there are many insecurities regarding the influence of climate change on agricultural activities in the Free State, but the high-risk scenarios for farmers will likely increase. This could lead to more fallow fields or fields with low vegetation cover, which could, in combination with the excepted increase in wind velocities, increase dust emissions.

1.5 Knowledge gap

Free State has been identified as the most emissive region in South Africa (Eckardt et al., 2020). This emission can be linked to large-scale agriculture that is practised on the sandy and loamy soils in this region. Due to these agricultural practices, fields are left with little plant cover between harvest and the start of the next rainy season, which leaves soil vulnerable to wind erosion. Harvest takes place anytime between May and August, and the planting season between November and January, depending on the crop type and the weather conditions. This time frame corresponds with the dust period from August to December described by Eckardt et al. (2020). Despite the yearly patterns of the dust events, the count of events appears to vary greatly (Figure 1-12) with the lowest number being recorded in 2009 when no events were detected, and more than 40 events recorded in 2016. Dust events cannot solely be explained by variations in wind velocity (Figure 1-12), which begs the question which surface characteristics play a role in the emission of dust, and to what extent dust emissions could be reduced?

Eckardt et al. (2020) already pointed out the increase in fallow fields during the dusty year of 2015/2016. As discussed in Chapter 1.3, a low cover of vegetation has often been seen as the dominant amplifier in dust emission and is also given as a reason for the specific dust season in the Free State. When a significant cover from stubble or vegetation is missing, the remaining factors that could play a role in the emission of dust from the soil surface are soil texture, moisture content, surface roughness, and the presence of a soil crust, as discussed in Chapter 1.2.

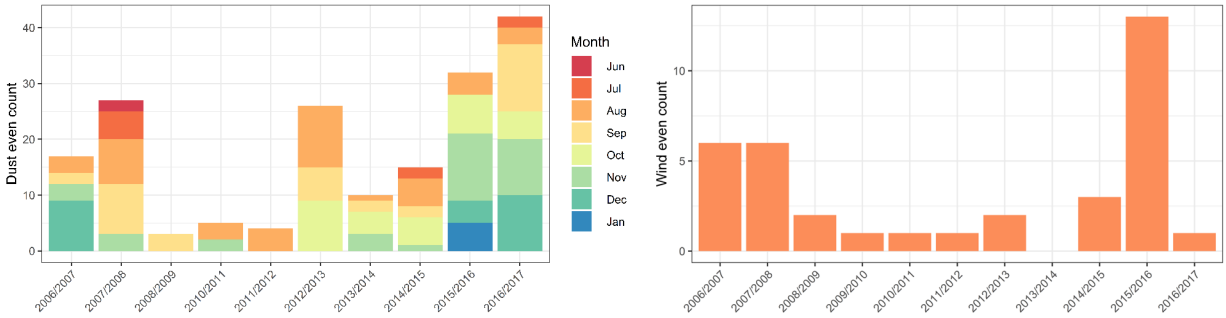

Figure 1-12. The monthly wind events count per year (left) and the wind event count (right) from 2006 to 2016. A wind event is defined as an event where the wind velocity exceeds 10 m s^{-1}. The dust event data comes from Eckardt et al. (2020) and the wind data comes from the weather station of ARC near Bultfontein.

The difference in soil type throughout the Free State is expected to result in different soil textures (Hensley et al., 2006), but Eckardt et al. (2020) described all emissive surfaces to consist of mainly fine sand and coarse silt. Wiggs and Holmes (2011) described the influence of moisture to be a minor control in limiting dust emission, partially because months with higher rainfall are accompanied by higher wind velocities. Furthermore, due to the low rainfall and quick evaporation, the moisture content of the soil surface is expected to only be relevant for short periods. However, since moisture could still strongly decrease soil erodibility during these short periods after rain events, it is still a significant factor for short periods. The influence of soil roughness from a bare, disturbed surface has been described by Wiggs and Holmes (2011). They demonstrated a linear relationship between the aerodynamic roughness, a value that was influenced by the tillage ridges and clods, with the threshold velocity, and the influence these factors have on the collection of dust. However, this study lacks a comparison with different field conditions.

In contrast to the moisture, roughness, soil texture, and soil cover from vegetation or crop residue, the presence of soil crusts on sandy soils and its relationship to dust emission has received little attention. Soil crusts on Free State croplands are expected to be exclusively physical since biological crusts develop over many years when a soil is not disturbed (Belnap, 2001). As described in Chapter 1.3.1, the influence of soil crusts has been described in experimental and natural settings, but their influence on agricultural fields has received little attention (Nerger et al., 2017). Another question that remains is whether soil crusts are relevant on such sandy soils, since clay, silt, and total organic carbon (TOC) contents are considered to be the main soil characteristic that drive the formation of crusts (Zobeck, 1991b). This also indicates that the influence and variation of soil type, texture, and chemistry are indirectly also relevant for dust emissions from surface crusts. For this thesis, the focus will be on the influence of crusts on the emission from the Free State cropland soils. Hereby, the interaction with crusts and the aforementioned factors, texture, moisture, chemistry, and soil cover will be taken into account.

The knowledge of the role of crusts on dust emission, and its interaction with other surface characteristics, is not only relevant in the framework of the Free State. As shown in Figure 1-1, regions with intensive land use are a significant dust source, with both on and off-site effects. Especially agricultural lands with sandy soils in semi-arid to arid regions are sensitive to wind erosion. Regions with conditions comparable to the Free State are, for example, Sahelian Africa (Sterk, 2003; Visser and Sterk, 2007), Northern China and Mongolia (Li et al., 2014; Liu et al., 2006; Xi and Sokolik, 2015; Zhou et al., 2015), Australia (McTainsh et al., 1990), Spain (López et al., 1998), India (Santra et al., 2017), the United States and Mexico (Hagen, 1991; Rivera Rivera et al., 2010; Sharratt and Collins, 2018), and Argentina (Buschiazzo et al., 1999). This makes the Free State a good analogue to study the emission from dry, sandy, croplands.

1.6 Research question, aims, and thesis structure

The main research question of this thesis is: *"What role do crusts play in the emission from Free State croplands?"*. To address this question, a combination of experimental and field studies has been performed. The dust emission potential was measured with the PI-SWERL since it is a light and easily portable instrument. This required a cross-comparison between the PI-SWERL and a traditional straight-line wind tunnel. Furthermore, pathogens and allergens in the dust needed to be assessed to determine the possible offsite risks for human health. To address these points and the main research question, the following aims were posed:

1. Create a cross-comparison between the PI-SWERL and a traditional wind tunnel;
2. Determine how soil crusts develop under rainfall;
3. Determine the difference in emissivity between crusts and loose surfaces and determine the surface characteristics that influence the emissivity of these surfaces;
4. Describe the main pathogens and allergens that are present in the suspended dust and the fractionation that these microbial organisms show compared to the emitting soil;
5. Determine under which conditions the soil cover is low enough for crusts to become a significant factor in dust emission.

These aims are addressed in Chapters 2 to 6. Chapter 2 focuses on the first aim: the cross-comparison between the PI-SWERL and a portable straight-line wind tunnel. Since the PI-SWERL is the main instrument for the measurement of dust emissions, this instrument requires verification and comparison with the more commonly used straight-line wind tunnel. The focus is on the threshold friction velocity of dust, which could be influenced by both deflation and saltation. This study has been published in 2021 in Aeolian Research, under the title *"A cross-comparison of threshold friction velocities for PM_{10} emissions between a traditional portable straight-line wind tunnel and PI-SWERL".*

Chapter 3 investigates the formation and emissivity of soil crusts in an experimental setting. This addresses the second aim and partially the third aim of this thesis. Rainfall simulations on Free State cropland soil provide insight into the formation of physical soil crusts and the increase of cohesion with rainfall. Hereby the simulated rainfall represents natural rainfall conditions in the Free State. Secondly, the emissions of crusts are compared with the emission from loose surfaces using the PI-SWERL. Hereby the possible influence of saltators is also taken into account since this has often been raised as an important factor in increasing the emission from crusts. This study has been published in 2020 in the journal, Land, under the title *"Physical Crust Formation on Sandy Soils and Their Potential to Reduce Dust Emissions from Croplands".*

The fourth chapter presents field measurements on emissions from loose and crusted surfaces and contributes to achieving the third aim. Furthermore, soil surfaces were characterised by their shear strength, texture, chemistry, moisture content, and the amount of saltating grains during the experiment. This gives insight into what other surface characteristics, besides the surface type, could

influence dust emissions from croplands. Besides the comparison between these crust and loose surfaces, these dust emission measurements enable a comparison to be drawn between experimental and field measurements. This study has been published in Aeolian Research in 2021, under the title *"Assessing the emission potential of sandy, dryland soils in South Africa using the PI-SWERL".*

Chapter 5 presents results from a microbial study using the PI-SWERL on the Free State croplands and addresses the fourth aim of this thesis. Considering the potential of the Free State dust to reach the densely populated Gauteng province, the negative health impact of this dust is of high relevance. The measurements focus on allergens and pathogens in the dust, which are suspected to be more significant in dust from agricultural areas than that from natural sources. It furthermore offers a comparison between the PI-SWERL and passive dust samplers for microbial research, which has relevance for future, high spatial resolution microbial dust research. This study has been published in Microbial Ecology in 2021 under the title *"Gone with the Wind: Microbial Communities Associated with Dust from Emissive Farmlands*".

The sixth chapter focuses on the fifth aim by presenting field monitoring measurements on four fields under different scenarios of crust and soil cover. Since the quantity of soil cover can differ greatly between fields during the dust season, partially by purposeful management and partially by weather conditions, it is important to understand the influence that soil cover has on the emission from a field. This study presents the sediment flux and saltation threshold of these fields, in combination with UAV analyses to quantify soil cover. This gives insight into the soil cover conditions which protect soil against wind erosion, and under which conditions crusts can play a significant role in preventing dust emission. This study has been published in Agronomy in 2022 under the title *"Influence of Crop and Land Management on Wind Erosion from Sandy Soils in Dryland Agriculture"*

In the last chapter, the results of the previous chapters will be summarised and discussed, together with the implications that these results could have for dryland crop farming, and the points that should be addressed by future research.

1.7 Study framework

This thesis is part of a Swiss National Science Foundation (SNSF) and National Research Foundation (NRF) funded joint research project (grant number 170942) with the title "*South African croplands dust emission risks: Physical thresholds, environmental and socio-economic impacts*". This research project is a collaboration between the University of Basel, the University of Cape Town, the Agricultural Research Council, and the University of Pretoria. The following two aims have been set for this project:

1. *"Improving the understanding of the environmental boundary conditions for dust emissions on South African cropland."*
2. *"Producing knowledge on land management best practices and sediment quality to mitigate the impact of dust emission on ecosystem services, climate and public health."*

To address these aims, five work packages were developed that have the following objectives:

1. "*To identify the spatial and temporal pattern of dust emissions from agricultural land in South Africa*
2. *To determine the environmental boundary conditions for dust emission on South African cropland identified as dust sources in work package 1*
3. *To identify the impact of land management practices on dust emission and ecosystem services losses*
4. *To identify microbiomics air contamination due to dust*
5. *To synthesize the above information and produce holistic knowledge on dispersal, impact of dust and thresholds to inform policy in farming systems"*

This thesis is part of the second and fourth work packages.

2.

A cross-comparison of threshold friction velocities for PM_{10} emissions between a traditional portable straight-line wind tunnel and PI-SWERL

Cynthia C.E. van Leeuwen*, Wolfgang Fister**, Heleen C. Vos**, Erik L.H. Cammeraat* & Nikolaus J. Kuhn**

*Institute for Biodiversity and Ecosystem Dynamics, Ecosystem and Landscape Dynamics Group, University of Amsterdam, Amsterdam, the Netherlands

**Physical Geography and Environmental Change, University of Basel, Basel, Switzerland

Published in Aeolian Research, 2021, Volume 49, 100661

doi.org/10.1016/j.aeolia.2020.100661

2.1 Abstract

Experiments in large wind tunnels have made vital contributions to our knowledge of aeolian processes. However, the size of these instruments makes them impractical for field application. To facilitate field measurements on the dust emission potential of soils, the Portable In-Situ Wind Erosion Lab (PI-SWERL) was developed. Previous research shows that the PI-SWERL can be used to quantify dust emission potentials and (threshold) friction velocities. Studies that compare the PI-SWERL to traditional wind tunnels mainly focus on the dust emission potential at various friction velocities. In the present study, we quantified the threshold friction velocity for PM_{10} emission using a PI-SWERL and compare it to results obtained with a straight-line wind tunnel: the Portable Wind and Rainfall Simulator of the University of Basel (PWRS). Tests were performed on two types of substrate: fine sand (NS1) and loamy sand (DS1). For NS1, a threshold friction velocity of 0.33 m s^{-1} was identified from both the PI-SWERL and the PWRS data. For DS1, identified threshold friction velocities showed differences: 0.25 m s^{-1} by the PI-SWERL and 0.39 m s^{-1} by the PWRS. The position of the DustTrak II monitor's inlet tube and variations of the fan's speed by different operators could explain the difference in identified thresholds. Although different threshold friction velocities were obtained for one of the substrates, we believe that comparable results can be achieved by adjusting the experimental design in future research. Therefore, the PI-SWERL can be successfully used to quantify thresholds, facilitating dust emission studies in more remote regions.

Keywords: Dust emission potential; threshold friction velocity; vertical PM_{10} flux; wind tunnel experiment; PI-SWERL

2.2 Introduction

Wind erosion occurs in a large variety of (semi-)arid areas around the globe, and is initiated when the wind exceeds the critical velocity for particle entrainment. This threshold friction velocity is influenced by multiple factors, such as vegetation cover, the presence of soil aggregates, and soil moisture (Fécan et al., 1999; Shao and Lu, 2000). Saltation fluxes and dust emission quantities in a specific region are dependent on the threshold friction velocity (Kok et al., 2014). Estimates of threshold values from various soil surfaces are required as input data in most dust emission models. To limit uncertainties in threshold friction velocity data, large quantities of local data are required (Li and Zhang, 2011). Generally, most of these data are collected using large field wind tunnels.

Much of our understanding of aeolian processes, and the susceptibility of a soil to wind erosion, comes from the outcomes of wind tunnel experiments (Van Pelt and Zobeck, 2013). Traditionally, friction velocities and dust emissions have been quantified in experiments with different types of wind tunnels (e.g., Bagnold, 1941; Gillette, 1988; Roney and White, 2006; Shao et al., 1993). A distinction can be made between small wind tunnels with lengths up to 3.5 m, and large wind tunnels that are above 4 m long (Raupach and Leys, 1990). Large wind tunnels are often preferred for studying aeolian processes, as their properties enable simulation of a more realistic, natural atmospheric boundary layer (White and Mounla, 1991). However, the wind tunnel's size results in

several practical disadvantages. Large wind tunnels are relatively heavy, making them less suitable for application in regions with low accessibility and thus limiting their overall benefits. In addition, the instrument's size requires relatively large areas of flat terrain to collect accurate measurements (Sweeney et al., 2008). Furthermore, the average construction time in the field is long and multiple people are needed to set up, pack and transport the instrument (Fister and Ries, 2009).

In order to reduce these disadvantages, the Portable In-Situ Wind Erosion Laboratory (PI-SWERL) was developed by the Desert Research Institute in Nevada, USA, to facilitate field measurements on the dust emission potential of soils. The main advantage of the PI-SWERL is its compact size, which requires a short set-up time and makes it easier to transport. In this research, we employed the PI-SWERL model MPS-2b (version November 2018), which is described in detail in the Methods Section.

Sweeney et al. (2008) acknowledge that the PI-SWERL violates most of the guidelines for large-field wind tunnel design, as listed by Raupach and Leys (1990). They mention that the PI-SWERL is not designed to simulate the natural atmospheric boundary layer, as large wind tunnels attempt to do. Instead, the device can provide a measure of soil erodibility, based on the relationship between friction velocity and dust emission. In their study, the PI-SWERL was compared with the straight-line, suction-type, field wind tunnel of the University of Guelph to test its reliability (Sweeney et al., 2008). A close to 1:1 correspondence was found between the dust emissions for most soil surfaces. However, the PI-SWERL systematically measured higher dust emissions for gravel-covered surfaces at all friction velocities. The size and distribution of non-erodible roughness elements, such as gravel, affect the boundary layer flow and thus, the amount of shear stress exerted on the surface. This different behaviour of the shear stress led to an underestimation of the threshold friction velocity for rough surfaces by the original relationship between RPM and friction velocity used for the PI-SWERL (Sweeney et al, 2008). To compensate for this underestimation, a surface roughness correction factor must be used for rough surfaces when calculating friction velocities based on the RPMs (Etyemezian et al., 2014).

Most studies that used the PI-SWERL have been focused on studying the dust emission potential of different soil surfaces at various friction velocities in different regions in the world, e.g., the Namib Desert in Namibia (von Holdt et al., 2017), the Tengger and Mu Us Desert in Northern China (Cui et al., 2019b), coastal dunes in California, USA (Mejia et al., 2019), the Colorado Plateau in the USA (Fick et al., 2020), Yellow Lake Playa, USA (Sweeney et al., 2016), Athabasca Oil Sands Region in Canada (Wang et al., 2015), and the Mongolian steppe (Munkhtsetseg et al., 2016). Others aimed to compare the dust emission potential of the PI-SWERL to a wind tunnel, for similar friction velocities (Kavouras et al., 2009; King et al., 2011; Sweeney et al., 2008). The PI-SWERL was also successfully used to quantify threshold friction velocities for various substrates, for example on volcanic ashes (Etyemezian et al., 2019) and off-road trails (Goossens and Buck, 2009). In the current study, we aimed to determine if thresholds for PM_{10} emission are comparable between both instruments for two substrates. To accomplish this aim, experiments with a similar design were performed with both

the PI-SWERL and a wind tunnel: the Portable Wind and Rainfall Simulator (PWRS) of the University of Basel.

2.3 Materials and methods

2.3.1 Materials

Two types of substrate with varying textures (Figure 2-1) were used to identify the effects of particle size and sorting on the threshold friction velocity of PM_{10} emission. The first substrate (NS1) originated from a silver sand mine in Limburg, The Netherlands, and was mined from a Miocene formation. The D50, or median particle diameter, of this first substrate was 212 µm, and 70% of its particles were categorized as very fine sand (range between 62.5 µm and 125 µm). The second substrate (DS1) is a loamy sand soil, which was collected from Central Jutland, near Foulum, Denmark, with a D50 of 246 µm. Both substrates have a similar D50, but differ substantially in their fraction with particles smaller than 100 µm. Approximately 25% of DS1's mass consists of particles below 100 µm, while NS1 only has 7% of its particles in this fraction.

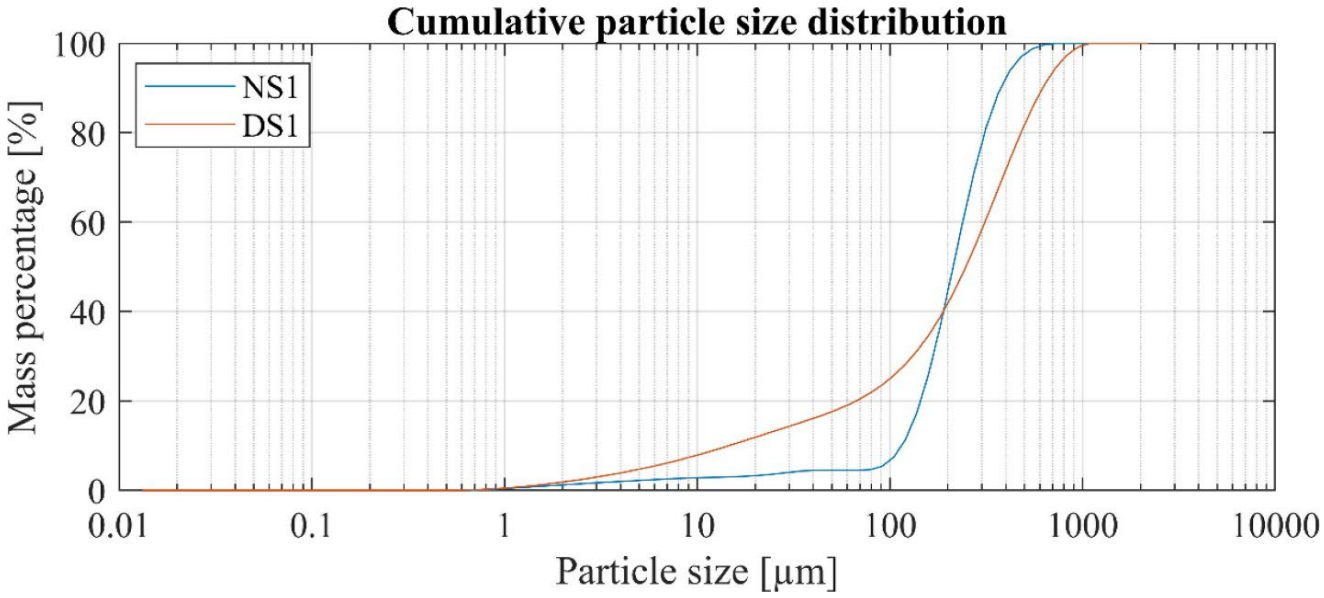

Figure 2-1. The cumulative particle size distribution of NS1 and DS1.

Both substrates were first oven-dried at 40 °C and then sieved through a 2 mm sieve. This sample preparation reduced the effect of various factors, such as the presence of aggregates and high soil moisture that were likely to affect dust entrainment. The particle size distribution of both substrates was analysed with the Mastersizer 2000, a laser diffraction particle size analyser, using wet dispersion.

2.3.2 Methods

2.3.2.1 PI-SWERL

In this research, we employed the PI-SWERL model MPS-2b (version November 2018) (Figure 2-2). This model has a cylindrical chamber with a diameter of 30 cm and a height of 20 cm. The chamber is open at the bottom and can be placed over the soil of interest. A foam seal surrounding the edge of the chamber ensures a direct connection with the soil surface. A computer-controlled 24-volt DC motor is attached to the top of the chamber, which provides power to a flat annular blade (⌀25 cm, 6 cm width). The blade is aligned in parallel to the soil surface while maintaining approximately 5 cm distance. As a result of the rotation of the blade, a velocity gradient is generated between the blade and the soil underneath, creating a shear stress on the soil surface (Sweeney et al., 2008). The magnitude of the shear stress depends on the revolutions per minute (RPM). A large enough shear stress leads to the entrainment of soil particles. During an experiment, the PM_{10} concentration inside the chamber of the PI-SWERL is monitored by a DustTrak II monitor (TSI Incorporated, 2018). A detailed description of the PI-SWERL system, based on a previous model version, is provided by Etyemezian (2018).

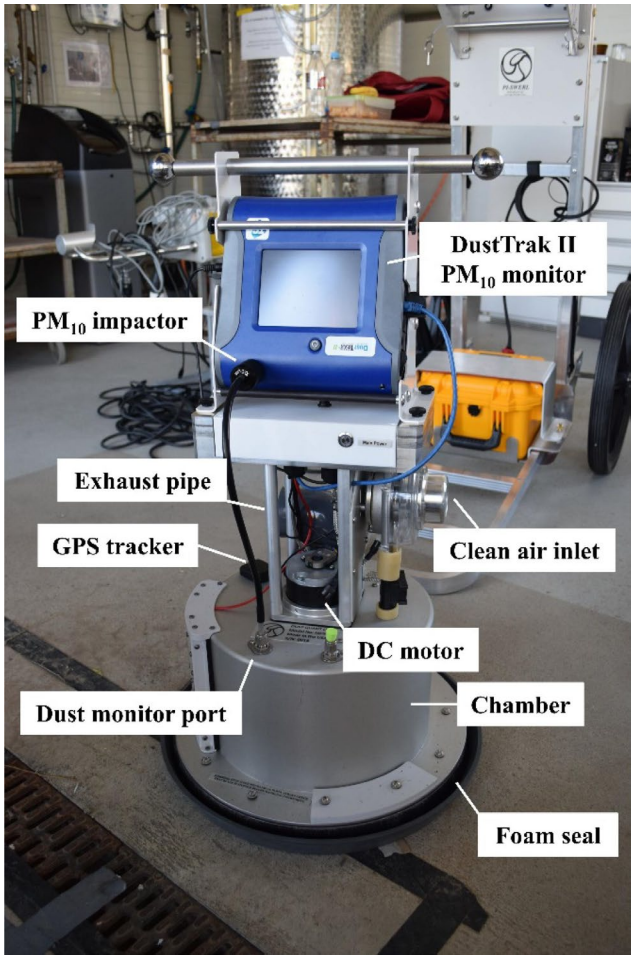

Figure 2-2. PI-SWERL model MPS-2b – Chamber with mounted DustTrak II monitor.

The PI-SWERL was programmed with the SwerlView application, provided by the Desert Research Institute. The same pre-programmed hybrid test was used for all experiments and consisted of the following phases: i) starting phase: a 30-second period of 0 RPM and running ventilation (100 L min-1) to clean the air in the chamber, ii) ramp phase: slow increase of RPM from zero to a target value of 3175 RPM within a time span of 120 s, iii) constant phase: RPM were kept constant for 240 s and iv) ending phase: RPM were reduced to zero within 30 s. The total duration of the experiment was 420 s.

The RPM is converted to a friction velocity, using

$$u_* = C_1 \alpha^4 RPM^{C_2/\alpha} \quad (1)$$

Where u_* is the friction velocity (m s^{-1}), C1 refers to a constant of 0.000683, C2 is a constant of 0.832 and α depends on the surface roughness (Etyemezian, 2018). Values of α are based on four roughness categories, where the lowest surface roughness is linked to category A, a silt–clay crusted playa with minimal cracking and sparse gravel, and the highest surface roughness refers to category D, a gravel covered surface. Furthermore categories B (sandy loam desert soil with <5% gravel cover) and C (a rippled dune surface with <10% gravel cover) are defined (Etyemezian et al., 2014). An α of 0.94, corresponding to roughness category B, was chosen to convert the set target value of 3175 RPM to a friction velocity of 0.67 m s^{-1} (Eq. (1)). This specific friction velocity was chosen for the experiment because previous research by Etyemezian et al. (2007) has shown that the corresponding friction velocity is sufficient to generate dust emission for most soil surfaces.

In addition to running the PI-SWERL program, the SwerlView application was also used to keep track of PM_{10} concentrations and the number of saltating particles during each hybrid test, PM_{10} concentrations in the chamber of the PI-SWERL were measured by a TSI DustTrak II monitor (model 8530) by active sampling with 3 L min-1 at a one-second interval. The optical gate sensors (OGS) peak area provides an indication of larger particles moving in the chamber. In the present set-up with high amounts of loose sand, the OGS sensors seemed to detect relatively unreliable numbers, due to the sheer number of particles. Therefore, they were not used in this research.

The hybrid test was repeated 10 times per test substrate (NS1 and DS1). A circular tray (⌀ 40.5 cm) was filled with 5 L of substrate before every test and an aluminium bar was used to flatten the surface. Left-over material from completed tests was recycled and mixed with new substrate before the start of each consecutive test run to guarantee a homogenous sample. During the experiment, the test surface was expected to become dust depleted, as dust was removed from the chamber via the exhaust pipe. To test this assumption, a surface sample was collected at the end of each test run. Additionally, to gain insight into the particle size distribution of the total emission, a Dyson V7 Trigger handheld vacuum cleaner was attached to the PI-SWERL (Figure 2-3a). A custom-made connector piece connected the Dyson with the exhaust pipe (Figure 2-3b). At both sides of the connector piece, two 2 cm holes were drilled to ensure an undisturbed air flow. The particles collected by the Dyson were sampled after every other test run and a corresponding sample was taken from the test surface.

The particle size distributions of the surface and Dyson samples were analysed with the Mastersizer 2000, using wet dispersion. Subsequently, these results were compared to the original particle size distribution of the substrates (Figure 2-1) to determine the degree of mobilization of PM10-sized dust and larger particles during each test run.

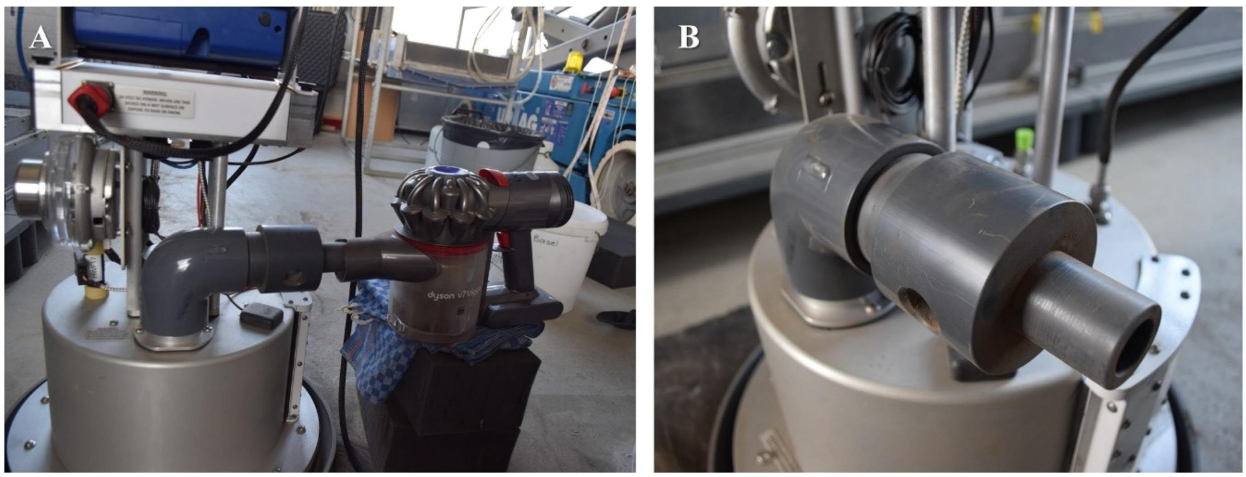

Figure 2-3. Modification to the PI-SWERL to collect emitted particles during the hybrid test. (a) Dyson V7 Trigger Handheld vacuum cleaner attached to the exhaust pipe, and (b) the custom-made connector piece.

To prevent cross-contamination between experiments, the chamber of the PI-SWERL had to be kept clean. Therefore, the inside of the chamber was cleaned with a brush after each test run. In addition, a cleaning cycle was performed after five consecutive test runs and before changing the test substrate. The cleaning cycle was a ramp test on a clean test surface (i.e., empty sample tray) at 5000 RPMs that lasted for 300 s. This procedure ensured that any dust that was left behind after simple cleaning with a brush was removed from the PI-SWERL's chamber. In addition, the impactor plate of the DustTrak II monitor was cleaned regularly to ensure accurate measurements.

2.3.2.2 Portable straight-line wind tunnel

For the cross-comparison with the PI-SWERL, the Portable Wind and Rainfall Simulator (PWRS) of the University of Basel was used (Figure 2-4). This straight-line wind tunnel is based on the device from Trier University (Fister et al., 2012, 2011). The Basel PWRS consists of five components that together have a length of 11 m: the fan, the transition section, the converter section, the honeycomb air-straightener and the test section. Airflow, or wind, is generated by a push-type fan, which is driven by a 3.7 kW electro-mechanical system. The velocity of the fan can be set between 2 and 12 m s^{-1}. The honeycomb consists of 448 PVC tubes, each 25 cm long and 4 cm in diameter and the adjacent test section that is 4 m long and has a 0.8 by 0.8 m cross-section.

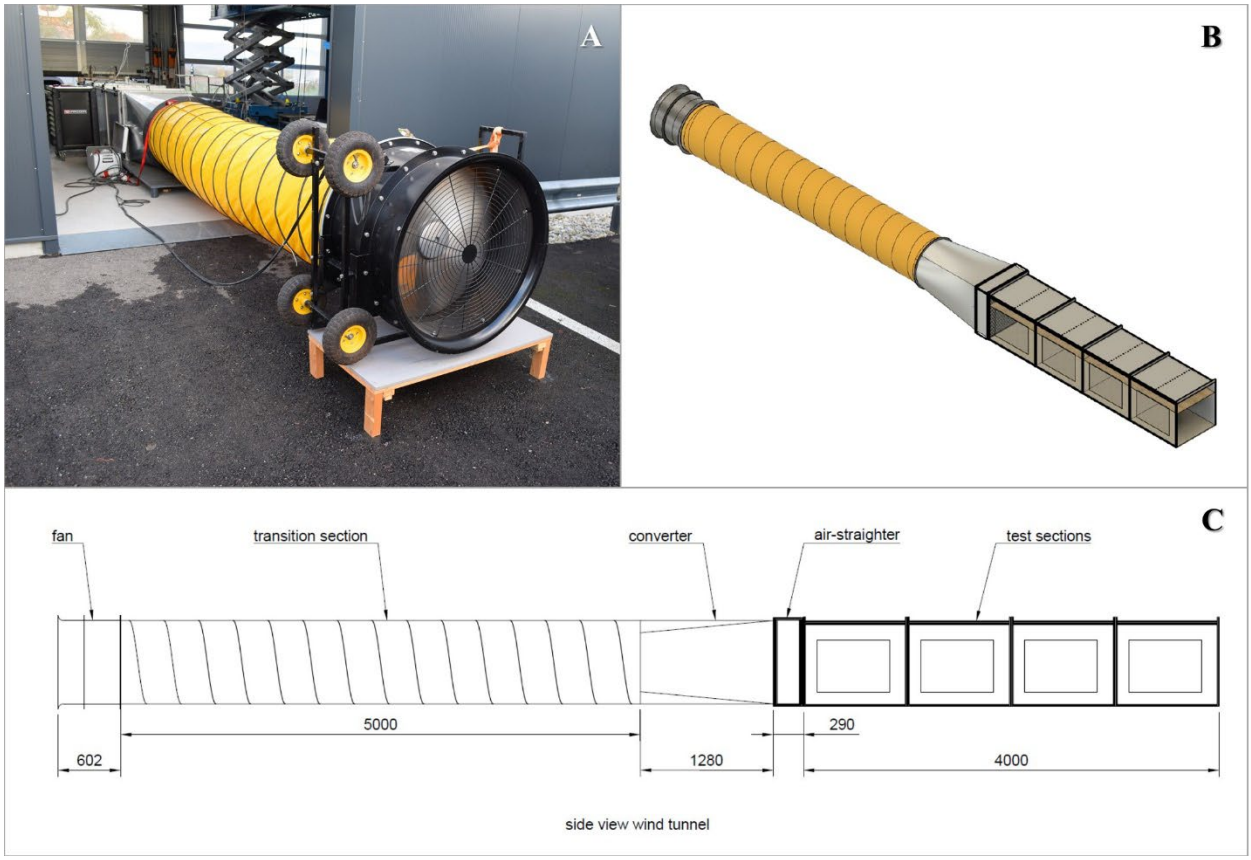

Figure 2-4. The Portable Wind and Rainfall Simulator of the University of Basel stationed in the experimental rainfall laboratory at Witterswil. a) The push-type fan, b) a technical 3D drawing of the wind tunnel from (top view) and c) a schematic 2D overview (side view). Dimensions are shown in millimetres (Figure 2-4b and c from Fabbri, 2018).

The test section has four detachable sections. The roof of the test section was lowered by wooden plates along its full length to reduce the tunnel height to 60 cm and thus increase wind velocities near the ground. The floor of the test section is covered with a 2 mm thick bitumen layer, which has a sanded top. At a 3.5 m distance from the start of the test section, a square tray (35 × 35 cm) with the substrate of interest was placed. The application of Irwin spires and roughness elements in the first metre of the test section creates an artificial boundary layer with a thickness of 26 cm.

During the experiment, no abraders or saltators were added to the set-up, meaning that for both substrates particle entrainment was initiated solely by the fluid force, i.e., the wind. To measure PM_{10} emissions from the test surfaces, a DustTrak II monitor was positioned at the end of the test section. This is the same instrument that was used to quantify PM_{10} concentrations during the PI-SWERL experiments. The inlet tube of the instrument was installed at 9 cm above the tunnel floor. Furthermore, sediment traps were installed over a height gradient at the end of the test section to provide information about the vertical distribution of emitted particles. Seven Modified Wilson and Cook (MWAC; Wilson and Cooke, 1980) samplers were positioned with their inlets at respectively 0.5, 3, 9, 15, 22, 27 and 32.5 cm above the tunnel floor.

In the test section of the PWRS, a vane anemometer probe and a hot wire probe were installed at 40 cm height at the end of the tunnel's test section. They were used as reference measurements for the wind speed, humidity, and air-temperature, respectively. The observed wind velocities by the vane anemometer probe can be transformed into friction velocities, using the logarithmic law of Prandtl-Karman

$$u_* = \frac{u * K}{\ln(\frac{z}{z_0})} \quad (2)$$

Where u is the velocity at height z, u_* is the friction velocity (m s^{-1}), κ is the dimensionless von-Kármán constant with a universal value of 0.40, z is the height (m) above the surface, and z_0 is the surface aerodynamic roughness length in metres (Prandtl, 1935). The PWRS has a surface roughness length of 50 μm (Fabbri, 2018). Measurements from the vane anemometer and the hotwire probe were collected with a hand-held Testo 480 digital temperature, humidity and air flow meter (Testo SE & Co. KGaA, n.d.).

The performed wind tunnel test was designed to mimic the pattern of the hybrid test of the PI-SWERL. The speed of the fan was increased over the course of 120 s, with 1 V per 4 s, creating a ramp towards its maximum of 50 V. This top speed, translating to 15 m s^{-1}, was maintained for 60 s before switching off the system. The rather short duration of 60 s was chosen, because otherwise, the depletion of the material in the sand tray would have been too big, causing further problems, such as scouring or sheltering of the surface by the rim of the tray. The test was repeated 10 times per substrate (NS1 and DS1). Before each test run, the square sample tray was refilled and the material was flattened with an aluminium bar to ensure low surface roughness. After every other test, surface samples were taken from the remaining substrate in the sample tray to verify if dust depletion occurred. The particle size distribution of the samples was analysed with the Mastersizer 2000 using wet dispersion. Unfortunately, due to human error, post-test surface samples were only collected for NS1. Therefore, no particle size distribution analysis was performed on DS1 post-test surface samples. Furthermore, the contents of the seven MWAC samplers were weighed.

2.3.2.3 Cross-comparison between instruments

To detect the start of PM_{10} emission, and thus the respective threshold friction velocity for the substrate, increasing trends were identified from the PI-SWERL and PWRS datasets. For the PI-SWERL, all replicates showed relatively large variance at the start of the experiment, which made a precise determination of the threshold friction velocity difficult. Therefore, as soon as ten data points (1 Hz interval) with an increasing trend could be identified in the measurements, the start of PM_{10} emission was defined, of which the first data point was marked as the threshold friction velocity. To quantify the threshold friction velocity in the PWRS data, the same method was applied. The reference wind velocities and the observed PM_{10} concentrations were plotted against time. Based on these data, an increasing trend in PM_{10} emissions was observed of which the first data point indicated the threshold friction velocity. To compare identified thresholds between the two experiments, a one-

way analysis of variance (ANOVA) was performed to determine if the group mean of the PI-SWERL threshold friction velocities for each substrate differed from those derived from the PWRS experiments. The analysis was done using MATLAB R2018b software.

Furthermore, the PM_{10} emission for both substrates was quantified. For the PI-SWERL experiments, the vertical dust flux (EF) was determined using Equation (3) (Etyemezian, 2018).

$$EF(t) = \frac{C_{dust} * FR * 0.0000167}{A_{eff}} \quad (3)$$

Here, C_{dust} (mg m^{-3}) is the average PM_{10} concentration in the PI-SWERL's chamber, FR (L min^{-1}) is the flow rate through the chamber and A_{eff} refers to the effective area of the instrument, which was estimated to be 0.035 m^2 for this model (Etyemezian et al., 2014). Unfortunately, it was impossible to measure dust emissions over a vertical profile and calculate the vertical PM_{10} fluxes for the PWRS, because only a single DustTrak II monitor was installed in the wind tunnel. Alternatively, the cumulative PM_{10} concentration (mg m^{-3}) was determined. Although not comparable to the vertical dust flux of the PI-SWERL measurements, the average PM_{10} concentration in the PWRS does show which substrate emitted more dust. These trends were expected to be similar to those in the PI-SWERL data.

2.4 Results

2.4.1 Threshold friction velocities

For both NS1 and DS1, the PI-SWERL data show a clear start of PM_{10} emission. The PM_{10} concentration of all replicate measurements followed a similar pattern with increasing RPM (Figure 2-5). The threshold friction velocity of NS1 was identified at 0.33 m s^{-1}, on average. DS1 emitted PM_{10} at a lower threshold friction velocity of 0.25 m s^{-1}. As illustrated by Figure 2-5, the PWRS data did not show a rapid increase in PM_{10} emissions, as was observed during the PI-SWERL experiments. Instead, PM_{10} emissions increased slower and with more fluctuations. Therefore, it was not possible to identify ten subsequent increasing points in the data, as planned in the original methodology. For NS1, only seven subsequent points could be identified that marked the start of PM_{10} emission. For DS1, the number of subsequent increasing points was even limited to three or four. For the PWRS measurements, PM_{10} was emitted from NS1 after exceeding a friction velocity of 0.33 m s^{-1}. This threshold friction velocity is the same as the threshold observed from the PI-SWERL experiment. In contrast, the PWRS did not yield comparable results for DS1. Here, a threshold friction velocity of 0.39 m s^{-1} was observed, which is higher compared to the 0.25 m s^{-1} from the PI-SWERL measurements. The PI-SWERL and the PWRS results both showed some degree of variation in the threshold friction velocity between replicates. However, the standard deviation of the PWRS data was larger (σ_{NS1} = 0.03 and σ_{DS1} = 0.04) than the standard deviation of the PI-SWERL data (σ_{NS1} = 0.01 and σ_{DS1} = 0.01).

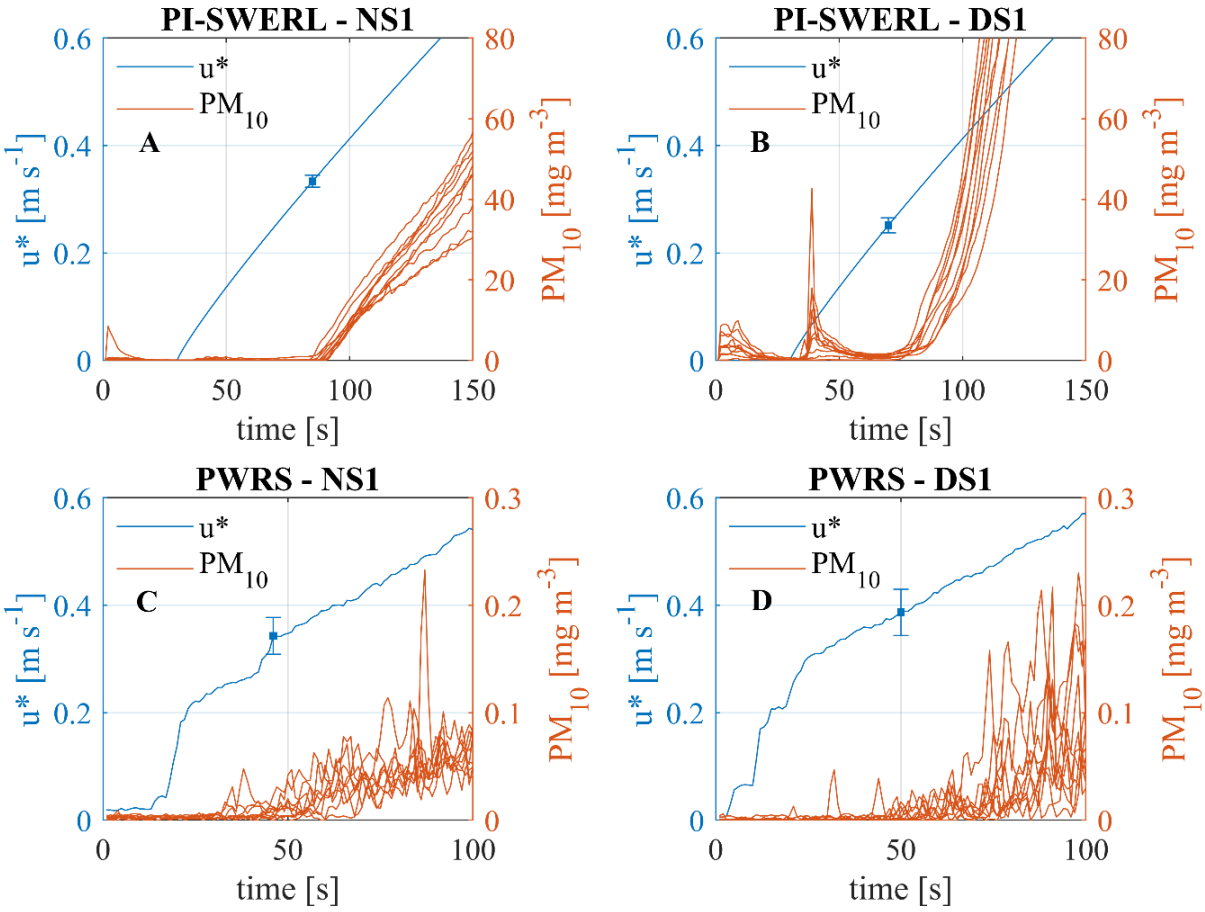

Figure 2-5. Identified threshold friction velocities for the PI-SWERL (5a, 5b) and PWRS (5c, 5d). The average critical friction velocity for PM_{10} emission is marked by the blue square. (For interpretation of the references to colour in this figure legend, the reader is referred to the web version of this article).

These findings suggest that the PI-SWERL and the PWRS yield similar results for NS1. The average threshold friction velocity of NS1 from the PI-SWERL was 0.9% higher than the threshold measured by the PWRS. In contrast, average threshold friction velocities for DS1 that were measured by the PI-SWERL were 34.7% higher than those derived from PWRS tests. Because the ANOVA returned a p-value of 0.716 for NS1, the null hypothesis could not be rejected. In other words, this finding suggests that the threshold friction velocities for NS1 are comparable. The group means of DS1, on the other hand, did differ significantly with a p-value of 1.5×10^{-8}.

2.4.2 Dust emission fluxes

NS1 and DS1 emitted highly variable PM_{10} concentrations for both instruments (Figure 2-6). Emission patterns differ between the instruments. Dust emission during the PI-SWERL experiments is marked by a sharp increase in PM_{10} concentrations, while PM_{10} values during PWRS experiments increase more gradually. Variability in PM_{10} emissions was much higher during the PI-SWERL experiments, compared to the PWRS data. Despite the large variance for both instruments, the pattern of PM_{10} emission behaved similarly between replicates of both NS1 and DS1. An average

PM_{10} emission flux of 2.86 mg m^{-2} s^{-1} was observed for NS1, which was about two times less than the emission flux of DS1 (6.91 mg m^{-2} s^{-1}). The standard deviations of the observed emission fluxes were 0.53 mg m^{-2} s^{-1} for NS1 and 0.88 mg m^{-2} s^{-1} for DS1. Unfortunately, the set-up of the DustTrak II monitor in the wind tunnel did not allow for the calculation of the PM_{10} emission flux. Alternatively, we determined the cumulative PM_{10} concentration during a wind tunnel test. Calculations show that an average of 10.12 mg m^{-3} was measured by the DustTrak II monitor for NS1, while DS1 emitted 10.91 mg m^{-3} on average. The total PM_{10} emission data had a standard deviation of 3.08 mg m^{-3} NS1 and 3.81 mg m^{-3} for DS1.

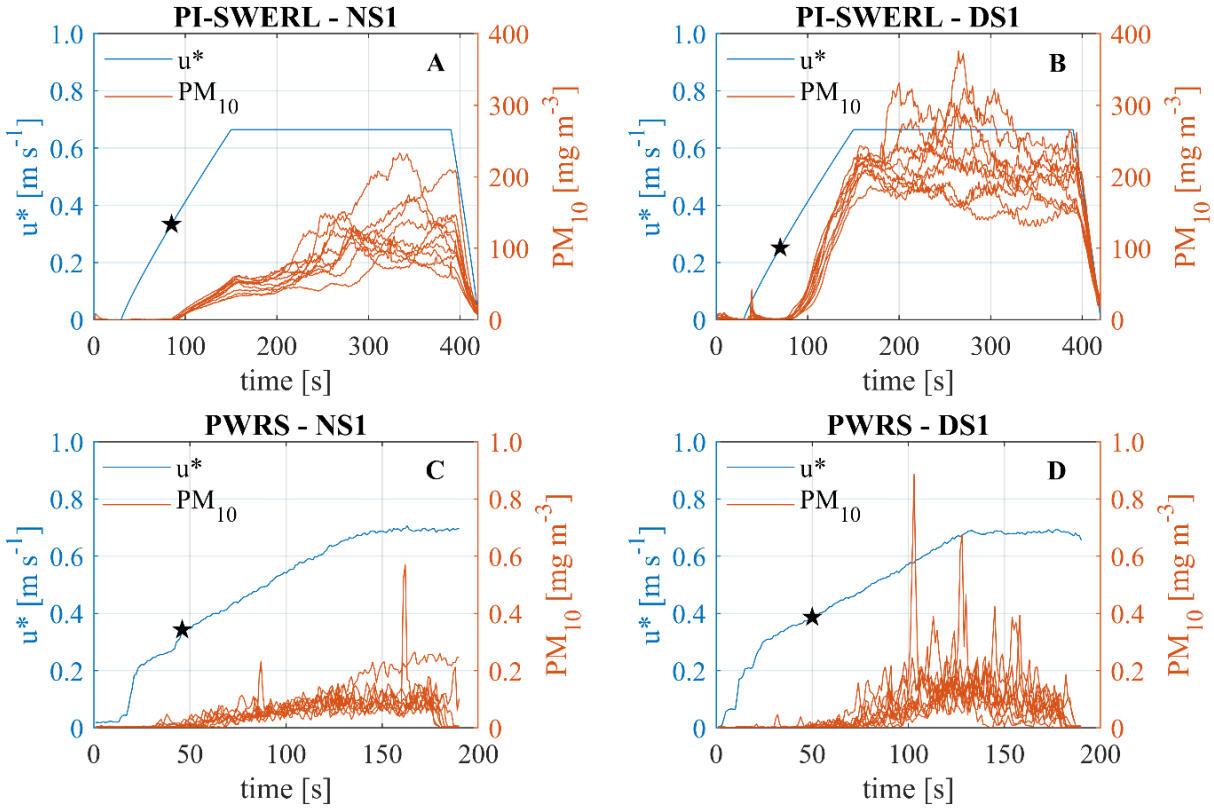

Figure 2-6. PM_{10} concentrations and corresponding friction velocities (u_*), measured by the PI-SWERL (6a, 6b) and the PWRS (6c, 6d). Star represents the identified threshold friction velocity. Note that the scale of the PM_{10} axis is different for the PI-SWERL and PWRS runs.

During the PWRS experiment, passive samplers 1 to 4 showed that more material was captured for NS1 than for DS1 (Table 2-1; Figure 2-7). MWAC 1 to 4 collected in sum 10.35 and 3.31 g for NS1 and DS1, respectively. For both test substrates, most material was trapped by MWACs 1 and 2. On average, 6.35 g in MWAC 1 and 3.85 g in MWAC 2 were trapped for NS1, while weights of DS1 were significantly lower with only 1.98 g in MWAC 1 and 1.19 g MWAC 2. MWACs 5, 6 and 7 did not collect any (measurable) material during the wind tunnel experiments, because they were located above the artificial boundary layer.

Table 2-1. Mass trapped by the MWAC passive samplers.

		Mass trapped			
MWAC nr.	**Height (cm)**	**NS1 – mean (g)**	**NS1 – std (g)**	**DS1 – mean (g)**	**DS1 – std (g)**
1	0.5	6.35	0.72	1.98	0.43
2	3	3.85	0.50	1.19	0.24
3	9	0.13	0.05	0.13	0.04
4	15	0.02	0.02	0.01	0.01
Total mass trapped (g)		10.35		3.31	

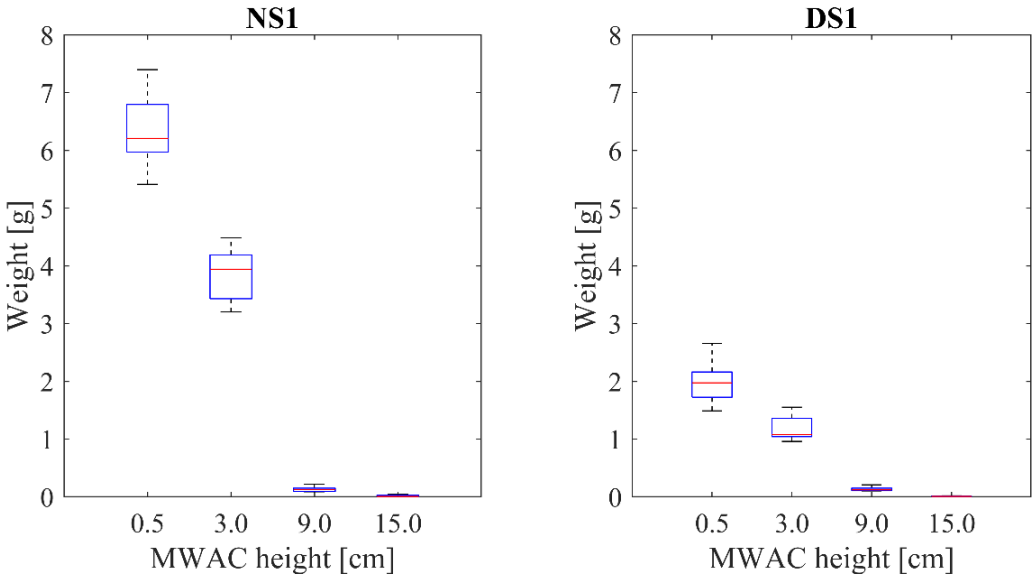

Figure 2-7. Average weights of trapped NS1 and DS1 in MWAC sampler 1 to 4.

Particle size analysis of NS1 showed that after the PWRS experiments, the cumulative mass percentages of the sample's surface were comparable to the original distribution of the substrate (Figure 2-8). This lack of depletion of fines could have been caused by either too short exposure times or a non-selectivity of the erosion process due to high shear stresses applied. Similarly, the PI-SWERL's post-experiment particle size distribution did not change much for NS1. On the contrary, for DS1, depletion of the finer fractions (<100 µm) was observed when comparing the surface samples to the particle size distribution of the original sample. Furthermore, for both substrates, the samples from the Dyson attachment showed that only smaller particles (<100 µm) were emitted from the PI-SWERL.

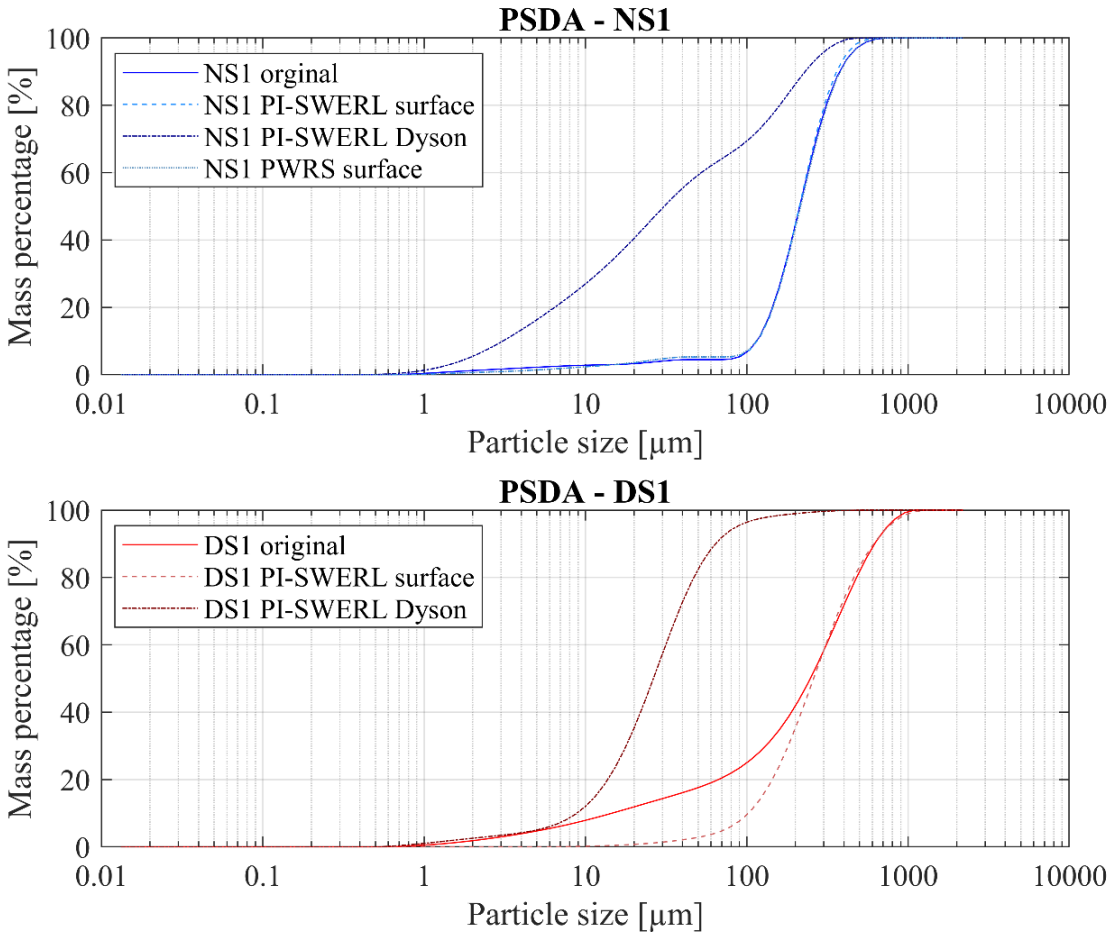

Figure 2-8. The average cumulative particle size distribution of the original substrates (NS1 and DS1), surface samples after the PI-SWERL and PWRS experiments, and the Dyson samples.

2.5 Discussion

In this research, we aimed to explore the ability of the PI-SWERL to quantify the threshold friction velocities for PM_{10} emissions. We hypothesised that the threshold friction velocities measured by the PI-SWERL and the PWRS would be comparable. For NS1, the threshold was identified at 0.33 m s^{-1} from the PI-SWERL data, which corresponds to a wind speed of 6.35 m s^{-1} at 2 m above the surface. The same threshold friction velocity was derived from the PWRS data, which indicates comparability of the two methods. However, for DS1 the threshold friction velocities differed significantly between instruments. The PI-SWERL obtained a critical value of 0.25 m s^{-1}, whereas a threshold of 0.39 m s^{-1} was identified from the PWRS data. For reference, these threshold friction velocities correspond to 4.79 and 7.33 m s^{-1} at 2 m above the surface for NS1 and DS1, respectively.

Another factor that might have caused the deviation of thresholds between devices for DS1 is that the PWRS experiments were performed on different days (NS1 on day 1, DS1 on day 2). Environmental conditions differed between the test days, with an average temperature of 16.5 °C and relative humidity of 58.8% on the first day. On the second day of the PWRS experiments, the average

temperature was 9.3 °C and the relative humidity decreased to 46.0%. Temperature and relative humidity during the PI-SWERL experiment were similar to the environmental conditions of the first PWRS test day. Humidity directly influences the threshold friction velocity of a soil, as it strengthens the interparticle forces (McKenna Neuman, 2004). Temperature has an indirect effect on the critical value for particle entrainment. The drag force is proportional to air density, meaning that with low temperature the drag force on a soil particle increases, therefore reducing the threshold friction velocity (Kok et al., 2012). Also, with low temperature, the matric potential is low, weakening the interparticle cohesive forces, thus reducing the threshold friction velocity (McKenna Neuman, 2004). Because of these deviating environmental conditions, we would expect that the threshold friction velocity of DS1 would be lower during the PWRS experiments, compared to the PI-SWERL tests. However, the opposite was observed. Therefore, the differences in environmental conditions do not explain the deviating threshold friction velocities for DS1. On the second day, DS1 was tested by a different operator, who might have manually controlled the fan slightly different, leading to variations in wind velocities and thus different threshold friction velocity during the experiment. This explanation is supported by the larger variation in observed PM_{10} emission patterns for DS1 replicates. Based on these assumptions, it is likely that the actual PWRS measurements on both substrates are valid. However, the increased variability between DS1 replicates, due to operator change, could have also resulted in inaccurate identification of the threshold friction velocity for DS1.

Lastly, some alterations should be made to the test set-up of the PWRS experiments to make it as similar as possible to the experimental design of the PI-SWERL. The PWRS tests lasted 190 s, while the PI-SWERL tests were much longer with 420 s. However, maintaining the PWRS test for 420 s was not possible because the sample tray in the tunnel floor would have been highly depleted in material before the end of the test. Increasing the size of the sample tray does not solve this problem. As soon as the material is below the rim of the tray, aerodynamic conditions change and material is emitted differently. This change in procedure would improve the comparability of the total dust flux between the instruments but not the issues with detecting the certain threshold friction velocities.

Based on the observed experimental issues, it is important for future research to focus on reducing these factors from the PWRS experiments. Most importantly, the regulation of the fan's speed must be done by a single observer or automatically. Ideally, both substrates should be tested on the same day to ensure repeatable environmental conditions between measurements. Furthermore, multiple DustTrak II monitors should be added to the PWRS' experimental set-up. In the current design, it was not possible to measure dust emissions over a vertical profile and calculate vertical PM_{10} emission fluxes. In comparison, the study by Sweeney et al. (2008) used four DustTrak II monitors at 0.05, 0.10, 0.17 and 0.25 m above the tunnel floor.

When more DustTrak II monitors are added to the PWRS set-up, comparison of measured dust fluxes by both instruments would be possible. When comparing such results, underestimation of dust emission by the PI-SWERL should be considered. Due to the rotating movement of the blade, the PI-SWERL behaves like a cyclone separator (Etyemezian et al., 2019). Particles will be separated based

on their particle size, and smaller particles are likely to follow the airflow and will be removed from the chamber by the exhaust pipe. However, larger particles remain in the chamber due to the cyclonic movement of the airflow. Etyemezian et al. (2019) suggest that this is the case for particles larger than 5 µm and that the effect strengthens with increasing particle size. In other words, PM_{10} dust emissions are likely to be underestimated. However, this potential underestimation needs further clarification and explanation because Sweeney et al. (2008) did not find such systematic variations. For NS1, 2.7% of its mass consists of particles with a diameter up to 10 µm (PM_{10}), while for DS1 this is 8.6%. In addition, 0.7% of the particles of NS1 have diameters between 5 and 10 µm, while for DS1 3.9% of the particles are within this size category. According to Etyemezian et al. (2019), we would expect slight underrepresentation, especially for DS1, of the PM_{10} emission during the PI-SWERL experiments. As a result, it is likely that the dust flux measurements of the PI-SWERL will systematically differ from the PWRS findings.

2.6 Conclusion

In previous research, the PI-SWERL has been successfully used to study the dust emission potential of various surfaces. In this research, we aimed to explore if the PI-SWERL can be used to quantify threshold friction velocities for PM_{10} emission by comparing its findings to those of a wind tunnel: the PWRS of the University of Basel. Two substrates were used during the experiments: NS1 and DS1. For NS1, threshold friction velocities of 0.33 m s^{-1} were found by both instruments. In contrast, the observed thresholds for DS1 were different. A threshold friction velocity of 0.25 m s^{-1} was quantified by the PI-SWERL, while the PWRS experiments yielded a different speed of 0.39 m s^{-1}. The good comparability of thresholds for NS1 indicate that the PI-SWERL can be used to assess threshold friction velocities for PM_{10} dust emission. However, the rather large difference for DS1 shows that experimental issues need to be improved, before reliable results and a definite answer to the hypotheses can be formulated.

The different threshold friction velocities can possibly be explained by the experimental design of the PWRS tests and also by the instrument's operation by different persons. Lowering the inlet tube of the DustTrak II monitor should result in higher observed PM_{10} concentrations, making the identification of threshold friction velocities easier. The lack of a rapid increase of PM_{10} and highly variable emission patterns make precise quantification of the threshold velocities difficult. Furthermore, operation of the PWRS by different persons could explain the difference in PM_{10} emission patterns between substrates. The mechanical regulation of the push-type fan made precise control of the wind velocity between operators difficult.

Furthermore, to improve quality and reliability of results, multiple DustTrak II monitors should be included in the experimental set-up and the duration of the PI-SWERL experiments should be shortened to increase similarity between experiments. Although our research did not yield a 1:1 correspondence in threshold friction velocities for both substrates, we believe that with an improved and more comparable test set-up, the comparison of thresholds between the two methods can be

achieved. This would indicate that the PI-SWERL could be used in future research to supplement and even substitute threshold friction velocity datasets based on wind tunnel experiments, in the laboratory and, most importantly, in the field.

3.

Physical crust formation on sandy soils and their potential to reduce dust emissions from croplands

Heleen C. Vos*, Wolfgang Fister*, Frank D. Eckardt**, Anthony R. Palmer*** & Nikolaus J. Kuhn*

* Physical Geography and Environmental Change, University of Basel, Basel, Switzerland

** Department of Environmental and Geographical Sciences, University of Cape Town, Cape Town, South Africa

*** Agricultural Research Council-Animal Production, Grahamstown, South Africa

Published in Land, 2020, Volume 9, Issue 12, 503

https://doi:10.3390/land9120503

3.1 Abstract

The sandy croplands in the Free State have been identified as one of the main dust sources in South Africa. The aim of this study was to investigate the occurrence and strength of physical soil crusts on cropland soils in the Free State, to identify the rainfall required to form a stable crust, and to test their impact on dust emissions. Crust strength was measured using a fall cone penetrometer and a torvane, while laboratory rainfall simulations were used to form experimental crusts. Dust emissions were measured with a Portable In-Situ Wind Erosion Laboratory (PI-SWERL). The laboratory rainfall simulations showed that stable crusts could be formed by 15 mm of rainfall. The PI-SWERL experiments illustrated that the PM_{10} emission flux of such crusts is between 0.14% and 0.26% of that of a non-crusted Luvisol and Arenosol, respectively. The presence of abraders on the crust can increase the emissions up to 4% and 8 % of the non-crusted dust flux. Overall, our study shows that crusts in the field are potentially strong enough to protect the soil surfaces against wind erosion during a phase of the cropping cycle when the soil surface in not protected by plants.

Keywords: Wind erosion; soil crusts; PI-SWERL; rainfall experiment; crust strength

3.2 Introduction

The emission of dust can have offsite effects on the regional and global climate (Boucher et al., 2013; Shao et al., 2011; Tegen et al., 1997), global geochemical fluxes (Lawrence and Neff, 2009; Mahowald et al., 2009), and human health (Goudie, 2013; Sprigg, 2016). For the emitting surface, dust emissions can lead to land degradation due to the removal of fine soil particles and organic material, especially in semi-arid and arid environments (Bridges and Oldeman, 1999; Chappell et al., 2019; Oldeman, 1992; Sterk et al., 1996; Visser and Sterk, 2007). Due to these impacts, many studies have focused on assessing the sources of dust and the factors controlling dust emission (Ginoux et al., 2012; Middleton, 2017; Prospero et al., 2002; Tegen et al., 2004). Dust is assumed to be largely emitted from natural surfaces, in particular deserts, but dust emissions from croplands are receiving increasing attention (Colazo and Buschiazzo, 2015; Funk et al., 2008; Prospero et al., 2002; Ries et al., 2009; Stout and Zobeck, 1996; Tegen et al., 2004; Zobeck et al., 2003; Zobeck and Van Pelt, 2006).

The central and western parts of the Free State province in South Africa experience elevated dust emissions from croplands (Tegen et al., 2004; Vickery et al., 2013). Eckardt et al. (2020) showed that 70% of the Meteosat Second Generation (MSG) identified dust source points of South Africa from 2006 to 2016 are located in this province. The fine, suspended particles could have a serious impact on public health in this region. The emissions from the Free State can be attributed to commercial, rain fed croplands with sandy soils in a semi-arid climate, which renders them very vulnerable to wind erosion (Webb et al., 2013). It should be noted that the frequency of dust events identified for the Free State is relatively low in comparison to nearby desert regions, such as the Kalahari or the Namib desert (Ginoux et al., 2012; Vickery et al., 2013). However, the close proximity of these dust sources to urban centres and rural populations in the Free State and beyond may have an effect on human health and contribute to the loss of fertile soil in the source areas (Goudie, 2013).

Wind erosion in the Free State has already been identified as both a current and a historical phenomenon (Holmes et al., 2008, 2012). Holmes et al. (2012) emphasize that the increase in agricultural activities during the 20th century is responsible for an increase in wind erosion due to the removal of vegetation. However, only one study from Wiggs and Holmes (2011) focused in detail on the interaction between wind and surface properties of agricultural fields in the Free State. Their results show that erosion of ridges and filling of furrows on bare agricultural fields without soil crusts reduce the aerodynamic roughness and, consequently, reduce threshold wind velocities. Eckardt et al. (2020) showed that 85% of the 75 dust event days between 2006 and 2016 took place between August and November. However, the annual variability of dust events is dependent on drought and field cover. Without sufficient cover, soil properties and surface conditions remain the only control to dust emission in the Free State. Besides the influence of roughness and cover, the main factors that can control the emissivity are the soil texture and cohesion, which in turn is mainly controlled by the moisture content, and the presence of a physical or biological crust. Due to the regular disturbance of the surface, we only expect the formation of physical soil crusts and no presence of biological crust. In this study, we focus therefore on the possible influence of physical soil crusts as a boundary condition for dust emissions, and on how crust formation is influenced by agricultural practices.

Soil crusts are commonly considered as enhancing water erosion (Belnap, 2001; Hu et al., 2013; Le Bissonnais et al., 1995). However, the positive influence of physical soil crusts on reducing wind erosion and dust emissions has been shown by experimental studies (Houser and Nickling, 2001b; Rice et al., 1996; Rice and McEwan, 2001; Zobeck, 1991a) as well as field measurements (Gillette, 1988; Gillette et al., 2001, 1982, 1980; Goossens, 2004; Klose et al., 2019; Sharratt and Vaddella, 2014; Sterk et al., 1999; Yan et al., 2015). However, some studies also described the abrading effect of saltating particles on crusted surfaces, which results in the degradation of a crust and the emission of fine particles (Houser and Nickling, 2001b; Klose et al., 2019; Rajot et al., 2003; Rice et al., 1999, 1996; Rice and McEwan, 2001). Especially for weaker crusts with a low content of fine particles, the ability of abraders to disrupt the crust appears to be very high.

This study identifies the potential significance of physical soil crusts on dust emissions from Arenosols and Luvisols, which are widespread in the semi-arid rangelands of the world (Sanchez et al., 2009). We hypothesise that crusts potentially play a critical role in increasing soil cohesion and thus reducing dust emissions in the Free State. Hereby we must take the soil texture, the crust strength, the presence or absence of abraders, and the rainfall into account. To test this hypothesis, the specific aims of this study are to:

1. Document the occurrence, structure, and properties of crusts on cropland during the emission season.
2. Identify the constraining rainfall conditions that lead to formation of crusts on sandy cropland soils.
3. Assess the potential impact of crusts and their abrasion on dust emissions using a Portable In-Situ Wind Erosion Laboratory (PI-SWERL).

The outcome of this study has implications beyond land degradation in the Free State and the air quality and human health in South Africa, because croplands on sandy soils are wide spread across the globe (Hartemink and Huting, 2008; Houyou et al., 2016; McTainsh et al., 1990; Sanchez et al., 2009) and often subject to wind erosion (Colazo and Buschiazzo, 2015; Guo et al., 2014; Harper and Gilkes, 1994; Nan et al., 2018). Findings could also have a positive impact on the potential of implementing practices that protect crusts or even enhance their formation to reduce dust emissions from sandy soils.

3.3 Materials and methods

3.3.1 Introduction

This study consists of three parts: (1) the field measurements of crust strength and soil sampling, (2) simulation of crust formation using laboratory rainfall, and (3) the dust emission measurements on crusts formed in the laboratory with the PI-SWERL. For both the field measurements and the laboratory rainfall experiments, the crust strength was analysed as an indication of its resistance against wind erosion (Goossens, 2004; Goossens and Buck, 2009; Houser and Nickling, 2001a; Rice et al., 1999; Rice and McEwan, 2001; von Holdt et al., 2019).

3.3.2 Site description and field measurements

The research area is located in the north-western part of the Free State province, north of Bultfontein (Figure 3-1). This area was selected because it is in the centre of the region with the greatest number of dust emission events identified by Eckardt et al. (2020). Furthermore, two soil types most commonly associated with these emissions and which are commonly used for crop farming are predominant in this area. Luvisols are characterised by a clay enrichment in the B horizon, whereas Arenosols are generally more homogenous in soil texture with depth. A climate station from the Agricultural Research Council (ARC) on the farm Arbeidskroon situated 10 km north of Bultfontein provided data on the recent climate of this area (Figure 3-2 and Figure 3-3). The rainy season is in summer (November - April), whereas during the winter months (May – October) dry periods are very common. The rainfall in this region can be characterized by high inter-annual and seasonal variability. Between 2006 and 2018, the average annual rainfall was 477 mm (representing the growing season), with a minimum rainfall of 294 mm in 2015/2016 and a maximum of 813 mm in 2010/2011. The mean annual air temperature in the aforementioned period was 17.1 °C with daily maximum values in summer that can exceed 35°C, but lowers in winter to below 0 °C. After the Köppen-Geiger classification, the climate is categorised as BSk (semi-arid, steppe climate). The predominant wind directions are NNE and SSW with the greatest velocities for winds coming from NW directions. The study area is prone to wind erosion due to the supply of fine silt associated with sandy soils, farming practices which make these available for entrainment, and frequent winds with high wind velocities, especially during the dry winter months which generate a high transport potential (Figure 3-2).

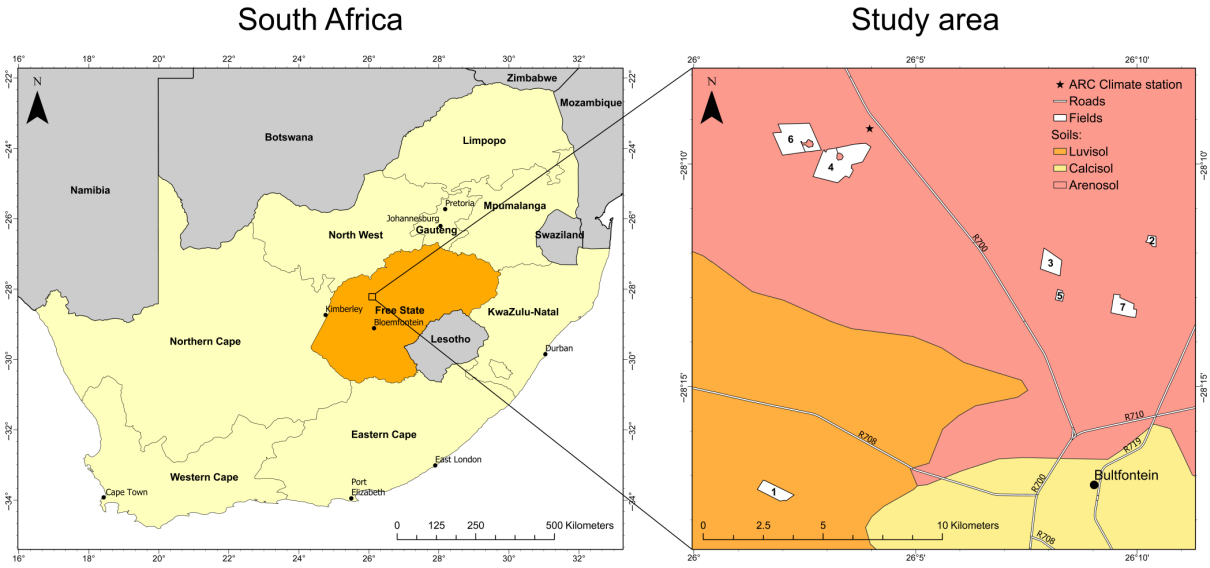

Figure 3-1. South Africa with the Free State province marked in dark orange (a) and the soil map of the research area with the location of the studied fields, see also Table 3-1 (b). Province borders come from the GADM database (www.gadm.org), version 2.5, July 2015. The soil map data was extracted from the Soil and Terrain Database (SOTER) for South Africa (FAO-ISRIC 2003).

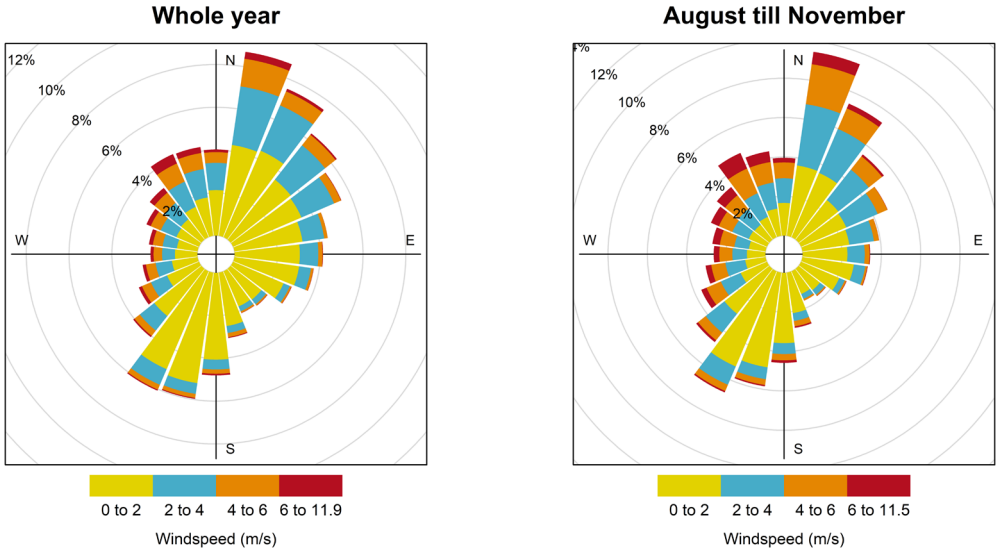

(a) (b)

Figure 3-2. Wind rose from the study area north of Bultfontein. (a) Shows the annual data from 2006 to 2016 and (b) shows the winds during the dust season, from August until November. This data was obtained from the ARC weather station.

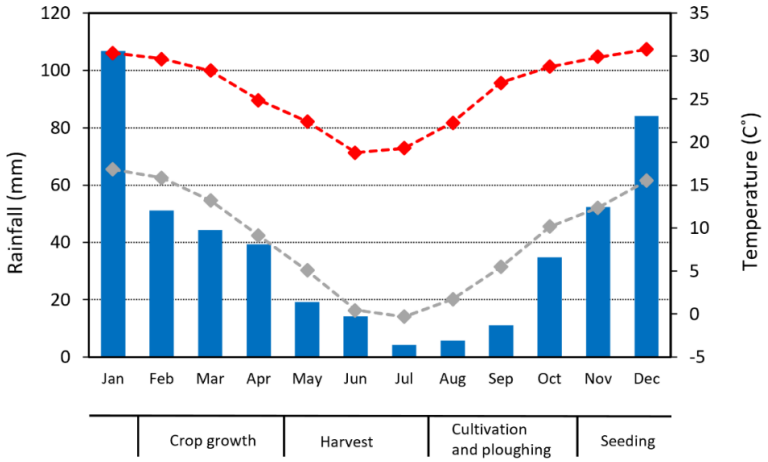

Figure 3-3. The average rainfall (blue bars), the minimum (grey) and maximum (red) temperature per month, and the general periods of agricultural activity (bottom). Note that these periods are generalized to present an overview and can differ depending on the weather, crop, and farmer's preference.

Roughly 31% of the land in the Free State is utilised as arable land. These croplands produce around one third of all the food in South Africa (DAFF, 2018). Maize is the main crop (81% of the total Free State crop production), but other annual crops include sunflower, groundnuts, soybeans, and a small number of cool season crops (wheat, barley) being cultivated for livestock fodder (DAFF, 2018). Maize is planted at the beginning of the rainy season, which usually starts in November or December, and is harvested between May and the beginning of August (Figure 3-3). As a result, most fields have a low amount of plant cover between August and November, which leaves soils vulnerable to wind erosion and dust emission. Cultivation practices, such as ploughing, deep ripping or burial of mineral fertiliser that take place between harvest and renewed crop cover, can break-up soil crust, thus loosening the soil and enhancing wind erosion. Wind erosion protection measures are not routinely practised.

The fields under investigation are shown in Figure 3-1 and Figure 3-4 and are further described in Table 3-1. They were chosen because of the presence of a physical soil crust (Figure 3-5) and the diversity in cropland management, such as a difference in crop and cultivation techniques. Unfortunately, the Luvisol fields were ploughed just prior to the field experiments and therefore lacked a crust. The strength of the field crusts was measured with a fall cone penetrometer and a torvane (paragraph 2.4).

Table 3-1. Field test sites in the study area and the soil chemistry from the observed fields.

Field	Soil	Description	Crust presence	TOC %	pH	Silt/Sand
Field 1	Luvisol	Ploughed and bare field	No	0.25	6.06	0.19
Field 2	Arenosol	Unharvested maize field	Yes	0.47	6.32	0.23
Field 3	Arenosol	Groundnut field, harvested	Yes	0.19	6.30	0.09
Field 4	Arenosol	Maize field, harvested and deep ripped	Yes	0.18	6.32	0.12
Field 5	Arenosol	Sunflower field, harvested	Yes	0.18	6.08	0.10
Field 6	Arenosol	Maize field, unharvested	Yes	0.32	6.81	0.19
Field 7	Arenosol	Harvested maize field, grazed by cattle	Yes	0.16	6.30	0.13

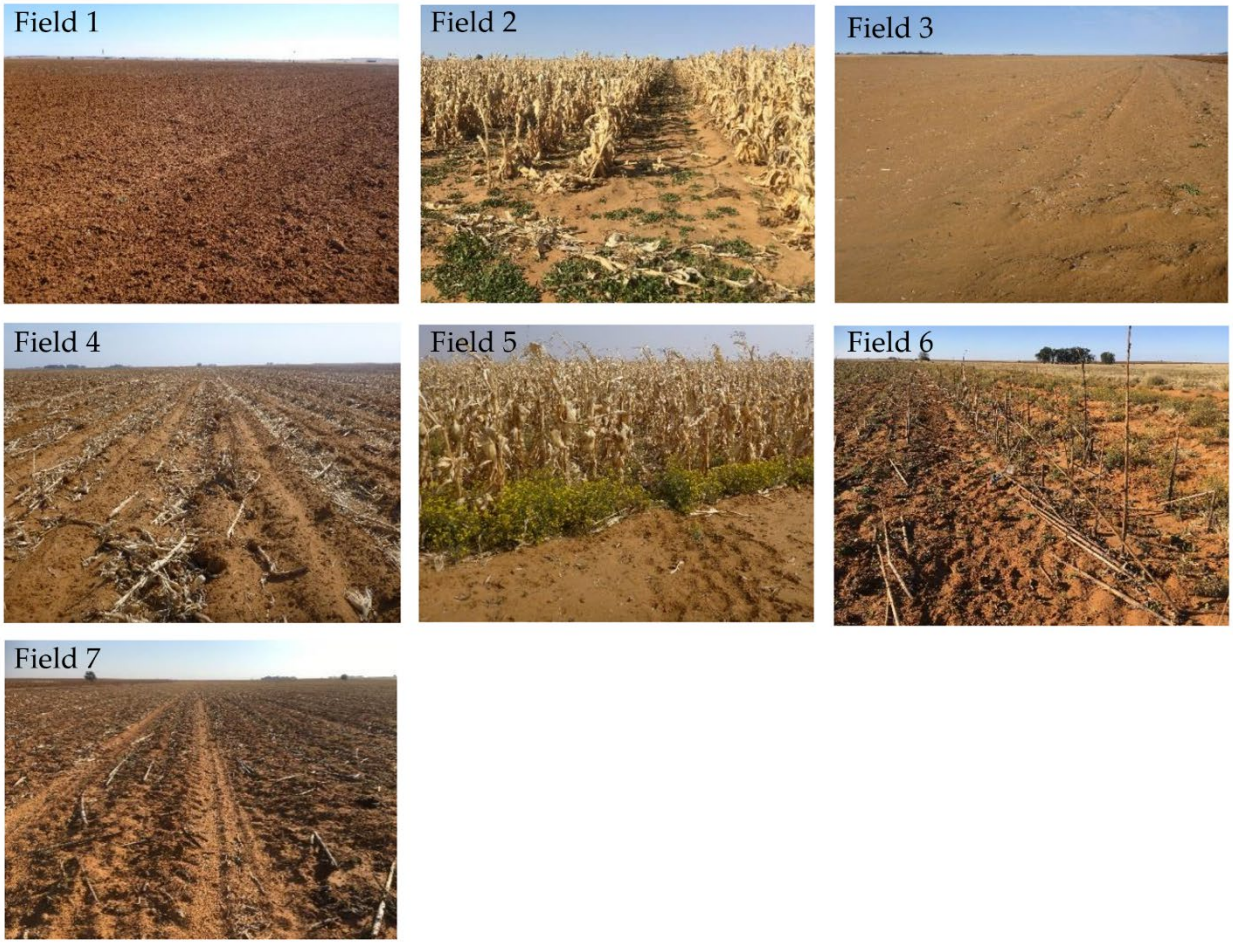

Figure 3-4. Overview of fields from which the crust strength was measured.

Figure 3-5. Intact crust on Arenosol in field 2.

The top 2 cm of soil the in these fields were sampled to measure soil properties. The grainsize distribution of the soils was obtained using the wet dispersion unit of the Malvern Mastersizer 2000. Before the measurements, the samples were dispersed at 60 J ml^{-1} using the Branson 250 Sonifier, which is in accordance to methods from Hu et al. (2016). Also the pH value (SevenExcellens pH meter,

Mettler Toledo) and the carbon content (RC612, Leco) was analysed, as described in Caviezel et al. (2017). The soil shows a texture ranging between sand and loamy sand with low organic carbon contents and silt/sand ratio (Table 3-1 and Figure 3-6). The pH is slightly acidic, except for the almost neutral pH of field 6 (Table 3-1). Both soils show a poor structure, with an aggregate stability of 8% and 13% for field 1 and field 4, respectively, as determined using the Eijkelkamp wet sieving apparatus.

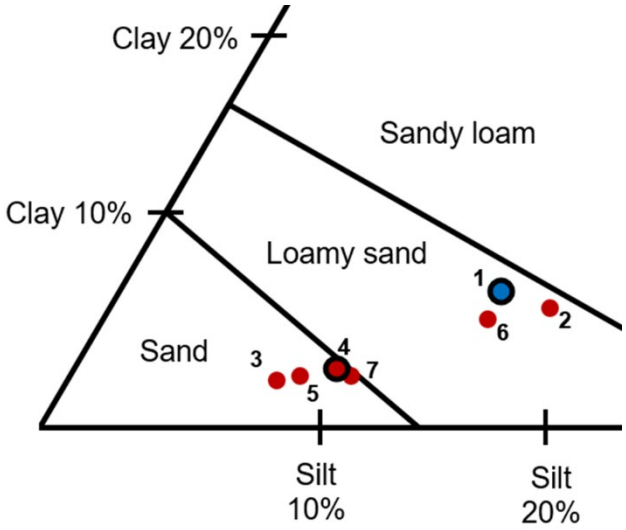

Figure 3-6. Close-up of the soil triangle with the measured soil points. The red point represent Arenosol and the blue one Luvisol according to the SOTER database. The marked points of field 1 and field 4 were used for further rainfall and wind erosion experiments.

3.3.3 Rainfall simulation and crust formation

A large sample (approximately 10 dm^3) of a Luvisol (from field 1) and an Arenosol (from field 4) were collected in 2018, transported back to the laboratory in Basel, and used to gain insight into the formation of physical crusts through artificial rainfall experiments. Prior to the rainfall simulation, the soils were dried at 40 ^{0}C and sieved through a 2 mm sieve to remove larger particles, such as stones, roots, and straw from the soil. For the rainfall experiments, containers of 10 x 10 x 12.5 cm (w x h x d) were used. The bottom 10 cm of these containers were filled with air-dried sand and the top 2.5 cm of the boxes were filled with the soil sample. The crusts for the PI-SWERL experiments were prepared on perforated round plates with a diameter of 50 cm and a depth of 5 cm, whereby again the top 2.5 cm was filled with soil sample and the bottom was filled with sand as filling material, see Figure 3-7. The sand has a similar texture to the cropland soils and was used to minimize the amount of soil required for each experiment.

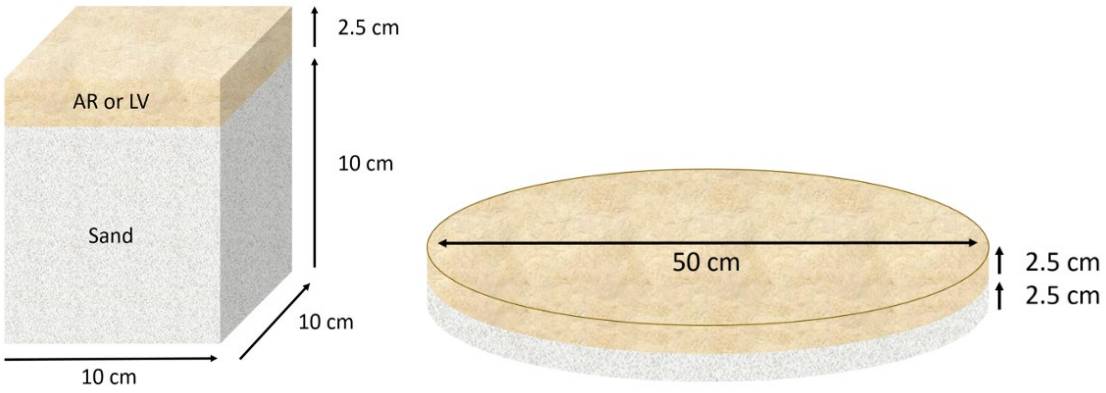

Figure 3-7. Schematic overview of the tray set-up for the rainfall experiments.

The rainfall experiments were performed using a high precision rainfall simulator from the Physical Geography and Environmental Change Research Group of the University of Basel in Switzerland, described by Fister et al. (2019). The rainfall experiments aimed at creating a crust with a rainfall amount that could occur realistically in the study area. A maximum of 20 mm of rainfall was chosen, because only 5% of the rainfall events deliver this amount or more (See supplementary material). Experiments were done at 100 mm h^{-1} with a drop fall height of 5.8 m and a drop diameter of 2.6 mm, which corresponds to a kinetic energy (kE) of 24.1 J mm^{-1} m^{-2}. The kinetic energy (kE) of the rainfall was determined by a Joss Waldvogel Distrometer. The high rainfall intensity was chosen to match the kinetic energy of natural rainfall (van Dijk et al., 2002). The soils were exposed to an increasing amount of rainfall up to the maximum of 20 mm. This would allow for identifying a change of crust strength with an increase in rainfall amount and kE. Besides this variation, two types of rainfall were tested: single event rainfall and a sequence event rainfall. For the single event rainfall, 12 rainfall quantities were tested, from 1.67 mm to 20 mm in steps of 1.67 mm. The sequenced rainfall was measured in steps of 5 mm, whereby a crust was dried before exposed again to rainfall. This approach gives an insight into whether crust strength is determined by the cumulative rainfall alone or if it is also affected by drying in between, as shown by Kuhn et al. (2004).

After the experiments, the crusts were dried for seven days in a Binder climate chamber (Model MK-240) at 30 °C and a humidity of 56%. The moisture content is of importance since moisture can influence both the surface strength (Zimbone et al., 1996) and, more notably, the resistance to erosion of a surface (Chen et al., 1996; Funk et al., 2008; Ishizuka et al., 2008; Munkhtsetseg et al., 2016). Measurements showed that the soil humidity of the top 2 mm did not decrease significantly after seven days of drying, and the moisture content was always below 1%.

Thin sections of the experimental crusts were made with an epoxy resin of laromin® C 260 and araldit® in a 40% - 60% ratio. Images of the thin sections were taken using a Nikon Super Coolscan 5000 ED.

3.3.4 Crust strength measurements

Crust strength is an indicator for the resistance of the surface to wind erosion (Feng et al., 2013; Goossens, 2004; Rice et al., 1996; Sharratt and Vaddella, 2014). For this study, crust strength was measured with two instruments, commonly used to describe soil resistance to erosion: a fall cone penetrometer for both field- as experimental crusts, and a torvane for only the field crusts. Fall cone penetrometer measurements have been used by several studies (Borselli et al., 1996; Bradford and Grossman, 1982; Campbell, 1976; Ghadiri, 2004; Han et al., 2016). The major advantages of using a fall cone penetrometer is the small scale of the measurement, both in surface as in depth. This makes the measurement more comparable to the impact of an abrading particle or single raindrop, in contrast to larger scale measurements with a torvane or a pocket penetrometer, as also discussed by Rice et al. (1997). Furthermore, the fall cone penetrometer delivers high precision measurements, and the instrument is easy to transfer and operate. The disadvantage of the fall cone penetrometer is that despite the high precision, the crust strength that is calculated is a relative value; see also Eq. 1. It is also slower to use and less common than the torvane. A torvane determines the torsional shear stress before failure, and is a very common instrument for wind erosion studies (Gillette et al., 2001; Goossens, 2004; Li et al., 2010; Sweeney and Mason, 2013; von Holdt et al., 2019; Zimbone et al., 1996) since it is physically closest to the shear stress that wind and abraders apply to a surface. Due to the scale of the measurement, torvane measurements require a large surface area which was not feasible. By performing measurements using both instruments on field crusts, where surface space is abundant, we can compare the two methods and make our experimental results comparable to the studies done with a torvane. A Humboldt Portable Penetrometer (Model H-1250 fall cone penetrometer) with an aluminium 10 o apex cone and a 0.8 mm stainless steel blunt tip, with a total weight of 142.5 g was used. The cone was raised 2 cm above the soil surface, after which it was released to fall onto the crust. The penetration depth was measured with an accuracy of 0.1 mm. For field crusts and experimental crusts, 20 and 10 measurements were taken, respectively. In addition, a torvane (n=10) was used to determine the field crust strength. This instrument is adapted from a table instrument to a handheld instrument for field use by Kuhn et al. (2004), and uses a vane with eight blades and a penetration depth of 3 mm.

A fall cone penetrometer links the penetration depth to an undrained shear strength (τ, in Pa or kg m^{-1} s^{-2}), meaning the maximum horizontal stress without any water flowing in or out of the soil. For this study we will use the following formula to calculate the shear strength index (τ^*) as a kPa index (Becher et al., 1997; Han et al., 2016; Hansbo, 1957).

$$\tau^* = \frac{Q}{{h_p}^2} * 10^{-3} \quad (1)$$

Whereby Q is the vertical force of the cone (in kg m s^{-2}, using a gravitational acceleration of 9.81 m s^{-2}), and hp is the penetration depth (m). The maximum penetration depth is 2 cm, which is in accordance with a shear strength index of 3.5 kPa.

To determine whether rainfall type (single event versus sequence rainfall) or soil type results in significantly different soil strength, two-tailed t-tests was performed on the crust strength measurements. An alpha value of 0.05 was used to determine the statistical significance.

3.3.5 PI-SWERL

To determine the influence of crust formation on dust emissions, a Portable In-Situ Wind Erosion Lab (PI-SWERL, Desert Research Institute) was used. The PI-SWERL is described in detail by Etyemezian et al. (2007, 2014). The PI-SWERL is ideally suited for the dust emission experiments carried out in this study for several reasons. Due to the small amount of soil required for experiments (ca. 3 kg per crust) a wide range of controlled tests can be carried out. Secondly, while the PI-SWERL can only be used on surfaces with small roughness elements, this limitation does not occur on smooth crusts. Finally, while not relevant in this study, the PI-SWERL is highly mobile and will be used in a later part of the project to measure emissions from crusts in the field as well.

The friction velocity exerted by the PI-SWERL to the effective area ($u_{*,\,eff}$) is determined by the revolutions per minute (RPM) of the blades that create the air stream in the measurement chamber, which is empirically determined by Etyemezian et al. (2014) as:

$$u_{*,eff}(RPM) = 0.000683 * \alpha^4 * RPM^{0.832/\alpha} \quad (2)$$

In this formula α is a roughness constant that is determined per surface. For our surface, a roughness parameter of 0.98 was used.

Table 3-2 shows the PI-SWERL runs that were performed. For each soil, PI-SWERL measurements were done on loose material, and on bare crusts formed by 15 mm of rain with and without the addition of 3 grams of abrader material. The abrader material was sampled from a sand accumulation in the field. To avoid any influence of the abrader on dust measurements, the abrader was sonified and wet sieved to extract all particles finer than 63 microns. Every PI-SWERL run started with a velocity increase from zero up to 3175 RPM within 120 seconds to detect the threshold of PM_{10} emission. 3175 RPM matches a friction velocity of 0.59 m s^{-1} (Eq. 2) which is in accordance with a wind speed of ca. 11 m s^{-1} at 2 metres (z_0 of 1 mm), a commonly occurring wind speed in the study area. When 3175 RPM were reached, the RPM were kept stable for two different times (Table 3-2): the experiment on loose soil for 30 seconds, and the experiment on crusted soil (with and without abrader) for 120 seconds. The experiments on loose soil were run for a shorter period to prevent a significant depletion of fines from the highly emissive soils. The crusted surfaces were run for a longer time to gain insight into the possible effect of abrasion and degradation. As shown in Eq. 3, the flux is calculated as an average for the entire run.

Table 3-2. Summary table of performed PI-SWERL runs.

Soil	Crust	Abrader addition	n (per soil type)	Time (s) at 0.59 m s^{-1}
AR and LV	Loose soil	No	6	30
	Crusted by 15 mm of rainfall	No	3	120
		Yes	3	120

To calculate the average emission flux of the soil during the PI-SWERL experiment ($E_{PI,i}$) in mg m^{-2} s^{-1} of each RPM step, Sweeney et al. (2008) proposed the following formula:

$$E_{PI,i} = \frac{\sum_{begin,1}^{end,i} C*F*1s}{(t_{end,i} - t_{begin,i})*A_{eff}}, \quad (3)$$

Whereby C is the dust concentration in mg m^{-3}, F the blow rate in l s^{-1}, and A_{eff} is the effective area of 0.035 m^2. The emission flux will be calculated for the period at which the RPM is at 3175. Furthermore, the threshold of PM_{10} will be determined. The threshold is defined as the point after which there is a subsequent increase in PM_{10} for a minimum of 10 seconds, after Van Leeuwen et al. (2021). The RPM of this PM_{10} threshold is converted into a friction velocity using Eq. 2.

As mentioned before, the bombardment of a crust by saltating grains is an important process resulting in the emission of fine particles and degradation of the crust. A common term to express the relationship between the saltation flux and the resulting dust emission is the abrasion efficiency (Houser and Nickling, 2001a; Zobeck, 1991a) or bombardment efficiency (Shao et al., 1993). For this study a relative abrasion efficiency (in µg m^{-2} s^{-1} $count^{-1}$) will be calculated by dividing the dust flux from Eq. 3 by the average saltation count. The relative abrasion efficiency represents the amount of PM_{10} that are released per saltating particle. The saltation count within the PI-SWERL is measured using four Optical Gate Sensors (OGS) on the sides of the PI-SWERL chamber that measure the passing of saltating grains in Hz. Since the OGS sensor cannot give an exact indication of the saltation transport rate, the relative abrasion efficiency only gives an indication on the relationship between abrasion and PM_{10} emission.

3.4 Results and discussion

3.4.1 Crust strength and structure of field crusts

The crust strength measured on Arenosols of the different agricultural fields are provided (Figure 3-8). The shear strength of field 4 was below the minimum value that can be measured with the fall cone penetrometer, namely 3.5 kPa, so this measurement will not be used for regression calculation. The measurements of the two types of crust strength, the vertical shear strength and the horizontal torsional shear strength, correlated well with each other (R^2 = 0.87). This indicates that the fall cone penetrometer can be regarded as a reliable and relevant method for crust strength measurements on smaller, experimental crusts.

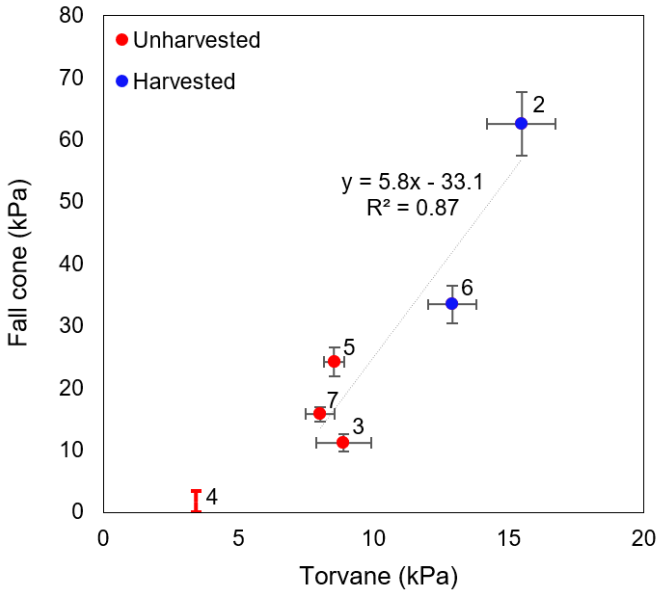

Figure 3-8. The crust strength measurements from crusts in the field measured using the fall cone (n = 20), torvane (n = 10). Error bars are 95% confidence intervals.

The field measurements show a difference between strong crusts on fields that have not been harvested yet (field 2 and 6), and weaker crusts on fields that had been harvested and cultivated (fields 3, 5 and 7). We speculate that the strong crusts developed at the beginning of the rainy season when the crops where small enough for raindrops to reach the surface, while the weaker crusts from field 3 and 4 formed after harvest when cultivation destroyed the former crusts. In June and July 2018, 2.8 and 3.8 mm of rainfall fell respectively, which could have made the formation of a weak crust on loose soil possible. These results lead us to the conclusion that crusts that form during the rainy season can survive throughout the dry season and that these crusts are significantly stronger than the crusts that form later during the dry season. The absence of crusts in the Luvisol field (field 1) and other non-crusted fields in our study area could have been caused by tillage operations in June or July or animal trampling (Hiernaux et al., 1999; Munkhtsetseg et al., 2017; Ries et al., 2009).

The torsional shear strength of the crusts was between 3.4 and 15.5 kPa, which is on average smaller compared to the crust strength measured by other studies: Goossens et al. (2004) measured crust strength on loamy and sandy soils with results between 12 and 37 kPa, and Zimbone et al. (1996) measured a strength of 10 kPa on a crusted sandy loam. This difference in crust strength could be caused by a smaller content of fines or TOC in our crusts, but also by the fact that our field crusts might have been less developed or more degraded. The degradation could have been the result of particle abrasion, plant root growth, hail impact, or freezing and thawing (Liu et al., 2017; Wang et al., 2014).

3.4.2 Crust formation by experimental rainfall

Rainfall experiments were performed on Arenosol and Luvisol samples to investigate the development of physical crusts in respect to varying rainfall amounts. Figure 3-9 shows a thin section of an Arenosol crust. This crust shows the formation of a thin dense layer of fine particles in the upper part of the crust. The results from these experiments show a clear positive correlation between the rainfall amount and the shear strength of the crusts (Figure 3-10). This increase is visible for both soils, and for both single event and sequenced rainfall.

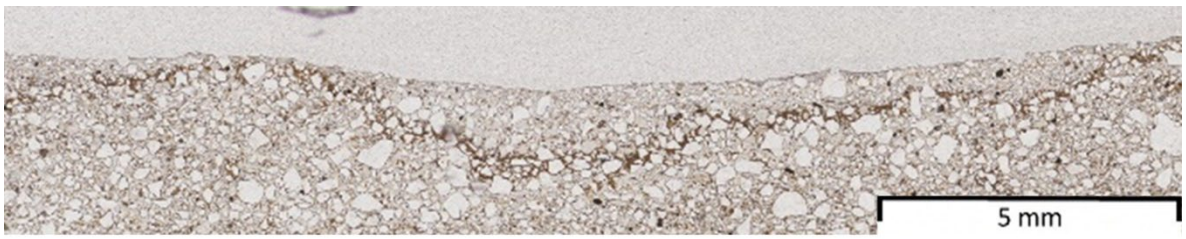

Figure 3-9. Thin section from the top of an Arenosol crust that formed with 20 mm of rainfall showing the thin dense layer of fine particles at the top of the crust.

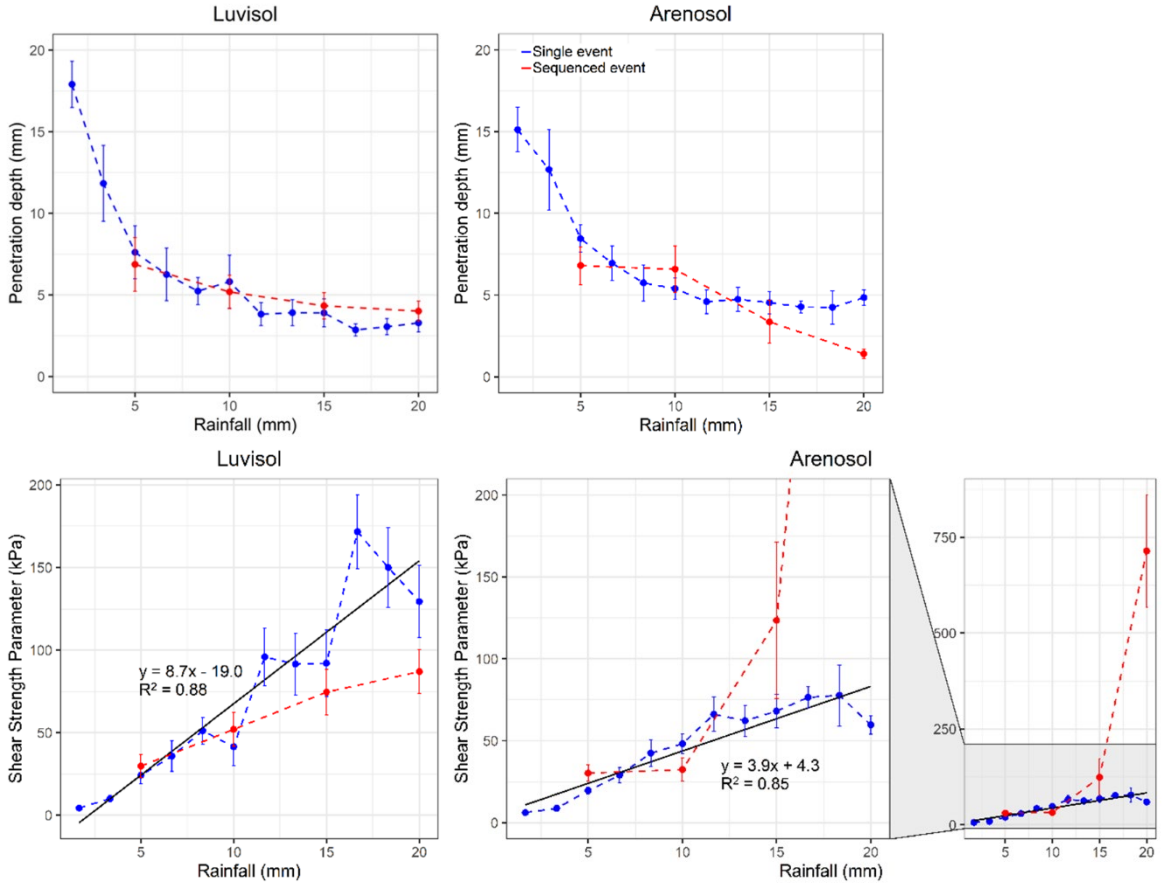

Figure 3-10. Results from the rainfall experiments, error bars show the standard deviation calculated from 9 measurements. The regression shown is calculated from the single event rainfall.

Table 3-3 shows the results of the t-tests between the shear strength from the Arenosol and Luvisol at 5, 10, 15, and 20 mm rainfall, and between single event and sequenced rainfall. Using an alpha value of 0.05, it can be stated that for single event rainfall Arenosol and Luvisol crusts have similar crust strength up to 15 mm of rainfall, after which Luvisol crusts are significantly stronger. The fact that Luvisols create stronger crusts can be attributed to the greater clay and silt content (21.4% for LV versus 13.1% for AR), a relationship that has been described elsewhere (Rice and McEwan, 2001; Sweeney and Mason, 2013).

Table 3-3. P-values from two-tailed t-test.

Rainfall amount	AR versus LV		Single event versus Sequenced rainfall	
	Single event	Sequenced	AR	LV
5 mm	0.140		-	
10 mm	0.995	0.066	0.074	0.497
15 mm	0.071	0.050	0.032	0.301
20 mm	0.001	0.001	0.000	0.025

Crust strength increased continuously with sequenced rainfall, a phenomenon that was also observed by Feng et al. (2013). For both soils, the crust strength between the single event and the sequenced rainfall is statistically similar until 15 mm of rainfall for the Arenosol and until 20 mm on the Luvisol. For greater rainfall, the strength of sequenced Luvisol crusts is smaller compared to the single event rainfall, whereas the Arenosol crusts from sequenced rainfall is much stronger than the single event crust. This could be caused by the fact that standing water during the experiment can reduce the kinetic energy of impacting drops acting on the soil surface (Gillette et al., 1982, 1980; Greenwood et al., 2013)(Greenwood et al., 2013)(Greenwood et al., 2013)(Greenwood et al., 2013). This building-up of crust strength would be an important process for physical crust formation, since smaller rainfall events are much more common (See supplementary material), especially between May and September, when the monthly rainfall is less than 20 mm. This successive buildup of crust strength with sequence rainfall events would be the most important process in crust formation during this period.

Using the Arenosol single rainfall event regression, calculated from the experimental results (Figure 3-10), it is possible to estimate the rainfall amount to which the field crusts that were studied in 2018 were exposed. The greatest shear strength of the crust from the harvested fields was 24.2 kPa, which would represent ca. 5.0 mm of experimental rainfall. For the crusts on the unharvested fields, the shear strength was between 33.5 kPa and 62.6 kPa, which is in accordance with 6.1 to 9.4 mm of experimental rainfall. The amount of rainfall that the soil had been exposed to in 2018 since the start of the growing season in 2017 was likely greater. According to the ARC weather station, 345 mm of rainfall fell from November 2017 till July 2018, whereas during the months after harvest, June and July, only 6.0 mm fell. The field crusts are weaker than the regression suggests, which could be caused by a difference in intensity of kE of natural rainfall, the protection of the soil from crusting by vegetation cover, or by any degradation of the field crust as mentioned before.

3.4.3 Dust emission thresholds and fluxes

The dust concentration observed during the PI-SWERL runs on loose and crusted surfaces are shown in Figure 3-11. The crusted surfaces do not show any significant dust emission, with the exception of one Luvisol crust experiment that shows a sudden increase in PM_{10}, 200 seconds into the experiment. This might have been caused by a crack in the crust due to swelling-and shrinking processes (Figure 3-14). A small concentration increase at the beginning of some runs, is attributed to small contaminations in the instrument. Figure 3-12 shows the relative abrasion efficiency of the abrader runs. Generally, this value shows a slight increase over time, which indicates that the crusts became more emissive under abrasion.

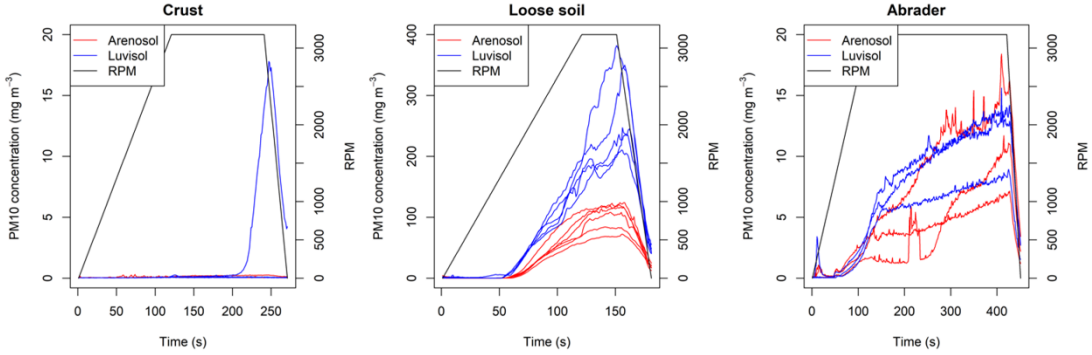

Figure 3-11. PM10 concentration measured during the PI-SWERL runs on several crusted and non-crusted surfaces (RPM = revolutions per minute).

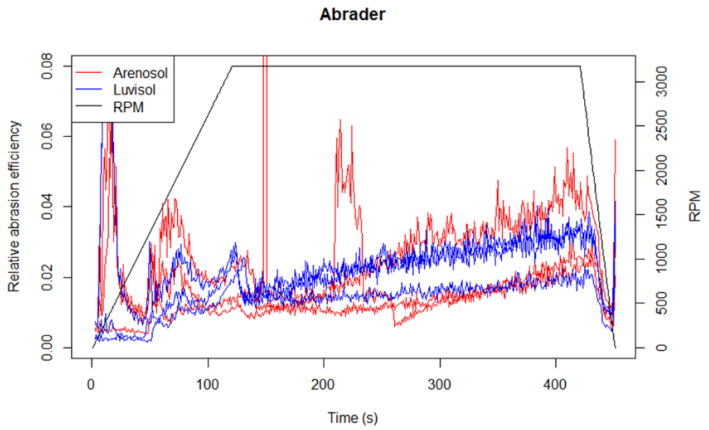

Figure 3-12. The relative abrasion efficiency over time during the PI-SWERL experiments with abraders.

For each PI-SWERL run, the dust emission flux and threshold were calculated (Figure 3-13 and Table 3-4). The effect of crusting on dust emission is clearly visible. In all experiments, the crusts significantly reduce dust fluxes in comparison to loose material. For Arenosol crusts, the dust emission is reduced from 3.87 to 0.005 mg m^{-2} s^{-1} on average, which is a reduction down to 0.14%, and the Luvisol the values went from 10.53 to 0.028 mg m^{-2} s^{-1}, which represent 0.26% of the emission from a loose surface.

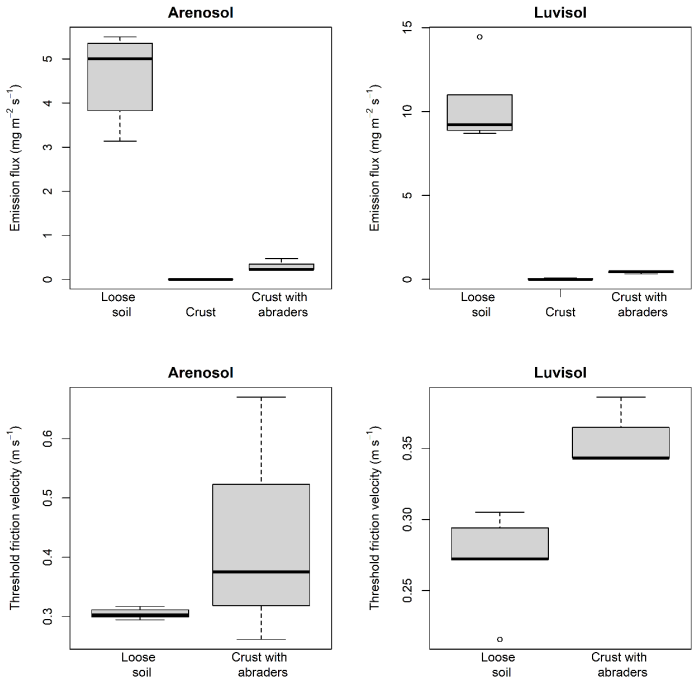

Figure 3-13. The emission flux calculated from the PI-SWERL experiments, using Eq. 3.

Table 3-4. Summary of results from PI-SWERL measurements on experimental crusts.

Soil type	Experiment type	Average threshold friction velocity (m s^{-1})	Average flux (mg m^{-2} s^{-1})	Flux ratio to loose run	Relative abrasion efficiency	Shear strength (kPa)
	Loose	0.305	3.872	-	-	-
AR	Crust	-	0.0053	0.14%	-	68.1
	Abraders	0.436	0.311	8.03%	0.012	-
	Loose	0.272	10.534	-	-	-
LV	Crust	-	0.0278	0.26%	-	92.0
	Abraders	0.357	0.425	4.03%	0.013	-

The threshold friction velocity is increased by the formation of a crust when abraders are present, which is a phenomenon that also been described in other studies (Gillette et al., 1982, 1980). Crusted soils without abraders do not have a threshold friction velocity since there is no significant emission. The thresholds of the loose and abrading surfaces translate into wind speeds of 5.7 and 8.1 m s^{-1} for Arenosol and 5.0 and 6.6 m s^{-1} for Luvisol respectively (z_0 = 1 mm). The difference between the threshold friction velocities between crusted and non-crusted surfaces is small compared to the difference in dust flux. The threshold of the abrader experiment is likely initiated by the movement of the loose abraders and is therefore not only influenced by the cohesion of the crust. Despite the fact that the threshold velocity will also be greatly influenced by larger roughness elements such as ridges and stubble (Marticorena et al., 1997; Wiggs and Holmes, 2011), this small-scale difference could have a significant influence on dust emissions form cropland.

The protection from crusts against wind erosion that our data presents is in line with other studies on the dust emission from crusted surfaces. Wind tunnel studies from Zobeck et al. (1991) and Yan

et al. (2015) describe how developed crusts can almost completely prevent wind erosion when there are no external abrader. Sweeney and Manson (2013) determine dust emission from loose and artificially crusted loess using the PI-SWERL. The dust emission from their loose material ranged from 0.1 to 4.5 mg m^{-2} s^{-1}, whereas the crusted surfaces range from zero to 1.4 mg m^{-2} s^{-1} at 0.69 m s^{-1}. Comparing these results to ours, here loose soils, especially the Luvisols, appeared to be more emissive, whereas the crusts appear to be more effective at protecting the surface. This difference could be attributed to differences in grainsize and the experimental set up for crust formation.

The protective effect of a crust is also smaller with the addition of abraders. In this case, the soils emit 8% and 4% of the emission of loose soils for Arenosols and Luvisols, respectively. Figure 3-14 shows an example of an Arenosol crust before and after an abrasion experiment. The crust is degraded, and large parts of the crust are removed by the abrading particles. This important influence of abraders on dust emission has been described by many wind tunnel studies (Houser and Nickling, 2001b; Rice et al., 1999, 1996; Zobeck, 1991a). Although the dust emission in runs with abraders is greater than without abraders, the amounts are still more than an order of magnitude smaller than those from loose surfaces. However, it might be possible that with longer duration of the experiments, the crusts could have been completely destroyed by abrasion and emission values could have reached the level of loose soils, as suggested by a field study on loamy sandy crusts from Goossens (2004). Future studies on field crusts will have to focus on the longevity of the crusting-induced reduction of dust emissions.

(a) **(b)**

Figure 3-14. A Luvisol crust from 15 mm rainfall before (a) and after (b) a PI-SWERL run with the addition of abraders.

Despite their greater strength (Table 3-4), the Luvisol crusts were on average more emissive for both the normal and abraded crusts, which is likely caused by the greater number of fine particles in the Luvisols. These findings do not agree with the field measurements on loamy to sandy crusts by Goossens (2004), which showed a negative exponential correlation between the crust shear strength and the horizontal and vertical dust flux. However, their wind tunnel measurements do not address

the influence of a continuous abrasion, which is simulated in the closed system of the PI-SWERL. Houser and Nickling (2001a) also described a negative correlation between crust strength and abrasion efficiency using wind tunnel experiments. The strength of their crust was greatly influenced by the presence of salts, whereas the differences in crust strength in our study are attributed to the concentration of fines. This suggests an interesting interplay of factors, where a greater concentration of fines results in a general greater PM_{10} emission, but also in a greater crust strength that limits the emission.

3.5 Conclusion

The high dust fluxes from loose Free State soils in this study support the result of Eckardt et al. (2020) that sandy cropland soils play a role as a source of atmospheric dust in southern Africa, in addition to the aerosols generated by natural surfaces. Our results show that physical soil crusts can form rapidly on loamy sand and sandy loam cropland soils, and that these crusts have the potential to reduce dust emissions on these fields which concurs with other studies on sandy loamy soils (Goossens, 2004; Yan et al., 2015). Crusts formed on Arenosols and Luvisols by 15 mm of experimental rainfall minimized the PM_{10} emission flux to less than 0.5% of the emission from a loose soil. We expect that the most significant formation of crusts occurs during the start of the rainy season, before the growth of crops protects the soil from the impact of raindrops, and that these crusts can last into the dust season. However, even during the dry season crust formation by sequenced rainfall appears possible.

Our results underline the importance of physical soil crusts in dust prevention on sandy soils in the Free State and in many other regions in the world. The results illustrate that crust-protecting land management could be very advantageous to minimize dust emission from bare agricultural fields. These practices may include the limitation of ploughing, mechanical cultivation, and animal trampling after harvest. The trade-off between reducing dust emission and increasing the risk of run-off and water erosion has to be further studied.

Abraders play an important role in increasing the PM_{10} emission and the erosion of crusts, as also suggested by previous studies (Houser and Nickling, 2001b; Langston and McKenna Neuman, 2005; Rajot et al., 2003; Rice et al., 1999, 1997). This indicates that active prevention of the mobilisation of abrading sand particles should also be considered as an important measure to minimize dust emissions. These measures could include the preservation of crop stubble or the placement of roughness elements, such as fences or shrubs at the border of fields combined with a reduction of the field sizes.

While the results of this study seem to be very plausible and straightforward, we would like to point out that this knowledge is gained under laboratory conditions and that further experiments and field measurements on natural crusts are necessary to test these findings. The influence of abraders is commonly studied with wind tunnel measurements (Houser and Nickling, 2001b, 2001a; Rice et al., 1999, 1996; Rice and McEwan, 2001). Wind tunnel experiments on abrasion conditions would offer

a cross-comparison with our PI-SWERL results, field dust emission monitoring, and synoptic weather data. Furthermore, measurements with the PI-SWERL in the field would offer the possibility to gain a more representative understanding on emission characteristics by testing a wider range of crust strengths, textures, and abrasion conditions.

Acknowledgments: We wish to thank the Swiss-South Africa Joint Research Programme, the Swiss National Science Foundation, and the National Research Foundation. We would also like to thank the Agricultural Research Council for making the data of their climate station available to us. We would like to thank Hannes and Sophia Prinsloo, A.C. van Wyk, and Sias van Rensburg for allowing us to take measurements on their field and providing us with information on their fields.

4.

Assessing the PM_{10} emission potential of sandy, dryland soils in South Africa using the PI-SWERL

Heleen C. Vos*, Wolfgang Fister*, Johanna R. Von Holdt**, Frank D. Eckardt**, Anthony R. Palmer*** & Nikolaus J. Kuhn*

* Physical Geography and Environmental Change, University of Basel, Basel, Switzerland

** Department of Environmental and Geographical Sciences, University of Cape Town, Cape Town, South Africa

*** Institute for Water Research, Rhodes University, Grahamstown, South Africa

Published in Aeolian Research, 2021, Volume 53, 100747

https://doi.org/10.1016/j.aeolia.2021.100747

4.1 Abstract

The Free State has been identified as the region with the most dust sources in South Africa. These dust sources can be linked with the large, heavily cultivated cropland areas in this province, which leaves fields vulnerable to wind erosion after the harvest in the winter. For this study, the focus was on the factors that influence the emission from bare, flat surfaces on agricultural lands in this region. The Portable In-Situ Wind Erosion Laboratory (PI-SWERL) was used to measure the emission flux from adjacent crusted and loose surfaces, which was combined with shear strength, moisture, and soil texture measurements. Boosted regression tree (BRT) analyses were used to identify the variable with the highest relevance on the emission flux.

On the whole dataset, that the shear strength is the most important variable that controls the emission. This is reflected in the significantly lower emission from the crusted surfaces (0.49 mg m^{-2} s^{-1}) compared to that of loose surfaces (2.34 mg m^{-2} s^{-1}). However, for crusted surfaces, the presence of abraders appeared to be the most significant factor in emission, showing a power relationship between the abrader count and the emission flux (R^2 = 0.76). In the case of the loose surfaces, the presence of clay and silt was a major influence in emissivity, with a linear relationship between the two variables (R^2 = 0.68). This difference in factors depending on the agricultural disturbance, asks for a more holistic approach when predicting emission from such arid cropland areas.

Keywords: PI-SWERL, dust emission, croplands, South Africa, soil crust

4.2 Introduction

Dust emission is an important process that has an impact on climate (Boucher et al., 2013; Shao et al., 2011; Tegen et al., 1997), the global chemical flux (Lawrence and Neff, 2009; Mahowald et al., 2009), public health (Goudie, 2013; Sprigg, 2016), and the degradation of croplands (Bridges and Oldeman, 1999; Chappell et al., 2019, 2012; Oldeman, 1992; Sterk et al., 1996; Visser and Sterk, 2007). Due to climate change, the emission of dust from disturbed soil surfaces from arid regions is expected to increase (Mahowald and Luo, 2003; Shepherd et al., 2016; Tegen et al., 2004; Woodward et al., 2005), which could enhance the on- and off-site effect of dust emission. Several studies have determined the sources of dust and the factors controlling the emissions. While remote sensing is suitable in the identification of emission hot spots (Vickery et al., 2013; von Holdt et al., 2017) small-scale factors that influence dust emission require detailed field observations (Bielders et al., 2001; Chappell et al., 2008; Goossens, 2004; von Holdt et al., 2019).

One region that has been recently identified as an important source for dust emissions, and is our focus here, is the central to north-western part of the Free State Province, South Africa (Eckardt et al., 2020) as seen from the MSG (Meteosat Second Generation) and SEVIRI (Spinning Enhanced Visible and Infrared Imager) imagery. It was reported that 71% of all South African dust sources in this record are situated in the Free State Province and are mainly associated with areas of extensive dryland crop farming, suggesting a strong anthropogenic origin of these dust emissions. This is in

contrast to natural dust sources that have been identified as the dominant source areas for dust emissions in the rest of southern Africa, where the Etosha pan, the Makgadikgadi pan, coastal regions, and the Kalahari Desert are the main emitter of dust (Ginoux et al., 2012; Vickery et al., 2013; von Holdt et al., 2017). Despite the significant presence of pans in the Free State (Geldenhuys, 1982), the size of pans is still very small compared to the croplands area. Eckardt et al. (2020) described the land cover of a 10 km radius of the dust source points and found that less than 1% consists of pans, whereas 34% consist of agricultural land, and 55% of grassland and low shrubland.

Agricultural areas are predicted to be subjected to climatic changes, including an increase in wind velocities and a decrease in rainfall (Archer and Tadross, 2009; Mahowald and Luo, 2003; Thomas et al., 2005), which would enhance dust emission. The impact of soil degradation by wind erosion, due to the loss of nutrients and organic carbon from agricultural lands, leads to reduced land productivity (Sterk et al., 2001; Visser and Sterk, 2007). The dust sources identified from MSG (Eckardt et al., 2020) revealed a dust season from August till November (late winter and spring) which correlated with the crop cycle and farming practices. The dust season was particularly pronounced during the drought cycle in 2016, which left many of the fields fallow and without wind protection. However, significant dust emission patterns between fields and years were noted in the decade long dust record (Eckardt et al., 2020) which raises questions regarding factors that control the dust emission from South Africa's maize production areas.

The main characteristics that control the emissivity from a surface include soil composition, surface cohesion, and surface roughness and cover (Fryrear et al., 1998; McKenna Neuman et al., 2005; Shao et al., 2011; Webb et al., 2013; Webb and Strong, 2011). These parameters are determined by the soil texture and chemistry, the moisture content, the presence and characteristics of crusts, the aggregate content, the presence of clods, the roughness from tillage practices, and the presence of crops or stubble cover, among others (Funk and Engel, 2015; Gillette, 1988; Leys et al., 1996; Munkhtsetseg et al., 2017; Sterk, 2003). Two studies from the Free State provide some preliminary characteristics. Wiggs and Holmes (2011) described the importance of aerodynamic roughness on the threshold friction velocity, by monitoring a disturbed, bare field, where the roughness was the result of ridges and clods. The crusts that form on the croplands are expected to be physical crusts since biological crusts are sensitive to disturbance and develop slowly, a process that can take multiple decennia (Belnap et al., 2001). Vos et al. (2020) developed and tested physical soil crusts in the laboratory from soils sampled in the Free State. The study described a strong reducing effect of the soil crusts on the emission of dust, in comparison to the emission from surfaces with Loose Erodible Material (LEM) (Zobeck, 1991b). Furthermore, Vos et al. (2020) found that even with the presence of abraders, dust emission from crusted sand and loamy sand surfaces is lower than from loose surfaces by a factor of 10. These recent findings contradict previous studies that described physical crusts on these soil types as weak, with little potential to minimize wind erosion (Rajot et al., 2003; Rice et al., 1999) due to the lack of fines. However, the soils in the Free State could have a range of soil textures, chemistry, cohesion, and abrasion conditions compared to those used in the laboratory. Furthermore, cropland

crusts could have experienced more degradation and might have formed under different rainfall conditions. Therefore, it is important to compare the results from the laboratory study to dust emission measurements from croplands.

To determine the emissivity of a surface, wind tunnels have been used in many studies since this offers a precise indication of the losses from a surface and response to measured wind velocity (Belnap et al., 2007; Fister and Ries, 2009; Leys and Eldridge, 1998; Li et al., 2015; Liu et al., 2006; McKenna Neuman and Scott, 1998). The disadvantage of wind tunnels is their large size, which makes it time-consuming to deploy the instrument and to measure on smaller surfaces. An alternative method is the Portable In-Situ Wind Erosion Laboratory (PI-SWERL) (Etyemezian et al., 2007). The PI-SWERL consists of a 30 cm diameter chamber that is placed on a surface, with an annular blade that exerts a controlled friction velocity to the surface. The particles with a diameter below 10 micrometre (PM_{10}) that are emitted as a response is measured with a DustTrak 8530. The advantage of the PI-SWERL, in comparison to wind tunnels, are its small size, lower weight, and high frequency of measurement runs, which enables many repeated measurements in a relatively short time. The major disadvantage of the PI-SWERL is its shallow annular blade (at 5 cm height) and lack of a naturally developed logarithmic wind profile, making it less representative of natural wind erosion and determining the influence of surface roughness then requires a separate assessment (Bacon et al., 2011; Etyemezian et al., 2014). Despite these disadvantages, the PI-SWERL was successfully used under laboratory conditions to assess dust emissions from crusts and loose substrates (van Leeuwen et al., 2021; Vos et al., 2020) and on different surface types in various regions of the world. Field studies have been performed on grasslands (Munkhtsetseg et al., 2017, 2016); alluvial landscapes (von Holdt et al., 2017, 2019); mining areas (Wang et al., 2015), and a variety of desert landforms (Bacon et al., 2011; Cui et al., 2019b, 2019a; Sweeney et al., 2016; Sweeney and Mason, 2013). Despite this large number of PI-SWERL studies, agricultural lands have received little attention so far, with the exception of Cui et al. (2019a). As emissions from agricultural surfaces represent between 10% (Tegen et al., 2004) and 25% (Ginoux et al., 2012) of global dust sources, it is paramount to understand such areas and the PI-SWERL presents the perfect opportunity to assess these surfaces.

Combining the need to further understand the relevance of crusts for reducing dust emissions from sandy dryland soils, the respective soil and surface properties, the processes that influence emissions in real-world conditions, and the suitability of the PI-SWERL to determine emissivity on cropland, the aims of this study were:

1. Determine to which extent physical soil crusts minimize dust emissions from cropland.
2. Determine the main factors that influence the emissivity of croplands from loose erodible material and crusted surfaces.
3. Determine how the emission from field surfaces compare to the emissions from laboratory surfaces.

In order to achieve these aims, this study combines dust emission measurements using PI-SWERL, data and observations, describe soil surface properties, such as moisture content, soil texture, carbon content, and surface cohesion. In addition, the emission from a pan and an adjacent grassland were measured to generate a reference emission value for dominant land cover and known dust sources. The research was carried out from August to October 2019 (the winter dust season) in the Free State province of South Africa. Measurements were made on crusted and loose erodible material surfaces at different fields with different agricultural management.

4.3 Materials and methods

4.3.1 Study area

The study area is in the north-western part of the Free State, 100 km north of the State capital, Bloemfontein (Figure 4-1). This area has been identified as a hotspot for dust emission (Eckardt et al., 2020) in southern Africa. This region was also chosen because it enables the investigation of two different soil types that are predominant in the region and known for sustaining agriculture: Luvisols and Arenosols (Jones et al., 2013). Both soil types are characterised by their sandy texture, which makes them highly suitable for water storage under the local climatic conditions (Hensley et al., 2006) and therefore suitable for dryland cropping.

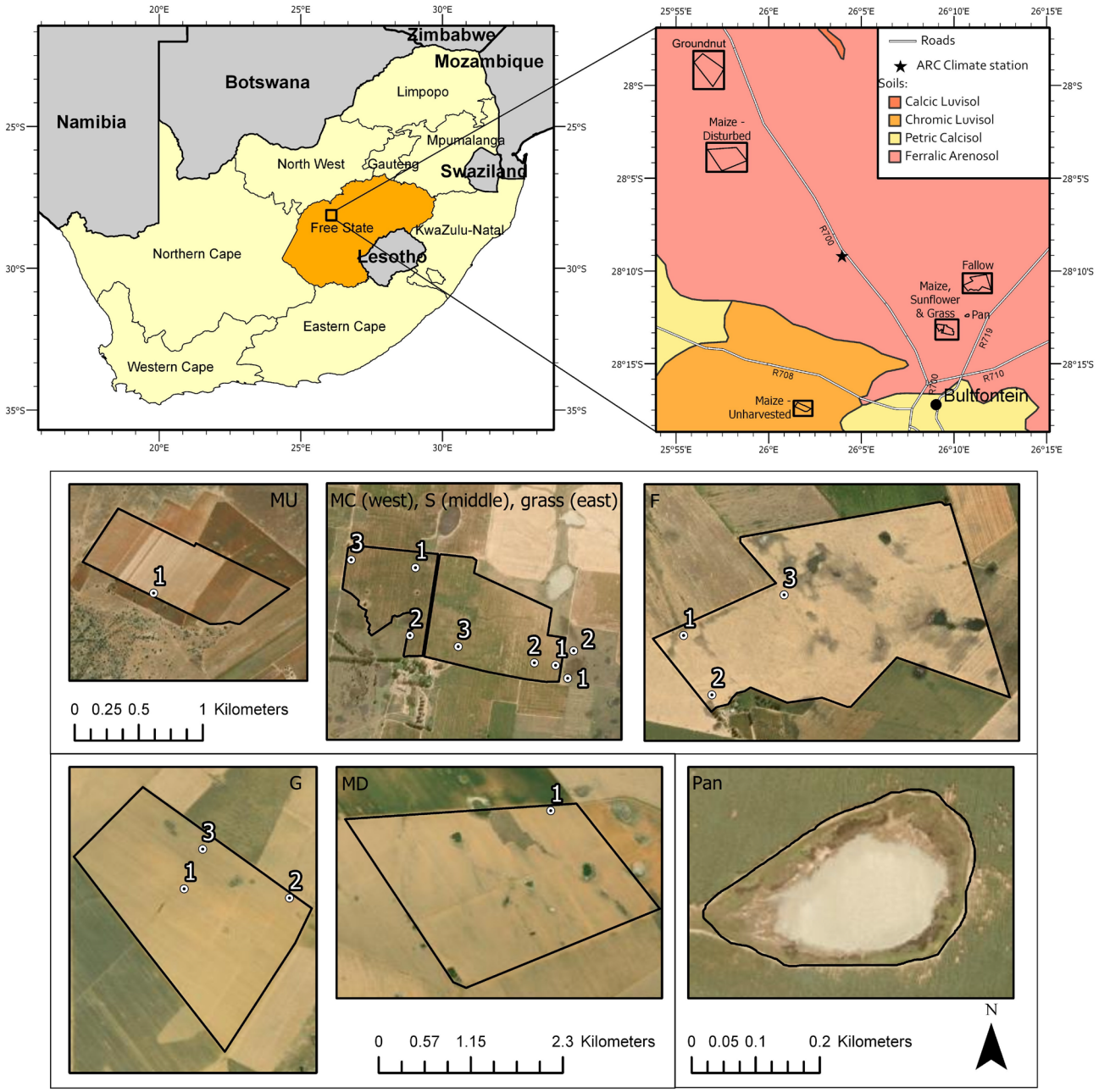

Figure 4-1. Maps depicting South Africa and the Free State province (top left) and the selected study area and test fields with dominant soil types (top right). The aerial images below illustrate the individual fields that were selected for emissivity measurements with respective positions of test plots. Soil data from the Soil and Terrain Database (SOTER) for South Africa (FAO-ISRIC-2).

The Free State has a semi-arid climate, with annual rainfall ranging from 400 to 600 mm (Hensley et al., 2006), 80% of which takes place between November to April (summer). During the dust event months, which is mainly between August and November, the average daily maximum wind velocity is 5.4 m s^{-1} and 10% of the days have a maximum wind speed above 7.7 m s^{-1}. The rainfall is on average 104 mm in total during the main dust season. The climate in the study area has been described in more detail by Vos et al. (2020). The main crop produced in this region is corn (maize) with about

82% of the total crop production in the Free State (DAFF, 2018). This is followed by sunflower (7%), soybean (6%), wheat (4%), and groundnuts (1%). Most of these crops are planted at the beginning of the rainy season and harvested between May and August. There are few exceptions from this cycle, for example, winter wheat, which is planted at the end of July as a cool-season fodder crop.

4.3.2 Field description

Six agricultural fields were selected for the field measurements: a fallow field (F), a harvested groundnut field (G), a harvested sunflower field (S), an unharvest maize field (MU), and two harvested maize fields (maize-crusted (MC) and maize-disturbed (MD)) (Figure 4-1, Figure 4-2, and Table 4-1). Furthermore, a pan and two grassland plots were selected for comparison measurements. All the agricultural fields were situated on Arenosols, apart from the unharvested maize field that was on a Luvisol. These fields were chosen for their variety of agricultural management practices, which resulted in a range of different surface characteristics, such as regarding soil crusts, roughness, cohesion and aggregate content. It should be noted that the crop type on each field can be alternated each year so that the used names are only a descriptor for the crops and agricultural management in the specific season preceding the fieldwork. The sunflower field was harvested at the end of July. Bordering on the west of the sunflower field is the crusted maize field, which was a field with crusted surfaces and tire tracks. On the disturbed maize field, the removal of loose plant material resulted in the disturbance of the crust. The groundnut field was harvested by removing the entire plant, leaving no stubble on the ground, which made this field different from the maize and sunflower fields that still held some stubble. The groundnut field showed sand deposits with ripple marks that covered the crusts, which is a sign of active movement by wind. The fallow land had not been planted the previous year and has been treated with herbicide (Round-up). Because this field has not been disturbed, it was fully covered with a soil crust. The selected Luvisol field carried unharvested maize and consisted fully of crusts. The selected grassland was not cultivated due to the high clay content in this area (personal communication with the farmer, Mr H. Prinsloo). The pan had a surface area of roughly 5 ha and consisted mainly of a clay surface, with salt deposits at the rim.

Table 4-1. Overview of the fields that were selected for this study. The plots, PI-SWERL runs, and surface types are explained in the text.

Field	Abbreviation	Plot count	PI-SWERL count	Surface types
Fallow field	F	3	48	Crust
Groundnut	G	3	48	Crust and sand deposits
Sunflower	S	3	40	Crust and loosened soil
Maize Unharvested	MU	1	2	Crust
Maize Crusted	MC	3	38	Crust and loosened soil
Maize Disturbed	MD	2	3	Loosened soil
Grass	-	2	14	-
Pan	-	Cross- section	37	-

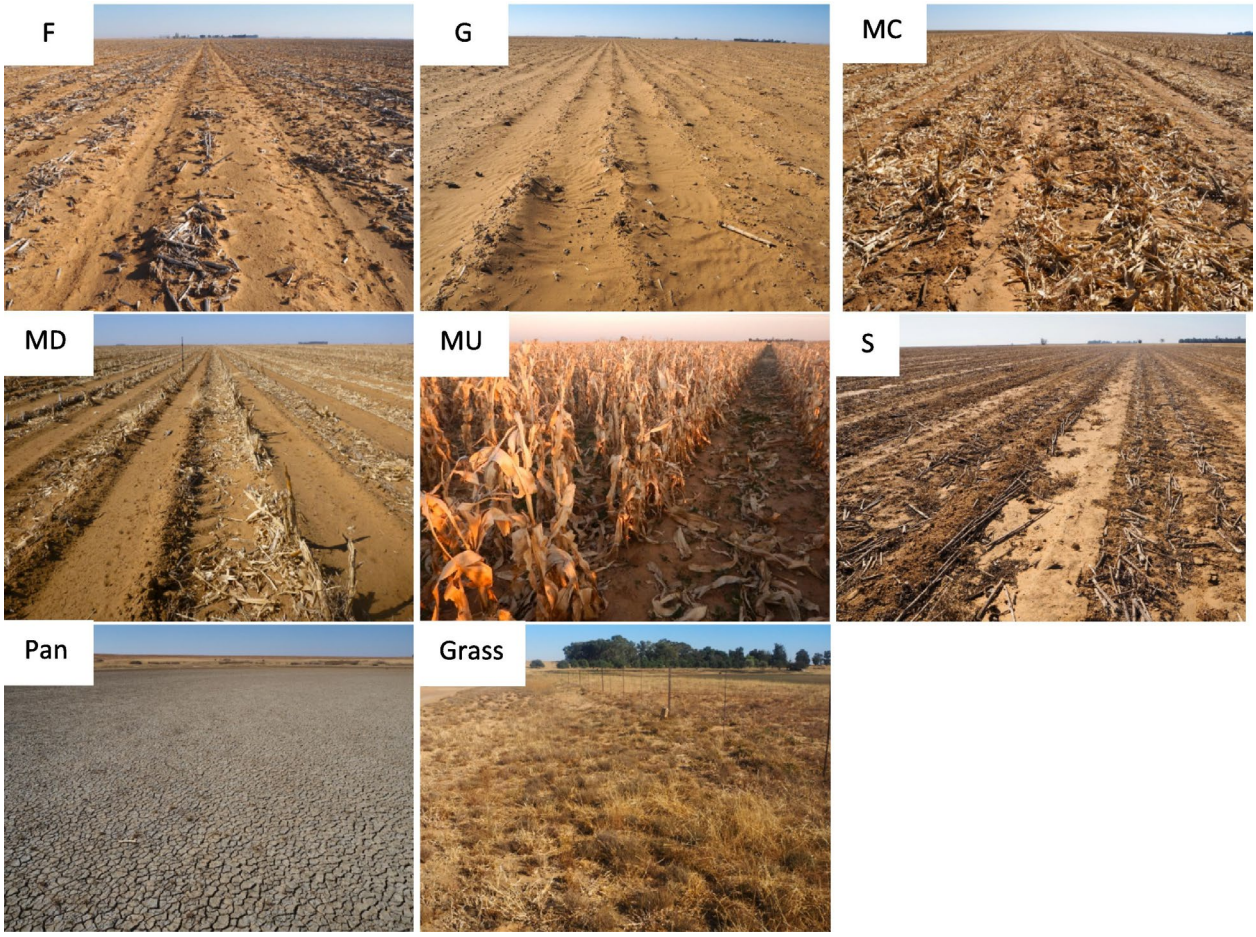

Figure 4-2. Examples of the six fields that were selected for field measurements.

The measurement sites were chosen using a stratified randomized approach. For each field, one to three plots which covered roughly a 10 x 10 metre area, were selected for measurements (Figure 4-1). These plots were selected based on a textural gradient or, when no clear texture gradient was initially visible, a spatial distribution. Figure 4-3 illustrates that a significant variation in grain size exists, both, between and within the fields. In general, the groundnut field, sunflower field, and maize-disturbed field had the lowest concentration of clay and silt, whereas the unharvested maize field with the Luvisol soil has the largest concentration. The within-field variation in texture appears to be the most significant in the groundnut and sunflower fields, which were the fields where a texture gradient was present. For the pan, a cross-section was made along which was measured to capture the heterogeneity of the pan.

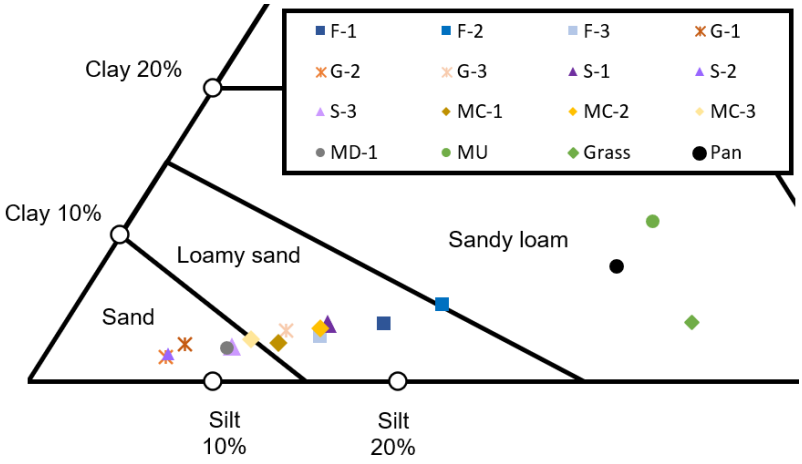

Figure 4-3. Average soil texture of the field plots (F = Fallow, G = Groundnut, S = Sunflower MC = Maize Crusted, MD = Maize Disturbed, MU = Maize Unharvested, Grass = Grassland surface).

Within each plot, crusted and LEM surfaces that held less than 5% clods were randomly selected for PI-SWERL measurements. The LEM surfaces consisted of sand deposits and soil that was loosened by tracks (Figure 4-4 and Table 4-1). In the field, clod content was estimated based on charts for surface proportion estimates. Later, the surface areas of the clods were determined by measuring the diameter and counting the number of clods in an image of the areas sampled by the PI-SWERL. Surfaces with more than 5% clods were excluded because the quality of PI-SWERL measurements on surfaces with high roughness is not well understood (Bacon et al., 2011; Etyemezian et al., 2014). Since the aim of this study was to understand the emissions of loose substrates and crusts in the field, this omission did not limit the scope of this study.

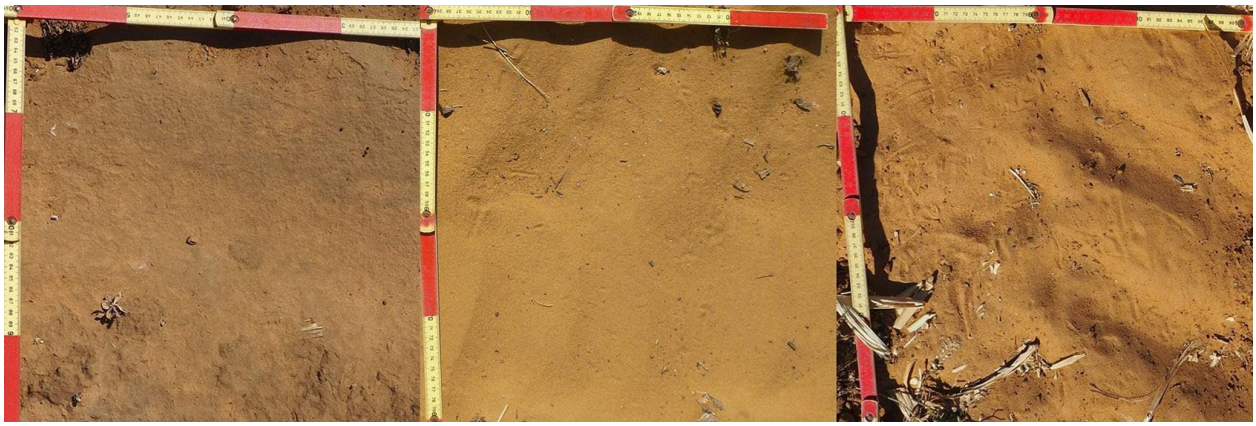

Figure 4-4. Examples of the surface types: left crust (S), middle sandy deposit (G), and right loosened soil (MC).

The PI-SWERL is an instrument that has been used by many different studies to assess the emissivity of small, flat surfaces, which can then give insight into the emission potential of different landforms and the controlling factors and processes (Etyemezian et al., 2007; Sweeney et al., 2016; von Holdt et al., 2019). The PI-SWERL used for this study has a diameter of 30 cm. The instrument was placed on representative areas, avoiding large stubble and clods that could disturb the airflow inside the PI-SWERL (Figure 4-5). A PI-SWERL run consisted of 30 seconds at 0 RPM, after which the

RPM was increased to 2250 RPM in 120 seconds, where it was kept for 5 minutes. At the end of the run, the RPM was brought back to zero in 10 seconds. An RPM of 2250 is in accordance with a friction velocity of 0.56 m s^{-1} assuming an alpha value of 0.90 as described by Etyemezian et al. (2014). This is a friction velocity that is similar to the one used in most PI-SWERL (Sweeney et al., 2011, 2008; Sweeney and Mason, 2013; von Holdt et al., 2019). It represents a wind velocity of approximately 11 m s^{-1} at 2 metre height, a common velocity during wind events in the Free State and has been linked with observed dust events (Eckardt et al., 2020; Vos et al., 2020). This friction velocity can mobilize particles above 1 mm diameter, according to models from both Bagnold (1941) and Greeley and Iversen (1985). For each run, a DustTrak 8530 measured the PM_{10} concentration from which the emission flux, E_{PI} in mg m^{-2} s^{-1} can be calculated using the formula from Sweeney et al. (2008):

$$E_{PI,i} = \frac{\sum_{begin,1}^{end,i} C*F*1s}{(t_{end,i} - t_{begin,i})*A_{eff}}, \quad (3)$$

Whereby C is the PM_{10} concentration in mg m^{-3}, F is the blow rate in m^3 s^{-1} which was approximately 0.1 m^{-3} s^{-1} throughout the run, t_{begin} is the start time and t_{end} is the end time in seconds of the aimed RPM step *i* (in this case 2250 RPM), and the A_{eff} is the effective surface which was 0.035 m^2. The PI-SWERL is also equipped with four Optical Gate Sensors (OGS), which measured the number of saltating particles passing the sensor, expressed in Hz, as described by Etyemezian et al. (2017). The count of the four sensors was averaged for the analyses on the abrader quantity during the PI-SWERL run.

Multiple PI-SWERL runs were conducted at each test plot on the six different fields. In order to increase the number of PI-SWERL measurements, without simultaneously increasing the time necessary to describe the positions and to take samples, pairwise test runs were chosen as the best solution. It was assumed that soil moisture, texture and roughness did not change significantly between the two directly adjacent positions. Therefore, only the surface strength measurements were done individually for all test runs.

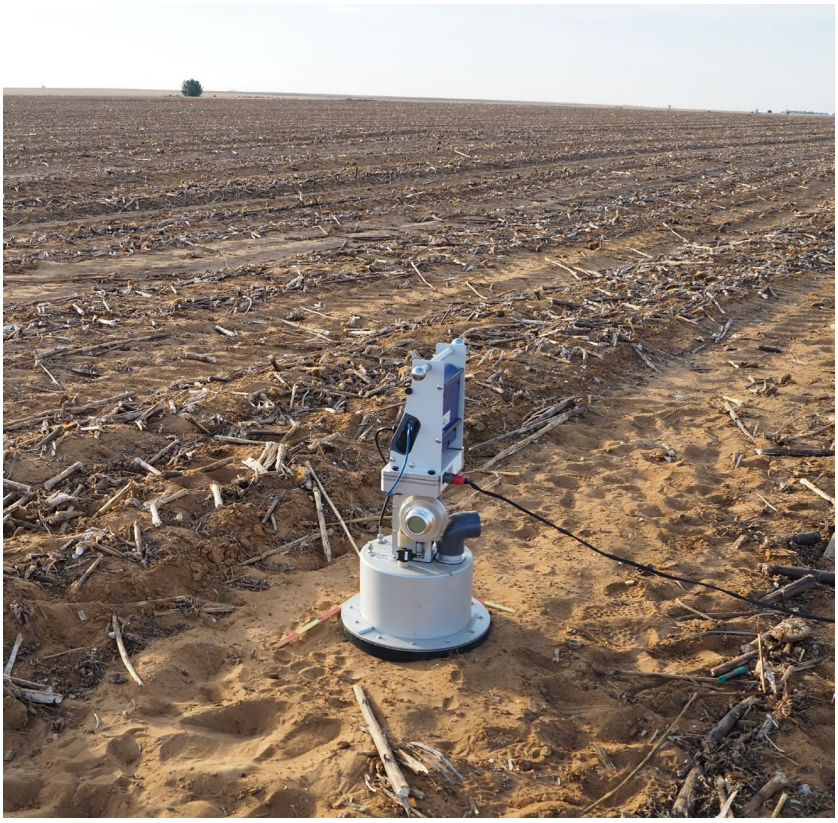

Figure 4-5. The PI-SWERL performing a measurement in the sunflower field.

4.3.3 Surface characterisation

For each PI-SWERL run, the soil surfaces were characterised to determine which factors control their emissivity. The soil properties that were measured are the surface strength, soil texture, moisture, and aggregate content. The surfaces were furthermore classified based on their morphology and structure into crusts or LEM surfaces, from which the latter can be split into loosened soil or sand deposits.

The surface strength was regarded as the most important indicator for the emission potential, both for crusted surfaces (Feng et al., 2013; Goossens, 2004; Houser and Nickling, 2001a; Rice et al., 1996; Rice and McEwan, 2001; Sharratt and Vaddella, 2014), as well as non-crusted surfaces (Goossens and Buck, 2009; von Holdt et al., 2019). The surface strength was measured with a torvane, an instrument that measures the torsional shear stress before failure in kPa, commonly used in wind erosion studies (Ellis et al., 2012; Gillette et al., 2001; Goossens, 2004; Goossens and Buck, 2009; Li et al., 2010; Sweeney and Mason, 2013; von Holdt et al., 2019). The torvane used in this study is custom-designed to capture the strength of just the topsoil surface and consists of eight blades with a penetration depth of three millimetres (Kuhn and Bryan, 2004). For each PI-SWERL run, 10 torvane measurements were performed next to the test surface and averaged.

For each pairwise PI-SWERL set, one sample each was collected for the measurement of soil moisture and soil texture. This aggregated sampling was executed in order to minimize the total

number of soil samples, because a significant variability in soil texture and soil moisture was not expected within the distance of 1 meter. The samples were taken from the top 1 cm to capture the characteristics of the surface exposed to the dust emission experiment. The soil samples were afterwards dried and analysed for their moisture content, grain size, and carbon content, using a Malvern Mastersizer 2000 and a Leco RC612, respectively. To disperse the sample before the grain size measurements, the samples were sonified at 60 J ml^{-1} in 12 seconds with no chemical dispersant. The moisture content was measured gravimetrically by drying the samples at 100 degrees Celsius. The effect of soil moisture on the emission of a surface has been described elsewhere (Cui et al., 2019b; Funk et al., 2008; Munkhtsetseg et al., 2016; von Holdt et al., 2019; Wang et al., 2015). The relative humidity and air temperature were recorded during the PI-SWERL measurements.

4.3.4 Statistical analyses

The statistical difference between crusted and LEM surfaces per field plot was determined using two-tailed t-tests, with an alpha value of 0.05 to determine statistical significance. A Boosted Regression Tree (BRT) machine learning analysis was used to determine the relative importance of and interactions between the measured soil surface properties and the emission flux from these surfaces as measured by the PI-SWERL (Elith et al., 2008). A BRT model was used by Von Holdt et al. (2019) to investigate the relationships between surface properties and emission flux measured with the PI-SWERL in the alluvial landscapes of Namibia. The BRT analysis provides the relative influence each input variable has on the dependent variable, which is in this case the emission flux measured by the PI-SWERL. The BRT models were run with the R package *gbm* was used (Ridgeway, 2007). A learning rate of 0.01, an interaction depth (or tree complexity) of 5, a bag fraction of 0.6, a cross fold of 10, and a maximum number of 1000 trees was used.

Per surface type, two different BRT analyses were performed. The BRT analyses presented in the text contains the main variables of interest, namely the surface shear strength, soil moisture, clay and silt content, and the content of Total Organic Carbon (TOC). For the crusted surfaces, also the OGS counts have been used which represents the count of abrading sand grains during a run. This can be regarded as an external factor for the emission flux in the case of undisturbed crusts. For the LEM surfaces, the OGS count is regarded as an indication of the disturbance or texture, rather than an external influence on emission. The clay and silt contents have been chosen as the only property to represent soil texture since there is a large covariance between these values and the sand content. Using all of these texture-related parameters would have reduced the strength of results received by this method. The second BRT analyses contain all the parameters that were measured, e.g., the surface shear strength, soil moisture, clay and silt content, TOC, Total Inorganic Carbon (TIC), and air humidity and air temperature. These analyses were performed to put the results of the first BRT in a wider context, at least qualitative, even if this is outside the immediate scope of the paper.

4.4 Results and discussion

4.4.1 Surface conditions and emissions

The results from the PI-SWERL runs and shear strength measurements show that crusted surfaces have the lowest emissions in general, but show significant variance per field (Figure 4-6 and Table 4-2). In contrast, loosened soils are the most emissive surfaces, among which the highest emissions are from loosened soil in maize fields. The sand deposits in the groundnut field, which can be associated with wind erosion, had a much lower emission than the loosened soils. T-tests of the emission fluxes between surface types on each field plot, where statistical significance is defined as $p < 0.05$, show that the LEM surfaces, the loosened soils and the sand deposits, have a higher emission flux than crusted surfaces. Regarding shear strength, crusted surfaces have a much higher average cohesion, considering the average is between 11.1 and 14.1 kPa for crusted surfaces and between 4.5 kPa and 6.9 kPa for loose surfaces. This relationship is reversed for the average OGS count, which is significantly higher for the LEM surfaces (between 291 Hz and 452 Hz) than the crusted surfaces (between 56 and 111 Hz).

The cropland surfaces have an average emission of 0.78 mg m^{-2} s^{-1} and are relatively high in comparison with other studies. Von Holdt et al. (2019) for example measured average emissions from LEM surfaces of 0.32 mg m^{-2} s^{-1} and for medium and high saltator crusts 0.086 mg m^{-2} s^{-1} and 0.34 mg m^{-2} s^{-1}, respectively. The arable land measured by Cui et al (2019) also showed lower average emissions of 0.231 mg m^{-2} s^{-1}. By comparing dust emissions from agricultural fields to emissions from natural grassland or pan surfaces their relative importance can be seen, despite the fact that causes and processes, for example, drag absorption by plants, are different. Grassland surfaces show very little dust emission (0.03 mg m^{-2} s^{-1} on average), whereas pans can show very high emissions, which are statistically comparable to the ones from loosened soils. The variance of emissions from pans is very high however, and the median of the emission flux is as low as that of crusted surfaces. Additional data on the measurements on the pan and grassland surfaces are shown in the supplementary materials (Table S1), which again demonstrates the high variability of surface characteristics within the pans. Combining this with their small size in comparison to that of agricultural fields indicates that more observations on Free State pans are required for a full assessment of their contribution to dust emissions. In contrast, grasslands can be considered insignificant, when it comes to dust emission in this region.

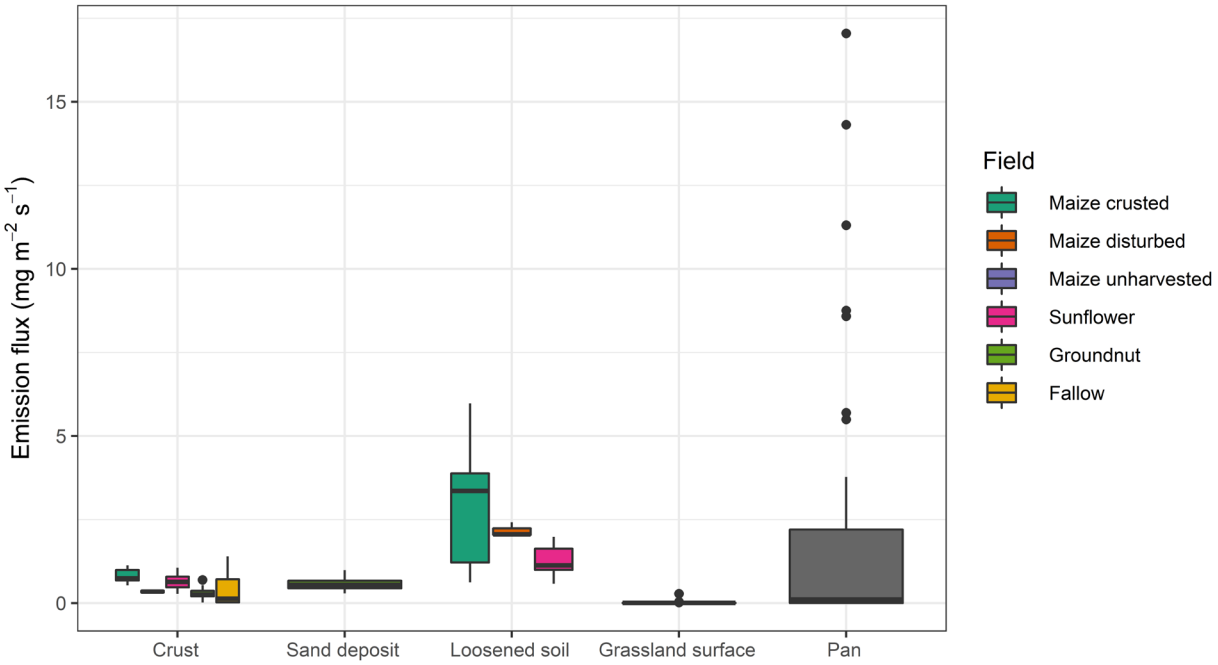

Figure 4-6. The emission flux of each surface type per field as measured by the PI-SWERL at a friction velocity of 0.56 m s-1 with Tukey test results showing the statistical significant groups. More information on these measurements are given in Table 4-2.

Table 4-2. The results from the PI-SWERL measurements at a friction velocity of 0.56 m s-1 per field and surface type. For shear strength measurement per PI-SWERL run n = 10.

		Flux emission (mg m^{-2} s^{-1})		Shear strength (kPa)		Average OGS count (Hz)	
Type	**Count**	**Mean**	**σ**	**Mean**	**σ**	**Mean**	**σ**
Crust	133	0.48	0.35	13.4	3.6	104	79
Sand deposit	18	0.57	0.22	6.1	1.7	291	178
Loosened soil	28	2.34	1.47	4.6	1.6	348	256

4.4.2 Surface properties determining emissivity on all sites

The generated data set can be used to identify the most relevant soil surface properties for emissivity by performing BRT analyses. The first analysis comprised the entire data set and aimed at identifying the main controlling factors for emissivity. The results of this analysis are shown in Figure 4-7, with the relative influence (in %) and the marginal effect of each factor. Hereby the marginal effect represents the influence of a variable on the emission flux without the influence from any of the other variables. These results show that shear strength has the greatest influence, with a relative influence of 74.7%. The marginal effect of shear strength shows the highest value below 5 kPa, where it has a value of 2.5, and the lowest value above 10 kPa, where it has a value of 0.5. This would mean that the shear strength alone increased the emission flux five-fold for our dataset when it is below 5 kPa compared to when it is above 15 kPa. Between these values, the marginal effect shows a steady decrease, which could represent an almost linear or exponential negative relationship between shear

strength and emission flux when only these two values are considered. It is important to note however that the marginal effect is calculated with the BRT analysis and is not based on any functional relationship. The high relevance and the marginal effect of the shear strength explain the high emissions observed on the loosened soils because these surfaces had the lowest shear strength (Figure 4-8). They also indicate that shear strength above 15 kPa is most effective in reducing emissions, which matches with the low emission from the crusted surfaces.

The BRT analysis furthermore shows a small positive influence of the TOC content, with the most significant increase in marginal effect being between 0.1 and 0.3%. This means that above a TOC of 0.3%, the influence of a change in TOC on emission is neglectable. The moisture content has a low effect, which was expected since the measured moisture content (0.25% mean, 0.17% STDV, 0.81% maximum) was below the level where moisture is described to have an effect, which is above 1% (Cui et al., 2019b; Funk et al., 2008; Munkhtsetseg et al., 2016; von Holdt et al., 2019). This would of course only be relevant for our PI-SWERL measurements, since moisture could still be a relevant factor for the temporal variability of wind erosion, as described by Wiggs and Holmes (2011). Surprisingly, the clay and silt content can be considered insignificant for the emission, when differences in surface type are not considered. Similar results can be found in the BRT analysis including the complete variable set (Supplementary). This analysis also shows a high importance of humidity and temperature, which is an influence also described by Etyemezian et al. (2019) and McKenna Neuman (2004). Since daily weather conditions and access to sampling sites limited the ability to carry out PI-SWERL tests systematically at constant relative air humidity and soil temperature, more research should be done to the influence of these variables. Also in this analysis, the shear strength remains the variable with the highest relative influence.

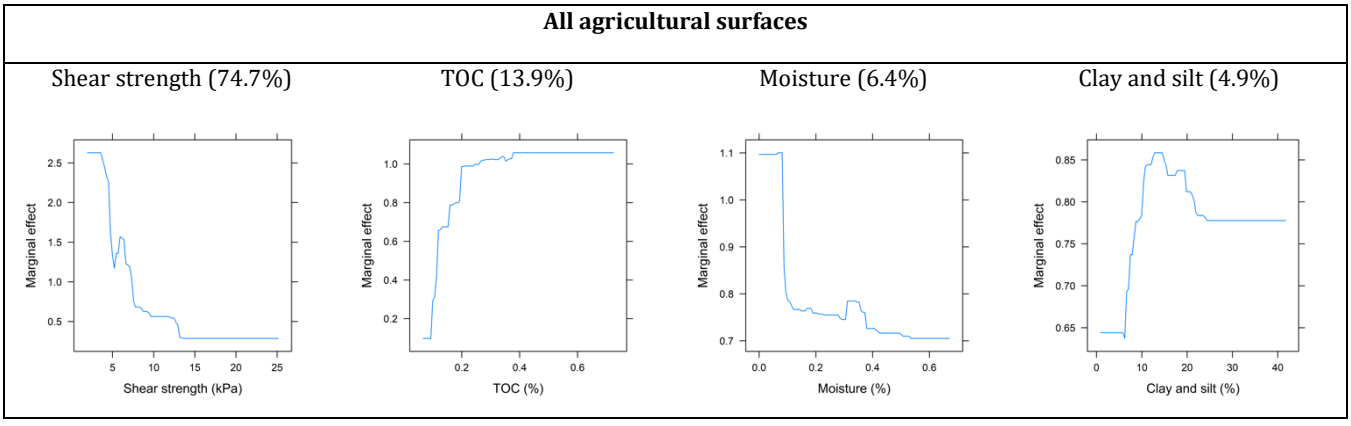

Figure 4-7. The results from the BRT analyses on the whole data set, showing the relative influence on the emission flux in percentage for each variable, and the marginal effect of this variable.

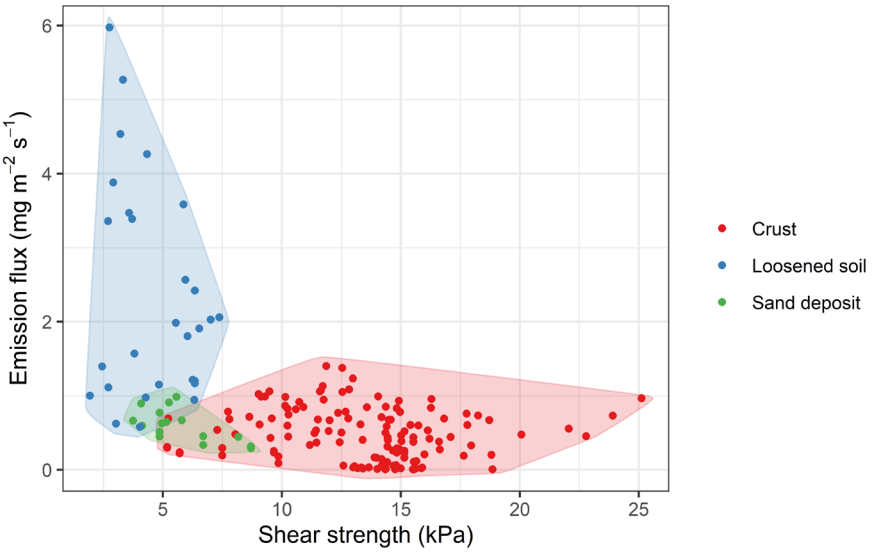

Figure 4-8. The average shear strength of the agricultural surfaces versus the emission flux at a friction velocity of 0.56 m s^{-1}.

4.4.3 Surface properties determining emissions on individual surface types

The large relative influence of shear strength when considering all surface types may mask some unexplained variability for individual surfaces (Figure 4-8). The crusts and loosened soils show no significant relationship between shear strength and emission flux (R^2 = 0.08 and 0.02 for the crusts and loosened soils, respectively) and the sand deposits show a negative trend with a R^2 of 0.48. The loosened soils have a very large range in emission (between 0.5 mg s^{-1} m^{-2} and 6 mg s^{-1} m^{-2}) that is not explained by a difference in shear strength. For example, a low emission has been measured on the sand deposits, regardless of their low shear strength. To determine the factors that are most important for the difference in emissivity of these surfaces, additional boosted regression tree models have been performed. This was done on the separate data of the crusted surfaces and on the LEM surfaces, which are the loosened soils and sand deposits. This separation will enable the identification of soil properties influencing the emissions from crusted and non-crusted surfaces.

4.4.3.1 Emissivity controls on crusted surfaces

For the BRT analysis of the crusted surfaces, the OGS count has been added to the data set. This was done because saltating grains and abrasion have been described as relevant external factors for emissions from crusted surfaces (Houser and Nickling, 2001a; Klose et al., 2019; McKenna Neuman et al., 1996; McKenna Neuman and Maxwell, 1999; Rice et al., 1999, 1996; Rice and McEwan, 2001; Zobeck et al., 2003). The results show that the OGS count is indeed the most prominent factor for crusted surfaces with a relative influence of 68.2% (Figure 4-9). The marginal effect of the OGS shows that the saltation count influences the emissivity greatly up to approximately 150 Hz. OGS count and the emission flux display a significant power relationship (Figure 4-10) which demonstrates that saltating sand is indeed an important trigger for the emission of dust from crusted surfaces on Free

State cropland. Considering that the abraders that trigger emission from crusts might originate from nearby disturbed or loosened soil surfaces, indicates that indirectly, the non-crusted surfaces could thus increase the emission on crusted surfaces. Consequently, the importance of minimizing the disturbance of crusts to limit the emissivity is also dependent on the interaction of crusted patches with adjacent surfaces.

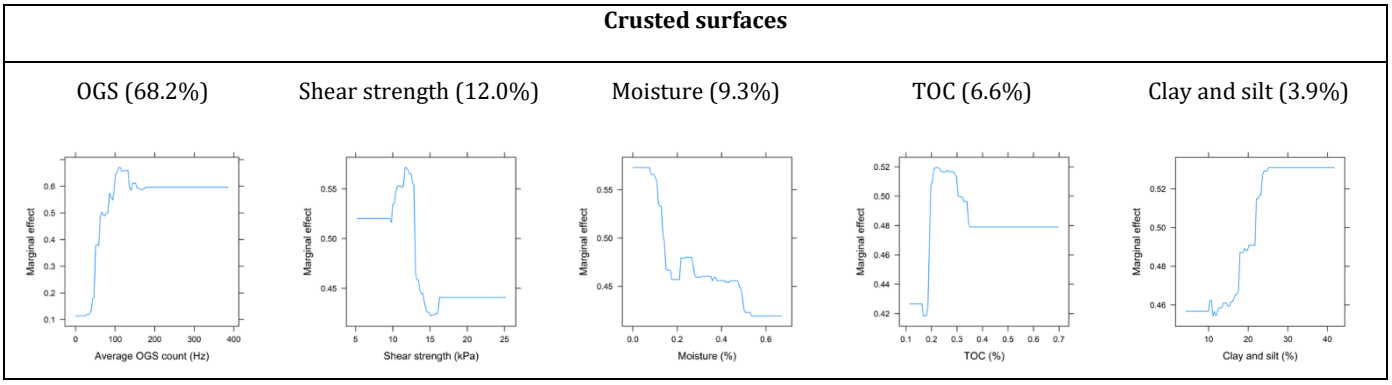

Figure 4-9. The results from the BRT analyses on the crust data, showing the relative influence on the emission flux in percentage for each variable, and the marginal effect of this variable.

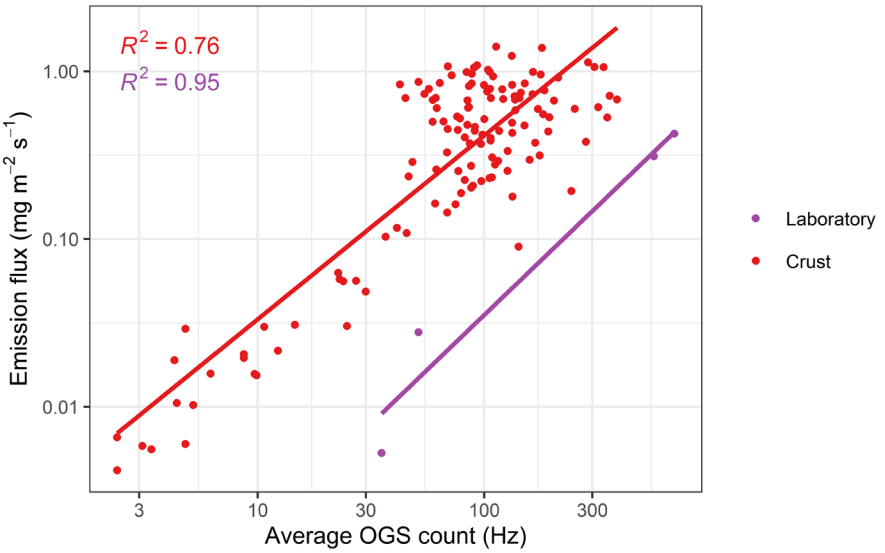

Figure 4-10. The OGS count versus the emission of the field crusts and the average emission from experimental crusts from Vos et al. (2020). Note the logarithmic scale of the OGS plot.

The BRT shows a small influence, almost binary relationship of the shear strength, with a threshold around 15 kPa. This shear strength value has also been identified by Goossens (2004) to be a threshold for the resistance to dust emissions from a crusted surface. However, the small relative influence of the crust strength (12%) indicates that such a high crust strength is not a prerequisite for a crust to prevent dust emission. Furthermore, the texture and chemistry of the soil appear to be almost insignificant for the emission from crusts. This points towards the universal protection soil crusts offer in relation to the presence of abraders.

4.4.3.2 Emissivity controls on LEM surfaces

Figure 4-11 shows the result of the BRT analysis for the LEM surfaces, which consist of the loosened soils and sand deposits. The most important factor is the clay and silt content with a relative influence of 44%. This influence of clay and silt is confirmed when plotting the clay and silt content versus the emission flux (Figure 4-12). The emission from purely LEM soils is increased by the presence of clay and silt, as described by Wang et al. (2015), Madden et al. (2010) and Sweeney and Mason (2013). This shows that the most emissive surfaces can be found on LEM surfaces with a higher clay and silt content (up to 20%). The sand deposits were notable due to their low emission, despite their very low cohesive strength. The low content of clay and silt in the sand deposits would be the result of a depletion of these particle sizes in the surfaces by previous wind erosion events. The high degree of sorting also explains the very low shear strengths of the sand deposits. This can also be seen when comparing the clay and silt from the sand deposits (1.3% and 4.2% clay and silt, respectively) to the crusts on the same test plot or field (2.7% and 9.2% clay and silt, respectively). The relevance of fines for dust emissions also illustrates that sandy surfaces, which are highly vulnerable to wind erosion, are not necessarily emitting large quantities of dust, because they could have been depleted of it.

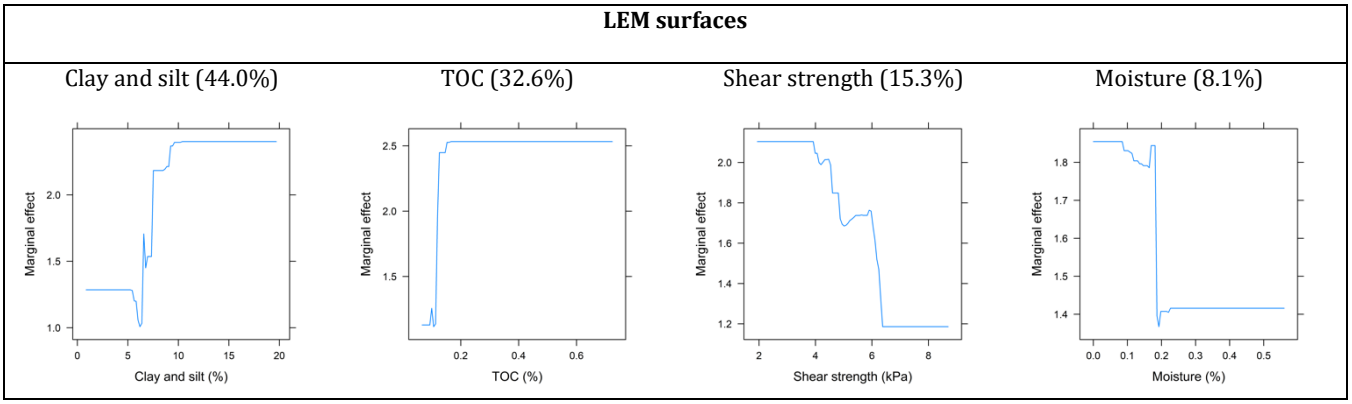

Figure 4-11. The results from the BRT analyses on the LEM data set (including the sand deposits and loosened soil), showing the relative influence on the emission flux in percentage for each variable, and the marginal effect of this variable.

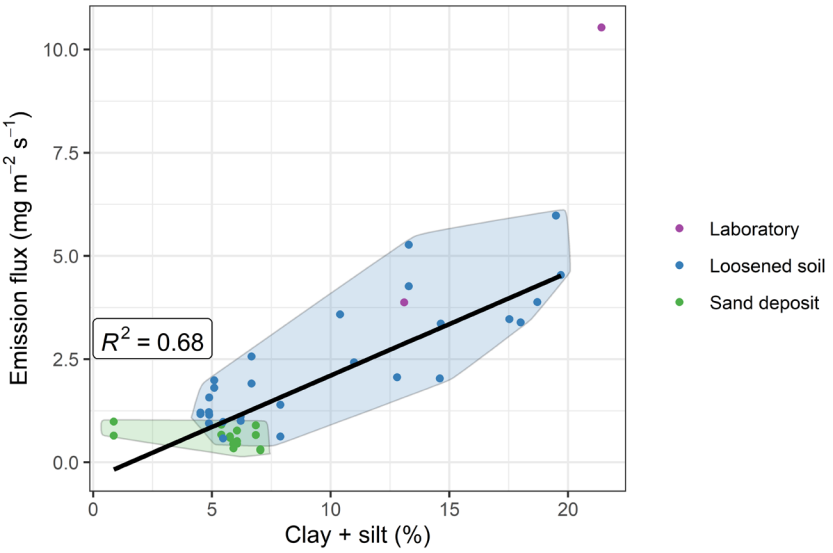

Figure 4-12. The clay and silt content versus the emission flux at a friction velocity of 0.56 m s-1, including the average experimental data from Vos et al. (2020).

4.4.4 Laboratory and field comparison

The third objective of this study was to compare the results from the field measurements to the measurements carried out in the laboratory by Vos et al. (2020). In their study rainfall simulations with 15 mm of rainfall were used to create physical crusts on small soil plots. Emissions from these crusted surfaces were then compared to emissions from non-crusted, loosened soil by using the PI-SWERL. The results showed that the emission from crusted Arenosols and Luvisols are 0.14 and 0.26%, respectively, of that of a loose surface. When introducing sand particles acting as abraders on the crusts, which simulates a likely scenario in the field, emissions observed in the laboratory were still only 10% of those observed on loose soil in the laboratory. The soils used in the laboratory study had a texture and shear strength similar to those in the field (Table 4-3). Comparing this data with the PI-SWERL measurements carried out for this study, the effect of crusts on dust emission appears smaller on actual cropland. This can be attributed to both, a higher emission from the field crusts and a lower emission from the loose surfaces in the field.

Table 4-3. The average shear strength and soil texture of the laboratory crusts from Vos et al. (2020).

	Emission (mg m^{-2} s^{-1})			Clay (%)	Silt (%)	Sand (%)	Crust shear strength (kPa)
	Crust	Crust with abrader	Loose				
Arenosol	0.00053	0.311	3.872	2.7	10.4	86.9	17.4
Luvisol	0.0278	0.425	10.534	6.3	15.1	78.4	21.5

When looking at the influence of saltators on the emission of crusts (Figure 4-10), laboratory and field crusts show a similar power relationship. However, at a similar OGS count, emissions in the lab were a magnitude smaller. This could be explained by loose fines that settled on these field surfaces

after wind events, and that get suspended again easily. These fines would be absent from the laboratory crusts. We furthermore speculate that this difference could also be caused by a difference in the composition of the abraders in the field and laboratory measurements. Grainsize measurements on the loose particles collected on field crusts showed an average of 5% clay and silt, whereas the abraders in the lab were sonified to rid them of fines, before being used as abraders. This means that in the lab, no additional emission of fines from the abraders took place which is in contrast to field measurements. Lastly, the crusts in the field could have been exposed to degradation which could have increased the emission from these crusts and the sensitivity to abraders. This degradation could have been caused by freeze-thawing processes and previous abrasion (Liu et al., 2017; Wang et al., 2014). While field and laboratory results generally indicate a similar effect of crusts on dust emissivity, the differences between them also highlight the risk of an overassessment of the relevance of crusts when looking at laboratory results alone.

When it comes to the loose surfaces and their relationship to texture, there is an overlap between the field and laboratory surfaces (Figure 4-12). The laboratory and field surfaces show approximately a similar relationship between texture and emission flux. The laboratory Arenosol plots in the same region as the field measurements, whereas the laboratory Luvisol has a higher clay and silt content and therefore a higher emission. The disturbance on the unharvested maize field, which held the Luvisol soil, left a much more aggregated surface with a higher roughness, which is why there was no measurement on a loose Luvisol soil. The sieving of soils before laboratory measurements could disturb a soil to a degree that might not always occur in the field, which should be taken into account for laboratory measurements.

4.5 Conclusion

The objectives of this study were to (1) determine the extent to which physical soil crusts reduce dust emissions from croplands, to (2) determine which factors influence the emissivity from loose and crusted surfaces, and to (3) compare emissions from laboratory surfaces to field surfaces. The dust emissions of the croplands appear much higher than of bare grassland soils, which is the largest surface area in the Free State. While the pan showed a dust flux statistically similar to that of the loose soil, more information on their emissivity is required. However, pan emissions would probably not match those of the cropland due to their small cumulative size. The cohesion of a surface, expressed as shear strength, appears to be the main factor influencing dust emissions on croplands. This influence can be seen in the lower emissions of the cohesive crusts, in comparison to the less cohesive loosened soils and sand deposits. Considering that crusts can build up quickly, even during the dry season (Vos et al., 2020), physical soil crusts could be the main factor limiting dust emissions from bare fields with low roughness and cover. This is in strong contrast to the conventional assumption that the clay and silt content of sandy soils are too low to form strong crusts (Rajot et al., 2003; Rice et al., 1999). The dust emissions from crusts themselves are controlled by the presence of abraders, which can originate from adjacent non-crusted surfaces. This shows that besides the higher emission from loose surfaces in the first place, these loose surfaces can have an additional increasing effect on

emissions from crusted surfaces. In the case of the fallow field, we speculate that the unlimited supply of abraders originates from bordering disturbed fields and that without these abraders, emissions from the fallow field would be much lower. Consequently, the emissions from the fallow field could be limited even further by keeping mobile sand to a minimum, e.g. by increasing sand traps such as fences or vegetation, maintaining a residue cover or crusts, and stabilizing sand on margins with vegetation.

The influence of texture on dust emissions appears to be ambiguous in our study since it is not identified as highly relevant when analysing the whole data set. However, it does appear to be a major influence for emissions from loose surfaces, where the presence of clay and silt increases the emission. This relationship does not take into account that higher contents of clay and silt could also potentially result in the development of clods and thus higher surface roughness. An increase in clay and silt could then increase the threshold friction velocities and reduce dust emissions. However, due to the very low content of clay and silt in the soils investigated in the Free State, this context was not within the scope of this study. The influence of texture also explains the unexpected low dust emissions from the sand deposits where depletion of fines had caused soil degradation by wind erosion. This also suggests that the fields that show the most signs of wind erosion, such as moving or ripple marks, might not be the fields that actually emit the most dust in their current state due to this degradation.

Our results are in line with the laboratory measurements from Vos et al. (2020) that showed a large difference in emissions between crusted and loose surfaces. For crusted surfaces, the field measurements showed that the majority of the crusts are subjected to abraders which leads to higher emissions. When taking the influence of abraders into account, field crusts still have a greater emission than in the laboratory, which could be the result of degradation of the surface and loose fines on top of the surface. For loose surfaces, the laboratory results are comparable to loose surfaces with similar clay and silt content. Laboratory studies on the emission from crusted surfaces should take the underestimation of emission from crusted surfaces into account.

Our data showed interesting implications for assessing or modelling dust emissions from sandy, rain-fed croplands in semi-arid to arid regions. The importance of cohesion and the presence of crusted surfaces in minimizing dust emissions should be taken into account when predictions of dust emissions are made for cropland areas. Especially during dry years, when the growth of crops is limited, protecting crusts could be used as an important land management technique to limit dust emissions from fallow fields with no protection from stubble. Hereby, the presence and input from neighbouring fields of saltating particles should be minimized. Furthermore, the importance of soil texture for the loose surface is noticeable, indicating that the emissions of surfaces with more clay and silt are only higher when it is disturbed by loosened soils. These contradictory influences should be considered for predictions on the emissivity of sandy, agricultural surfaces.

For future work, the focus should be on assessing a wider range of surfaces present on these agricultural lands. This includes the disturbed surfaces with a certain roughness or clod content. These surfaces were present on agricultural fields, but these surfaces are too rough to be measured with the PI-SWERL. Furthermore, the influence of larger roughness elements in these croplands, such as stubble or ploughing ridges, should be determined since windbreaks at the margins of fields are not practised in the region as a measure against wind erosion. This could then give insight under which conditions the roughness and cover are not sufficient to protect a surface, and therefore the formation of crusts and the limitation of saltators could be the primary solution of protection against dust emission.

Acknowledgement: We would like to thank the Swiss-South Africa Joint Research Programme, the Swiss National Science Foundation, and the National Research Foundation. We also wish to thank Hannes and Sophia Prinsloo, A.C. van Wyk, and Sias van Rensburg for allowing us to measure on their fields.

5.

Gone with the wind: Microbial communities associated with dust from emissive farmlands

Adeola Salawu-Rotimi*, Pedro H. Lebre*, Heleen C. Vos**, Wolfgang Fister**, Nikolaus Kuhn**, Frank D. Eckardt*** & Don A. Cowan*

* Centre for Microbial Ecology and Genomics, Department of Biochemistry, Genetics and Microbiology, University of Pretoria, Pretoria, South Africa

** Physical Geography and Environmental Change, University of Basel, Basel, Switzerland

*** Department of Environmental and Geographical Sciences, University of Cape Town, Cape Town, South Africa

Publish in Microbial Ecology, 2021, 82

doi.org/10.1007/s00248-021-01717-8

5.1 Abstract

Dust is a major vehicle for the dispersal of microorganisms across the globe. While much attention has been focused on microbial dispersal in dust plumes from major natural dust sources, very little is known about the fractionation processes that select for the "dust microbiome." The recent identification of highly emissive, agricultural land dust sources in South Africa has provided the opportunity to study the displacement of microbial communities through dust generation and transport. In this study, we aimed to document the microbial communities that are carried in the dust from one of South Africa's most emissive locations, and to investigate the selective factors that control the partitioning of microbial communities from soil to dust. For this purpose, dust samples were generated at different emission sources using a Portable In-Situ Wind Erosion Lab (PI-SWERL), and the taxonomic composition of the resulting microbiomes was compared with the source soils. Dust emission processes resulted in the clear fractionation of the soil bacterial community, where dust samples were significantly enriched in spore-forming taxa. Conversely, little fractionation was observed in the soil fungal communities, such that the dust fungal fingerprint could be used to identify the source soil. Dust microbiomes were also found to vary according to the emission source, suggesting that land use significantly affected the structure and fractionation of microbial communities transported in dust plumes. In addition, several potential biological allergens of fungal origin were detected in the dust microbiomes, highlighting the potential detrimental effects of dust plumes emitted in South Africa. This study represents the first description of the fractionation of microbial taxa occurring at the source of dust plumes and provides a direct link between land use and its impact on the dust microbiome.

Keywords: Comparative phylogenetic; dust microbiome; fractionation anthropogenic land-use dust allergens; PI-SWERL.

5.2 Introduction

Atmospheric mineral aerosols are recognized as an integral component of the earth's biogeochemical cycle (Fryrear, 1986; Ravi et al., 2011). It is estimated that the yearly quantity of dust that makes district or worldwide airborne migrations ranges from 0.5 to 5.0 billion tons (Behzad et al., 2018; Perkins, 2001). Dust minerals fertilize terrestrial (Okin et al., 2004) and aquatic (Neff et al., 2008) environments and modulate the earth's radiation budget (Schepanski, 2018). Wind erosion constitutes not only a loss of mineral particles and causes abrasion and damage to plants but also a displacement and transfer of microbial biomass (Behzad et al., 2018; Rosselli et al., 2015). For example, large increases in the concentration of airborne bacteria and fungi are associated with dust clouds during sandstorm events (Kellogg and Griffin, 2006).

Global dust sources are represented by persistent hotpots, mostly associated with dry environments (Prospero et al., 2002). The dispersion of dust from such hotpots is a function of the supply of dry, pulverized soil aggregates, its availability to entrainment, usually determined by the lack of soil cover, stubble and soil roughness, and transport sustained by sufficient wind speeds

(Bullard et al., 2011). A recent decade-long satellite data survey established the Free State province of South Africa, in particular areas north of Bloemfontein, to be such a hotspot, more so than any other area in South Africa (Eckardt et al., 2020). Here, dust events are common during the months of July to September, after commercial, rain-fed arable crops have been harvested coinciding with the dry season and the strongest winds (Wiggs and Holmes, 2011). Dust events were particularly frequent during the 2015–2016 drought, when 790 thousand hectares in the Free State remained fallow and weather satellite imagery identified more than 20 major dust days. Satellite data and air parcel trajectory models suggest the widespread dispersal of windborne mineral aerosols, reaching the neighbouring provinces to the east, along with Lesotho and the Indian Ocean (Eckardt et al., 2020).

Anthropogenic activities (particularly farming practices) have been recognized as major drivers of dust emission elsewhere, generating between 10 and 60% of the total atmospheric dust loads per year (Webb and Pierre, 2018), and are clearly linked to dust emissions in the Free State province of South Africa (Eckardt et al., 2020; Wiggs and Holmes, 2011).

Recent phylogenetic analyses of dust microbiomes (Gat et al., 2017; Tang et al., 2018; Weil et al., 2017) have identified a wide variety of bacterial taxa, representing all the common soil phyla (Behzad et al., 2018), while dust-associated fungal taxa include a wide range of both soil- and plant-associated taxa (Behzad et al., 2018; Maki et al., 2019; Tang et al., 2018). The dispersal of soil microbial communities in dust plumes is also thought to have far-reaching effects on human health (Graham et al., 2016; Kellogg and Griffin, 2006). Several studies have linked dust generation to various diseases, including meningitis outbreaks, asthma attacks, and to respiratory and other cardiovascular complications (Behzad et al., 2018; Jusot et al., 2017). Farming practices and crop rotations have also been shown to play a role in shaping the dust microbiome (Kirjavainen et al., 2019; Luiken et al., 2020; White et al., 2019). However, to date there is no information on dust microbiomes originating from sub-Saharan Africa, or how farming practices might shape this microbiome.

In this study, we document the fractionation process that shapes the dust microbiome in emissive farmland soils in the Free State province of South Africa and assess whether the latter can provide a diagnostic fingerprint for identification of source soils. In addition, we assess the potential impact of the dust microbiome generated from arable farmland soils by identifying taxa that may be implicated in human and agricultural crop health issues.

5.3 Materials and methods

5.3.1 Soil and dust sampling

Soil and dust sampling took place in August 2019, near Bultfontein, Free State province, South Africa (- 28.27 S, 26.15 E), a region of large-scale agriculture including maize (*Zea mays*), sunflower (*Helianthus annuus*), soyabeans (*Glycine max*), sorghum (*Sorghum bicolor*), wheat (*Triticum aestivum*), and peanut (*Arachis hypogaea*) (Supplementary Figure 5-1a). The soil is principally

comprised of Luvisols and Arenosols (Jones et al., 2013), which are rich in silt and sand, making them particularly susceptible to wind erosion (Eckardt et al., 2020). At each site, 4 soil samples ("Source Soils") were collected at the vertices of a 10 × 10 m metres quadrat. Surface soil samples (0–2 cm) were recovered with a sterile trowel into sterile Whirlpak® bags. A single dust sample ("PS sample") was artificially generated at the GPS coordinate for each site, using a portable In-Situ Wind Erosion Lab (Pi-SWERL) (Supplementary Figure 5-1b), which simulates wind-driven dust emissions and is used to measure emission thresholds (Etyemezian et al., 2007). Each PS sample was collected in a sterile Whirlpak® bag attached to the outlet of the PI-SWERL. For each PS sample, dust was collected from a 15-min run of the PI-SWERL at 3500 RPM, which represents a friction velocity of 0.85 m s^{-1}, using an alpha value of 0.90 and the relationship as proposed by Etyemezian et al. (2014). This corresponds to a wind speed of approximately 16 m s^{-1} (57 km h^{-1}). Six "control" dust samples (DT samples) (Supplementary Figure 5-1b) were also collected from Big Spring Number Eight (BSNE) collectors established prior to the study. The BSNE was developed by Fryrear (1986) and has been used frequently in wind erosion research (Goossens and Buck, 2011; Goossens and Offer, 2000; Sharratt et al., 2007; Webb et al., 2013). For the purposes of this study, BSNE dust traps were deployed in the peanut fields at heights of 10, 35, and 60 cm, calculated from the geometric mean of the opening. Collection of the DT samples was done after a dust storm event that occurred in the area on the 21st September 2019, with gust wind speeds of 14 m s^{-1} (50 km h^{-1}). Only samples from heights 10 and 35 cm were used for downstream analysis, as they contained enough biomass for DNA extraction. All samples were stored at room temperature before transport to the Centre of Microbial Ecology and Genomics (CMEG), University of Pretoria, Pretoria, South Africa, and subsequently stored at 4 °C until downstream processing. Grainsize of the DT and PS samples was measured using the Mastersizer 2000, after dispersing the samples using a Branson 250 Sonifier at 60 J ml^{-1} (Hu and Kuhn, 2014). Physical (silt/clay/sand content) and chemical (ammonia/nitrate and organic carbon) properties of the soil were measured from 200 grams of bulk soil by Intertek (Gauteng, South Africa).

5.3.2 DNA extraction and sequencing

Prior to DNA extraction, quadruplicate source soil samples from individual sites were combined into a composite sample and passed through a sterile 2-mm sieve in order to remove large mineral particles that might interfere with the extraction protocol. DNA from all samples was extracted using the DNeasy PowerSoil Kit (QIAGEN, Germany) with 0.5 to 1 g of initial sample material. Extracted DNA was quantified using the NanoDrop 2000 spectrophotometer (ThermoScientific, USA), and quality-checked by PCR amplification with 16S rRNA gene and ITS-specific primers. Thermocycling was conducted with a 25 µl reaction volume following the protocol recommended by the provider (New England Biolabs, USA) (initial denaturation 95 °C, 30 s; 30 × (denaturation 95 °C, 15 s annealing 55 °C, 30 s; elongation 68 °C, 60 s); final extension 68 °C, 5 min; hold 4 °C). After the quality of the DNA was confirmed, the samples were sent to Omega Bioservices (Georgia, USA) for sequencing of the v3-v4 hypervariable region of the 16S RNA gene and the ITS1-ITS4 region, using 2 × 300 bps PE Illumina MiSeq technology with a read coverage of 100,000 reads per sample.

5.3.3 Phylogenetic analysis

Sequenced reads were filtered and assembled using the QIIME2 pipeline (Bolyen et al., 2019), using DADA2 (Callahan et al., 2016) for read filtering and unique sequence inference, with a trunc-length of 280 bps for forward reads and 250 bps for reverse reads for bacterial reads, and 300 bps for fungal reads. Taxonomic analysis of the resulting assembled reads was carried out using the SILVA ver132 classifier (Quast et al., 2013) for prokaryotic species (with 99% similarity cut-off), and the UNITE fungal database (with 99% similarity cut-off) for fungal species. The Amplicon Sequence Variant (ASV) count table generated by the QIIME2 pipeline was manually curated to remove ASVs that were present in less than three samples. This step was performed to minimize false-positives originating from the sequencing platform. To assess if the sequencing depth for each sample was adequate, rarefaction curves were generated using the Vegan (Oksanen et al., 2019) package in RStudio.

5.3.4 Community composition analysis

Alpha-diversity metrics, beta-diversity metrics, and ordination were calculated using the Phyloseq (McMurdie and Holmes, 2013) and Vegan packages in Rstudio. The distribution of relative abundances and alpha-diversity indices was tested using the Shapiro test (Royston, 1982), and the significance of differences in phylum relative abundances was calculated using ANOVA (for normally distributed data) (Chambers and Hastie, 1992) and the Kruskal-Wallis test (for non-normally distributed data) (McKight and Najab, 2010). To perform beta-diversity analyses, the ASVs count table was first rarefied using the sample with the lowest ASV number as the reference sample, and counts were $\log(x + 1)$ transformed. Beta-diversity between groups was calculated using the Bray-Curtis dissimilarity metric (Lozupone et al., 2011) and visualized in a Principal Coordinates Analysis (PCoA) plot (Jolliffe and Cadima, 2016). PERMANOVA (Anderson and Walsh, 2013) with 999 permutations was used to test for statistical differences between sample beta-diversity, while the variation within sample groups was tested using the analysis of multivariate homogeneity of group dispersions (β-disper) (Anderson, 2006). Similarity within groups of samples was calculated with ANOSIM (Anderson and Walsh, 2013), using the same number of permutations as the PERMANOVA test. Redundancy analysis (RDA) was performed to access the explanatory effects of soil physical and chemical properties on the microbial community beta-diversity distribution. RDA models were calculated with forward selection model building using the Vegan package in Rstudio with an adjusted *p*-value threshold of 0.01.

5.3.5 Sample biomarkers and sink-source analysis

Biomarker taxa, i.e., taxa that were significantly over-represented in dust compared to soil samples, were identified using linear discriminant analysis effect size (LEfSe) analysis (Segata et al., 2011). ASV abundance values were converted to relative abundances (from 0 to 100%) prior to the LEfSe analysis, and data were normalized using the normalization step included in the galaxy version of the LEfSe software (http://huttenhower.sph.harvard.edu/galaxy/). Significant differences in abundance

were calculated using a Kruskal-Wallis test with a *p*-value threshold of 0.01, and effect size estimates were calculated using linear discriminant analysis (LDA).

Sink-source analysis was performed using the SourceTracker2 package (Knights et al., 2011) in RStudio. The ASV counts table was supplied as an input, together with a metadata file containing the classification of "sink" and "source," for each of the dust and soil samples, respectively. Data were rarefied using the SourceTracker2 default settings. Significant differences in sink-source proportions for each dust sample set, according to field type, were calculated with the Kruskal-Wallis test.

5.4 Results and Discussion

5.4.1 PI-SWERL Samples Are a Valid Surrogate for the Study of Dust-Associated Microbial Communities

The PI-SWERL, which generates dust from soil surfaces through shear generated by a rapidly rotating annular ring positioned above the soil surface, has been used extensively to quantify spatial and temporal patterns of dust emissions (Etyemezian et al., 2007; Sankey et al., 2011). However, to the authors' knowledge, this technology has not previously been employed in studies of dust microbiomics. In order to first validate the method, we compared the microbial communities in dust generated by the PI-SWERL (PS samples) to those in dust collected in BSNE dust traps (DT samples). Both PS and DT samples showed comparable number of ASVs (measured as observed species) between each other and compared to the source soil samples (Supplementary Figure 5-2b), corroborating the hypothesis that microorganisms undergo near-ubiquitous dispersal through dust (Bottos et al., 2014; Prospero et al., 2005). In addition, the majority of ASVs assigned to DT samples was shared by both the source soils and PS samples (Supplementary Figure 5-2b). We note that the PI-SWERL-generated dust samples exhibited a much higher variability in species richness than DT samples, which mimicked the variability observed in the soil samples from which the dust was collected.

Further analysis of the PS samples, collected in same vicinity as the DT samples, showed that both PS and DT samples shared a higher number of species (ASVs) compared with the source soils (Figure 5-1). These results suggest that the dust samples collected from the PI-SWERL are more representative of dust samples collected in conventional dust traps than of the source soils, and that PI-SWERL technology is an effective method for generating dust samples for microbiome analysis.

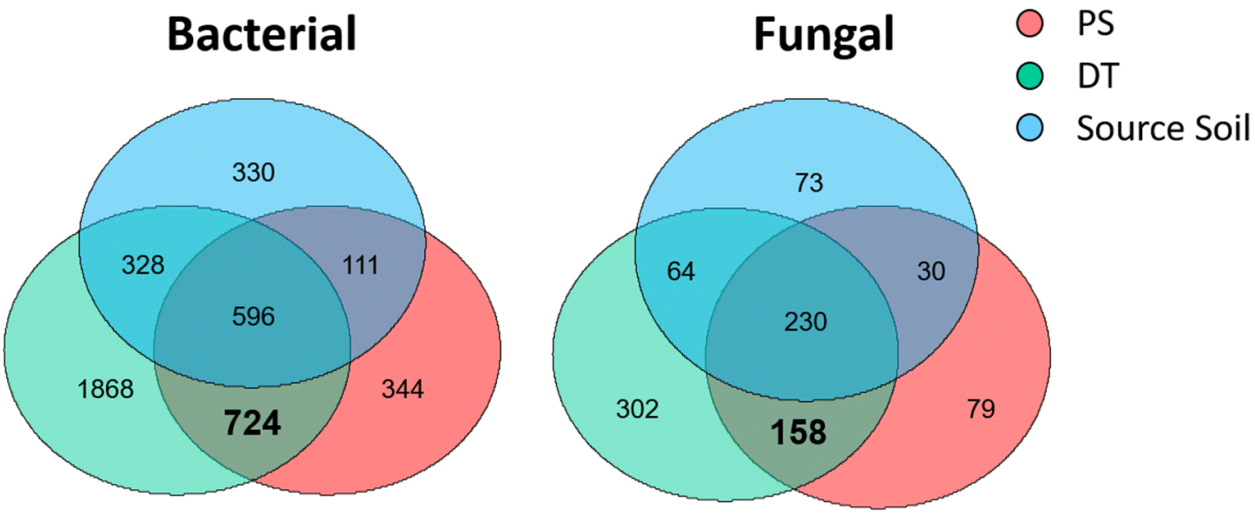

Figure 5-1. Shared bacterial and fungal ASVs shared between DT, PS, and source soil samples taken in close proximity from each other. The number of shared ASVs between PS and DT samples is highlighted in bold.

The high number of unique ASVs in DT samples, particularly those not shared with source soil samples from the vicinity, is consistent with the practical observation that conventional dust traps collect aeolian material from more distant sources (c.f., the PI-SWERL, which generated dust from a point location). In this regard, the use of the PI-SWERL could simplify the comparison of source and dust microbiomes in terms of community fractionation by avoiding confounding issues relating to the mixing of dust from multiple sources during transport. Additionally, differences in microbial composition between DT and PS samples could be correlated with differences in particle retention between the two sample collection methods. At high wind speeds, the efficiency of the BSNE is reduced with small particulate sizes (<10 μm), as described by Sharratt et al. (2007). Correspondingly, DT samples had a clay and silt content of 3.0% and 16.5%, respectively, while PS samples were composed of approximately 3.1% clay and 70.2% silt. The difference in grainsize between these samples can be explained by the fact that the PS samples only consist of smaller particles that can be suspended in the air, whereas the DT samples from BSNEs hold the larger, sand-sized fraction of saltating particles. Future work needs to address how different particle compositions affect the microbiome of the dust plumes.

5.4.2 Dust Emissions Select for Specific Taxa from Soil Microbial Communities

In order to understand the fractionation process of soil microbiota that occurs during dust emission, the taxonomic composition of the three sample sets (PS, DT, Source Soil) was analyzed and compared. All sample sets showed a similar composition in both the dominant (99% of ASVs) bacterial and fungal phyla (Figure 5-2a), with communities being dominated by *Proteobacteria* and *Ascomycota*, respectively. The top 10 bacterial and 3 fungal phyla observed in the source soil used in this study have previously been reported to be abundant in arable lands across the globe, and are often connected to the productivity of the soils (Trivedi et al., 2016; Wang et al., 2018). A recent report (Maki et al., 2019) documenting the microbial composition of dust from desert and anthropogenic sources also reported similar prokaryote compositions to those reported in this study.

Significant differences in relative abundances of taxa at the Phylum level were detected between dust and source soil samples (Figure 5-2b). Most notably, *Proteobacteria* were significantly enriched in PS and DT samples compared to source soils (34% PS/DT vs 26% source soils average relative abundance), while *Firmicutes* were over-represented in source soils (8% source soils vs 4.6% DT/ 2.3% PS).

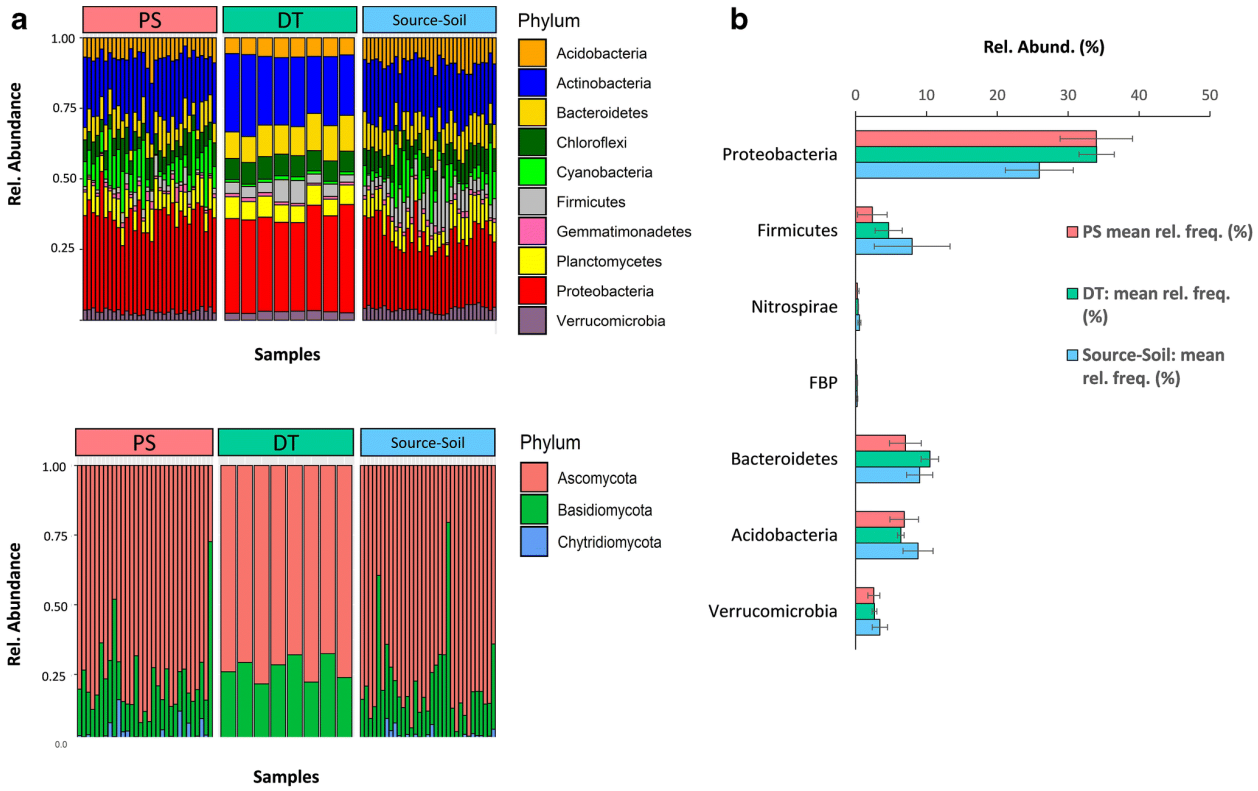

Figure 5-2. (a) Distribution of the dominant prokaryotic and fungal phyla across the three sample sets. Abundances were calculated as the fraction of total ASVs belonging to each phyla. (b) Relative abundance of phyla that which show significant (p-value >0.01) difference in abundance between the three data sets. Relative abundance was calculated as the average percentage of the fraction of each phylum across the three data sets.

To further explore the differences in microbial abundance between dust and source soil samples, LEfSe analysis was performed to identify taxa that were significantly over-represented in PS and DT samples (Figure 5-3). A total of 12 bacterial taxa were identified as being over-represented in the dust samples, suggesting that some level of selective fractionation does occur during dust generation. Several of the bacterial taxa identified in this analysis, including *Cryptosporangium*, *Micromonosporaceae*, and *Actinoplanes*, are associated with the ability to sporulate (Buttner, 2017; Tamura et al., 1998). By comparison, only 3 fungal taxa were over-represented in the dust samples. Together with the lack of differentiation in fungal phylum abundances between the sample groups, these results suggest that the fungal communities do not undergo the same fractionation process as bacteria. We suggest that this is due to their inate capacity for aeolian transport (Egan et al., 2014; Kendrick, 2001).

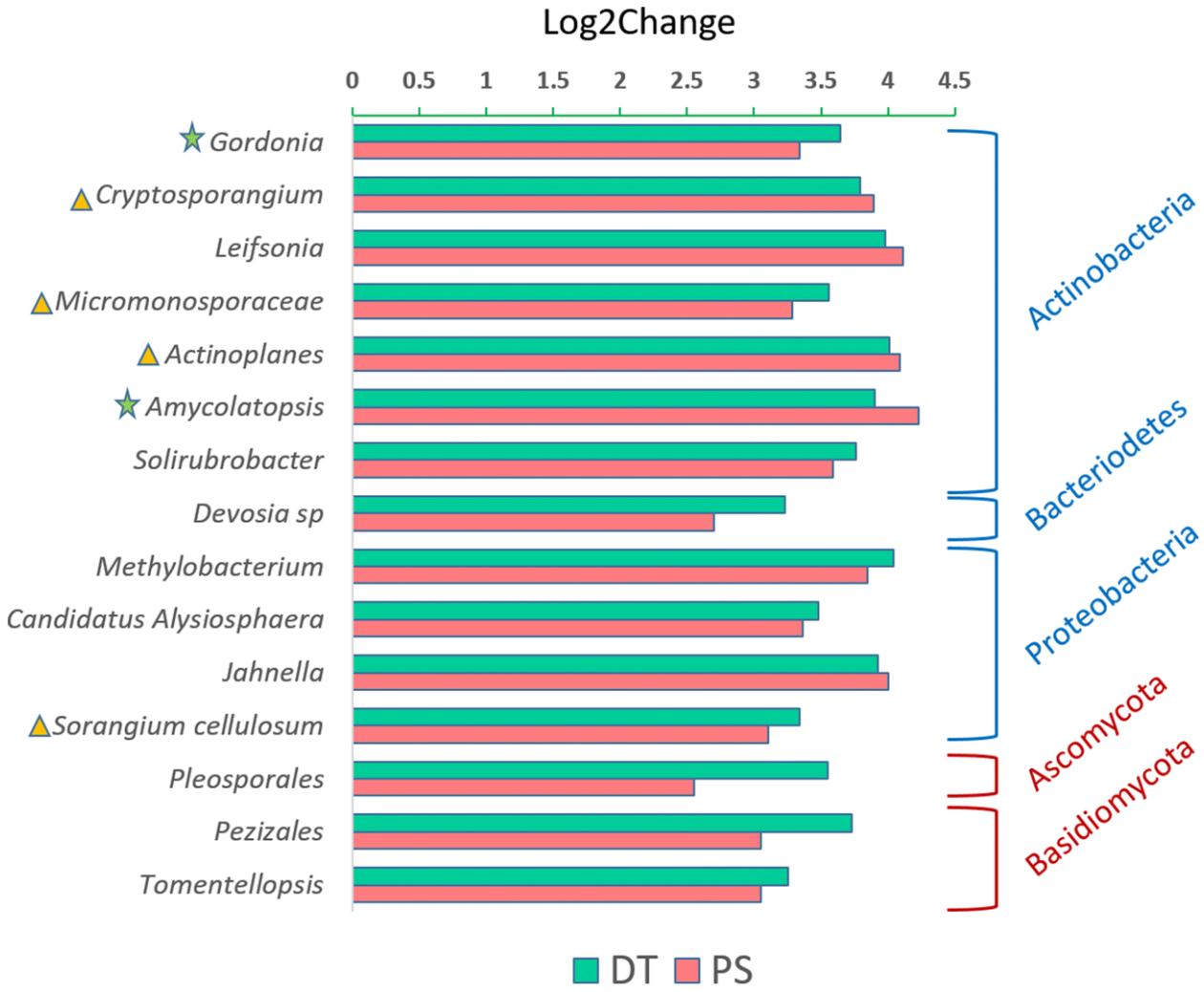

Figure 5-3. LEfSe analysis of taxa that were significantly over-represented in dust samples (p-value < 0.01) compared to the source soils. Over-representation is expressed as Log2 change compared to soil samples. Bacterial taxa are highlighted within the blue brackets, while fungal taxa are highlighted within the red brackets. Taxa marked with the yellow triangles are associated with the capabilities to form spores.

5.4.3 Dust Microbial Communities Can Be Linked to the Soil from Which They Originate

Analysis of the differences in community composition using the Bray-Curtis beta-diversity dissimilarity showed that both bacterial and fungal communities clustered significantly (*p*-value <0.01) according to sample type (PS vs DT vs Source Soil) (Supplementary Figure 5-3), corroborating the suggestion that microbial communities do undergo some level of compositional fractionation during dust production. However, this grouping only weakly explained the dissimilarity in bacterial and fungal communities between sample sets (R^2 = 0.09 and R^2 = 0.11, respectively). By comparison, dissimilarities between microbial communities could be explained more robustly by the type of field/crop from which samples were taken (i.e., peanut vs sunflower vs maize vs fallow) (Figure 5-4). Both bacterial and fungal communities were found to be significantly (*p*-value <0.0009) dissimilar between field types (R^2 = 0.18 and R^2 = 0.22, respectively), and significantly similar within each field

type (R = 0.49; R = 0.57). This result indicates that the different field/crop types have distinct soil microbial communities, and these dissimilarities might be explained by a conjunction of different factors, including soil physico-chemistry (Lauber et al., 2008), type of crop planted (Azeem et al., 2020), and tillage method (Smith et al., 2016).

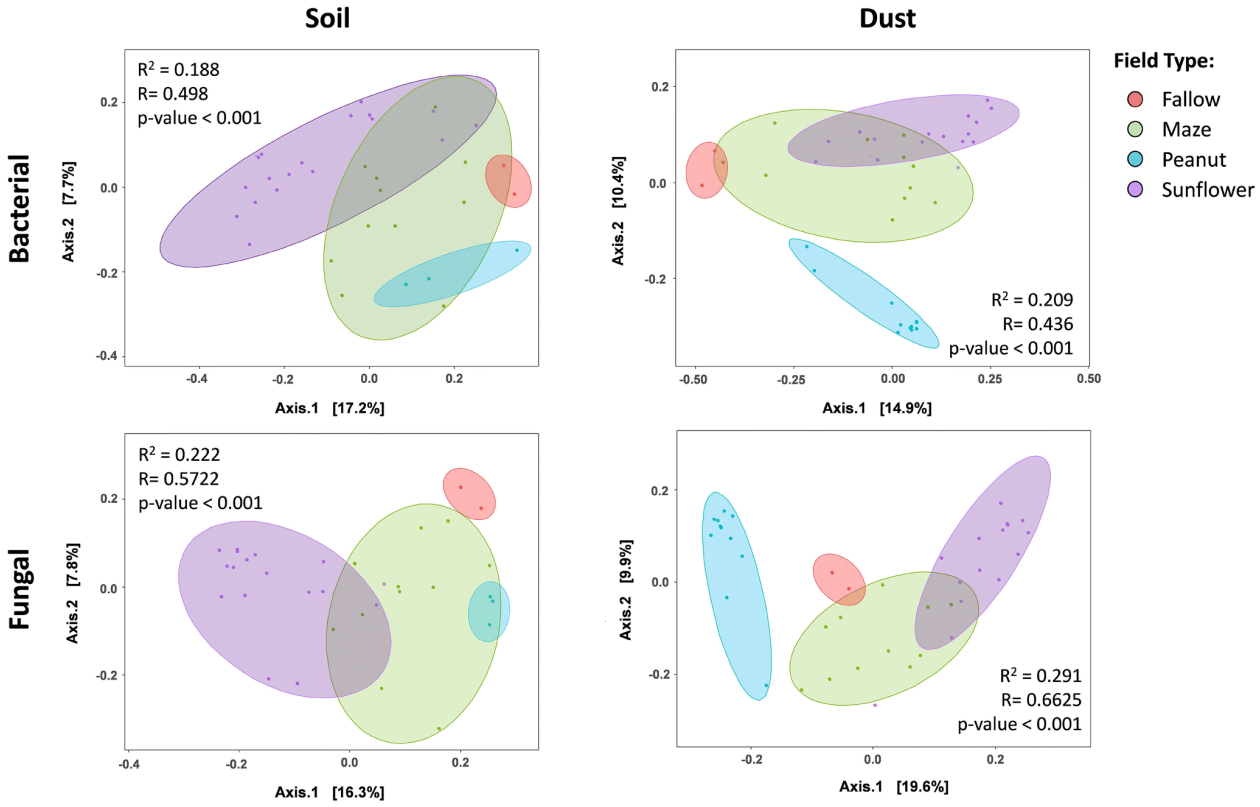

Figure 5-4. Dissimilarities in microbial communities between dust and soil samples according to type of field from which the samples were collected. The Principal Component Analysis (PCoA) plots display the Bray-Curtis dissimilarity matrices for subsets of the sample community (Soil vs Dust; Bacterial vs Fungal). For the purposes of this analysis, PS and DT samples were considered Dust samples. The sample clusters corresponding to the different field types are highlighted within the ellipses using the following color-coding: Peanut - blue; Sunflower - purple; Fallow - red; Maize – green.

Dust samples (PS and DT) formed distinct communities relative to the field type from which they were collected, with fungal communities being more associated with field type than bacterial communities (R = 0.66 versus R = 0.43 for bacterial communities). This result might also be explained by a high capacity for fungal tissue (spores, mycelial fragments) to mobilize via aeolian transport (Adhikari et al., 2009; Crawford et al., 2009; Després et al., 2012). Consequently, the fungal diversity in dust samples should more accurately represent those in source soils, compared to their bacterial counterparts. To further explore this hypothesis, sink-source analysis was used to determine if microbial communities in dust samples could be traced to their respective sources. The results from the analysis (Figure 5-5) showed a significant (p-value <0.01) positive correlation between the dust fungal communities and the fields from which these were collected. By comparison, only dust bacterial communities originating from the sunflower fields could be significantly correlated to their source soils. Together, these results suggest that microbial communities found in dust samples,

particularly fungal communities, can be linked to the soils from which they are sourced, at least at the point of origin. Surprisingly, even dust control (DT) communities could be significantly distinguished from dust samples from other fields in the sampling area, suggesting that BSNE dust traps collect microbial communities that are primarily sourced from the immediate vicinity of the dust trap.

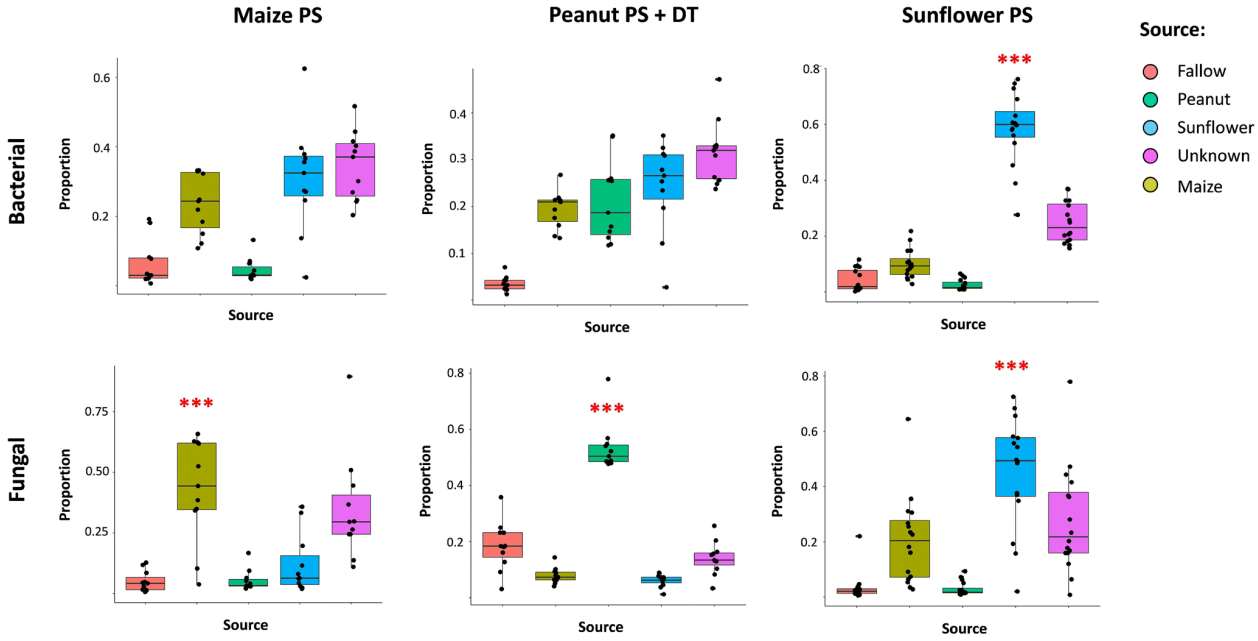

Figure 5-5. Correlation between the DT + PS communities (sink), and the communities in the soil from which the dust was collected (source). The y-axis values express the proportion of shared ASVs between the sink samples and the source, representation as fractions from 0 to 1. Significant correlations (p-value <0.01) are highlighted by the red asterisks (***).

5.4.4 Amonia and Clay Content Affect Soil Microbial Composition of Different Fields

As suggested above, the differences in microbial community structure observed in the soil and dust from different field types might be explained by differences in chemical and structural properties of the soils. In order to investigate this hypothesis further, the general soil properties (silt/clay/sand fraction, nitrogen, and organic carbon content) of the sampled soils were measured and correlated with the soil microbial communities. All soils were found to have a similar soil silt/sand composition as well as organic carbon content, while soils from sunflower fields were found to be significantly enriched in both ammonia and clay content (Supplementary Figure 5-4). Redundancy analysis (RDA) of the soil properties (Figure 5-6) revealed that ammonia and clay content significantly (adj. *p*-value <0.01) explained 9% of the beta-diversity distribution observed for prokaryotic communities, while clay content on its own explained 6% of the beta-diversity distribution of fungal communities. Together, these results indicate that these two properties have a significant, albeit small, effect on the microbial composition of different fields.

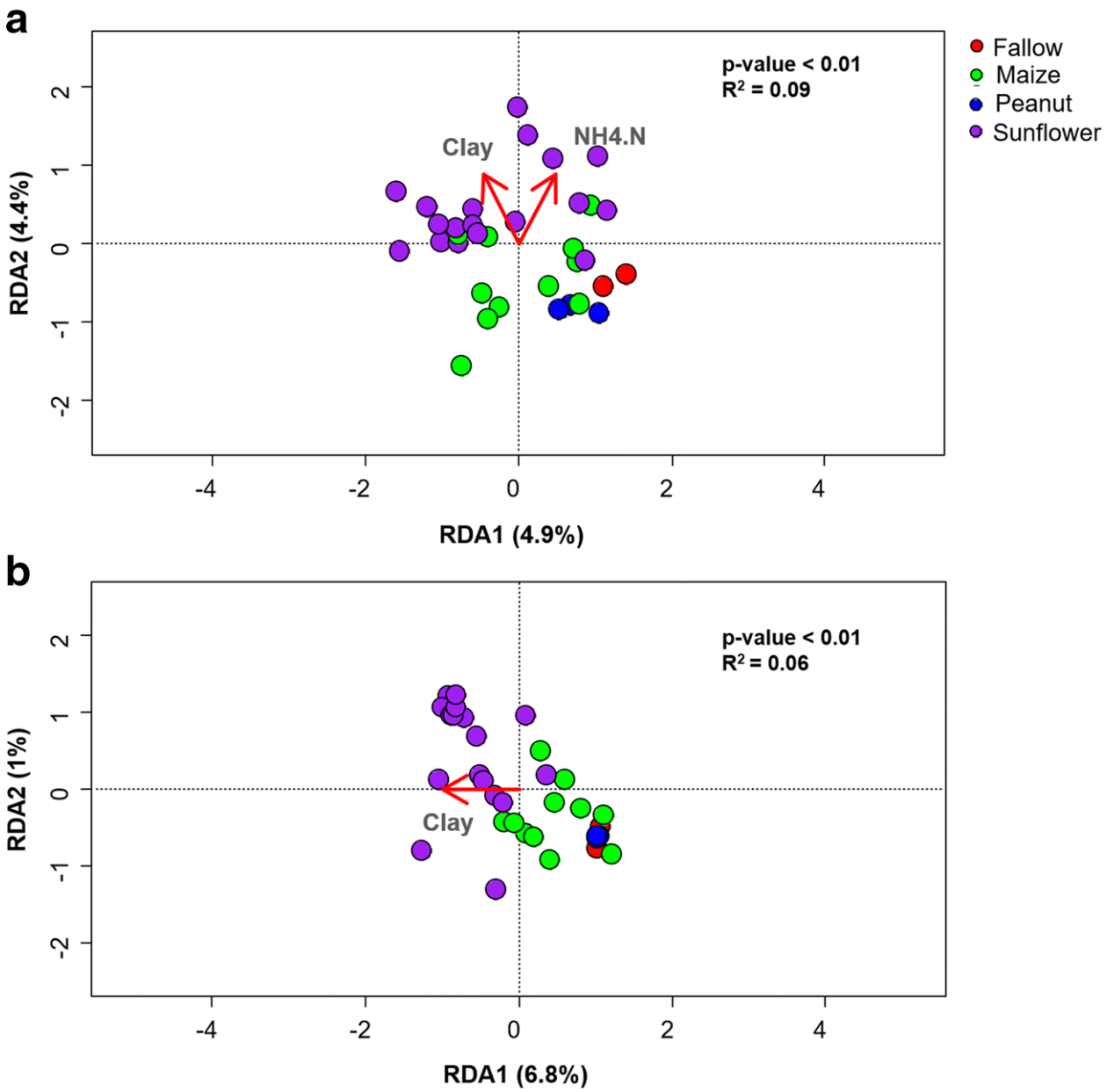

Figure 5-6. The effects of physical and chemical properties of the soil on the prokaryotic (a) and fungal (b) communities of the different field types. The distance-based redundancy analysis (db-RDA) plots show the soil properties (represented by red arrows) that significantly (adjusted p-value < 0.01) explain the Bray-Curtis distribution of the soil microbial communities. Samples are colored according to field type. The following abbreviations were used to represent soil properties: Clay - clay content (%) in soil; NH4.N - ammonia content (mg kg-1) in soil.

5.4.5 Dust Carries a High Proportion of Potentially Allergenic Fungal Taxa

Analysis of the dust fungal community at the Genus level showed high levels of putative fungal allergens and plant pathogens. Examples include *Cladosporium*, which represented an average of 9.5% of PS and DT fungal ASV counts, as well as *Alternaria* and *Fusarium*, which accounted for 6.5% and 5.8% of ASV counts, respectively (Figure 5-7). *Alternaria* species, such as *Alternaria alternata*, are allergens associated with serious asthma and hay fever symptoms (Meena et al., 2017). *Alternaria*

alternata and *Cladosporium herbarum* have also been linked to severe cases of asthma, eczema, and rhinitis in children (Tariq et al., 1996). *Alternaria* and *Fusarium* species are known plant pathogens that can cause spoilage of agricultural products (Bhat et al., 2010; Pinto and Patriarca, 2017; Torbati et al., 2019).

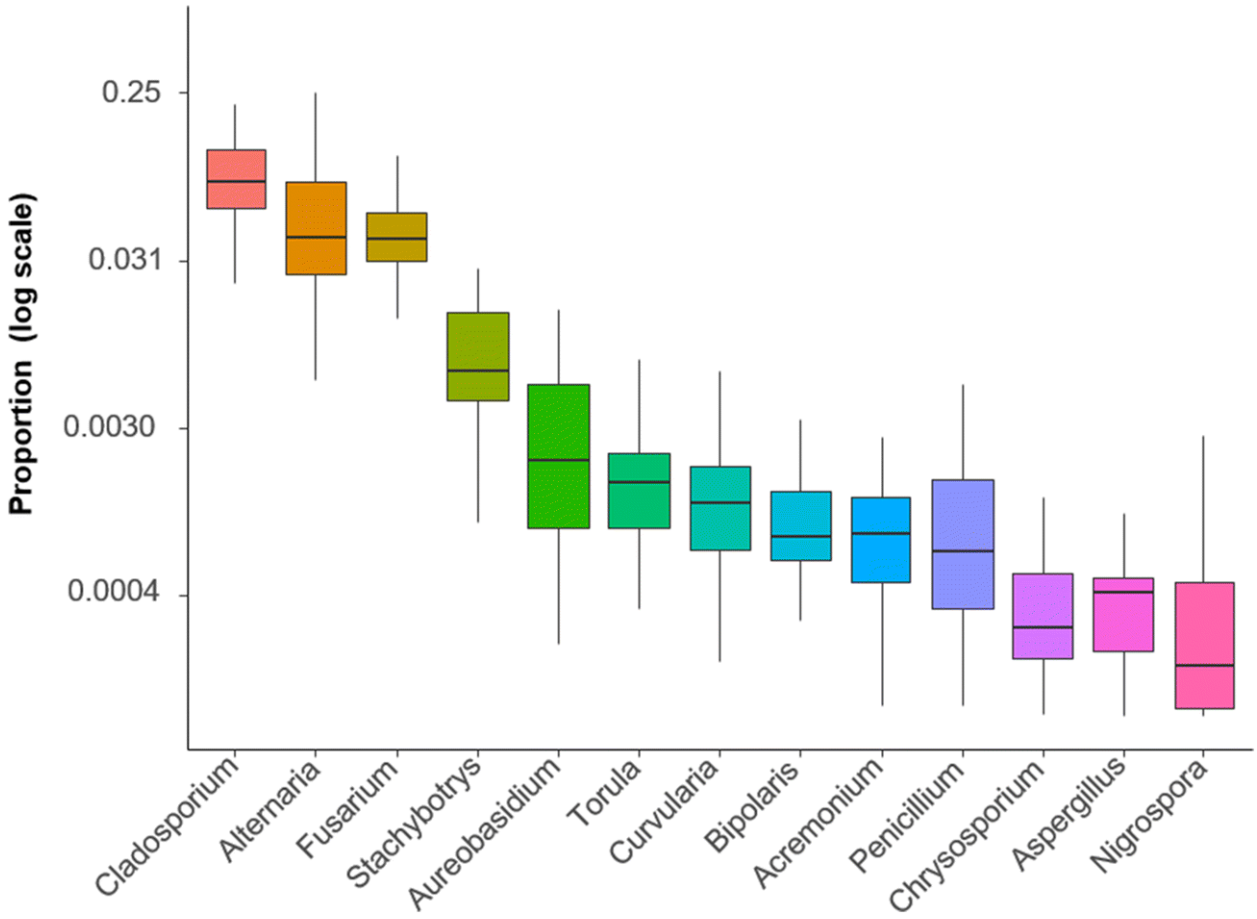

Figure 5-7. Relative proportion (relative to total fungal ASV counts) of potentially allergenic fungal pathogens present in both PS and DT samples.

A number of studies have linked farming practices to over-representation of allergens in dust (Corden et al., 2003; Friesen et al., 2001; Hyde and Williams, 1946; Nasser and Pulimood, 2009; Stein et al., 2016). For instance, mechanized harvesting methods have been reported to release large quantities of *Alternaria* spores which can be wind-transported for long distances (Corden et al., 2003; Friesen et al., 2001). Here, we demonstrate that "natural" aeolian processes also have the potential to trigger the mobilization of high levels of potentially pathogenic and health-related fungal taxa. While the impacts of this process on human and plant health have not been directly quantified, we note that dust generated from the Bultfontein area of South Africa can be widely transported to other areas of the country, including the North West province, Mpumalanga, Gauteng province, and the Western Cape (Eckardt et al., 2020).

5.5 Conclusions

To the authors' knowledge, this is the first study to document the microbial fractionation process that occurs during dust emissions at the source of the emissions. The results reported in this study lead us to conclude that microbial communities undergo a selective fractionation process during dust emissive events, which may be dependent on the ability of certain species to differentiate into structures that are prone to aeolian transport. Given that most fungal taxa have this capacity, either through the production of spores or from fragmentation of hyphae, it is perhaps not surprising that fungal taxa associated with dust samples can be readily linked to the source from which they originate, and therefore potentially be used as biomarkers for the sources of dust plumes. By comparison, bacteria communities in dust samples were generally only weakly associated with the source soil microbiomes, suggesting that bacteria undergo a greater degree of selective fractionation during dust generation. The mechanisms underlying the fractionation process, and the differences in fractionation between bacterial and fungal taxa, are worthy of further investigation. Possible avenues for future exploration include analyses of possible differences in adsorption and/or entrapment of different cell types in/to different minerals or different mineral particle sizes.

In addition, results in this study support the growing body of evidence that crop-plant selection has a significant impact on the composition of associated soil microbial community (González-Chávez et al., 2010; Hartman et al., 2018; Larkin, 2008; Maarastawi et al., 2018; Smith et al., 2016) and therefore, by extension, a significant impact on the microbiomes of dust generated from such soils. Correspondingly, a proportion of the dust microbiome, particularly the fungal taxa, can be used as a biomarker of emission sources. However, we accept that aeolian mixing processes over distance may rapidly obscure this signature.

The observation that dust samples also carry a significant load of potentially pathogenic and/or allergenic fungal taxa is also worthy of further investigation. The extent to which this transport process has a negative impact on human and plant populations would inevitably be difficult to quantify, although carefully constructed epidemiological surveys of crop disease and human respiratory disease issues in areas both upstream and downstream of major dust plumes might offer some supporting evidence.

Acknowledgements: The authors wish to thank the University of Pretoria for postdoctoral grants (ASR and PHL).

6.

Influence of crop and land management on wind erosion from sandy soils in dryland agriculture

Heleen. C. Vos*, Isabel Karst*, Frank D. Eckardt**, Wolfgang Fister* & Nikolaus J. Kuhn*

* Physical Geography and Environmental Change, University of Basel, Basel, Switzerland

** Department of Environmental and Geographical Sciences, University of Cape Town, Cape Town, South Africa

Published in Agronomy, 2022, 12, 457

https://doi.org/10.3390/agronomy12020457

6.1 Abstract

Minimizing wind erosion on agricultural fields is of great interest to farmers. There is a general understanding that vegetation can greatly minimize wind erosion taking place. However, after harvest, a low vegetation cover can be inevitable, whereby the amount of stubble that remains on a field is dependent on the crop type and land management. This study aims at quantifying the vulnerability to wind erosion of different crops, and the possibility to predict the vulnerability based on high-precision aerial images. The study area was the semi-arid Free State, which holds large intensive agriculture on sandy soils. These croplands have been identified as the largest emitter of dust in South Africa. The main crop in the region is maize, but also sunflower, groundnut and fallow fields are common land-use types. On these fields, the horizontal sediment flux, the saltation threshold, and aerodynamic roughness length were measured, and the soil cover was assessed using Unmanned Aerial Vehicle (UAV) imagery. The results showed a strong relationship between the soil cover and the sediment flux, whereby fallow and groundnut fields have the highest wind erosion risk. These results emphasize the great importance of soil cover management to prevent wind erosion.

Keywords: Wind erosion; land management; soil cover; UAV image analysis; sediment flux

6.2 Introduction

Wind erosion is known for the disastrous effects it can have on agricultural lands due to the damage it can bring to the crops by saltation (Sterk, 2003; Sterk et al., 2001) and the degrading effect on the soil, because of the removal of nutrients and topsoil (Bielders et al., 2002; Lawrence and Neff, 2009; Van Pelt and Zobeck, 2007; Visser and Sterk, 2007; Zobeck and Bilbro, 2001). The dust that is transported from the fields can become part of the global chemical flux and can, furthermore, have offsite effects on human health and climate. Wind erosion is especially a problem in semi-arid and arid regions (Ginoux et al., 2012), where fields are most vulnerable after harvest, when the soil cover from plants or residue is low. The total global wind erosion is estimated to be s 6577 t km^{-2} yr^{-1} (Yang et al., 2022). During these wind erosion processes, roughly 500 to 3320 Tg yr^{-1} of dust is emitted (Shao et al., 2011). The dust emission from anthropogenic areas has been estimated to be 10% to 25% of the total dust load, whereby the contribution of anthropogenic dust differs greatly per region (Ginoux et al., 2012; Tegen et al., 2004).

The most important method for preventing wind erosion from agricultural fields is the maintenance of a residue and vegetation cover (Abdourhamane Toure et al., 2011; Fryrear et al., 1998; Funk and Engel, 2015; Lyles, 1985; Riksen et al., 2003; Tibke, 1988; Woodruff and Siddoway, 1965). The erodibility of a surface can furthermore be influenced by the presence of a soil crust that increases cohesion and thus in turn by the tillage operations that disturb the crust (Fister and Ries, 2009; Li et al., 2015; López et al., 2000). The influence of soil cover on wind erosion can be expressed as a ratio of wind erosion from a surface with vegetation to a surface without vegetation. Exact exponential relationships have been developed by Fryrear (1985), Findlater et al. (1990), and Lancaster and Baas (1998) based on different vegetation types. The soil cover percentage is different

from the roughness effect from the silhouette shape of vegetation density, even though they expect to correlate (Bilbro and Fryrear, 1994).

The amount of residue and the cohesion of a surface is dependent on the crop and land-use type, and the harvesting and cultivation technique (Lin et al., 2021; López et al., 2000; Nelson, 2002; Nordstrom and Hotta, 2004; Yang et al., 2020). These surface conditions then also rely on favourable annual weather conditions. For example, droughts can result in higher amounts of fallow land since this can result in crop failure. Farmers can also decide to keep a field unplanted during a drought. Despite the general knowledge of the relationship between surface conditions and surface erodibility, the relationship between crop and land management, and field erodibility is often missing.

The percentage of soil cover has often been quantified by image analyses from photos in wind tunnel studies (Burri et al., 2011; Funk and Engel, 2015) or by certain formulas that combine the dimensions and densities of the plant (Lancaster and Baas, 1998; Li et al., 2007). However, image analyses from manually taken pictures are only suitable for small-scale measurements, and formulas depend largely on the type and the maturity of the vegetation. A new method to determine the soil cover is the image analyses of Unmanned Aerial Vehicle (UAV) images, since this had the precision of image analyses but can cover larger areas. The feasibility of using UAV analyses to determine the soil cover has been demonstrated by Zhang et al. (Zhang et al., 2021) but has not been used often.

One region that experiences high-intensity wind erosion is the Free State province in South Africa, where the majority of the dust sources can be linked to agricultural land (Eckardt et al., 2020). Roughly a third of the land in the Free State is used for agriculture (DAFF, 2018). The dust season in this region occurs between August and November, when the fields have been harvested and often ploughed in preparation for the beginning of the rainy season in December. The amount of dust events varies greatly per year (Eckardt et al., 2020), which raises the question of which other factors influence the emission of dust in the Free State, and to which extent these factors can be controlled by agricultural management.

Maize is the most common crop in the Free State, but depending on the soil and climate, also other crops such as sunflower, soya beans, wheat, sorghum, and groundnuts are cultivated. Furthermore, a significant number of fields is fallow. Fallow fields can either be a conscious decision to increase the water level or the result of low or late rains, causing farmers to miss the window of seeding (Moeletsi and Walker, 2012). Figure 6-1 shows the average land use from an average rainfall of 487 mm per year, and the land use during the drought in 2015–2016 when only 294 mm of rainfall fell. These figures show the importance of maize as the main crop in this region and the increase in fallow fields during drought.

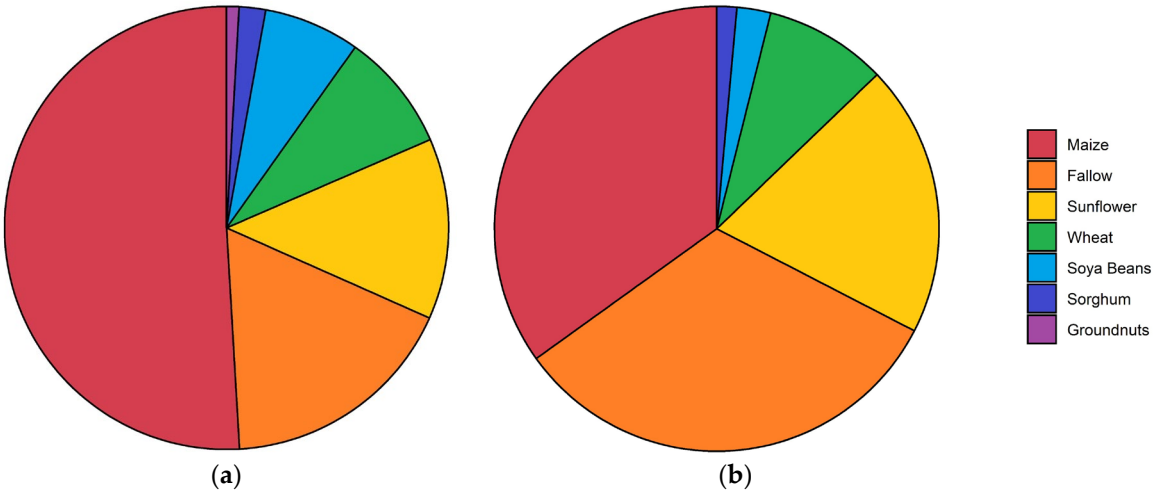

Figure 6-1. The land use in the Free State on average from 2006 to 2017 (a) and during the drought year of 2015–2016 (b). Data provided by the South African Department of Agriculture, Fisheries and Forestry (DAFF).

In the Free State, especially groundnut and fallow fields have been linked with wind erosion and dust events. Local farmers have indicated that groundnut fields show the highest intensity in wind erosion. Furthermore, Eckardt et al. (2020) connected a year with a high number of dust source points with the large number of fallow areas that were caused by drought. The number of fallow fields does show a relationship with the rainfall with an R^2 value of 0.15 (Figure 6-2). However, Vos et al. (2021) measured a low dust emission flux on these fields as long as the presence of sandy saltators and abrasion are limited, due to the crusted nature and high cohesion of these fields.

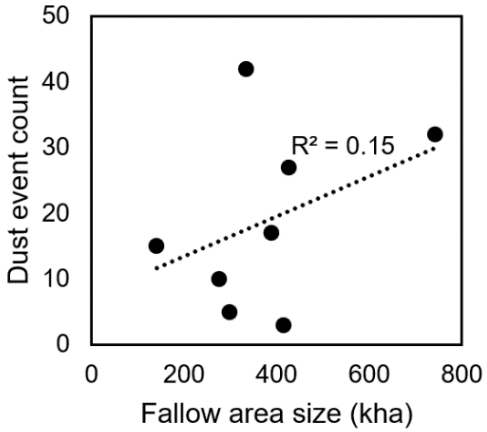

Figure 6-2. The yearly fallow area size versus the dust event count. Data from Eckardt et al. (Eckardt et al., 2020) and the Department of Agriculture, Forestry and Fisheries (DAFF).

The question of the factors influencing dust emissions in this region has been raised previously by Vos et al. (2021). Using the Portable In-Situ Wind Erosion Laboratory (PI-SWERL), they identified the presence of a crust to be an important factor in minimizing emission. In addition, the texture of a loose surface affected the PM_{10} emission flux greatly. However, the PI-SWERL is too small to capture the influence of the plant cover and the roughness from ploughing ridges or stubble. Wiggs et al. (2011) monitored the erosion from a ploughed bare field in the Free State using saltation sensors, anemometers, and dust deposition traps and found a correlation between roughness and the

threshold velocity. They furthermore described the minor role of moisture and rainfall in minimizing emission due to high wind velocities during similar periods. However, both of these studies do not address the influence of plant cover and stubble.

This study aims at quantifying wind erosion on a range of the most common field conditions encountered on Free State cropland during the dust season and at developing an understanding of the land management and cropping systems that potentially generate the most wind erosion and dust emission in this region. To address this, the sediment flux and threshold velocity of four fields with typical combinations of cover and surface characteristics were measured. The monitored surface characteristics consist of cohesion, soil cover, and roughness. The soil erodibility is described by the threshold velocity and the horizontal sediment flux. The objectives of this study are to determine the following:

1. The surface characteristics of the fields;
2. The sediment flux and threshold velocity on the different fields during the dust season;
3. The influence of the field characteristics on the soil erodibility;
4. A wind erosion risk assessment associated with different land use.

6.3 Methods

6.3.1 Study area and Sites

The study area is located in the northwestern part of the Free State (Figure 6-3), a region that shows the most dust source points as described by Eckardt et al. (2020). A climate station from the Agricultural Research Council (ARC) provided hourly data on the weather conditions (Figure 6-3). The rainfed agriculture in this mainly semi-arid region is largely sustained by the deep, sandy Arenosol and Luvisol, as classified using the Soil Atlas of Africa (Jones et al., 2013). Such soils commonly have an infiltration rate between 15 and 70 mm h^{-1}, depending on the moisture content, soil chemistry, and the stage of tillage or compaction throughout the cropping cycle (Meek et al., 1992; Patle et al., 2019). The sandy soils in the Free State can function as a water reservoir (Hensley et al., 2006). No irrigation is taking place on these fields, which makes agriculture highly dependent on favourable rainfall conditions. The seeding of the crop starts at the beginning of the rainy season in early spring (Moeletsi and Walker, 2012), except for winter wheat which is planted during fall due to its frost resistance (DAFF, 2016).

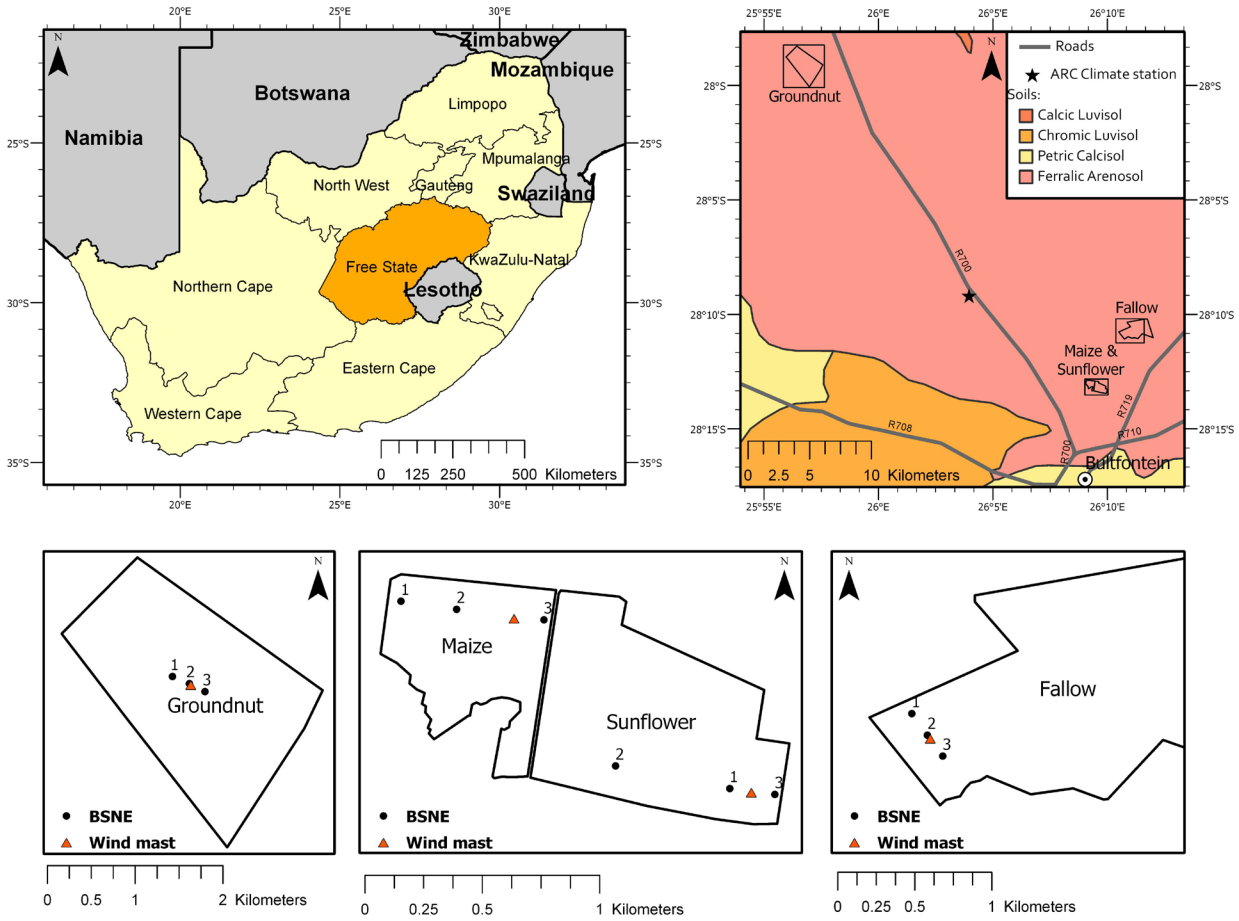

Figure 6-3. South Africa (top left), the soil map of the study area (top right), and the fields that were selected for monitoring (bottom) with the location of the Big Spring Number Eight (BSNE) and wind masts.

Four fields, representing the most important fields and crop types and showing a range of soil cover and cohesion conditions were monitored (Figures 6-3 and 6-4). The selected fields are a harvested maize, a sunflower, a groundnut and a fallow field. Maize and sunflower constitute over 90% of the crop production in the region and thus leave the largest proportion of cropland exposed to potentially erosive winds after harvest (DAFF, 2018). Groundnut and fallow fields have been linked to higher wind erosion risks.

The height of the stubble on the different fields is described in Table 6-1. All fields except for the fallow field were planted in January and harvested in July and August. No further tillage or cultivation has been performed on these fields yet. The maize field was a harvest field that had still standing straw and stubble after harvesting. The bare soil of this field was partially crusted and partially disturbed by tracks. The sunflower field was a harvested sunflower field with standing and laying stubble and had rows of low plant stubble, crusted rows, and track rows. The groundnut field was a harvested groundnut field with a mainly loose soil surface caused by the full removal of the crop and mechanical breakup of the soils during harvest. This field was furthermore largely covered by sand deposits that showed signs of wind erosion. Vos et al. (2021) showed that these sand deposits are

depleted in fines. The fallow field was a maize field that had not been planted during the past rainy season, causing the maize stubble from the year before to deteriorate. This resulted in a much lower soil cover than the maize field, but a fully crusted surface. Despite the lack of agricultural activities, this field still showed significant ridges and furrows, attributed to past seeding operations.

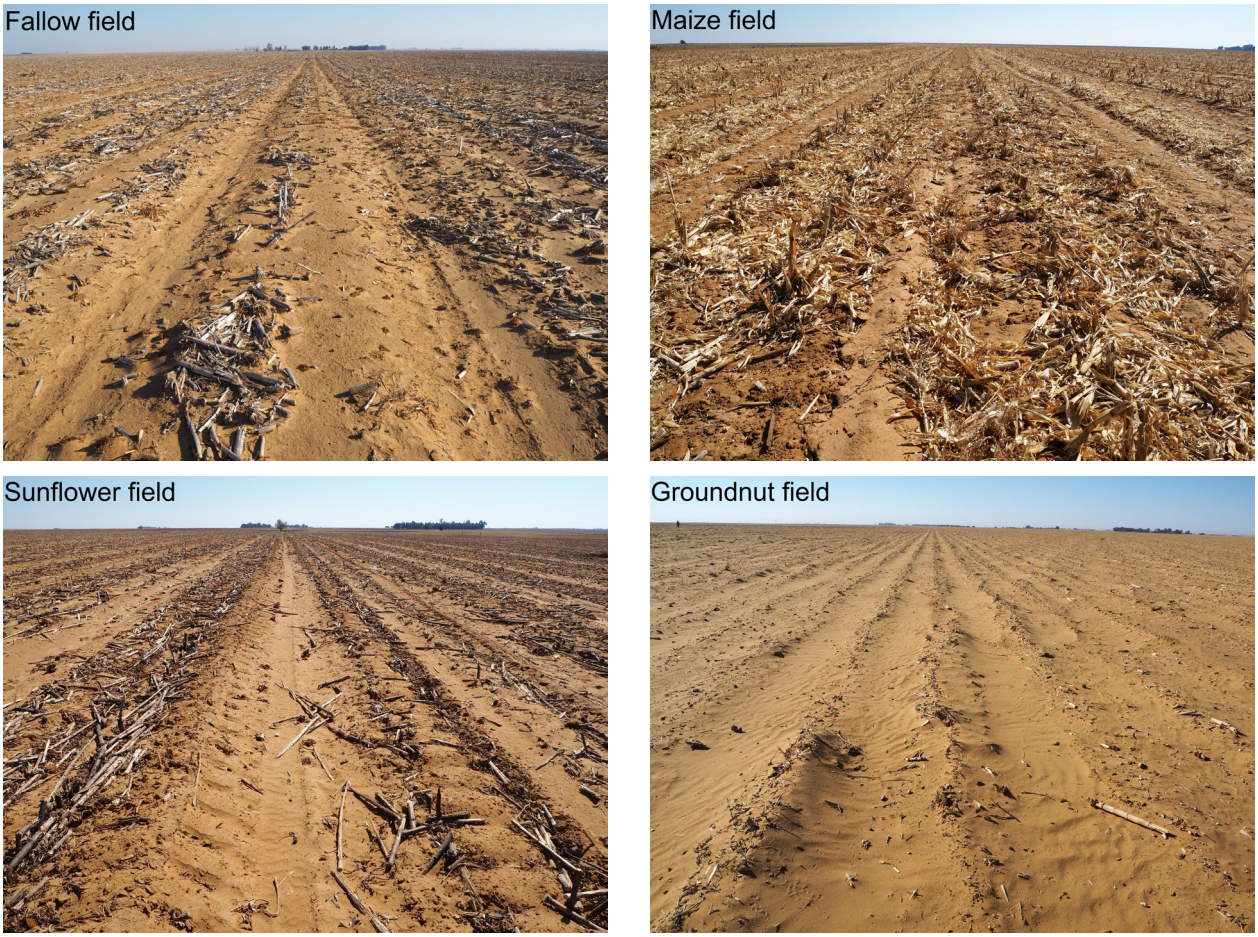

Figure 6-4. The four fields that were monitored during the field study.

Table 6-1. The height from the laying and standing stubble of the four fields.

Field	Stubble Laying	Stubble Standing
Sunflower	2–5 cm	10 to 20 cm
Maize	0–10 cm	30 cm
Groundnut	0–2 cm	None
Fallow	None	None

The soil type of all fields in this study is Arenosol, which is a prominent type in the Free State and commonly used for high-intensity agriculture (Hensley et al., 2006). Arenosols make up 15.3% of the soil area of South Africa. The texture of the soils ranged from loamy sand to sandy loam (Table 6-2).

Table 6-2. The average soil texture and Total Organic Carbon (TOC) content of the four fields.

Field	Average Clay %	Average Silt %	Average Sand %	Average TOC %
Maize field	12.3	3.0	84.7	0.227

Sunflower field	10.2	2.7	87.1	0.200
Groundnut field	8.7	2.6	88.8	0.184
Fallow field	17.1	4.1	78.8	0.318

6.3.2 Experimental Design

In each field, an anemometer mast, three Big Spring Number Eight (BSNE) masts, and a Sensit sensor were installed, see Figure 6-3. The fields were monitored from 26 August to 23 September.

BSNE sediment samples were used (Fryrear, 1986) to get an indication of the sediment flux during the period of monitoring. This is a commonly used sediment sampler due to its low cost, high efficiency, and general stability at different wind velocities (Fryrear, 1986; Goossens and Offer, 2000; Yang et al., 2018). Per field, three BSNE masts were installed (Figure 6-3) in a line following the observed soil texture gradient in the field to capture the within-field variations. The masts were positioned at a distance of 200 to 500 m from each other. The sediment was sampled after each wind event day, but the sediment flux is only calculated from the entire field monitoring period.

The data collected by the traps enable the calculation of the sediment transport and allow a general comparison between the fields. However, it will not give us precise insight into the spatial variability of a field since this would have required a much higher number of sampling positions, as discussed by Klose et al. (2019) and Webb et al. (2019). Each mast held three BSNEs at 0.10, 0.35, and 0.60 m height, defined from the geometric mean of the opening as proposed by Ellis et al. (2009). These heights were determined by the minimal possible distance of the lowest sampler to the ground, and of the minimal possible distance from the samplers to each other. The BSNE samples were weighted with a scale with a precision of 0.01 g. The efficiency of the BSNE correlates positively with the grainsize (Goossens and Offer, 2000; Sharratt et al., 2007; Yang et al., 2018). Since the efficiency of saltating grains is described to be near 100% (Abdourhamane Toure et al., 2011; Goossens and Offer, 2000), we will assume this efficiency for the horizontal mass flux samples.

During the field monitoring, wind velocity and direction were also observed, from which the aerodynamic roughness length of each field was calculated (see Section 2.3.2). The wind velocity and directions were monitored using Davis cup anemometers (Decagon Devices, Inc., Pullman, WA 99163, USA) attached to Decagon ZL6 loggers. These anemometers measure the wind velocity and wind direction with a precision of 5% and 7°, respectively, at a minimum of 0.9 m s^{-1} and a one-minute interval. Four anemometers were installed on a wind mast at 0.25, 0.5, 0.85, and 1.65 m to measure the logarithmic wind profile.

The threshold of wind erosion is often regarded as an important indicator of the erodibility of a surface (Fryrear et al., 1991; Gillette, 1988; Gillette et al., 1980; Li et al., 2010; Sharratt and Vaddella, 2014). In order to detect this threshold for the monitored sites, the saltation was monitored using the Sensit TM-H14-LIN (Sensit Inc., Redlands, CA 92374, USA). This instrument uses a cylindrical piezo-electric cylinder that counts the impact of saltating grains. The advantage of the Sensit is its sensitivity to smaller particles and low wind velocities. Van Pelt et al. (2009) described the threshold

diameter size of the Sensit to be below 125 mm for a wind velocity of 7.5 m s^{-1}. It has been used by several field- and wind tunnel studies (Fryrear et al., 1998; Goossens and Offer, 2000; Sharratt et al., 2007; Wiggs et al., 2004; Yang et al., 2018) to measure the saltation threshold. The Sensit data were recorded using the Campbell CR300 data logger and combined with the wind velocity measured at 1.65 m. Both values were aggregated to an interval with a one-minute interval. Two Sensit sensors were used to monitor four fields, therefore, positioning had to be alternated. Consequently, the saltation activity was only recorded partially. The Sensit sensor was installed close to the wind mast as shown in Figure 6-3.

6.3.3 Computation of Parameters

6.3.3.1 Sediment Flux

The mass data from the BSNEs is transformed into a horizontal sediment flux. For these calculations, we will use a power relationship as proposed by Zobeck and Fryrear (1986) as well as others, Abdourhamane Toure et al. (2011), Sharratt et al. (2007), and Webb et al. (2013). Therefore, the sediment flux q (g m^{-2}) with height z (m) is described as:

$$q = \alpha z^{\beta} \quad (1)$$

This relationship is integrated between 0.025 and 2 m height to calculate the sediment flux Q (g m^{-2}), following the study on agricultural fields by Sharratt et al. (2007). This kind of integration was found to be the best option, despite the risk of errors in the extrapolation of the sediment flux near the ground, especially considering the differences in roughness between the fields. The regression and heights for integration to calculate the horizontal sediment flux remains debated (Ellis et al., 2009; Mendez et al., 2011).

6.3.3.2 Aerodynamic Roughness Length

From the wind profile measured per minute by the anemometers, the aerodynamic roughness length was measured using a least-square fit on the Karman-Prandtl law-of-the-wall:

$$\frac{u_z}{u_*} = \frac{1}{k} \ln \frac{z}{z_0} \quad (2)$$

Whereby u_* is the friction velocity (m s^{-1}), u_z is the wind velocity (m s^{-1}) at height z (m), k is the von Karman constant (0.40), and z_0 is the aerodynamic roughness length (m). To calculate the aerodynamic roughness length, only measurements with a wind velocity above 0.9 m s^{-1} at the bottom anemometer were used. All the measured values were averaged per field for a final value.

6.3.4 Saltation threshold

To calculate the threshold velocity, the time fraction equivalence method (TFEM) from Stout and Zobeck (1997)and modified by Wiggs et al. (2004) was used. This formula assumes that the fraction of time units that saltation has been recorded is the same as the fraction of time units that the threshold wind velocity has been exceeded. Therefore, the minute saltation data ($p(t)$) is turned into binary data ($b_p(t)$). This gives the following formula:

$$\gamma_p = \frac{1}{N}\sum_{i=1}^{N} b_{pi} \quad (3)$$

Here, γp is the intermittency function, which can be linked to a certain wind velocity, which represents the threshold velocity. As discussed by Stout and Zobeck (1997), there is a negative correlation between the interval length of the measurements and the calculated threshold. Therefore, it is important to take into account that looking at second or hourly data, the threshold will be higher or lower, respectively.

6.3.5 Soil Cover from UAV Imagery

UAV imagery was collected during the dust season field campaign in 2019 to determine the surface area of the bare soil and the plant cover in each field. The UAV used for this study was a DJI Mavic Pro. To achieve a high resolution of the orthomosaic and digital surface model (DSM), the flight altitude was 10 m. The fields could only be partially covered, due to the large size of the fields in combination with the low flight low altitude. However, the obtained imagery is considered to generate a good index for the actual straw and stubble cover, because of the uniformity of soil properties and tillage practices. Image processing including orthorectification and production of a high-resolution orthomosaic and DSM was done with the photogrammetry software Pix4Dmapper.

The Ground Sampling Distance of the orthomosaic and DSM ranged from 3.1 mm to 4.1 mm. This enables a good distinction of features such as leaves and plant stumps. For the field cover analysis, the topographic ruggedness index (TRI) was calculated following Wilson et al. (2007) and was used as additional input data. For the land cover classification, three land cover classes were used: cover, soil, and shadow. To identify these classes, a supervised random forest algorithm was implemented using R. The ground truth data was collected virtually for each field. To reduce bias in the data, spatial distribution was regarded as well as the random separation of the data into training and validation data for the model. The random forest model was trained with 70% of this ground truth data and the model output was then validated with the remaining 30%, while a minimum distance of two pixels between a training- and a validation pixel was required for the random data separation. The model was then run using the RGB orthomosaic as well as the TRI raster as input data, resulting in classifications with an overall accuracy of above 90% for all fields. The final classification maps were made with ArcGIS and provided the basis for the statistical analyses on the distribution of land cover classes (Figure 6-5). For further analyses, the identified shadows were used as the error range. Lastly, for the maize and sunflower fields different row types (crop, crust, and track) were manually assigned and their spatial extent was calculated.

Figure 6-5. The results of the image analysis on the sunflower field: green represents the identified stubble cover, black represents shadow, and the remaining surface has been identified as soil (a). Distribution of the row types in the sunflower fields, where green is used for the planting rows, brown is the track rows, and crust is beige (b).

6.4 Results

6.4.1 Wind Characteristics and Sediment Flux

Figure 6-6 shows the wind rose for all the measured wind velocities during the period of field monitoring and the wind rose only including the velocities above the saltation threshold of 6 m s^{-1} (see Section 3.2). This wind velocity was reached during six wind events during the time of field monitoring. The general main wind direction appeared to be a southwesterly one. However, erosive winds occur in similar frequencies from NE, NW, and SW directions. This is in accordance with Eckardt et al. (Eckardt et al., 2020) who described that the daily dust events usually come from north to westerly winds, which change into a southern and eastern direction at night. Wiggs et al. (2011) also reported that most wind originates from southwestern to northwestern directions.

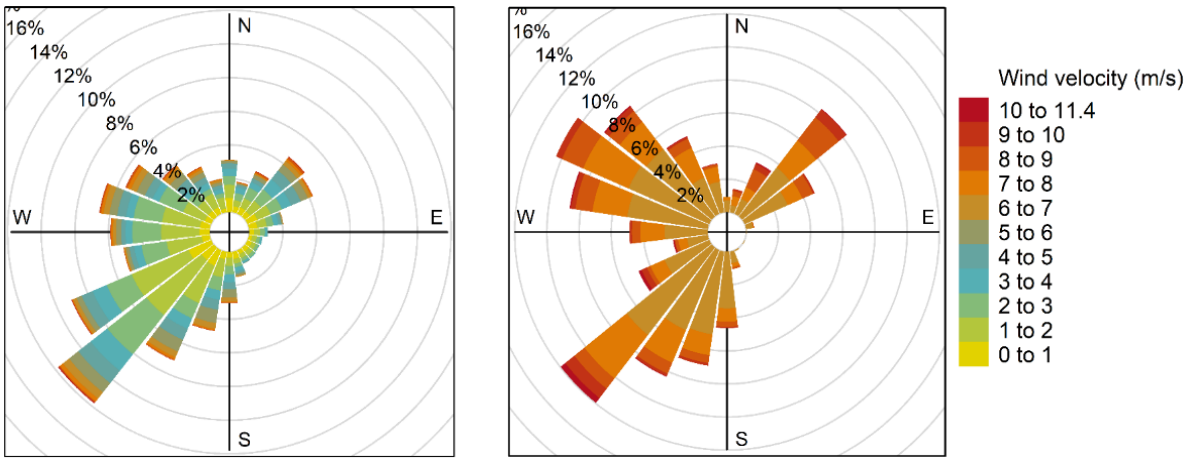

(**a**) (**b**)

Figure 6-6. The wind roses from the wind data that were measured at an hourly interval at the ARC climate station during the period of field monitoring of all the wind velocities (a) and the wind velocities above 6 m s^{-1} (b).

Eckardt et al. (2020) used 6 m s^{-1} as the average hourly threshold velocity for dust emission. During the field monitoring, 2.3% of the hours had an average hourly wind velocity above 6 m s^{-1}, which is roughly 17 h per month. This is a percentage that is observed during most months of the dust season from 2006 to 2016. Dust events have been associated with an average maximum wind velocity of 9.8 m s^{-1}, whereas the maximum hour wind velocity during the field monitoring period was 8.15 m s^{-1}. However, dust events have also been observed at 6.7 m s^{-1}, so these lower wind velocities do not have to be regarded as irrelevant. Most important are probably gust wind velocities, which are unfortunately not recorded in the available datasets.

The calculated sediment flux that was calculated based on the BSNE traps during this period is shown in Figure 6-7. The sediment flux on the groundnut field is at least 17 times larger than on the other fields. The maize field has the lowest sediment flux, followed by the sunflower field. The fallow field has on average a higher sediment flux than the sunflower field, but both fields showed a high variation in this value. This within-field variation of the sediment flux can be explained by the influence of bordering fields or changes in the erodibility in the field, as described by Bielders et al. (2001), but also a certain standard variability can be expected (Webb et al., 2019).

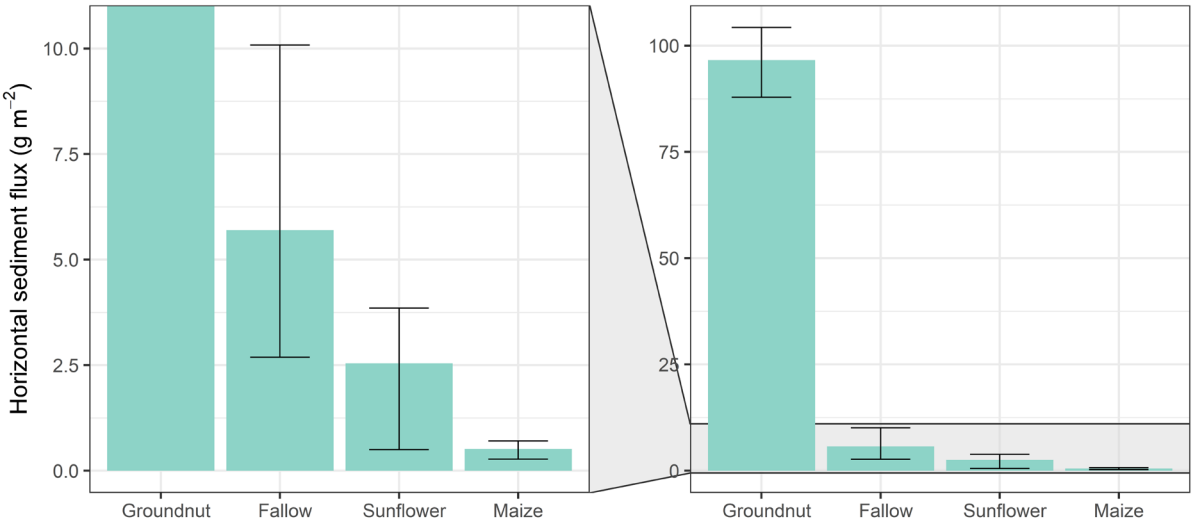

Figure 6-7. Average sediment flux on fields. Error bars illustrate maximum and minimum values.

6.4.2 Aerodynamic roughness and saltation threshold

Table 6-3 shows the average aerodynamic roughness length and the saltation threshold velocity measured on each field. As expected, the groundnut field had the lowest aerodynamic roughness length, with a height of 0.8 mm. In contrast, the maize field had a roughness length of 31.1 mm. Somewhat surprisingly, the sunflower field and groundnut field differed only a little, despite the difference in cover. Notably, the fallow field has a higher roughness length than the sunflower field, considering the similarities in soil cover. This supports the importance of preservation of the ridge and furrow pattern for increasing aerodynamic roughness, even on fields that have not been ploughed for approximately a year.

Table 6-3. Measured average aerodynamic roughness length and saltation threshold velocity of the different fields.

Field	Aerodynamic Roughness Length (mm)			Saltation Threshold Velocity (m s^{-1})			Minutes that Threshold Is Exceeded (%)	Days that Threshold Is Exceeded (%)
	Mean	n	σ	Mean	n	σ		
Maize field	31.1	46	9.66	>7.7			<2.1%	<30%
Sunflower field	1.9	410	1.25	5.96	61	2.22	6.1%	45%
Groundnut field	0.8	1203	0.76	5.95	36	1.15	8.8%	62%
Fallow field	3.0	794	10.0	6.54	11	2.48	6.1%	45%

The groundnut field and sunflower field have similarly low threshold wind velocities, despite their difference in soil cover. There was no definite threshold wind velocity measured on the maize field because it was not reached during our measurement period on that field. The maximum wind velocity measured on the maize field was 7.7 m s^{-1}, leading us to assume that the threshold velocity is definitely above this value. However, it cannot be told how much higher the threshold velocity precisely is. Despite the very limited saltation, the maize field could still emit dust due to deflation. Furthermore, the saltation of particles could have occurred outside of the detection range of the

Sensit. This limit is 100 mm for wind velocities below 10 m s^{-1} (Van Pelt et al., 2009), whereas particles of around 70 µm have the lowest threshold friction velocity (Greeley and Iversen, 1985). Table 6-3 also shows the percentage of minutes and days that the threshold velocity is crossed. As expected, this is the highest for the groundnut field. The sunflower and fallow fields have similar values. For the maize field, only estimations can be made, assuming a minimum threshold velocity of 7.8 m s^{-1}.

6.4.3 Cover Percentage

The identified cover and soil percentages are shown in Table 6-4. As expected, the maize field has the highest soil cover, which is almost twice as high as the sunflower field and six times greater than the groundnut field. The fallow field has a cover that is comparable to the sunflower field but with a lower error from the low shadow percentage. A year ago, the soil cover on the fallow field would have been similar to the maize field. Comparing the cover percentage of the current maize field to that of the fallow field, the cover is reduced by deterioration by roughly from approximately 66% to 40%. This is a significant decrease within one year, which is expected to decrease even further when no new crop is being planted in the following year, which could be the case if, for example, a drought year occurs

Table 6-4. The cover and soil percentages of each field as identified by the UAV analysis.

	Maize Field		Sunflower Field		Groundnut Field		Fallow Field	
Cover	66%	±7%	38%	±5%	11%	±0.4%	40%	±0.5%
Soil	34%		62%		89%		60%	

For the maize field and sunflower field, it was possible to differentiate rows in the fields and calculate the soil cover for each row (Table 6-5). As expected, the soil cover was highest for the crop rows, whereas the tracks and crusts have approximately the same soil cover percentages. This is roughly 38% for the maize field and 24% for the sunflower field. For the groundnut field and the fallow field, it was not possible to make a distinction between different rows. The cover distribution can be assumed as being rather homogenous.

Table 6-5. The percentage of the planting row, track, and crusts in size, and the identified surface area of each row type.

	Maize Field						Sunflower Field					
	Crop		Crust		Track		Crop		Crust		Track	
Fraction of field	82%		6%		12%		55%		16%		30%	
Cover	85%	±8%	39%	±7%	37%	±6%	48%	±7%	26%	±2%	22%	±3%
Soil	15%		61%		63%		52%		74%		78%	

6.5 Discussion

6.5.1 Field Characteristics

The first aim of this study was to determine the field characteristics of the maize field (high soil cover), the sunflower field (medium soil cover), the groundnut field (low soil cover), and the fallow field (medium soil cover). Our results show a positive relationship between the soil cover and the roughness (Figure 6-8). The groundnut field has the lowest roughness length (0.8 mm) in combination with the lowest stubble cover (11%). The maize field had a much higher roughness than the other fields (31.1 mm), which is likely related to the higher cover percentage (66%) and the height of this soil cover. The sunflower field and fallow fields are close in characteristics when it comes to roughness length (1.9 and 3.0 mm, respectively) and cover percentage (38 ± 5 and 40 ± 0.5%, respectively). The higher error in the sunflower field is caused by the relatively large area of shadow. Therefore, this field could have a higher or lower cover percentage than the fallow field depending on the surface type that the shadows in this field represent.

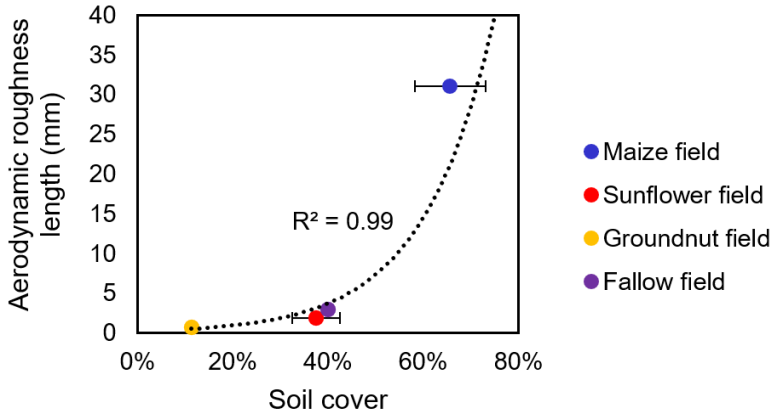

Figure 6-8. The soil cover versus the aerodynamic roughness length from the monitored fields.

The maize field and the sunflower field showed a spatial distribution of the soil cover, which was determined by the planting, crust and track rows. The planting rows had a much higher soil cover (85 and 48% for the maize field and sunflower field, respectively), than that on the track and crusted rows (38% and 24% on average, respectively). This difference in soil cover raises the question of whether the highest, lowest, or average soil cover controls erosion on a field within a typical pattern of surface conditions.

6.5.2 Erodibility and the influence of the field use on wind erosion

The second and third aim of this study was to determine the threshold velocity and sediment flux of fields and how these values relate to the field characteristics. The threshold velocity has a positive correlation with the roughness. The estimated threshold velocity of the maize field was above 7.7 m s^{-1}, which can be explained by the high roughness and protection of the maize stubble. Cohesion is

not expected to play a significant role in the threshold velocity, since the moving sand grains are expected to be loose top grains, as described by Vos et al. (2020).

The sediment flux showed greater deviance between the fields than the threshold velocity and the surface characteristics, with a 117-fold difference between the groundnut field and maize field. The relationship between the soil cover and sediment flux shows a good exponential relationship as described by Funk et al. (2015) and Fryrear (1985, 1984) (Figure 6-9). The mentioned studies compare the sediment flux relative to the flux without soil cover, or the soil loss ratio (SLR). For our data, the soil flux of the bare soil is unknown, hence the SLR cannot be calculated. It can be expected that the soil flux from the bare soil would be different for each field, considering the difference in cohesion and roughness from ridges and furrows (Gillette, 1988; Liu et al., 2006). Despite the limitations of our data, the relevance of soil cover is illustrated by the observed sediment flux.

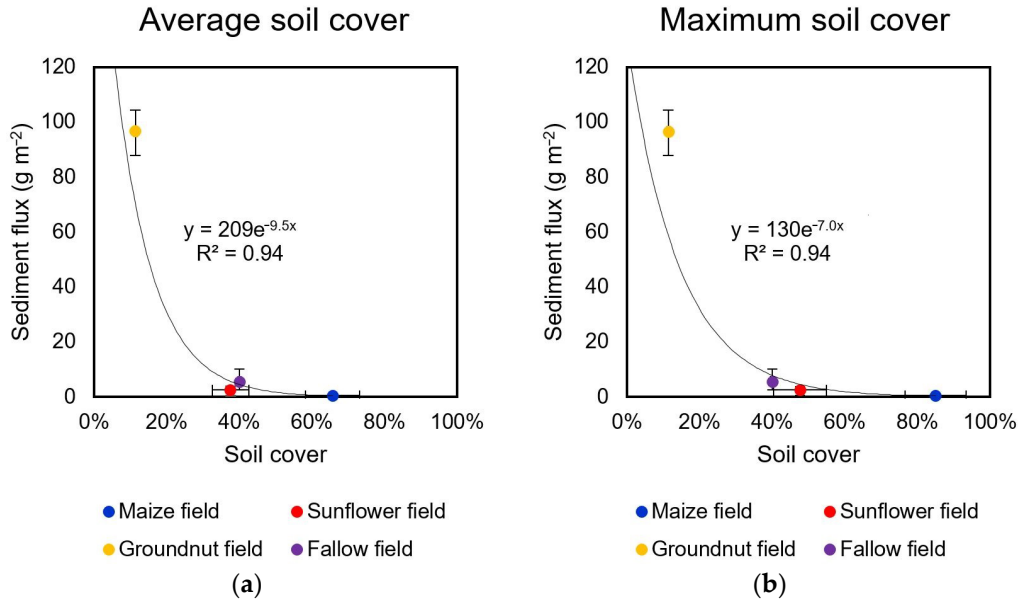

Figure 6-9. Relation between average sediment flux and soil cover. (a) Relations with average soil cover and (b) maximum soil cover from planting rows. The error bars indicate the variance for soil cover due to shadows in the UAV images, and the minimum and maximum value of the sediment flux.

A notable deviance from the relationship in Figure 6-9a is the low sediment flux on the sunflower field compared to the fallow field. This was against initial expectations, considering the higher roughness and cohesion of the fallow field. This difference could be explained by the relatively high vegetation cover in the planting rows in the sunflower field. We, therefore, hypothesize that the high plant cover in the planting rows can limit the transport from the bare rows significantly. We assume that Figure 6-9b, where the maximum soil cover in the rows is taken into account, is a better representation of the relationship between the soil cover and the sediment flux for the sunflower field and maize fields. Considering the NS direction of the ploughing ridges and the predominantly SW, NE, and NW wind directions, the sediment transport would be impeded across the field by the cover-rich plant rows and the ploughing ridges. This would emphasize the importance of highly dense, centred vegetation rows compared to the randomized stubble in the fallow field. This effect is

expected to be most pronounced when the plant row direction is at a minimum of 45° to the wind direction (Funk and Engel, 2015). Another explanation for the low sediment flux on the sunflower field could be caused by the relatively high degree of uncertainty as a result of the detected shadows from the UAV images, which could represent mainly soil cover. The maximum cover percentage on this field does show accordance with the calculated regression. This shows the limitation of UAV analyses in precisely quantifying soil cover and its influence on erodibility.

The difference between erodibility characterised by the threshold velocity and sediment flux is notable. Where the sunflower field and groundnut field had similar threshold velocities, the groundnut field had a sediment flux that was 38 times higher than the sunflower field. Furthermore, the fallow field has an average sediment flux twice as high as the less rough sunflower field with a low threshold velocity. This difference illustrates again that the protection from cover is not just caused by the increased roughness, but also by the proportion of the surface that is covered and the spatial pattern of the cover. Both have to be considered when assessing the erodibility of a field.

The fully crusted fallow field does not show a clear influence of cohesion, since the sediment flux does plot on the regression from Figure 6-9 and does not show a significantly lower sediment flux. To determine the influence of crusts on the sediment flux, measurements on a field with similar cover characteristics but different levels of disturbance would be required.

6.5.3 Risk assessment for land-use types and implications for dryland agriculture

Certain land-use types can have a specific range of surface characteristics that are related to the stubble quantity and cohesion of the surface. This could result in certain land-use types having a higher general wind erosion risk than others, in other words, the cover or cohesion during one crop rotation cycle alone is not sufficient to assess erodibility in situations where drought may interrupt such cycles. Considering the degrading effect of dust emission on soils, this is also important for the benefit of crop production itself. To determine the risk of both influences, the measured sediment fluxes of these crops were multiplied by their surface area, see Figure 6-10. This calculation does not take any variance in the sediment flux per crop type into account, and it should be noted that the total sediment flux might not be directly linked to the vertical dust flux, as described by Sterk et al. (1996). Furthermore, data on sorghum, soybeans, and wheat are missing. Wheat is expected to have a low wind erosion risk since the growing season is in winter. Meaning that it has a very high soil cover during the dust season. The relative importance of soybeans and sorghum, which cover 9% of the agricultural land in the Free State still needs to be assessed. Nonetheless, Figure 6-10 shows the high relevance of groundnuts and fallow fields. This would fit with the conclusions from Eckardt et al. (2020), who associated the high emissions of 2015/16 with the large proportion of fallow fields. Furthermore, the high emissions from groundnut fields in the Free State have not received any attention despite being identified as a problematic crop not just in this study, but also by Santra et al. (2017).

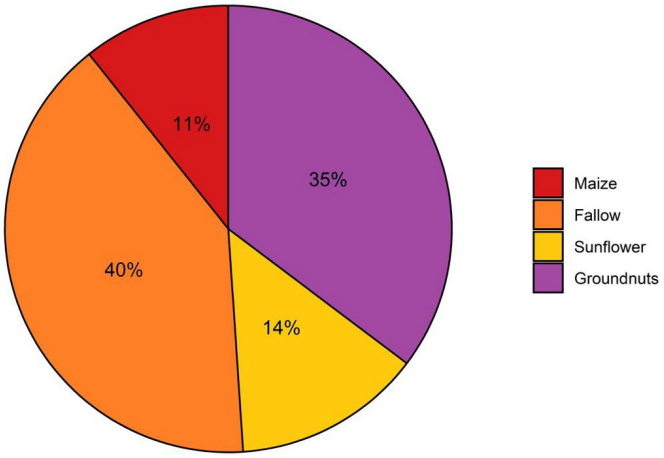

Figure 6-10. The relative sediment transport calculated from the average sediment flux. Note that flux data from wheat, sorghum, and soya beans are missing and that this data was excluded.

The groundnut field experienced the highest sediment flux. Considering the methods of groundnut harvest, this crop does not offer options for stubble-saving harvesting techniques. Current harvesting methods destroy all crusts. The percentage of groundnut fields in the Free State is currently quite low, but the highly erosive surfaces that these crops create should be considered as potential hotspots of emissions. Other crops that leave little soil cover after harvest, such as many bean types, could pose similar risks to dust emission. The high erosion risks associated with such crops, especially in the more arid regions with erodible sandy soils, should therefore be taken into account when making land management decisions.

The cover on the fallow field originates from the deteriorated maize stubble, which created a field condition with the second-highest sediment flux. This indicates that the missing of a planting window, or the purposeful decision to do so, is a process that potentially results in a low cover that makes the field sensitive to wind erosion. The exponential relationship between soil cover and sediment flux emphasizes the even greater danger of missing the second window of planting. The sensitivity to erosion from these fallow fields would potentially become even higher if the crusts of these fields would be disturbed by tillage operations for the next rainy season.

Lastly, the maize field had a much lower sediment flux than the sunflower field, which could also be attributed to their difference in cover. This illustrates that in general, maize stubble offers enough protection to minimize wind erosion in the Free State. The sunflower field showed an average sediment flux that was half of that on the fallow field, making it a lower risk crop than the fallow field. Sunflower is often grown during a delayed rainy season (personal communication with farmers) and should be considered as a preferred crop compared to keeping a field fallow.

The impact of soil cohesion on emissions observed in the study of Vos et al. (2021) illustrates that the preservation of crusts could be an important land management practice. In addition to conservation or reduced tillage, as described by Gicheru et al. (2004); Pi et al. (2018); Sharratt and Collins (2018), delaying tillage or necessary cultivation practices could reduce dust emissions, as

proposed by Funk et al. (2008). In addition to avoiding the destruction of crusts by tillage, their abrasion should also be reduced by limiting the sources of abrading sands from tracks, roads, and tillage on adjacent fields.

6.6 Conclusion

This study focused on characterizing the roughness and soil cover and measuring the associated wind erosion on four fields in typical Free State dust season conditions. The selected fields represent different scenarios that are common during the dust season: medium cohesion (maize field), medium cover and medium cohesion (sunflower field), high cover and low cover and low cohesion (groundnut field), and medium cover and high cohesion scenario (fallow field). This study also used UAV imagery for assessing the soil cover percentage with high resolution in the framework of a wind erosion study. The results showed a variance between 11 and 66% of soil cover. The sediment flux differed greatly among the different fields, but broadly followed a negative, exponential relationship with soil cover. The data collected at the study sites will illustrate the risk and intensity of wind erosion from different crops and field conditions. It will also provide a base to predict the behaviour of fields with different soil cover and roughness characteristics. In more general terms, this will help with the prediction of dust events and thus improve the quality of the output of wind erosion models. This study is therefore not only relevant for the Free State, but will also give an insight into factors controlling wind erosion and dust emissions on other rainfed croplands in drylands with strong seasonal contrasts in precipitation and cover (Bunn, 1998; López et al., 1998; Santra et al., 2017; Sterk et al., 2001).

The relationship between field condition and wind erosion observed in this study also illustrates the importance of maintaining stubble as a method to minimize wind erosion. In certain cases, the maintenance of stubble can be relatively easy, for example, by refraining from growing crops that leave little stubble after harvest such as groundnut. Maize is the most common crop in the Free State and leaves a high straw and stubble cover and has therefore a low wind erosion risk. However, it is not always possible to grow maize because of little or late rainfall. In those cases, farmers are forced to plant sunflowers or leave a field fallow, both increasing the wind erosion risk. On a fallow field, the stubble cover will deteriorate and decline over time, in which case the focus on dust emission prevention should shift to the maintenance of soil crusts. This can involve delaying tillage operations as close as possible to the first rainfall, as well as limiting external saltators and introducing stable roughness elements such as grasslands (Bielders et al., 2001; Rajot, 2001).

Overall, the results of this study have implications for all cropland experiencing dry and windy periods outside the growing season. This raises several research questions for future research. More measurements and knowledge on the sediment flux of bare surfaces and the influence of vegetation are necessary to create a precise expression for this relationship. The influence of row width on emission appears relevant from our data, highlighting the need for studying (or at least measuring and mentioning) not just the total or average percentage of straw and stubble but, taking into account their spatial patterns. Furthermore, the erosion of crusts by abraders that may have originated

outside the eroding field demonstrates that the mutual influence of neighbouring fields on their respective emissions should become a focus of wind erosion research. This involves, for example, measuring the mass balance of fallow fields and to which extent erosion can be prevented by any saltator traps on the border of a field, such as fences or grass rows. Finally, more insight into the influence of ridges from seeding and ploughing, i.e., the form roughness of the surface (Fryrear, 1984; Liu et al., 2006; Raupach et al., 1993; Wiggs and Holmes, 2011), on low cover fields is necessary. In such conditions, crusts in combination with tillage-induced soil surface roughness could be an important way to reduce erosion. However, the question remains whether tillage would increase emissions due to the disturbance of crusts, as suggested by Gicheru et al. (2004) or decrease emissions by increasing the roughness, as suggested by Wiggs et al. (2011).

7.

Summary and conclusion

7.1 Summary

This thesis aimed at answering the research question "*What role do crusts play in the emission from Free State croplands*?". Five aims were developed to answer this question:

1. Create a cross-comparison between the PI-SWERL and a traditional wind tunnel;
2. Determine how soil crusts develop under rainfall;
3. Determine the difference in emissivity between crusts and loose surfaces and determine the surface characteristics that influence the emissivity of these surfaces;
4. Describe the main pathogens and allergens that are present in the suspended dust and the fractionation that these microbial organisms show compared to the emitting soil;
5. Determine under which conditions the soil cover is low enough for crusts to become a significant factor in dust emission.

The first aim was addressed in Chapter 2, the second in Chapter 3, the third in Chapters 3 and 4, the fourth in Chapter 5, and the fifth in Chapter 6. This subchapter will first summarize the primary conclusions from the different chapters, after which the extent to which the aims have been addressed will be discussed.

Chapter 2 involves a lab-based comparison between the PI-SWERL and the portable straight-line wind tunnel of the University of Basel. The threshold friction velocities from fine sand and loamy sand, measured by both instruments, were compared. The sandy soil showed a similar threshold friction velocity for the wind tunnel and PI-SWERL, whereas the loamy sand showed a lower threshold friction velocity for the wind tunnel. The difference between the two instruments for the loamy sand is attributed to the sensitivity of the PI-SWERL which enables it to detect the small, initial PM10 emission. This indicates that the PI-SWERL is capable of measuring the threshold friction velocity for dust from soil surfaces.

In Chapter 3, both the formation of crusts by experimental rainfall on a Free State Luvisol and Arenosol and the dust emission from these crusts were examined. The rainfall experiments illustrate an increase in shear strength with rainfall quantity, whereby the more clay and silt-rich Luvisol shows greater cohesion than the Arenosol. Notably, sequenced rainfall increases the crust strength in a similar way to single event rainfall. Within 15 mm of rainfall, crust strength is significantly developed and protects soil well against dust emission. For both Arenosol and Luvisol, the emission of a crust formed by 15 mm of rainfall is less than 1% of the emission from a loose soil. The presence of abraders increases the emission from a crust, but these emissions remain less than 10% of that of a loose surface. However, the apparent unlimited supply of PM_{10} from an abrading crust is an indication of the degradation, which, through time, could destroy it. The results of this chapter show that crusts with the potential to reduce dust emissions can form rapidly on Free State cropland soils.

The fourth chapter presents the emissions that were measured with the PI-SWERL on cropland surfaces in the Free State, with a focus on crusts and loose surfaces. This is combined with soil surface

measurements on the texture, chemistry, moisture, and shear strength to identify the variables that influence emissivity. The results illustrate a greater emission from loose surfaces, which is confirmed by the high relevance of cohesion as identified by Boosted Regression Tree (BRT) analysis. When considering each surface type separately, the data show that the emission from crusted surfaces is controlled by abraders, whereas the emission from loose surfaces is mainly controlled by their clay and silt content. The depletion of silt and clay from the sand deposited on the highly erodible groundnut field also indicates that Free State cropland is already affected by soil degradation through wind erosion and dust emission. Chapter 4 supports the conclusion of chapter 3 that crusts could potentially reduce emissions from Free State cropland soils.

The fifth chapter presents a novel microbial study on particles that suspend into the atmosphere from the Free State soils using the PI-SWERL. Little fractionation was found in fungal communities, while bacterial communities did show a clear fractionation in spore-forming taxa in the dust. The lack of fractionation in fungi shows the potential for using certain microbial signatures to determine the origin of dust. The sampled dust shows high levels of allergens and pathogens, from which *Cladosporium*, *Alternaria*, and *Fusarium* are the most enriched. These fungal microbes are associated with asthma, eczema, hay fever symptoms in humans, and plant spoilage. Their presence in suspended dust indicates that aerosols from these croplands could have an amplified negative offsite effect on human health. This study furthermore shows the potential of the PI-SWERL for sampling suspended dust for microbial analyses.

The sixth chapter presents data from the sediment flux monitoring of four fields that represent different scenarios of cropland surface conditions during the Free State dust season. The results mainly illustrate the strong relationship between soil cover from crop residue and the measured horizontal sediment flux. The soil cover ranged from 11% to 66% and the associated horizontal sediment flux ranged from 97 g m^{-2} to 0.52 g m^{-2}, respectively. The highest flux was measured on the groundnut field, a field that besides a low soil cover also has a highly disturbed surface due to the harvesting activities. The data also pointed towards the importance of soil cover-rich planting rows instead of a homogenous distribution of cover. The fallow field showed the second-highest horizontal sediment flux, which indicates that abrasion on these crusted fields is a highly relevant process

7.2 Conclusion

This thesis addressed the influence of crusts on dust emission from Free State croplands by using a combination of laboratory experiments and field studies. The results of this research show the high potential of crusts to minimize dust emission, even on sandy soils. The shear strength threshold for a protective crust has been identified to be 15 kPa by the BRT analysis, a shear strength that can develop within 15 mm of rainfall. Figure 7-1 shows the influence of abraders and clay and silt content for crusts and loose soil, respectively, which shows the general higher emission on loose surfaces. However, the reduction of dust emission by crusts is dependent on abrasion, illustrating the need to reduce external saltators on fields when low soil cover cannot be avoided. Despite the strong

influence of crusts on emissions, the cover of soil, when present, is the dominant factor controlling wind erosion and dust emissions in the Free State whereby a lower soil cover leads to a higher importance of soil crusts. The presence of crust would therefore be especially important in fields with a soil cover of 40% or less.

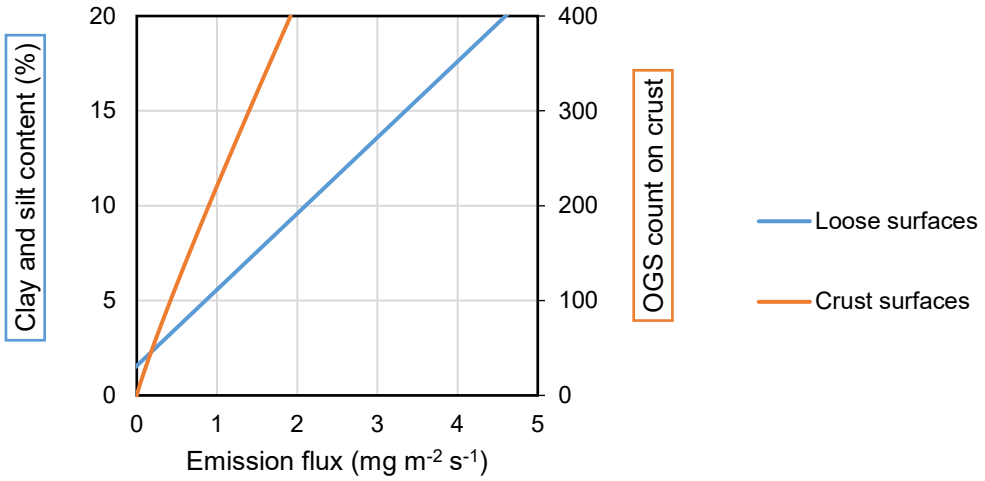

Figure 7-1. The influence of the clay and silt content and the OGS count on the emission flux from loose and crusted surfaces, respectively. The OGS count is an indication of the abrasion on a surface. These relationships are based on the regression from chapter four and do not include any variations in the data. The y-axis limits are based on the maximum values measured in the field.

This thesis also reveals that wind erosion has caused soil degradation already. In addition, the presence of specific allergens and pathogens illustrates the potential public health implications, further highlighting the need for reducing dust emissions in the Free State. Wind erosion reduction strategies can involve known practices of residue or vegetation cover management, but in situations, such as fallow or prolonged drought, the protection of crusts could be an important tool for reducing emissions. Furthermore, the significant increase in erosion caused by abrasion on crusted soils illustrates the need for identifying their sources and reducing their impact within clusters of fields when managing emissions.

The importance of crust on dust emission and wind erosion as shown by this study demonstrates the improvements possible for wind erosion models. As discussed in the introduction, most of the wind erosion models do not account for the presence of a crust. From the models that do account for the presence of a soil crust, only the WEPS includes the presence of abraders. The RWEQ wind erosion model, which has been used most commonly, described the influence of a crust based on the clay and silt content, whereby a crust builds up in 12 mm of rainfall and is fully destroyed by tillage operations. The 12 mm of rainfall to build a crust can be confirmed by our rainfall experiments. The crust factor of the experimental soils would be 0.95 and 0.79 for the Arenosol and Luvisol, respectively, meaning that the wind erosion of these surfaces is only slightly smaller than on a loose surface. The predicted wind erosion differs greatly from the experimentally measured dust emission. Partially this could be caused by the difference between wind erosion and dust emission, and the fact that the crust factor

is not developed for soils with a silt and clay content and TOC content below 6.4% and 0.18%, respectively, which is the case for some of the Arenosols. However, this shows again the underestimation of the effect of soil crusts on such sandy soils. Furthermore, this crust factor has been described the crust factor as a resistance against abrasion (Fryrear et al., 1998). However, the quantity of abraders, which is the main trigger in dust emission from crusts, is not included in the model. This shows the possibilities for improving the crust factor for this already extensive wind erosion model.

The RWEQ has been used by a recent study from Zhao et al. (2020) to model wind erosion in Southern Africa. The model was calculated for a resolution of 8 km and used the soil data from the International Soil Reference and Information Center and land use data from the Climate Change Initiative (CCI-LC) from the European Space Agency. Figure 7-2 shows the results from this wind erosion modelling from 2011 to 2015. Notable is the low wind erosion modelled for the Free State, which does not give predictions that are comparable with the observations from Eckardt et al. (2020). This would indicate an error or inaccuracy of the model or input variables, or that there is a large mismatch between the wind erosion modulus and the occurrence of a dust event.

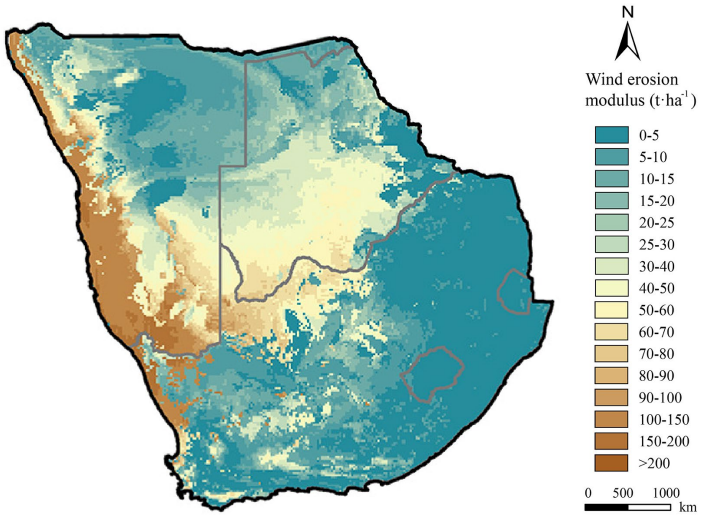

Figure 7-2. Map from Zhao et al. (2020) showing the calculated wind erosion based on the RWEQ model from 2011 to 2015.

7.3 Outlook

Several knowledge gaps and topics for further research can also be identified from the thesis. This study showed the potential of UAVs for mapping soil cover from crop residue, but the field monitoring data does not differentiate between the influence of soil cover, roughness and cohesion. More field monitoring and mapping are necessary to differentiate between the influences of these factors on erodibility. Future studies should also address the influence of external sediment on the measured sediment flux, something that could be especially relevant for the fallow fields since this would indicate the extent to which crust abrasion could be prevented. Furthermore, the difference between

the sediment flux and the dust flux should be examined, since this will give a better understanding of the dust emission per field when traps such as the BSNEs are used for monitoring. The BSNE has a low efficiency for PM_{10} particles, so a more precise sampler for PM_{10} particles is required to calculate the horizontal PM_{10} flux.

The influence of clods and other roughness elements generated by tillage or ridges and furrows have not been included in the PI-SWERL measurements. Clods are the remains of a crust after disturbance and have relatively high cohesion and roughness and are expected to decrease the emission from a disturbed surface. These surfaces have been excluded from measurements because the PI-SWERL is only developed for relatively flat surfaces. Etyemezian et al. (2014) only investigated surfaces with roughness elements up to a maximum of 10 mm, even though higher roughness elements are very common and should be considered for future studies. To measure rougher surfaces, a more extensive study of the use of the PI-SWERL on rough surfaces is required. However, certain roughness elements are too rough to be analyzed by the PI-SWERL and their influence on the erodibility can only be assessed by field monitoring, as mentioned before. Furthermore, the BRT analyses on the emission from both crusted and loose surfaces showed a high relevance for the air temperature and humidity. This can either be a result of a change in the soil moisture content, or a change in air density that influences the shear strength of the air. It is difficult to determine the exact relationship using the BRT analyses alone, so this should be considered for future studies. Another point that deserves further study is the degradation of crusts. Both in experimental and field settings the abrasion of crusts leaves marks on the surface. Furthermore, crusts could have degraded by freezing and thawing, as suggested by Liu et al. (2017) and Wang et al. (2014). To which extent degraded crusts remain relevant for minimizing erosion is not known.

The results of this thesis also show that more effort is required to assess the on- and offsite impacts of wind erosion and dust emissions. The depletion of clay and silt from the highly erodible groundnut fields in the Free State is a sign of the land degradation that is taking place in this region, but the exact depletion over time is unknown. Furthermore, the offsite effect of allergens and pathogens on human health requires further investigation.

7.4 Implications for dryland agriculture

As discussed in the introduction, wind erosion from croplands is not limited to the Free State. Generally, sandy soils in semi-arid and arid regions are sensitive to wind erosion. The decrease of surface cohesion and cover by agricultural practices makes these surfaces even more vulnerable. Emissive regions differ when it comes to soil, climate, and agriculture. However, some general recommendations can be made based on the findings of this thesis. One important consideration is the minimization of crops that leave a low residue cover and destroy the crust of a surface. In the case of the Free State, these crops include groundnuts, but also crops like potatoes and beans (Larney et al., 1997; Riksen et al., 2003) could create similar surface conditions. Soil cover has been shown to be of high importance, but a cover cannot always be maintained due to drought or crop type. In this case,

the management of crusts and their protection of it should become a priority. Crust management practices can include the minimization of soil disturbance and the delay of any necessary cultivation or ploughing until as close as possible to the start of the rainy season. The limitation of external saltators would also be very important, which could be done by introducing barriers at the field edges, preferably in combination with small field sizes.

These recommendations are likely to have financial and agricultural aspects that need further consideration. There are often economic reasons why certain crops are cultivated in a region, and some crops are crucial for food production for the local population. The shift from one crop type to another, or the exclusion of certain crop types, should be considered with local farmers. Similarly, the use of smaller fields and barriers at the boundaries must be considered taking the financial and logistical aspects into account. Lastly, the effect of low or delayed tillage and ploughing practices on the soil conditions has to be considered, since low tillage could compact soil and result in a lower crop yield (Ren et al., 2019). Despite these potential challenges for implementing soil conservation measures, the results of this thesis demonstrate that both soil degradation and public health would benefit from reducing dust emissions and thus contribute to more sustainable crop production in the Free State.

References

Abdourhamane Toure, A., Rajot, J.-L., Garba, Z., Marticorena, B., Petit, C., Sebag, D., 2011. Impact of very low crop residues cover on wind erosion in the Sahel. CATENA 85, 205–214.

Adhikari, A., Jung, J., Reponen, T., Lewis, J.S., DeGrasse, E.C., Grimsley, L.F., Chew, G.L., Grinshpun, S.A., 2009. Aerosolization of fungi, (1→3)-β-d glucan, and endotoxin from flood-affected materials collected in New Orleans homes. Environmental Research 109, 215–224.

Anderson, M.J., 2006. Distance-Based Tests for Homogeneity of Multivariate Dispersions. Biometrics 62, 245–253.

Anderson, M.J., Walsh, D.C.I., 2013. PERMANOVA, ANOSIM, and the Mantel test in the face of heterogeneous dispersions: What null hypothesis are you testing? Ecological Monographs 83, 557–574.

Archer, E., Tadross, M., 2009. Climate change and desertification in South Africa - Science and response. African Journal of Range & Forage Science - AFR J RANGE FOR SCI 26.

Azeem, M., Sun, D., Crowley, D., Hayat, R., Hussain, Q., Ali, A., Tahir, M.I., Jeyasundar, P.G.S.A., Rinklebe, J., Zhang, Z., 2020. Crop types have stronger effects on soil microbial communities and functionalities than biochar or fertilizer during two cycles of legume-cereal rotations of dry land. Science of The Total Environment 715, 136958.

Baas, A.C.W., 2004. Evaluation of saltation flux impact responders (Safires) for measuring instantaneous aeolian sand transport intensity. Geomorphology 59, 99–118.

Bacon, S.N., McDonald, E. V, Amit, R., Enzel, Y., Crouvi, O., 2011. Total suspended particulate matter emissions at high friction velocities from desert landforms. Journal of Geophysical Research: Earth Surface 116.

Bagnold, R.A., 1941. The physics of blown sand and desert dunes. Methuen, London.

Bali, K., Mishra, A.K., Singh, S., 2017. Impact of anomalous forest fire on aerosol radiative forcing and snow cover over Himalayan region. Atmospheric Environment 150, 264–275.

Barker, C.H., 2002. n Morfometriese ondersoek na landskapontwikkeling in die Sentraal-Vrystaat:n toepassing met behulp vann geografiese inligtingstelsel. University of the Free State.

Basaran, M., Erpul, G., Uzun, O., Gabriels, D., 2011. Comparative efficiency testing for a newly designed cyclone type sediment trap for wind erosion measurements. Geomorphology 130, 343–351.

Becher, H.H., Breuer, J., Klingler, B., 1997. An index value for characterizing hardsetting soils by fall-cone penetration. Soil Technology 10, 47–56.

Behzad, H., Mineta, K., Gojobori, T., 2018. Global Ramifications of Dust and Sandstorm Microbiota. Genome Biology and Evolution 10, 1970–1987.

Belnap, J.., Kaltenecker, J.H.., Rosentreter, R.. et al., 2001. Biological soil crusts: Ecology and management, Technical Reference 1730-2. Denver.

Belnap, J., 2006. The potential roles of biological soil crusts in dryland hydrologic cycles. Hydrological Processes 20, 3159–3178.

Belnap, J., 2001. Comparative structure of physical and biological soil crusts, in: Biological Soil Crusts:

Structure, Function, and Management. Springer, pp. 177–191.

Belnap, J., Gillette, D.A., 1998. Vulnerability of desert biological soil crusts to wind erosion: the influences of crust development, soil texture, and disturbance. Journal of Arid Environments 39, 133–142.

Belnap, J., Phillips, S., Herrick, J., Johansen, J., 2007. Wind erodibility of soils at Fort Irwin, California (Mojave Desert), USA, before and after trampling disturbance: Implications for land management. Earth Surface Processes and Landforms 32, 75–84.

Belnap, J., Phillips, S.L., Witwicki, D.L., Miller, M.E., 2008. Visually assessing the level of development and soil surface stability of cyanobacterially dominated biological soil crusts. Journal of Arid Environments 72, 1257–1264.

Bennie, A.T.P., Hensley, M., 2001. Maximizing precipitation utilization in dryland agriculture in South Africa - A review. Journal of Hydrology 241, 124–139.

Bhat, R., Rai, R. V, Karim, A.A., 2010. Mycotoxins in Food and Feed: Present Status and Future Concerns. Comprehensive Reviews in Food Science and Food Safety 9, 57–81.

Bielders, C.L., Rajot, J.-L., Amadou, M., 2002. Transport of soil and nutrients by wind in bush fallow land and traditionally managed cultivated fields in the Sahel. Geoderma 109, 19–39.

Bielders, C.L., Vrieling, A., Rajot, J.-L., Skidmore, E.L., 2001. On-farm evaluation of field-scale soil losses by wind erosion under traditional management in the Sahel. In: Soil Research for the 21ste Century, Hawaii 2001. - [S.l.] : [s.n.], 2001.

Bilbro, J.D., Fryrear, D.W., 1994. Wind Erosion Losses as Related to Plant Silhouette and Soil Cover. Agronomy Journal 86, 550–553.

Bolyen, E., Rideout, J.R., Dillon, M.R., Bokulich, N.A., Abnet, C.C., Al-Ghalith, G.A., Alexander, H., Alm, E.J., Arumugam, M., Asnicar, F., Bai, Y., Bisanz, J.E., Bittinger, K., Brejnrod, A., Brislawn, C.J., Brown, C.T., Callahan, B.J., Caraballo-Rodríguez, A.M., Chase, J., Cope, E.K., Da Silva, R., Diener, C., Dorrestein, P.C., Douglas, G.M., Durall, D.M., Duvallet, C., Edwardson, C.F., Ernst, M., Estaki, M., Fouquier, J., Gauglitz, J.M., Gibbons, S.M., Gibson, D.L., Gonzalez, A., Gorlick, K., Guo, J., Hillmann, B., Holmes, S.P., Holste, H., Huttenhower, C., Huttley, G.A., Janssen, S., Jarmusch, A.K., Jiang, L., Kaehler, B.D., Kang, K. Bin, Keefe, C.R., Keim, P., Kelley, S.T., Knights, D., Koester, I., Kosciolek, T., Kreps, J., Langille, M.G.I., Lee, J., Ley, R., Liu, Y.-X., Loftfield, E., Lozupone, C., Maher, M., Marotz, C., Martin, B.D., McDonald, D., McIver, L.J., Melnik, A. V, Metcalf, J.L., Morgan, S.C., Morton, J.T., Naimey, A.T., Navas-Molina, J.A., Nothias, L.F., Orchanian, S.B., Pearson, T., Peoples, S.L., Petras, D., Preuss, M.L., Pruesse, E., Rasmussen, L.B., Rivers, A., Robeson, M.S., Rosenthal, P., Segata, N., Shaffer, M., Shiffer, A., Sinha, R., Song, S.J., Spear, J.R., Swafford, A.D., Thompson, L.R., Torres, P.J., Trinh, P., Tripathi, A., Turnbaugh, P.J., Ul-Hasan, S., van der Hooft, J.J.J., Vargas, F., Vázquez-Baeza, Y., Vogtmann, E., von Hippel, M., Walters, W., Wan, Y., Wang, M., Warren, J., Weber, K.C., Williamson, C.H.D., Willis, A.D., Xu, Z.Z., Zaneveld, J.R., Zhang, Y., Zhu, Q., Knight, R., Caporaso, J.G., 2019. Reproducible, interactive, scalable and extensible microbiome data science using QIIME 2. Nature Biotechnology 37, 852–857.

Borselli, L., Biancalani, R., Giordani, C., Carnicelli, S., Ferrari, G.A., 1996. Effect of gypsum on seedling emergence in a kaolinitic crusting soil. Soil Technology 9, 71–81.

Bottos, E.M., Woo, A.C., Zawar-Reza, P., Pointing, S.B., Cary, S.C., 2014. Airborne Bacterial Populations Above Desert Soils of the McMurdo Dry Valleys, Antarctica. Microbial Ecology 67, 120–128.

Boucher, O., Randall, D., Artaxo, P., Bretherton, C., Feingold, G., Forster, P., Kerminen, V.-M., Kondo, Y.,

Liao, H., Lohmann, U., 2013. Clouds and aerosols, in: Climate Change 2013: The Physical Science Basis. Contribution of Working Group I to the Fifth Assessment Report of the Intergovernmental Panel on Climate Change. Cambridge University Press, pp. 571–657.

Bradford, J.M., Grossman, R.B., 1982. In-situ Measurement of Near-surface Soil Strength by the Fall-cone Device. Soil Science Society of America Journal 46, 685–688.

Bridges, E.M., Oldeman, L.R., 1999. Global Assessment of Human-Induced Soil Degradation. Arid Soil Research and Rehabilitation 13, 319–325.

Brotons, J., Díaz, A., Alonso, F., Serrato, F., 2010. Wind Erosion on Mining Waste in Southeast Spain. Land Degradation & Development 21, 196–209.

Bryan, R.B., 2000. Soil erodibility and processes of water erosion on hillslope. Geomorphology 32, 385–415.

Bullard, J.E., Harrison, S.P., Baddock, M.C., Drake, N., Gill, T.E., McTainsh, G.H., Sun, Y., 2011. Preferential dust sources: A geomorphological classification designed for use in global dust-cycle models. Journal of Geophysical Research: Earth Surface 116.

Bunn, J.A., 1998. Government Policy, Wind Erosion, And Economic Viability In Semi-Arid Agriculture: The Case Of The Southern Texas High Plains. Journal of Agricultural and Applied Economics 30, 339–351.

Burri, K., Gromke, C., Lehning, M., Graf, F., 2011. Aeolian sediment transport over vegetation canopies: A wind tunnel study with live plants. Aeolian Research 3, 205–213.

Buschiazzo, D.E., Zobeck, T.M., Aimar, S.B., 1999. WIND EROSION IN LOESS SOILS OF THE SEMIARID ARGENTINIAN PAMPAS. Soil Science 164.

Buttner, M., 2017. Actinoplanes Swims into the Molecular Age. Journal of bacteriology 199.

Callahan, B.J., McMurdie, P.J., Rosen, M.J., Han, A.W., Johnson, A.J.A., Holmes, S.P., 2016. DADA2: High-resolution sample inference from Illumina amplicon data. Nature Methods 13, 581–583.

Campbell, D.J., 1976. Plastic limit determination using a drop-cone penetrometer. Journal of Soil Science 27, 295–300.

Capone, D.G., Hutchins, D.A., 2013. Microbial biogeochemistry of coastal upwelling regimes in a changing ocean. Nature Geoscience 6, 711–717.

Catuneanu, O., Wopfner, H., Eriksson, P.G., Cairncross, B., Rubidge, B.S., Smith, R.M.H., Hancox, P.J., 2005. The Karoo basins of south-central Africa. Journal of African Earth Sciences 43, 211–253.

Caviezel, C., Hunziker, M., Kuhn, N.J., 2017. Bequest of the Norseman—The Potential for Agricultural Intensification and Expansion in Southern Greenland under Climate Change. Land 6, 87.

Chambers, J.M., Hastie, T.J., 1992. Statistical Models in S, 1st ed. Routledge.

Chappell, A., Sanderman, J., Thomas, M., Read, A., Leslie, C., 2012. The dynamics of soil redistribution and the implications for soil organic carbon accounting in agricultural south-eastern Australia. Global Change Biology 18, 2081–2088.

Chappell, A., Warren, A., O'Donoghue, A., Robinson, A., Thomas, A., Bristow, C., 2008. The implications for dust emission modeling of spatial and vertical variations in horizontal dust flux and particle size in the Bodélé Depression, Northern Chad. Journal of Geophysical Research: Atmospheres 113.

Chappell, A., Webb, N.P., Leys, J.F., Waters, C.M., Orgill, S., Eyres, M.J., 2019. Minimising soil organic carbon erosion by wind is critical for land degradation neutrality. Environmental Science & Policy 93, 43–52.

Chen, W., Zhibao, D., Zhenshan, L., Zuotao, Y., 1996. Wind tunnel test of the influence of moisture on the erodibility of loessial sandy loam soils by wind. Journal of Arid Environments 34, 391–402.

Chepil, W.S., 1944. Utilization of crop residues for wind erosion control. Scientific Agriculture 24, 307–319.

Cleveland, C.C., Townsend, A.R., Schmidt, S.K., 2002. Phosphorus Limitation of Microbial Processes in Moist Tropical Forests: Evidence from Short-term Laboratory Incubations and Field Studies. Ecosystems 5, 680–691.

Colazo, J.C., Buschiazzo, D.E., 2015. The Impact of Agriculture on Soil Texture Due to Wind Erosion. Land Degradation & Development 26, 62–70.

Corden, J.M., Millington, W.M., Mullins, J., 2003. Long-term trends and regional variation in the aeroallergen Alternaria in Cardiff and Derby UK – are differences in climate and cereal production having an effect? Aerobiologia 19, 191–199.

Cornelis, W.M., Gabriels, D., 2003. A simple low-cost sand catcher for wind-tunnel simulations. Earth Surface Processes and Landforms 28, 1033–1041.

Cowie, S.M., Knippertz, P., Marsham, J.H., 2013. Are vegetation-related roughness changes the cause of the recent decrease in dust emission from the Sahel? Geophysical Research Letters 40, 1868–1872.

Crawford, C., Reponen, T., Lee, T., Iossifova, Y., Levin, L., Adhikari, A., Grinshpun, S.A., 2009. Temporal and spatial variation of indoor and outdoor airborne fungal spores, pollen, and (1→3)-β-d-glucan. Aerobiologia 25, 147–158.

Csavina, J., Field, J., Taylor, M., Gao, S., Landázuri, A., Betterton, E., Sáez, A., 2012. A Review on the Importance of Metals and Metalloids in Atmospheric Dust and Aerosol from Mining Operations. The Science of the total environment 433, 58–73.

Cui, M., Lu, H., Etyemezian, V., Su, Q., 2019a. Quantifying the emission potentials of fugitive dust sources in Nanjing, East China. Atmospheric Environment 207, 129–135.

Cui, M., Lu, H., Wiggs, G.F.S., Etyemezian, V., Sweeney, M.R., Xu, Z., 2019b. Quantifying the effect of geomorphology on aeolian dust emission potential in northern China. Earth Surface Processes and Landforms 44, 2872–2884.

DAFF, 2018. Abstract of Agricultural Statistics. Department of Agriculture, Forestry and Fisheries, Republic of South Africa.

DAFF, 2016. Production Guidline For Wheat. Republic of South Africa.

Dansie, A.P., Wiggs, G.F.S., Thomas, D.S.G., Washington, R., 2017. Measurements of windblown dust characteristics and ocean fertilization potential: The ephemeral river valleys of Namibia. Aeolian Research 29, 30–41.

DEA, 2013. Long-Term Adaptation Scenarios Flagship Research Programme (LTAS) for South Africa. Climate Trends and Scenarios for South Africa. Pretoria, South Africa.

Derry, L., Chadwick, O.A., 2007. Contributions from Earth's Atmosphere to Soil. Elements 3, 333–338.

Després, V., Huffman, J.A., Burrows, S.M., Hoose, C., Safatov, A., Buryak, G., Fröhlich-Nowoisky, J., Elbert, W., Andreae, M., Pöschl, U., Jaenicke, R., 2012. Primary biological aerosol particles in the atmosphere: a review. Tellus B: Chemical and Physical Meteorology 64, 15598.

Eckardt, F.D., Bekiswa, S., Von Holdt, J., Jack, C., Kuhn, N.J., Mogane, F., Murray, J.E., Ndara, N., Palmer, A., 2020. South Africa's agricultural dust sources and events from MSG SEVIRI. Aeolian Research 47, 100637.

Egan, C., Li, D.-W., Klironomos, J., 2014. Detection of arbuscular mycorrhizal fungal spores in the air across different biomes and ecoregions. Fungal Ecology 12, 26–31.

Eglington, B.M., 2006. Evolution of the Namaqua-Natal Belt, southern Africa – A geochronological and isotope geochemical review. Journal of African Earth Sciences 46, 93–111.

Eldridge, D.J., Leys, J.F., 2003. Exploring some relationships between biological soil crusts, soil aggregation and wind erosion. Journal of Arid Environments 53, 457–466.

Elith, J., Leathwick, J.R., Hastie, T., 2008. A working guide to boosted regression trees. Journal of Animal Ecology 77, 802–813.

Ellis, J.T., Li, B., Farrell, E.J., Sherman, D.J., 2009. Protocols for characterizing aeolian mass-flux profiles. Aeolian Research 1, 19–26.

Ellis, J.T., Sherman, D.J., Farrell, E.J., Li, B., 2012. Temporal and spatial variability of aeolian sand transport: Implications for field measurements. Aeolian Research 3, 379–387.

Etyemezian, V., 2018. User's Guide for the Miniature Portable In-Situ Wind ERosion Lab (PI-SWERL). Last Vegas.

Etyemezian, V., Gillies, J.A., Mastin, L.G., Crawford, A., Hasson, R., Van Eaton, A.R., Nikolich, G., 2019. Laboratory Experiments of Volcanic Ash Resuspension by Wind. Journal of Geophysical Research: Atmospheres 124, 9534–9560.

Etyemezian, V., Gillies, J.A., Shinoda, M., Nikolich, G., King, J., Bardis, A.R., 2014. Accounting for surface roughness on measurements conducted with PI-SWERL: Evaluation of a subjective visual approach and a photogrammetric technique. Aeolian Research 13, 35–50.

Etyemezian, V., Nikolich, G., Ahonen, S., Pitchford, M., Sweeney, M.R., Purcell, R., Gillies, J.A., Kuhns, H., 2007. The Portable In Situ Wind Erosion Laboratory (PI-SWERL): A new method to measure PM10 windblown dust properties and potential for emissions. Atmospheric Environment 41, 3789–3796.

Etyemezian, V., Nikolich, G., Nickling, W.G., King, J.S., Gillies, J.A., 2017. Analysis of an optical gate device for measuring aeolian sand movement. Aeolian Research 24, 65–79.

Fabbri, C., 2018. Simulation of natural winds in a portable wind tunnel using full-depth and part-depth atmospheric boundary layer approaches for soil erosion research.

Falkowski, P.G., Barber, R.T., Smetacek, V., 1998. Biogeochemical Controls and Feedbacks on Ocean Primary Production. Science 281, 200 LP – 206.

Farmer, A.M., 1993. The effects of dust on vegetation—a review. Environmental Pollution 79, 63–75.

Fécan, F., Marticorena, B., Bergametti, G., 1999. Parameterization of the increase of the Aeolian erosion threshold wind friction velocity due to soil moisture for arid and semi-arid areas. Annales Geophysicae 17, 149–157.

Feng, G., Sharratt, B.S., Vaddella, V., 2013. Windblown soil crust formation under light rainfall in a semiarid region. Soil and Tillage Research 128, 91–96.

Fernandez, D.P., Neff, J.C., Reynolds, R.L., 2008. Biogeochemical and ecological impacts of livestock grazing in semi-arid southeastern Utah, USA. Journal of Arid Environments 72, 777–791.

Fick, S.S.E., Barger, N., Tatarko, J., Duniway, M.C., 2020. Induced biological soil crust controls on wind erodibility and dust (PM10) emissions. Earth Surface Processes and Landforms 45, 224–236.

Findlater, P.A., Carter, D.J., Scott, B., 1990. A model to predict the effects of prostrate ground cover on wind erosion. Australian Journal of Soil Research - AUST J SOIL RES 28, 609–622.

Fister, W., Goldman, N., Mayer, M., Suter, M., Kuhn, N.J., 2019. Testing of photogrammetry for differentiation of soil organic carbon and biochar in sandy substrates. Geographica Helvetica 74, 81–91.

Fister, W., Iserloh, T., Ries, J.B., Schmidt, R.-G., 2012. A portable wind and rainfall simulator for in situ soil erosion measurements. CATENA 91, 72–84.

Fister, W., Iserloh, T., Ries, J.B., Schmidt, R.G., 2011. Comparison of rainfall characteristics of a small portable rainfall simulator and a portable wind and rainfall simulator. Zeitschrift für Geomorphologie, Supplementary Issues 55, 109–126.

Fister, W., Ries, J.B., 2009. Wind erosion in the central Ebro Basin under changing land use management. Field experiments with a portable wind tunnel. Journal of Arid Environments 73, 996–1004.

Forster, P., Ramaswamy, V., Artaxo, P., Berntsen, T., Betts, R., Fahey, D.W., Haywood, J., Lean, J., Lowe, D.C., Myhre, G., 2007. Changes in atmospheric constituents and in radiative forcing. Chapter 2, in: Climate Change 2007. The Physical Science Basis.

Friesen, T.L., De Wolf, E.D., Francl, L.J., 2001. Source strength of wheat pathogens during combine harvest. Aerobiologia 17, 293–299.

Fryrear, D.W., 1986. A field dust sampler. Journal of Soil and Water Conservation 41, 117–120.

Fryrear, D.W., 1985. Soil cover and wind erosion. Transactions of the ASAE 28, 781–784.

Fryrear, D.W., 1984. Soil Ridges-Clods and Wind Erosion. Transactions of the ASAE 27, 445–448.

Fryrear, D.W., Saleh, A., Bilbro, J.D., Schromberg, H.M., Stout, J.E., Zobeck, T.M., Schomberg, H.M., Stout, J.E., Zobeck, T.M., 1998. Revised wind erosion equation, Technical Bulletin. USDA-ARS, Big Spring.

Fryrear, D.W., Stout, J.E., Hagen, L.J., Vories, E.D., 1991. Wind Erosion: Field Measurement And Analysis. Transactions of the ASAE 34, 155–160.

Funk, R., Engel, W., 2015. Investigations with a field wind tunnel to estimate the wind erosion risk of row crops. Soil and Tillage Research 145, 224–232.

Funk, R., Reuter, H., Hoffmann, C., Engel, W., Oettl, D., 2008. Effect of moisture on fine dust emission from tillage operations on agricultural soils. Earth Surface Processes and Landforms 33, 1851–1863.

Gal, M., Arcan, L., Shainberg, I., Keren, R., 1984. Effect of Exchangeable Sodium and Phosphogypsum on Crust Structure—Scanning Electron Microscope Observations1. Soil Science Society of America Journal 48, 872–878.

Gat, D., Mazar, Y., Cytryn, E., Rudich, Y., 2017. Origin-Dependent Variations in the Atmospheric Microbiome Community in Eastern Mediterranean Dust Storms. Environmental Science & Technology 51, 6709–6718.

Geist, H.J., Lambin, E.F., 2004. Dynamic Causal Patterns of Desertification. BioScience 54, 817–829.

Geldenhuys, J.N., 1982. Classification of the pans of the western Orange Free State according to vegetation structure with reference to avifaunal communities. South African Journal of Wildlife Research 12, 55–62.

Ghadiri, H., 2004. Crater formation in soils by raindrop impact. Earth Surface Processes and Landforms 29, 77–89.

Gicheru, P., Gachene, C., Mbuvi, J., Mare, E., 2004. Effects of soil management practices and tillage systems on surface soil water conservation and crust formation on a sandy loam in semi-arid {Kenya}. Soil and Tillage Research 75, 173–184.

Gillette, D.A., 1988. Threshold friction velocities for dust production for agricultural soils. Journal of Geophysical Research: Atmospheres 93, 12645–12662.

Gillette, D.A., 1977. Fine particulate emissions due to wind erosion. Transactions of the ASAE 20, 890–897.

Gillette, D.A., Adams, J., Endo, A., Smith, D., Kihl, R., 1980. Threshold velocities for input of soil particles into the air by desert soils (Mojave). Journal of Geophysical Research 85, 5621–5630.

Gillette, D.A., Adams, J., Muhs, D., Kihl, R., 1982. Threshold friction velocities and rupture moduli for crusted desert soils for the input of soil particles into the air. Journal of Geophysical Research: Oceans 87, 9003–9015.

Gillette, D.A., Niemeyer, T.C., Helm, P.J., 2001. Supply-limited horizontal sand drift at an ephemerally crusted, unvegetated saline playa. Journal of Geophysical Research: Atmospheres 106, 18085–18098.

Ginoux, P., Prospero, J.M., Gill, T.E., Hsu, N.C., Zhao, M., 2012. Global-scale attribution of anthropogenic and natural dust sources and their emission rates based on MODIS Deep Blue aerosol products. Reviews of Geophysics 50, 3005.

González-Chávez, M. del C.A., Aitkenhead-Peterson, J.A., Gentry, T.J., Zuberer, D., Hons, F., Loeppert, R., 2010. Soil microbial community, C, N, and P responses to long-term tillage and crop rotation. Soil and Tillage Research 106, 285–293.

Goossens, D., 2004. Effect of soil crusting on the emission and transport of wind-eroded sediment: field measurements on loamy sandy soil. Geomorphology 58, 145–160.

Goossens, D., Buck, B.J., 2011. Gross erosion, net erosion and gross deposition of dust by wind: field data from 17 desert surfaces. Earth Surface Processes and Landforms 36, 610–623.

Goossens, D., Buck, B.J., 2009. Dust dynamics in off-road vehicle trails: Measurements on 16 arid soil types, Nevada, USA. Journal of Environmental Management 90, 3458–3469.

Goossens, D., Offer, Z.Y., 2000. Wind tunnel and field calibration of six aeolian dust samplers. Atmospheric Environment 34, 1043–1057.

Goudie, A.S., 2013. Desert dust and human health disorders. Environment International 63C, 101–113.

Goudie, A.S., 1991. Pans. Progress in Physical Geography 15, 221–237.

Goudie, A.S., Thomas, D.S.G., 1986. Lunette dunes in southern Africa. Journal of Arid Environments 10, 1–12.

Goudie, A.S., Wells, G.L., 1995. The nature, distribution and formation of pans in arid zones. Earth-Science Reviews 38, 1–69.

Graham, E.B., Knelman, J.E., Schindlbacher, A., Siciliano, S., Breulmann, M., Yannarell, A., Beman, J.M., Abell, G., Philippot, L., Prosser, J., Foulquier, A., Yuste, J.C., Glanville, H.C., Jones, D.L., Angel, R., Salminen, J., Newton, R.J., Bürgmann, H., Ingram, L.J., Hamer, U., Siljanen, H.M.P., Peltoniemi, K., Potthast, K., Bañeras, L., Hartmann, M., Banerjee, S., Yu, R.-Q., Nogaro, G., Richter, A., Koranda, M., Castle, S.C., Goberna, M., Song, B., Chatterjee, A., Nunes, O.C., Lopes, A.R., Cao, Y., Kaisermann, A., Hallin, S., Strickland, M.S., Garcia-Pausas, J., Barba, J., Kang, H., Isobe, K., Papaspyrou, S., Pastorelli, R., Lagomarsino, A., Lindström, E.S., Basiliko, N., Nemergut, D.R., 2016. Microbes as Engines of Ecosystem Function: When Does Community Structure Enhance Predictions of Ecosystem Processes? Frontiers in Microbiology 7, 214.

Grantz, D.A., Garner, J.H.B., Johnson, D.W., 2003. Ecological effects of particulate matter. Environment International 29, 213–239.

Greeley, R., Iversen, J.D., 1985. Wind as a Geological Process on Earth, Mars, Venus and Titan, 2009/05/01. ed, Cambridge Planetary Science Series. Cambridge University Press, Cambridge.

Greenwood, P., Fister, W., Kinnell, P.I.A., Rüegg, H.-R., Kuhn, N.J., 2013. Developing and testing a precision erosion measurement facility for elucidating mobilization mechanisms in shallow-flow conditions. Desertification and Land Degradation 105.

Guo, Z., Huang, N., Dong, Z., Van Pelt, R.S., Zobeck, T.M., 2014. Wind Erosion Induced Soil Degradation in Northern China: Status, Measures and Perspective. Sustainability 6, 8951–8966.

Hagen, L.J., 1991. A wind erosion prediction system to meet user needs. Journal of Soil and Water Conservation 46, 106 LP – 111.

Hall, D.J., Upton, S.L., Marsland, G.W., 1993. 11 - Improvements in dust gauge design, in: Couling, S. (Ed.), Measurement of Airborne Pollutants. Butterworth-Heinemann, pp. 171–217.

Han, Y., Fan, Y., Zhongbao, X., Wang, L., Cai, Q., Wang, X., 2016. Effects of wetting rate and simulated rain duration on soil crust formation of red loam. Environmental Earth Sciences 75.

Hancox, P.J., Götz, A.E., 2014. South Africa's coalfields — A 2014 perspective. International Journal of Coal Geology 132, 170–254.

Hansbo, S., 1957. A new approach to determination of shear strength of clay by the fall cone test. Swedish Geotechnical Institute Proceedings 14, 5–47.

Hansen, Z., Libecap, G., 2004. Small Farms, Externalities, and the Dust Bowl of the 1930s. Journal of Political Economy 112, 665–694.

Harper, R.J., Gilkes, R.J., 1994. Evaluation of the ^{137}Cs techniques for estimating wind erosion losses for some sandy Western Australian soils. Soil Research 32, 1369–1387.

Hartemink, A., Huting, J.R.M., 2008. Land Cover, Extent, and Properties of Arenosols in Southern Africa. Arid Land Research and Management 22.

Hartman, K., van der Heijden, M.G.A., Wittwer, R.A., Banerjee, S., Walser, J.-C., Schlaeppi, K., 2018. Cropping practices manipulate abundance patterns of root and soil microbiome members

paving the way to smart farming. Microbiome 6, 14.

Hensley, M., Le Roux, P., Preez, C.D.U., van Huyssteen, C.W., Kotze, E., Van Rensburg, L., 2006. Soils: The Free State's Agricultural Base. South African Geographical Journal 88, 11–21.

Herman, J.R., Bhartia, P.K., Torres, O., Hsu, C., Seftor, C., Celarier, E., 1997. Global distribution of UV-absorbing aerosols from Nimbus 7/TOMS data. Journal of Geophysical Research: Atmospheres 102, 16911–16922.

Hiernaux, P., Bielders, C.L., Valentin, C., Bationo, A., Fernández-Rivera, S., 1999. Effects of livestock grazing on physical and chemical properties of sandy soils in Sahelian rangelands. Journal of Arid Environments 41, 231–245.

Holmes, P., Barker, C.H., 2006. Geological and geomorphological controls and the physical landscape of the Free State. South African Geographical Journal 88, 3–10.

Holmes, P., Bateman, M., Thomas, D.S.G., Telfer, M., Barker, C.H., Lawson, M., 2008. A Holocene late Pleistocene aeolian record from lunette dunes in the western Free State panfield, South Africa. The Holocene 18, 1193–1205.

Holmes, P., Thomas, D.S.G., Bateman, M., Wiggs, G.F.S., Rabumbulu, M., 2012. Evidence for land degradation from aeolian sediment in the West-Central Free State province, South Africa. Land Degradation and Development 23.

Horowitz, A., Sampson, C.G., Scott, L., Vogel, J.C., 1978. Analysis of the Voigtspost Site, O.F.S., South Africa. The South African Archaeological Bulletin 33, 152–159.

Houser, C.A., Nickling, W.G., 2001a. The factors influencing the abrasion efficiency of saltating grains on a clay-crusted playa. Earth Surface Processes and Landforms 26, 491–505.

Houser, C.A., Nickling, W.G., 2001b. The emission and vertical flux of particulate matter <10 μm from a disturbed clay-crusted surface. Sedimentology 48, 255–267.

Houyou, Z., Bielders, C.L., Benhorma, H.A., Dellal, A., Boutemdjet, A., 2016. Evidence of Strong Land Degradation by Wind Erosion as a Result of Rainfed Cropping in the Algerian Steppe: A Case Study at Laghouat. Land Degradation & Development 27, 1788–1796.

Hu, Y., Berhe, A.A., Fogel, M.L., Heckrath, G.J., Kuhn, N.J., 2016. Transport-distance specific SOC distribution: Does it skew erosion induced C fluxes? Biogeochemistry 128, 339–351.

Hu, Y., Fister, W., Kuhn, N.J., 2013. Temporal variation of SOC enrichment from interrill erosion over prolonged rainfall simulations. Agriculture 3, 726–740.

Hu, Y., Kuhn, N.J., 2014. Aggregates reduce transport distance of soil organic carbon: are our balances correct? Biogeosciences Discussions 11.

Hurtt, G., Chini, L., Frolking, S., Betts, R., Feddema, J., Fischer, G., Fisk, J., Hibbard, K., Houghton, R., Janetos, A., Jones, C., Kindermann, G., Kinoshita, T., Klein Goldewijk, K., Riahi, K., Shevliakova, E., Smith, S., Stehfest, E., Thomson, A., Wang, Y., 2011. Harmonization of Land-Use Scenarios for the Period 1500-2100: 600 Years of Global Gridded Annual Land-Use Transitions, Wood Harvest, and Resulting Secondary Lands. Climatic Change 109, 117–161.

Hyde, H.A., Williams, D.A., 1946. A daily census of Alternaria spores caught from the atmosphere at Cardiff in 1942 and 1943. Transactions of the British Mycological Society 29, 78-IN5.

Ishizuka, M., Mikami, M., Leys, J.F., Yamada, Y., Heidenreich, S., Shao, Y.P., McTainsh, G.H., 2008. Effects of soil moisture and dried raindroplet crust on saltation and dust emission. Journal of

Geophysical Research: Atmospheres 113.

Janssen, W., Tetzlaff, G., 1991. Entwicklung und Eichung einer registrierenden Suspensionsfalle. Zeitschrift Für Kulturtechnik und Landentwicklung 32, 167–180.

Jiang, Y., Yang, X.-Q., Liu, X., Qian, Y., Zhang, K., Wang, M., Li, F., Wang, Y., Lu, Z., 2020. Impacts of Wildfire Aerosols on Global Energy Budget and Climate: The Role of Climate Feedbacks. Journal of Climate 33, 3351–3366.

Jickells, T.D., 1995. Atmospheric inputs of metals and nutrients to the oceans: their magnitude and effects. Marine Chemistry 48, 199–214.

Jolliffe, I.T., Cadima, J., 2016. Principal component analysis: a review and recent developments. Philosophical Transactions of the Royal Society A: Mathematical, Physical and Engineering Sciences 374, 20150202.

Jones, A., Breuning-Madsen, H., Brossard, M., Dampha, A., Deckers, J., Dewitte, O., Gallali, T., Hallett, S., Jones, R., Kilasara, M., Le Roux, P., Michéli, E., Montanarella, L., Spaargaren, O., Thiombiano, L., Van Ranst, E., Yemefack, M., Zougmore, R., 2013. Soil Atlas of Africa. European Commission, Publications Office of the European Union, Luxembourg.

Jusot, J.-F., Neill, D.R., Waters, E.M., Bangert, M., Collins, M., Bricio Moreno, L., Lawan, K.G., Moussa, M.M., Dearing, E., Everett, D.B., Collard, J.-M., Kadioglu, A., 2017. Airborne dust and high temperatures are risk factors for invasive bacterial disease. Journal of Allergy and Clinical Immunology 139, 977-986.e2.

Kavouras, I., Etyemezian, V., Nikolich, G., Gillies, J.A., Sweeney, M.R., Young, M., Shafer, D., 2009. A New Technique for Characterizing the Efficacy of Fugitive Dust Suppressants. Journal of the Air & Waste Management Association (1995) 59, 603–612.

Kellogg, C.A., Griffin, D.W., 2006. Aerobiology and the global transport of desert dust. Trends in Ecology & Evolution 21, 638–644.

Kendrick, B., 2001. pore dispersal in fungi – airborne spores and allergy. Focus Publishing, Newburyport.

King, J., Etyemezian, V., Sweeney, M.R., Buck, B.J., Nikolich, G., 2011. Dust emission variability at the Salton Sea, California, USA. Journal of Aeolian Research 3, 67–79.

Kirjavainen, P. V, Karvonen, A.M., Adams, R.I., Täubel, M., Roponen, M., Tuoresmäki, P., Loss, G., Jayaprakash, B., Depner, M., Ege, M.J., Renz, H., Pfefferle, P.I., Schaub, B., Lauener, R., Hyvärinen, A., Knight, R., Heederik, D.J.J., von Mutius, E., Pekkanen, J., 2019. Farm-like indoor microbiota in non-farm homes protects children from asthma development. Nature Medicine 25, 1089–1095.

Klose, M., Gill, T.E., Etyemezian, V., Nikolich, G., Ghodsi Zadeh, Z., Webb, N.P., Van Pelt, R.S., 2019. Dust emission from crusted surfaces: Insights from field measurements and modelling. Aeolian Research 40, 1–14.

Knights, D., Kuczynski, J., Charlson, E.S., Zaneveld, J., Mozer, M.C., Collman, R.G., Bushman, F.D., Knight, R., Kelley, S.T., 2011. Bayesian community-wide culture-independent microbial source tracking. Nature Methods 8, 761–763.

Koch, D., Bond, T.C., Streets, D., Unger, N., van der Werf, G.R., 2007. Global impacts of aerosols from particular source regions and sectors. Journal of Geophysical Research: Atmospheres 112.

Kok, J.F., Albani, S., Mahowald, N.M., Ward, D., 2014. An improved dust emission model – Part 2: Evaluation in the Community Earth System Model, with implications for the use of dust source

functions. Atmospheric Chemistry and Physics 14, 13043–13061.

Kok, J.F., Parteli, E.J.R., Michaels, T.I., Karam, D.B., 2012. The physics of wind-blown sand and dust. Reports on Progress in Physics 75, 106901.

Kruger, A.C., Goliger, A.M., Retief, J., Sekele, S., 2010. Strong wind climatic zones in South Africa. Wind and Structures, An International Journal 13.

Kruger, A.C., Service, S.A.W., 2004. Climate of South Africa: Climate regions, Klimaat van Suid-Afrika. South African Weather Service.

Kuhn, N.J., Bryan, R.B., 2004. Drying, soil surface condition and interrill erosion on two Ontario soils. CATENA 57, 113–133.

Lancaster, N., Baas, A., 1998. Influence of vegetation cover on sand transport by wind: field studies at Owens Lake, California. Earth Surface Processes and Landforms 23, 69–82.

Langston, G., McKenna Neuman, C., 2005. An experimental study on the susceptibility of crusted surfaces to wind erosion: A comparison of the strength properties of biotic and salt crusts. Geomorphology 72, 40–53.

Larkin, R.P., 2008. Relative effects of biological amendments and crop rotations on soil microbial communities and soilborne diseases of potato. Soil Biology and Biochemistry 40, 1341–1351.

Larney, F.J., Bullock, M.S., Lindwall, C.W., 1997. Residue Cover versus Soil Clods for Wind Erosion Protection on Fallow. Alberta.

Lauber, C.L., Strickland, M.S., Bradford, M.A., Fierer, N., 2008. The influence of soil properties on the structure of bacterial and fungal communities across land-use types. Soil Biology and Biochemistry 40, 2407–2415.

Lawrence, C., Neff, J.C., 2009. The contemporary physical and chemical flux of Aeolian dust: A synthesis of direct measurements of dust deposition. Chemical Geology 267, 46–63.

Le Bissonnais, Y., Renaux, B., Delouche, H., 1995. Interactions between soil properties and moisture content in crust formation, runoff and interrill erosion from tilled loess soils. CATENA 25, 33–46.

Lee, J.A., Gill, T.E., 2015. Multiple causes of wind erosion in the Dust Bowl. Aeolian Research 19, 15–36.

Leys, J.F., Eldridge, D.J., 1998. Influence of cryptogamic crust disturbance to wind erosion on sand and loam rangeland soils. Earth Surface Processes and Landforms 23, 963–974.

Leys, J.F., Koen, T., McTainsh, G.H., 1996. The effect of dry aggregation and percentage clay on sediment flux as measured by a portable wind tunnel. Australian Journal of Soil Research 34.

Li, H., Tatarko, J., Kucharski, M., Dong, Z., 2015. PM2.5 and PM10 emissions from agricultural soils by wind erosion. Aeolian Research 19, 171–182.

Li, J.-T., Zhang, B., 2007. Paddy Soil Stability and Mechanical Properties as Affected by Long-Term Application of Chemical Fertilizer and Animal Manure in Subtropical China. Pedosphere 17, 568–579.

Li, J., Okin, G.S., Alvarez, L., Epstein, H., 2007. Quantitative effects of vegetation cover on wind erosion and soil nutrient loss in a desert grassland of southern New Mexico, USA. Biogeochemistry 85, 317–332.

Li, J., Okin, G.S., Herrick, J., Belnap, J., Munson, S., Miller, M.E., 2010. A simple method to estimate threshold friction velocity of wind erosion in the field. Geophysical Research Letters 37, L10402.

Li, X., Zhang, H., 2011. Research on threshold friction velocities during dust events over the Gobi Desert in northwest China. Journal of Geophysical Research 116.

Li, Y., Yu, H., Chappell, A., Zhou, N., Funk, R., 2014. How much soil organic carbon sequestration is due to conservation agriculture reducing soil erosion? Soil Research 52, 717–726.

Lin, X., Niu, J., Yu, X., Berndtsson, R., Wu, S., Xie, S., 2021. Maize residue effects on PM2.5, PM10, and dust emission from agricultural land. Soil and Tillage Research 205, 104738.

Liu, M.-X., Wang, J.-A., Yan, P., Liu, L.-Y., Ge, Y.-Q., Li, X.-Y., Hu, X., Song, Y., Wang, L., 2006. Wind tunnel simulation of ridge-tillage effects on soil erosion from cropland. Soil and Tillage Research 90, 242–249.

Liu, T., Xu, X., Yang, J., 2017. Experimental study on the effect of freezing-thawing cycles on wind erosion of black soil in Northeast China. Cold Regions Science and Technology 136, 1–8.

López, M. V, Gracia, R., Arrúe, J.L., 2000. Effects of reduced tillage on soil surface properties affecting wind erosion in semiarid fallow lands of Central Aragón. European Journal of Agronomy 12, 191–199.

López, M. V, Sabre, M., Gracia, R., Arrúe, J.L., Gomes, L., 1998. Tillage effects on soil surface conditions and dust emission by wind erosion in semiarid {Aragón} ({NE} {Spain}). Soil and Tillage Research 45, 91–105.

Lozupone, C., Lladser, M.E., Knights, D., Stombaugh, J., Knight, R., 2011. UniFrac: an effective distance metric for microbial community comparison. The ISME Journal 5, 169–172.

Luiken, R.E.C., Van Gompel, L., Bossers, A., Munk, P., Joosten, P., Hansen, R.B., Knudsen, B.E., García-Cobos, S., Dewulf, J., Aarestrup, F.M., Wagenaar, J.A., Smit, L.A.M., Mevius, D.J., Heederik, D.J.J., Schmitt, H., 2020. Farm dust resistomes and bacterial microbiomes in European poultry and pig farms. Environment International 143, 105971.

Lyles, L., 1985. Predicting and Controlling Wind Erosion. Agricultural History 59, 205–214.

Lyles, L., Tatarko, J., 1986. Wind erosion effects on soil texture and organic matter. Journal of Soil and Water Conservation 41.

Maarastawi, S.A., Frindte, K., Linnartz, M., Knief, C., 2018. Crop Rotation and Straw Application Impact Microbial Communities in Italian and Philippine Soils and the Rhizosphere of Zea mays . Frontiers in Microbiology .

Madden, N.M., Southard, R.J., Mitchell, J.P., 2010. Soil water and particle size distribution influence laboratory-generated PM10. Atmospheric Environment 44, 745–752.

Mahowald, N.M., Albani, S., Kok, J.F., Engelstaedter, S., Scanza, R.A., Ward, D.S., Flanner, M.G., 2014. The size distribution of desert dust aerosols and its impact on the Earth system. Aeolian Research 15, 53–71.

Mahowald, N.M., Engelstaedter, S., Luo, C., Sealy, A., Artaxo, P., Benitez-Nelson, C., Bonnet, S., Chen, Y., Chuang, P., Cohen, D., Dulac, F., Herut, B., Johansen, A., Kubilay, N., Losno, R., Maenhaut, W., Prospero, J.M., Shank, L., Siefert, R., 2009. Atmospheric Iron Deposition: Global Distribution, Variability, and Human Perturbations*. Annual review of marine science 1, 245–278.

Mahowald, N.M., Kloster, S., Engelstaedter, S., Moore, J.K., Mukhopadhyay, S., McConnell, J.R., Albani,

S., Doney, S.C., Bhattacharya, A., Curran, M.A.J., Flanner, M.G., Hoffman, F.M., Lawrence, D.M., Lindsay, K., Mayewski, P.A., Neff, J.C., Rothenberg, D., Thomas, E., Thornton, P.E., Zender, C.S., 2010. Observed 20th century desert dust variability: impact on climate and biogeochemistry. Atmospheric Chemistry and Physics 10, 10875–10893.

Mahowald, N.M., Kohfeld, K., Hansson, M., Balkanski, Y., Harrison, S.P., Prentice, I.C., Schulz, M., Rodhe, H., 1999. Dust sources and deposition during the last glacial maximum and current climate: A comparison of model results with paleodata from ice cores and marine sediments. Journal of Geophysical Research: Atmospheres 104, 15895–15916.

Mahowald, N.M., Luo, C., 2003. A less dusty future? Geophysical Research Letters - GEOPHYS RES LETT 30.

Maki, T., Lee, K.C., Kawai, K., Onishi, K., Hong, C.S., Kurosaki, Y., Shinoda, M., Kai, K., Iwasaka, Y., Archer, S.D.J., Lacap-Bugler, D.C., Hasegawa, H., Pointing, S.B., 2019. Aeolian Dispersal of Bacteria Associated With Desert Dust and Anthropogenic Particles Over Continental and Oceanic Surfaces. Journal of Geophysical Research: Atmospheres 124, 5579–5588.

Marticorena, B., Bergametti, G., 1995. Modeling the atmospheric dust cycle. Part 1: Design of a soil-derived dust emission scheme. Journal of Geophysical Research 100, 16415–16430.

Marticorena, B., Bergametti, G., Gillette, D.A., Belnap, J., 1997. Factors controlling threshold friction velocity in semiarid and arid areas of the United States. Journal of Geophysical Research: Atmospheres 102, 23277–23287.

Martinelli, N., Olivieri, O., Girelli, D., 2013. Air particulate matter and cardiovascular disease: A narrative review. European journal of internal medicine.

McConnell, J.R., Aristarain, A.J., Banta, J.R., Edwards, P.R., Simões, J.C., 2007. 20th-Century doubling in dust archived in an Antarctic Peninsula ice core parallels climate change and desertification in South America. Proceedings of the National Academy of Sciences 104, 5743 LP – 5748.

McCourt, S., 2016. A brief geological history of southern Africa, in: Knight, J., Grab, S.W. (Eds.), Quaternary Environmental Change in Southern Africa: Physical and Human Dimensions. Cambridge University Press, Cambridge, pp. 18–29.

McKenna Neuman, C., 2004. Effects of temperature and humidity upon the transport of sedimentary particles by wind. Sedimentology 51, 1–17.

McKenna Neuman, C., Boulton, J.W., Sanderson, S., 2009. Wind tunnel simulation of environmental controls on fugitive dust emissions from mine tailings. Atmospheric Environment 43, 520–529.

McKenna Neuman, C., Maxwell, C.D., 1999. A wind tunnel study of the resilience of three fungal crusts to particle abrasion during aeolian sediment transport. CATENA 38, 151–173.

McKenna Neuman, C., Maxwell, C.D., Boulton, J.W., 1996. Wind transport of sand surfaces crusted with photoautotrophic microorganisms. CATENA 27, 229–247.

McKenna Neuman, C., Maxwell, C.D., Rutledge, C., 2005. Spatial and temporal analysis of crust deterioration under particle impact. Journal of Arid Environments 60, 321–342.

McKenna Neuman, C., Scott, M.M., 1998. A wind tunnel study of the influence of pore water on aeolian sediment transport. Journal of Arid Environments 39, 403–419.

McKight, P.E., Najab, J., 2010. Kruskal-Wallis Test. The Corsini Encyclopedia of Psychology, Major Reference Works.

McMurdie, P.J., Holmes, S.P., 2013. phyloseq: An R Package for Reproducible Interactive Analysis and Graphics of Microbiome Census Data. PLOS ONE 8, e61217.

McTainsh, G.H., Lynch, A.W., Burgess, R.C., 1990. Wind erosion in eastern Australia. Soil Research 28, 323–339.

Meek, B.D., Rechel, E.R., Carter, L.M., DeTar, W.R., Urie, A.L., 1992. Infiltration Rate of a Sandy Loam Soil: Effects of Traffic, Tillage, and Plant Roots. Soil Science Society of America Journal 56, 908–913.

Meena, M., Gupta, S.K., Swapnil, P., Zehra, A., Dubey, M.K., Upadhyay, R.S., 2017. Alternaria Toxins: Potential Virulence Factors and Genes Related to Pathogenesis . Frontiers in Microbiology .

Mejia, J.F., Gillies, J.A., Etyemezian, V., Glick, R., 2019. A very-high resolution (20m) measurement-based dust emissions and dispersion modeling approach for the Oceano Dunes, California. Atmospheric Environment 218, 116977.

Mendez, M.J., Funk, R., Buschiazzo, D.E., 2011. Field wind erosion measurements with Big Spring Number Eight (BSNE) and Modified Wilson and Cook (MWAC) samplers. Geomorphology 129, 43–48.

Middleton, N.J., 2017. Desert dust hazards: A global review. Aeolian Research 24, 53–63.

Middleton, N.J., Thomas, D.S.G., 1997. World atlas of desertification, 2nd ed. Arnold, Hodder Headline, PLC.

Miller, S.D., 2003. A consolidated technique for enhancing desert dust storms with MODIS. Geophysical Research Letters 30.

Moeletsi, M.E., 2010. Agroclimatological risk assessment of rainfed maize production for the Free State Province of South Africa. University of the Free State.

Moeletsi, M.E., Walker, S., 2012. Rainy season characteristics of the Free State Province of South Africa with reference to rain-fed maize production. Water SA 38, 775–782.

Moore, C.M., Mills, M.M., Arrigo, K.R., Berman-Frank, I., Bopp, L., Boyd, P.W., Galbraith, E.D., Geider, R.J., Guieu, C., Jaccard, S.L., Jickells, T.D., La Roche, J., Lenton, T.M., Mahowald, N.M., Marañón, E., Marinov, I., Moore, J.K., Nakatsuka, T., Oschlies, A., Saito, M.A., Thingstad, T.F., Tsuda, A., Ulloa, O., 2013. Processes and patterns of oceanic nutrient limitation. Nature Geoscience 6, 701–710.

Morin, J., 1993. Chapter 5, Soil crusting and sealing, in: Soil Tillage in Africa: Needs and Challenges. Food and Agriculture Organization of the United Nations.

Moulin, C., Chiapello, I., 2006. Impact of human-induced desertification on the intensification of Sahel dust emission and export over the last decades. Geophysical Research Letters 33.

Mulitza, S., Heslop, D., Pittauerova, D., Fischer, H.W., Meyer, I., Stuut, J.-B., Zabel, M., Mollenhauer, G., Collins, J.A., Kuhnert, H., Schulz, M., 2010. Increase in African dust flux at the onset of commercial agriculture in the Sahel region. Nature 466, 226–228.

Munkhtsetseg, E., Shinoda, M., Gillies, J.A., Kimura, R., King, J., Nikolich, G., 2016. Relationships between soil moisture and dust emissions in a bare sandy soil of Mongolia. Particuology 28, 131–137.

Munkhtsetseg, E., Shinoda, M., Ishizuka, M., Mikami, M., Kimura, R., Nikolich, G., 2017. Anthropogenic dust emissions due to livestock trampling in a Mongolian temperate grassland. Atmospheric Chemistry and Physics 17, 11389–11401.

Myhre, G., Shindell, D., Bréon, F.M., Collins, W., Fuglestvedt, J., Huang, J., Koch, D., Lamarque, J.F., Lee, D., Mendoza, B., 2013. Climate change 2013: the physical science basis. Contribution of working group I to the fifth assessment report of the intergovernmental panel on climate change 659–740.

Nan, L., Dong, Z., Xiao, W., Li, C., Xiao, N., Song, S., Xiao, F., Du, L., 2018. A field investigation of wind erosion in the farming–pastoral ecotone of northern China using a portable wind tunnel: A case study in Yanchi County. Journal of Arid Land 10, 27–38.

Nasser, S.M., Pulimood, T.B., 2009. Allergens and thunderstorm asthma. Current Allergy and Asthma Reports 9, 384.

Neff, J.C., Ballantyne, A.P., Farmer, L., Mahowald, N.M., Conroy, J., Landry, C., Overpeck, J., Painter, T., Lawrence, C., Reynolds, R., 2008. Increasing eolian dust deposition in the western United States linked to human activity. NATURE GEOSCIENCE 1, 189–195.

Neff, J.C., Reynolds, R.L., Belnap, J., Lamothe, P., 2005. MULTI-DECADAL IMPACTS OF GRAZING ON SOIL PHYSICAL AND BIOGEOCHEMICAL PROPERTIES IN SOUTHEAST UTAH. Ecological Applications 15, 87–95.

Nelson, R.G., 2002. Resource assessment and removal analysis for corn stover and wheat straw in the Eastern and Midwestern United States—rainfall and wind-induced soil erosion methodology. Biomass and Bioenergy 22, 349–363.

Nerger, R., Funk, R., Cordsen, E., Fohrer, N., 2017. Application of a modeling approach to designate soil and soil organic carbon loss to wind erosion on long-term monitoring sites (BDF) in Northern Germany. Aeolian Research 25, 135–147.

Nickling, W.G., Gillies, J.A., 1989. Emission of fine-grained particulates from desert soils, in: Paleoclimatology and Paleometeorology: Modern and Past Patterns of Global Atmospheric Transport. Springer, pp. 133–165.

Nickling, W.G., McKenna Neuman, C., 1997. Wind tunnel evaluation of a wedge-shaped aeolian sediment trap. Geomorphology 18, 333–345.

Nordstrom, K.F., Hotta, S., 2004. Wind erosion from cropland in the USA: a review of problems, solutions and prospects. Geoderma 121, 157–167.

Okin, G.S., Baker, A.R., Tegen, I., Mahowald, N.M., Dentener, F.J., Duce, R.A., Galloway, J.N., Hunter, K., Kanakidou, M., Kubilay, N., Prospero, J.M., Sarin, M., Surapipith, V., Uematsu, M., Zhu, T., 2011. Impacts of atmospheric nutrient deposition on marine productivity: Roles of nitrogen, phosphorus, and iron. Global Biogeochemical Cycles 25.

Okin, G.S., Mahowald, N.M., Chadwick, O.A., Artaxo, P., 2004. Impact of desert dust on the biogeochemistry of phosphorus in terrestrial ecosystems. Global Biogeochemical Cycles 18.

Oksanen, J., Blanchet, F.G., Friendly, M., Al., E., 2019. Vegan: community ecology package. R package version 2.5-5.

Oldeman, L.R., 1992. Global extent of soil degradation, in: Bi-Annual Report 1991-1992/ISRIC. ISRIC, pp. 19–36.

Oriolo, S., Becker, T., 2018. The Kalahari Craton, Southern Africa: From Archean Crustal Evolution to Gondwana Amalgamation, in: Siegesmund, S., Basei, M.A.S., Oyhantçabal, P., Oriolo, Sebastian (Eds.), . Springer International Publishing, Cham, pp. 133–159.

Partridge, T.C.& M.R.R., 1987. Geomorphic evolution of southern Africa since the Mesozoic . South

African Journal of Geology 90, 179–208.

Patle, G.T., Sikar, T.T., Rawat, K.S., Singh, S.K., 2019. Estimation of infiltration rate from soil properties using regression model for cultivated land. Geology, Ecology, and Landscapes 3, 1–13.

Pekel, J.-F., Cottam, A., Gorelick, N., Belward, A.S., 2016. High-resolution mapping of global surface water and its long-term changes. Nature 540, 418–422.

Perkins, S., 2001. Dust, the thermostat: How tiny airborne particles manipulate global climate. Science News 160, 200–202.

Peterson, B.J., Deegan, L., Helfrich, J., Hobbie, J.E., Hullar, M., Moller, B., Ford, T.E., Hershey, A., Hiltner, A., Kipphut, G., Lock, M.A., Fiebig, D.M., McKinley, V., Miller, M.C., Vestal, J.R., Ventullo, R., Volk, G., 1993. Biological Responses of a Tundra River to Fertilization. Ecology 74, 653–672.

Pi, H., Sharratt, B.S., Schillinger, W.F., Bary, A.I., Cogger, C.G., 2018. Wind erosion potential of a winter wheat–summer fallow rotation after land application of biosolids. Aeolian Research 32, 53–59.

Pinto, V.E.F., Patriarca, A., 2017. Alternaria Species and Their Associated Mycotoxins BT - Mycotoxigenic Fungi: Methods and Protocols, in: Moretti, A., Susca, A. (Eds.), . Springer New York, New York, NY, pp. 13–32.

Prospero, J.M., Blades, E., Mathison, G., Naidu, R., 2005. Interhemispheric transport of viable fungi and bacteria from Africa to the Caribbean with soil dust. Aerobiologia 21, 1–19.

Prospero, J.M., Ginoux, P., Torres, O., Nicholson, S.E., Gill, T.E., 2002. Environmental Characterization Of Global Sources Of Atmospheric Soil Dust Identified With The Nimbus 7 Total Ozone Mapping Spectrometer (TOMS) Absorbing Aerosol Product. Reviews of Geophysics 40, 2–31.

Pryor, S.C., Barthelmie, R.J., 2010. Climate change impacts on wind energy: A review. Renewable and Sustainable Energy Reviews 14, 430–437.

Qiang-guo, C., 2001. Soil erosion and management on the Loess Plateau. Journal of Geographical Sciences 11, 53–70.

Quast, C., Pruesse, E., Yilmaz, P., Gerken, J., Schweer, T., Yarza, P., Peplies, J., Glöckner, F.O., 2013. The SILVA ribosomal RNA gene database project: improved data processing and web-based tools. Nucleic Acids Research 41, D590–D596.

Rajot, J.-L., 2001. Wind blown sediment mass budget of Sahelian village land units in Niger. Bulletin de la Société Géologique de France 172, 523–531.

Rajot, J.-L., Alfaro, S.C., Gomes, L., Gaudichet, A., 2003. Soil crusting on sandy soils and its influence on wind erosion. CATENA 53, 1–16.

Raupach, M.R., Gillette, D.A., Leys, J.F., 1993. The effect of roughness elements on wind erosion threshold. Journal of Geophysical Research: Atmospheres 98, 3023–3029.

Raupach, M.R., Leys, J.F., 1990. Aerodynamics of a portable wind erosion tunnel for measuring soil erodibility by wind. Soil Research 28, 177–191.

Ravi, S., D'Odorico, P., Breshears, D., Field, J., Goudie, A.S., Huxman, T., Li, J., Okin, G.S., Swap, R., Thomas, A., Van Pelt, R.S., Whicker, J., 2011. Aeolian processes and the biosphere. Reviews of Geophysics 49.

Ren, L., Nest, T. Vanden, Ruysschaert, G., D'Hose, T., Cornelis, W.M., 2019. Short-term effects of cover crops and tillage methods on soil physical properties and maize growth in a sandy loam soil. Soil

and Tillage Research 192, 76–86.

Rice, M.A., McEwan, I.K., 2001. Crust strength: a wind tunnel study of the effect of impact by saltating particles on cohesive soil surfaces. Earth Surface Processes and Landforms 26, 721–733.

Rice, M.A., McEwan, I.K., Mullins, C.E., 1999. A conceptual model of wind erosion of soil surfaces by saltating particles. Earth Surface Processes and Landforms 24, 383–392.

Rice, M.A., Mullins, C.E., McEwan, I.K., 1997. An analysis of soil crust strength in relation to potential abrasion by saltating particles. Earth Surface Processes and Landforms 22, 869–883.

Rice, M.A., Willetts, B.B., McEwan, I.K., 1996. Wind Erosion Of Crusted Soil Sediments. Earth Surface Processes and Landforms 21, 279–293.

Ridgeway, G., 2007. Generalized Boosted Models: A guide to the gbm package. Update 1.

Ridley, D., Heald, C., Prospero, J.M., 2014. What controls the recent changes in African mineral dust aerosol across the Atlantic? ATMOSPHERIC CHEMISTRY AND PHYSICS 14.

Ries, J.B., Hirt, U., 2008. Permanence of soil surface crusts on abandoned farmland in the Central Ebro Basin/Spain. CATENA 72, 282–296.

Ries, J.B., Seeger, M., Iserloh, T., Wistorf, S., Fister, W., 2009. Calibration of simulated rainfall characteristics for the study of soil erosion on agricultural land. Soil and Tillage Research 106, 109–116.

Riksen, M., Brouwer, F., de Graaff, J., 2003. Soil conservation policy measures to control wind erosion in northwestern Europe. CATENA 52, 309–326.

Rivera Rivera, N.I., Gill, T.E., Bleiweiss, M.P., Hand, J.L., 2010. Source characteristics of hazardous Chihuahuan Desert dust outbreaks. Atmospheric Environment 44, 2457–2468.

Roney, J.A., White, B.R., 2006. Estimating fugitive dust emission rates using an environmental boundary layer wind tunnel. Atmospheric Environment 40, 7668–7685.

Rosselli, R., Fiamma, M., Deligios, M., Pintus, G., Pellizzaro, G., Canu, A., Duce, P., Squartini, A., Muresu, R., Cappuccinelli, P., 2015. Microbial immigration across the Mediterranean via airborne dust. Scientific Reports 5, 16306.

Roux, J.S., Le Roux, J.S., 1978. The origin and distribution of pans in the Orange Free State. South African geographer/Suid-Afrikaanse geograaf Stellenbosch 6, 167–176.

Royston, J.P., 1982. Algorithm AS 181: The W Test for Normality. Journal of the Royal Statistical Society. Series C (Applied Statistics) 31, 176–180.

Ruddiman, W., 2003. The Anthropogenic Greenhouse Era Began Thousand so Years Ago. Climatic Change 61, 261–293.

Rutherford, M.C., Mucina, L., Powrie, L., 2006. Biomes and bioregions of Southern Africa, in: The Vegetation of South Africa, Lesotho and Swaziland: Strelitzia 19. pp. 30–51.

Samset, B.H., Sand, M., Smith, C.J., Bauer, S.E., Forster, P.M., Fuglestvedt, J.S., Osprey, S., Schleussner, C.-F., 2018. Climate Impacts From a Removal of Anthropogenic Aerosol Emissions. Geophysical Research Letters 45, 1020–1029.

Sanchez, P., Ahamed, S., Carré, F., Hartemink, A., Hempel, J., Huising, J., Lagacherie, P., Mcbratney, A., McKenzie, N., Mendonça Santos, M., Minasny, B., Montanarella, L., Okoth, P., Palm, C., Sachs, J., Shepherd, K., Vågen, T.-G., Vanlauwe, B., Walsh, M., Zhang, G.-L., 2009. Digital Soil Map of the

World. Science (New York, N.Y.) 325, 680–681.

Sankey, J.B., Eitel, J.U.H., Glenn, N.F., Germino, M.J., Vierling, L.A., 2011. Quantifying relationships of burning, roughness, and potential dust emission with laser altimetry of soil surfaces at submeter scales. Geomorphology 135, 181–190.

Santra, P., Moharana, P.C., Kumar, M., Soni, M.L., Pandey, C.B., Chaudhari, S.K., Sikka, A.K., 2017. Crop production and economic loss due to wind erosion in hot arid ecosystem of India. Aeolian Research 28, 71–82.

Schepanski, K., 2018. Transport of Mineral Dust and Its Impact on Climate. Geosciences .

Schepanski, K., Tegen, I., Laurent, B., Heinold, B., Macke, A., 2007. A new Saharan dust source activation frequency map derived from MSG-SEVIRI IR-channels. Geophysical Research Letters 34.

Segata, N., Izard, J., Waldron, L., Gevers, D., Miropolsky, L., Garrett, W.S., Huttenhower, C., 2011. Metagenomic biomarker discovery and explanation. Genome Biology 12, R60.

Seneviratne, S., Nicholls, N., Easterling, D., Goodess, C., Kanae, S., Kossin, J., Luo, Y., Marengo, J., Mcinnes, K., Rahimi, M., Reichstein, M., Sorteberg, A., Vera, C., Zhang, X., 2012. Changes in climate extremes and their impacts on the natural physical environment.

Shao, Y.P., Lu, H., 2000. A simple expression for wind erosion threshold friction velocity. Journal of Geophysical Research: Atmospheres 105, 22437–22443.

Shao, Y.P., Raupach, M.R., Findlater, P.A., 1993. Effect of saltation bombardment on the entrainment of dust by wind. Journal of Geophysical Research: Atmospheres 98, 12719–12726.

Shao, Y.P., Raupach, M.R., Leys, J.F., 1996. A model for predicting aeolian sand drift and dust entrainment on scales from paddock to region. Soil Research 34, 309–342.

Shao, Y.P., Wyrwoll, K.-H., Chappell, A., Huang, J., Lin, Z., McTainsh, G.H., Mikami, M., Tanaka, T.Y., Wang, X., Yoon, S., 2011. Dust cycle: An emerging core theme in Earth system science. Aeolian Research 2, 181–204.

Sharratt, B.S., Collins, H.P., 2018. Wind Erosion Potential Influenced by Tillage in an Irrigated Potato–Sweet Corn Rotation in the Columbia Basin. Agronomy Journal 110, 842–849.

Sharratt, B.S., Feng, G., Wendling, L., 2007. Loss of soil and PM10 from agricultural fields associated with high winds on the Columbia Plateau. Earth Surface Processes and Landforms 32, 621–630.

Sharratt, B.S., Vaddella, V., 2014. Threshold friction velocity of crusted windblown soils in the Columbia Plateau. Aeolian Research 15, 227–234.

Shepherd, G., Terradellas, E., Baklanov, A., Kang, U., Sprigg, W.A., Nickovic, S., Darvishi Boloorani, A., Al-Dousari, A., Basart, S., Benedetti, A., Sealy, A., Tong, D., Zhang, X., Guillemot, J., Kebin, Z., Knippertz, P., Mohammed, A., Al-Dabbas, M., Cheng, L., Cha, J., 2016. Global Assessment of Sand and Dust Storms.

Siegesmund, S., Basei, M.A.S., Oyhantçabal, P., Oriolo, S., 2018. Geology of Southwest Gondwana. Springer, Cham.

Smith, C.R., Blair, P.L., Boyd, C., Cody, B., Hazel, A., Hedrick, A., Kathuria, H., Khurana, P., Kramer, B., Muterspaw, K., Peck, C., Sells, E., Skinner, J., Tegeler, C., Wolfe, Z., 2016. Microbial community responses to soil tillage and crop rotation in a corn/soybean agroecosystem. Ecology and Evolution 6, 8075–8084.

Soderberg, K., Compton, J., 2007. Dust as a Nutrient Source for Fynbos Ecosystems, South Africa. Ecosystems 10, 550–561.

Spaan, W.P., van den Abeele, G.D., 1991. Wind borne particle measurements with acoustic sensors. Soil Technology 4, 51–63.

Sprigg, W.A., 2016. Dust Storms, Human Health and a Global Early Warning System BT - Extreme Weather, Health, and Communities: Interdisciplinary Engagement Strategies, in: Steinberg, S.L., Sprigg, W.A. (Eds.), . Springer International Publishing, Cham, pp. 59–87.

Stanelle, T., Bey, I., Raddatz, T., Reick, C., Tegen, I., 2014. Anthropogenically induced changes in twentieth century mineral dust burden and the associated impact on radiative forcing. Journal of Geophysical Research: Atmospheres 119, 13,513-526,546.

Stein, M.M., Hrusch, C.L., Gozdz, J., Igartua, C., Pivniouk, V., Murray, S.E., Ledford, J.G., Marques dos Santos, M., Anderson, R.L., Metwali, N., Neilson, J.W., Maier, R.M., Gilbert, J.A., Holbreich, M., Thorne, P.S., Martinez, F.D., von Mutius, E., Vercelli, D., Ober, C., Sperling, A.I., 2016. Innate Immunity and Asthma Risk in Amish and Hutterite Farm Children. New England Journal of Medicine 375, 411–421.

Sterk, G., 2003. Causes, consequences and control of wind erosion in Sahelian Africa: a review. Land Degradation & Development 14, 95–108.

Sterk, G., Herrmann, L., Bationo, A., 1996. Wind-blown nutrient transport and soil productivity changes in southwest Niger. Land Degradation & Development 7, 325–335.

Sterk, G., López, M. V, Arrúe, J.L., 1999. Saltation transport on a silt loam soil in northeast Spain. Land Degradation & Development 10, 545–554.

Sterk, G., Riksen, M., Goossens, D., 2001. Dryland Degradation by Wind Erosion and its Control. Annals of Arid Zone 40, 351–367.

Stockton, P.H., Gillette, D.A., 1990. Field measurement of the sheltering effect of vegetation on erodible land surfaces. Land Degradation \& Development 2, 77–85.

Stout, J.E., Zobeck, T.M., 1997. Intermittent saltation. Sedimentology 44, 959–970.

Stout, J.E., Zobeck, T.M., 1996. The Wolfforth Field Experiment: A Wind Erosion Study. Soil Science 161, 616–632.

Strode, S., Jaeglé, L., Selin, N.E., 2009. Impact of mercury emissions from historic gold and silver mining: Global modeling. Atmospheric Environment 43, 2012–2017.

Swap, R., Garstang, M., Greco, S., Talbot, R., Källberg, P., 1992. Saharan dust in the Amazon Basin. Tellus B: Chemical and Physical Meteorology 44, 133–149.

Sweeney, M.R., Etyemezian, V., Macpherson, T., Nickling, W.G., Gillies, J.A., Nikolich, G., McDonald, E. V, 2008. Comparison of PI-SWERL with dust emission measurements from a straight-line field wind tunnel. Journal of Geophysical Research: Earth Surface 113.

Sweeney, M.R., Mason, J.A., 2013. Mechanisms of dust emission from Pleistocene loess deposits, Nebraska, USA. Journal of Geophysical Research: Earth Surface 118, 1460–1471.

Sweeney, M.R., McDonald, E. V, Etyemezian, V., 2011. Quantifying dust emissions from desert landforms, eastern Mojave Desert, USA. Geomorphology 135, 21–34.

Sweeney, M.R., Zlotnik, V.A., Joeckel, R.M., Stout, J.E., 2016. Geomorphic and hydrologic controls of

dust emissions during drought from Yellow Lake playa, West Texas, USA. Journal of Arid Environments 133, 37–46.

Tait, A., Zheng, X., 2003. Mapping Frost Occurrence Using Satellite Data. Journal of Applied Meteorology - J APPL METEOROL 42, 193–203.

Tamura, T., Hayakawa, M., Hatano, K., 1998. A new genus of the order Actinomycetales, Cryptosporangium gen. nov., with descriptions of Cryptosporangium arvum sp. nov. and Cryptosporangium japonicum sp. nov. International Journal of Systematic and Evolutionary Microbiology 48, 995–1005.

Tanaka, T.Y., Chiba, M., 2006. A numerical study of the contributions of dust source regions to the global dust budget. Global and Planetary Change 52, 88–104.

Tang, K., Huang, Z., Huang, J., Maki, T., Zhang, S., Shimizu, A., Ma, X., Shi, J., Bi, J., Zhou, T., Wang, G., Zhang, L., 2018. Characterization of atmospheric bioaerosols along the transport pathway of Asian dust during the Dust-Bioaerosol 2016 Campaign. Atmospheric Chemistry and Physics 18, 7131–7148.

Tariq, S.M., Matthews, S.M., Stevens, M., Hakim, E.A., 1996. Sensitization to Alternaria and Cladosporium by the age of 4 years. Clinical & Experimental Allergy 26, 794–798.

Tegen, I., Hollrig, P., Chin, M., Fung, I., Jacob, D., Penner, J., 1997. Contribution of different aerosol species to the global aerosol extinction optical thickness: Estimates from model results. Journal of Geophysical Research: Atmospheres 102, 23895–23915.

Tegen, I., Werner, M., Harrison, S.P., Kohfeld, K.E., 2004. Relative importance of climate and land use in determining present and future global soil dust emission. Geophysical Research Letters 31, L05105.

Thomas, D.S.G., Knight, M., Wiggs, G.F.S., 2005. Remobilization of southern African desert dune systems by twenty-first century global warming. Nature 435, 1218–1221.

Tibke, G., 1988. 5. Basic principles of wind erosion control. Agriculture, Ecosystems & Environment 22–23, 103–122.

Torbati, M., Arzanlou, M., Sandoval-Denis, M., Crous, P.W., 2019. Multigene phylogeny reveals new fungicolous species in the Fusarium tricinctum species complex and novel hosts in the genus Fusarium from Iran. Mycological Progress 18, 119–133.

Trivedi, P., Delgado-Baquerizo, M., Anderson, I.C., Singh, B.K., 2016. Response of Soil Properties and Microbial Communities to Agriculture: Implications for Primary Productivity and Soil Health Indicators . Frontiers in Plant Science .

Uno, I., Eguchi, K., Yumimoto, K., Takemura, T., Shimizu, A., Uematsu, M., Liu, Z., Wang, Z., Hara, Y., Sugimoto, N., 2009. Asian dust transported one full circuit around the globe. Nature Geoscience 2, 557–560.

Valentin, C., Bresson, L.M., 1997. Soil crusting. Methodology for assessment of soil degradation. Adv Soil Sc 89–107.

Valentin, C., Bresson, L.M., 1992. Morphology, genesis and classification of surface crusts in loamy and sandy soils. Geoderma 55, 225–245.

van Dijk, A.I.J.., Bruijnzeel, L.A., Rosewell, C.J., 2002. Rainfall intensity–kinetic energy relationships: a critical literature appraisal. Journal of Hydrology 261, 1–23.

van Leeuwen, C.C.E., Fister, W., Vos, H.C., Cammeraat, L.H., Kuhn, N.J., 2021. A cross-comparison of threshold friction velocities for PM10 emissions between a traditional portable straight-line wind tunnel and PI-SWERL. Aeolian Research 49, 100661.

Van Pelt, R.S., Peters, P., Visser, S.M., 2009. Laboratory wind tunnel testing of three commonly used saltation impact sensors. Aeolian Research 1, 55–62.

Van Pelt, R.S., Zobeck, T.M., 2013. Portable wind tunnels for fields testing of soils and natural surfaces, in: Wind Tunnels Designs and Their Diverse Engineering Applications. pp. 59–73.

Van Pelt, R.S., Zobeck, T.M., 2007. Chemical Constituents of Fugitive Dust. Environmental Monitoring and Assessment 130, 3–16.

Vickery, K.J., Eckardt, F.D., Bryant, R.G., 2013. A sub-basin scale dust plume source frequency inventory for southern Africa, 2005–2008. Geophysical Research Letters 40, 5274–5279.

Visser, J.N.J., Joubert, A., 1991. Cyclicity in the late Pleistocene to Holocene spring and lacustrine deposits at Florisbad, Orange Free State. South African Journal of Geology 94, 123–131.

Visser, S.M., Sterk, G., 2007. Nutrient dynamics—wind and water erosion at the village scale in the Sahel. Land Degradation & Development 18, 578–588.

von Holdt, J.R., Eckardt, F.D., Wiggs, G.F.S., 2017. Landsat identifies aeolian dust emission dynamics at the landform scale. Remote Sensing of Environment 198, 229–243.

von Holdt, J.R.C., Eckardt, F.D., Baddock, M.C., Wiggs, G.F.S., 2019. Assessing Landscape Dust Emission Potential Using Combined Ground-Based Measurements and Remote Sensing Data. Journal of Geophysical Research: Earth Surface 124, 1080–1098.

Vos, H.C., Fister, W., Eckardt, F.D., Palmer, A., Kuhn, N.J., 2020. Physical Crust Formation on Sandy Soils and Their Potential to Reduce Dust Emissions from Croplands. Land 9, 503.

Vos, H.C., Fister, W., von Holdt, J.R., Eckardt, F.D., Palmer, A.R., Kuhn, N.J., 2021. Assessing the PM10 emission potential of sandy, dryland soils in South Africa using the PI-SWERL. Aeolian Research 53, 100747.

Wang, F., Chen, S., Wang, Y., Zhang, Y., Hu, C., Liu, B., 2018. Long-Term Nitrogen Fertilization Elevates the Activity and Abundance of Nitrifying and Denitrifying Microbial Communities in an Upland Soil: Implications for Nitrogen Loss From Intensive Agricultural Systems . Frontiers in Microbiology .

Wang, L., Shi, Z.H., Wu, G.L., Fang, N.F., 2014. Freeze/thaw and soil moisture effects on wind erosion. Geomorphology 207, 141–148.

Wang, X., Chow, J.C., Kohl, S.D., Yatavelli, L.N.R., Percy, K.E., Legge, A.H., Watson, J.G., 2015. Wind erosion potential for fugitive dust sources in the Athabasca Oil Sands Region. Aeolian Research 18, 121–134.

Webb, N.P., Chappell, A., Edwards, B.L., McCord, S.E., Van Zee, J.W., Cooper, B.F., Courtright, E.M., Duniway, M.C., Sharratt, B.S., Tedela, N., Toledo, D., 2019. Reducing Sampling Uncertainty in Aeolian Research to Improve Change Detection. Journal of Geophysical Research: Earth Surface 124, 1366–1377.

Webb, N.P., Pierre, C., 2018. Quantifying Anthropogenic Dust Emissions. Earth's Future 6, 286–295.

Webb, N.P., Strong, C.L., 2011. Soil erodibility dynamics and its representation for wind erosion and dust emission models. Aeolian Research 3, 165–179.

Webb, N.P., Strong, C.L., Chappell, A., Marx, S.K., McTainsh, G.H., 2013. Soil organic carbon enrichment of dust emissions: magnitude, mechanisms and its implications for the carbon cycle. Earth Surface Processes and Landforms 38, 1662–1671.

Weil, T., De Filippo, C., Albanese, D., Donati, C., Pindo, M., Pavarini, L., Carotenuto, F., Pasqui, M., Poto, L., Gabrieli, J., Barbante, C., Sattler, B., Cavalieri, D., Miglietta, F., 2017. Legal immigrants: invasion of alien microbial communities during winter occurring desert dust storms. Microbiome 5, 32.

White, B.R., Mounla, H., 1991. An experimental study of Froude number effect on wind-tunnel saltation BT - Aeolian Grain Transport 1, in: Barndorff-Nielsen, O.E., Willetts, B.B. (Eds.), . Springer Vienna, Vienna, pp. 145–157.

White, J.K., Nielsen, J.L., Madsen, A.M., 2019. Microbial species and biodiversity in settling dust within and between pig farms. Environmental Research 171, 558–567.

WHO, 2005. WHO Air quality guidelines for particulate matter, ozone, nitrogen dioxide and sulfur dioxide.

Widdicombe, J., 1891. Fourteen years in Basutoland: a sketch of African Mission Life. Church Printing Company, London.

Wiggs, G.F.S., Baird, A.J., Atherton, R.J., 2004. The dynamic effects of moisture on the entrainment and transport of sand by wind. Geomorphology 59, 13–30.

Wiggs, G.F.S., Holmes, P., 2011. Dynamic controls on wind erosion and dust generation on west-central Free State agricultural land, South Africa. Earth Surface Processes and Landforms 36, 827–838.

Wilson, M.F.J., O'Connell, B., Brown, C., Guinan, J.C., Grehan, A.J., 2007. Multiscale Terrain Analysis of Multibeam Bathymetry Data for Habitat Mapping on the Continental Slope. Marine Geodesy 30, 3–35.

Wilson, S.J., Cooke, R.U., 1980. Wind erosion. Soil erosion 17251.

Woodruff, N.P., Siddoway, F.H., 1965. A Wind Erosion Equation. Soil Science Society of America Journal 29, 602–608.

Woodward, S., Roberts, D.L., Betts, R.A., 2005. A simulation of the effect of climate change–induced desertification on mineral dust aerosol. Geophysical Research Letters 32.

Wu, J., Sunda, W., Boyle, E., Karl, D., 2000. Phosphate Depletion in the Western North Atlantic Ocean. Science (New York, N.Y.) 289, 759–762.

Xi, X., Sokolik, I.N., 2015. Seasonal dynamics of threshold friction velocity and dust emission in Central Asia. Journal of Geophysical Research: Atmospheres 120, 1536–1564.

Yan, Y., Wu, L., Xin, X., Wang, X., Yang, G., 2015. How rain-formed soil crust affects wind erosion in a semi-arid steppe in northern China. Geoderma 249–250, 79–86.

Yang, C., Geng, Y., Fu, X.Z., Coulter, J.A., Chai, Q., 2020. The Effects of Wind Erosion Depending on Cropping System and Tillage Method in a Semi-Arid Region. Agronomy.

Yang, G., Sun, R., Jing, Y., Xiong, M., Li, J., Chen, L., 2022. Global assessment of wind erosion based on a spatially distributed RWEQ model. Progress in Physical Geography: Earth and Environment 46, 28–42.

Yang, X., Wang, M., He, Q., Mamtimin, A., Huo, W., Yang, F., Zhou, C., 2018. Estimation of sampling

efficiency of the Big Spring Number Eight (BSNE) sampler at different heights based on sand particle size in the Taklimakan Desert. Geomorphology 322, 89–96.

Zejun, T., Tingwu, L., Qingwen, Z., Jun, Z., 2002. Sealing Process and Crust Formation at Soil Surface Under the Impacts of Raindrops and Polyacrylamide. Acta Ecologica Sinica 22, 674—681.

Zender, C.S., Miller, R.L.R.L., Tegen, I., 2004. Quantifying mineral dust mass budgets:Terminology, constraints, and current estimates. Eos, Transactions American Geophysical Union 85, 509–512.

Zhang, J., Guo, W., Zhou, B., Okin, G.S., 2021. Drone-Based Remote Sensing for Research on Wind Erosion in Drylands: Possible Applications. Remote Sensing .

Zhou, Y., Guo, B., Wang, S., Tao, H., 2015. An estimation method of soil wind erosion in Inner Mongolia of China based on geographic information system and remote sensing. Journal of Arid Land 7, 304–317.

Zielinski, T., Petelski, T., Strzalkowska, A., Pakszys, P., Makuch, P., 2016. Impact of wild forest fires in Eastern Europe on aerosol composition and particle optical properties. Oceanologia 58, 13–24.

Zimbone, S.M., Vickers, A., Morgan, R.P.C., Vella, P., 1996. Field investigations of different techniques for measuring surface soil shear strength. Soil Technology 9, 101–111.

Zobeck, T., Bilbro, J., 2001. Crop Productivity and Surface Soil Properties of a Severely Wind-Eroded Soil, in: D.E. Stott, R.H. Mohtar and G.C. Steinhardt (Eds). 2001. Sustaining the Global Farm. Perdue University, West Lafayette, pp. 617–622.

Zobeck, T.M., 1991a. Abrasion of Crusted Soils: Influence of Abrader Flux and Soil Properties. Soil Science Society of America Journal 55, 1091–1097.

Zobeck, T.M., 1991b. Soil properties affecting wind erosion. Journal of Soil and Water Conservation 46, 112 LP – 118.

Zobeck, T.M., Baddock, M.C., 2013. Anthropogenic environments. Treatise on geomorphology 11, 395–413.

Zobeck, Ted M, Fryrear, D.W., 1986. Chemical and physical characteristics of windblown sediment I. Quantities and physical characteristics. Transactions of the ASAE 29, 1032–1036.

Zobeck, T M, Fryrear, D.W., 1986. Chemical and Physical Characteristics of Windblown Sediment II. Chemical Characteristics and Total Soil and Nutrient Discharge. Transactions of the ASAE 29, 1037–1041.

Zobeck, T.M., Sterk, G., Funk, R., Rajot, J.-L., Stout, J.E., Van Pelt, R.S., 2003. Measurement and data analysis methods for field-scale wind erosion studies and model validation. Earth Surface Processes and Landforms 28, 1163–1188.

Zobeck, T.M., Van Pelt, R.S., 2006. Wind-induced dust generation and transport mechanics on a bare agricultural field. Journal of Hazardous Materials 132, 26–38.

Supplementary material

Chapter 3

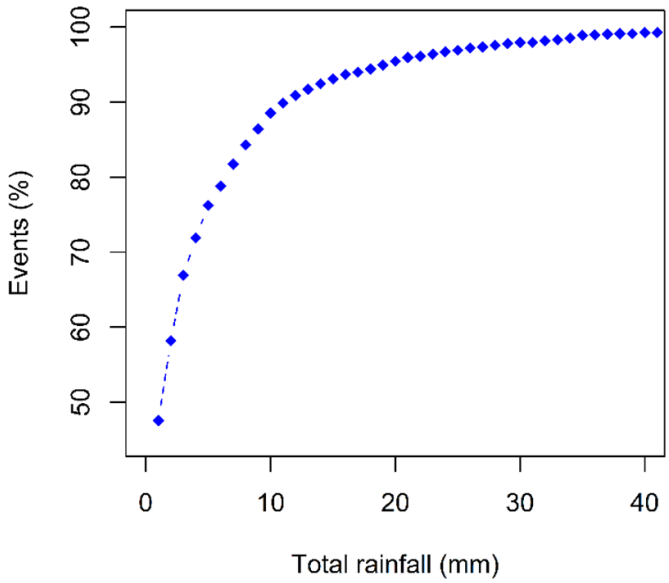

Supplementary Figure 3-1. The rainfall quantity distribution per rainfall event in the Free State. Data is coming from the weather station from the ARC near Bultfontein.

Chapter 4

Supplementary Table 4-1. The results from the PI-SWERL and shear strength measurements at a friction velocity of 0.56 m s^{-1} on the grassland and pan surfaces. In certain situation the shear strength of the pan surfaces was too high to measure, which was above 25 kPa. These measurements have been marked as such.

Name	Emission flux (mg m^{-2} s^{-1})	Average OGS count (Hz)	Shear strength (kPa)
Pan-1-B	0.003	2.9	>25
Pan-1-A	0.003	1.7	>25
Pan-1-D	0.003	1.9	>25
Pan-1-C	0.003	3.2	>25
Pan-2-A	0.003	2.2	>25
Pan-2-B	0.003	2.4	>25
Pan-3-A	0.004	2.4	>25
Pan-3-B	0.003	2.7	>25
Pan-4-B	0.297	63.1	10.63
Pan-4-A	0.107	7.9	10.88
Pan-5-B	0.019	4.3	6.95
Pan-5-A	1.538	65.4	7.17
Pan-6-B	0.006	1.6	>25
Pan-6-A	0.004	1.8	>25
Pan-7-A	0.006	1.6	6.98
Pan-7-B	2.199	140.4	7.39
Pan-8-B	2.06	69.4	7.02
Pan-8-A	8.582	295.3	9.01
Pan 9-A	0.004	1.9	>25
Pan 9-B	0.005	2.3	>25
Pan 10-A	0.004	1.5	>25
Pan 10-B	0.004	1.4	>25
Pan 10-C	0.021	0	>25
Pan 11-A	0.421	43.1	>25
Pan 11-B	0.188	28	>25
Pan 12-A	0.608	16.1	>25
Pan 12-B	0.593	13.4	>25
Pan 13-A	0.014	1.1	>25
Pan 13-B	0.128	52.2	>25
Pan 14-A	5.691	310.8	>25
Pan 14-B	3.776	54.8	>25
Pan 15-A	8.753	471.3	>25
Pan 15-B	11.302	323	>25
Pan 16-A	14.313	735.8	>25
Pan 16-B	17.042	927.6	>25
Pan 17-A	5.493	190.2	>25
Pan 17-B	2.819	156.9	>25
Grassland-1	0.279	8.6	14.3
Grassland-2	0.039	2.5	16.46
Grassland-3	0.011	2	17.35
Grassland-4	0.010	2.3	15.93
Grassland-5	0.004	6.3	-
Grassland-5	0.020	13.1	-
Grassland-6	0.005	3.4	16.75
Grassland-7	0.006	1.9	23.87
Grassland-8	0.006	2.6	20
Grassland-8	0.007	2.6	20
Grassland-9	0.004	2.3	19.72
Grassland-9	0.006	5	19.72
Grassland-10	0.009	2.8	26.06
Grassland-10	0.008	2.6	26.06

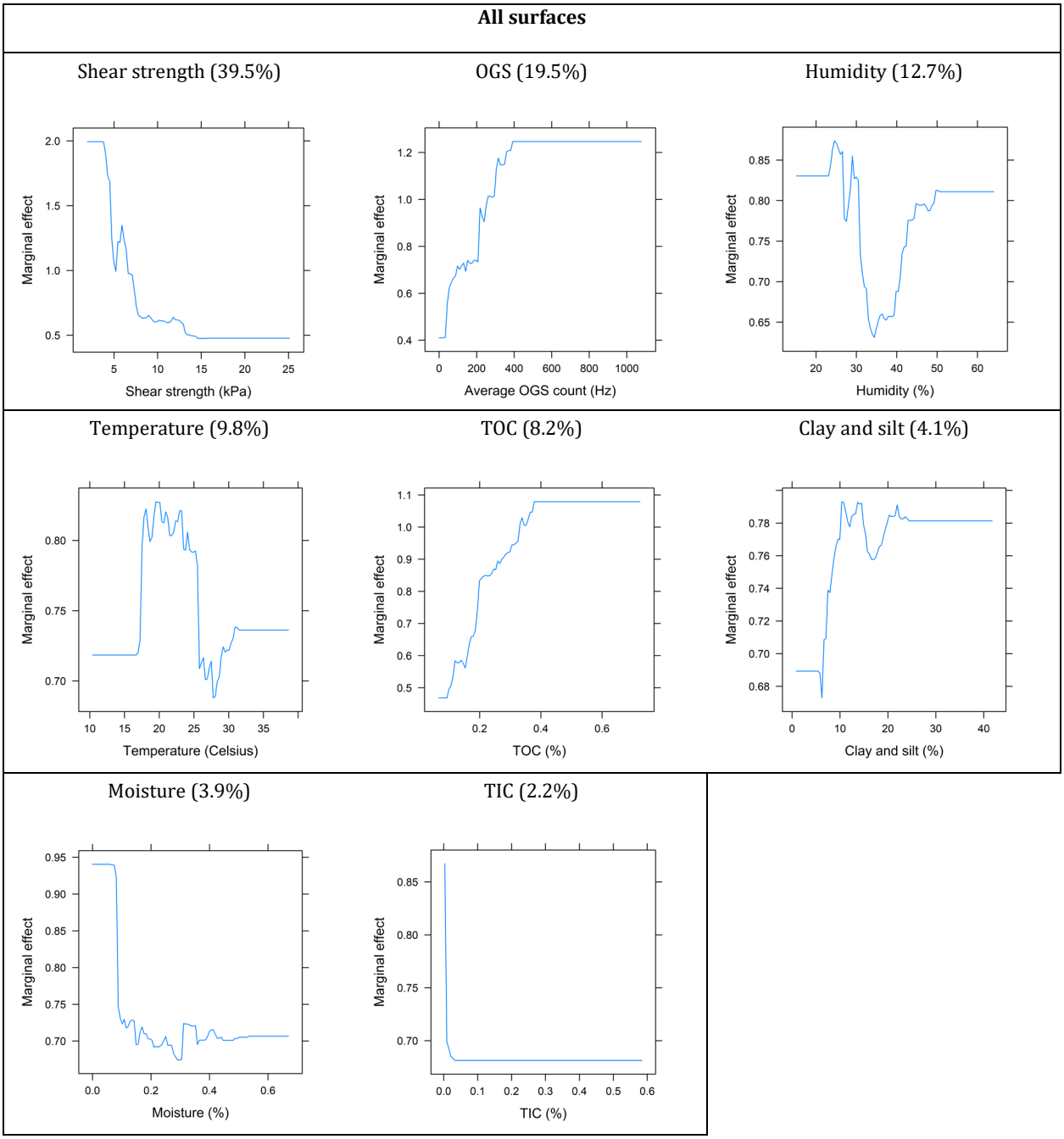

Supplementary Figure 4-1. The BRT results from the complete dataset, as described in Chapter 4.3.5.

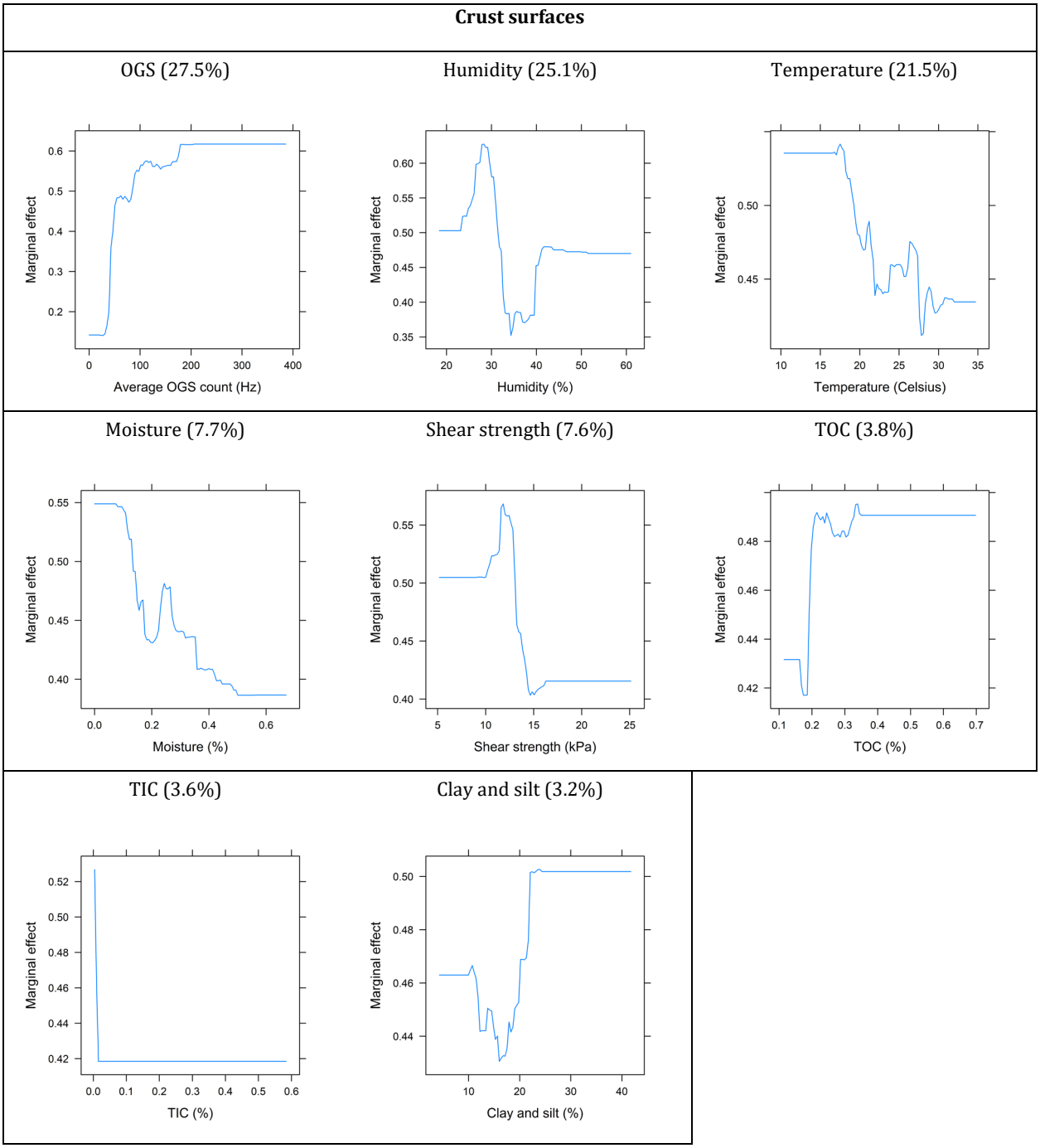

Supplementary Figure 4-2. The BRT results from the crusted surfaces, as described in Chapter 4.3.5 and Chapter 4.4.3.1.

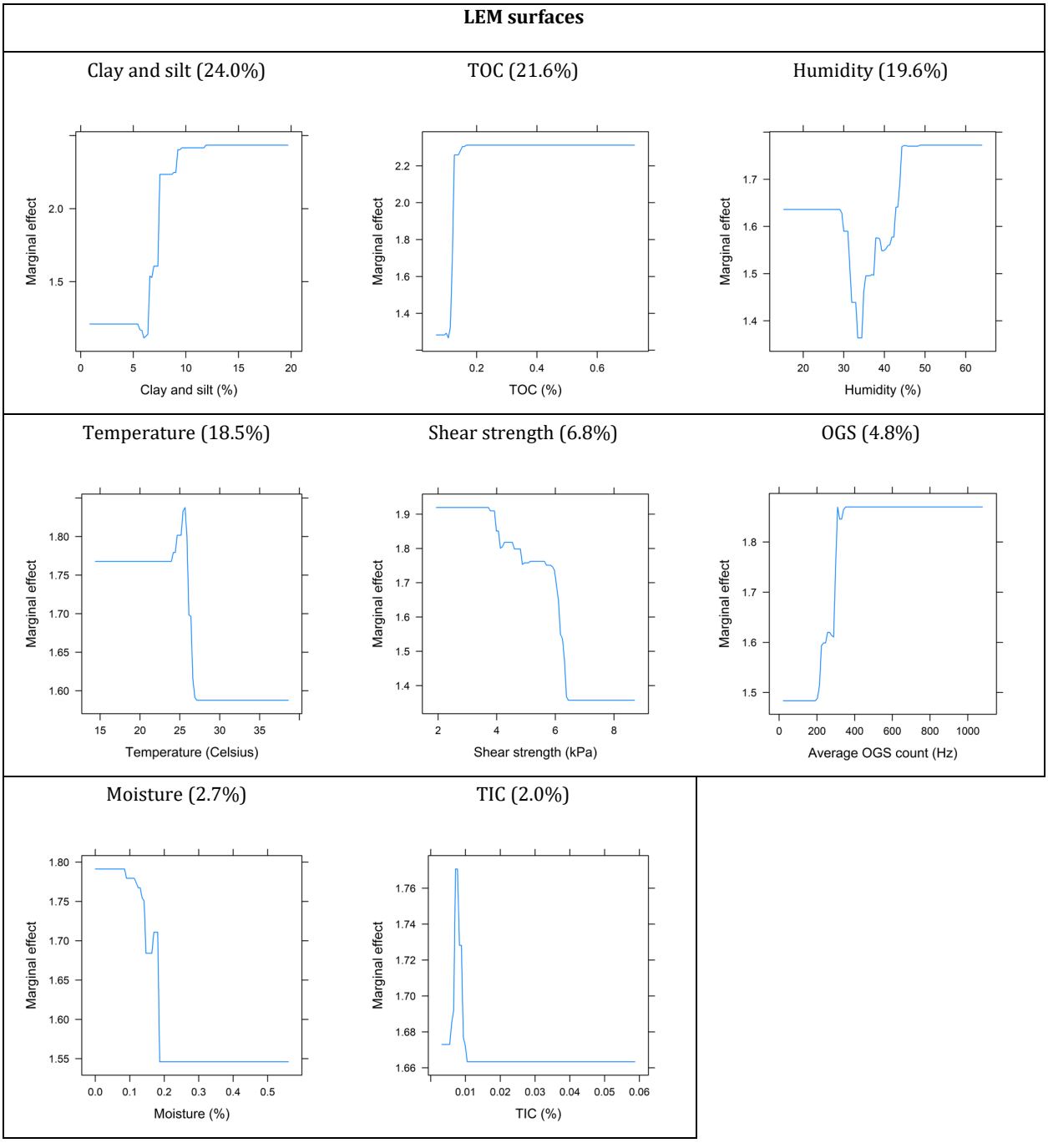

Supplementary Figure 4-3. The BRT results from the crusted surfaces, as described in Chapter 4.3.5 and Chapter 4.4.3.2.

Chapter 5

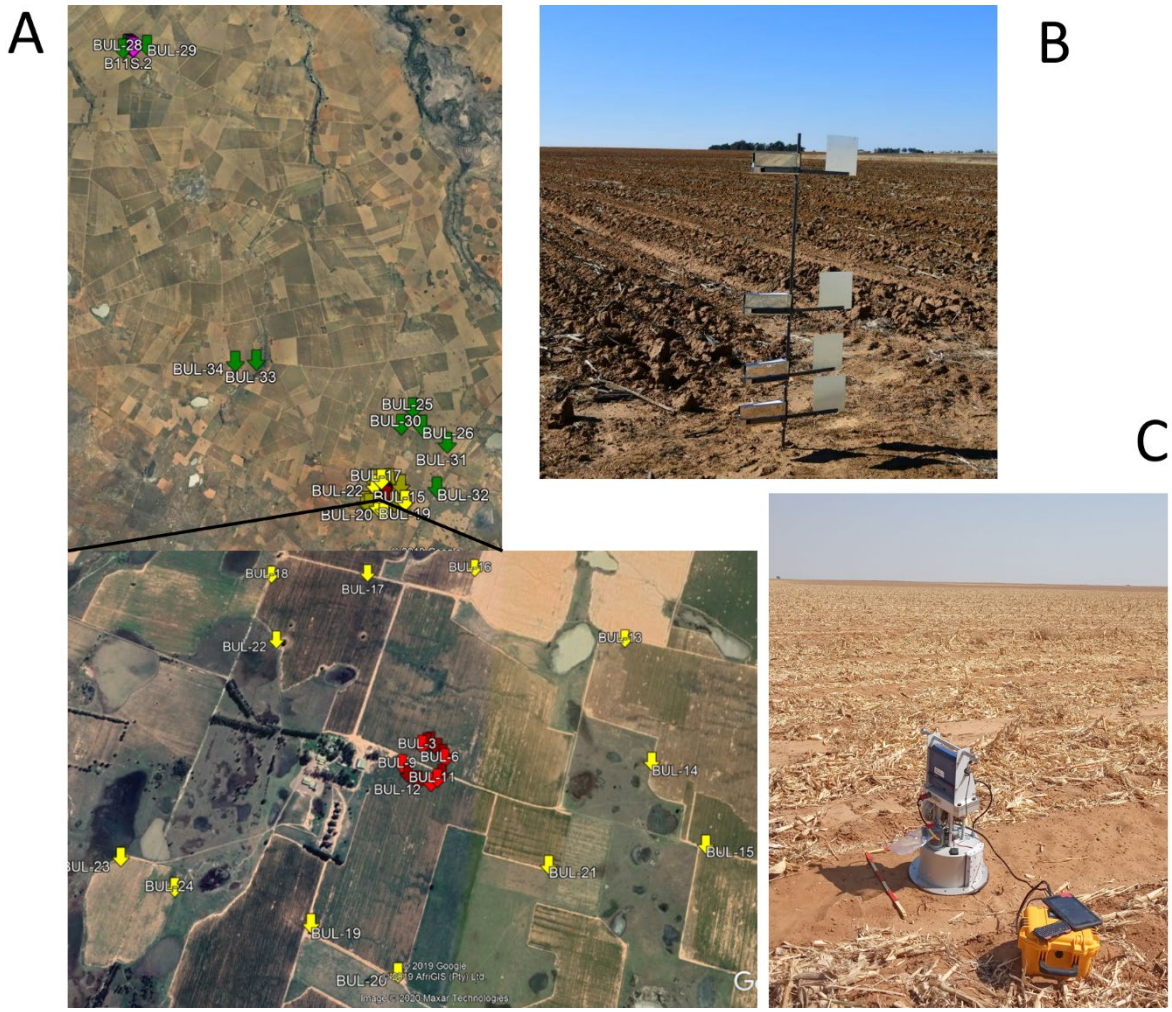

Supplementary Figure 5-1. a) Area of the study and location of the samples around a 30 km radius. b) Dust-trap used to collect dust from the air. c) PI-SWERL dust collector operating during field-work.

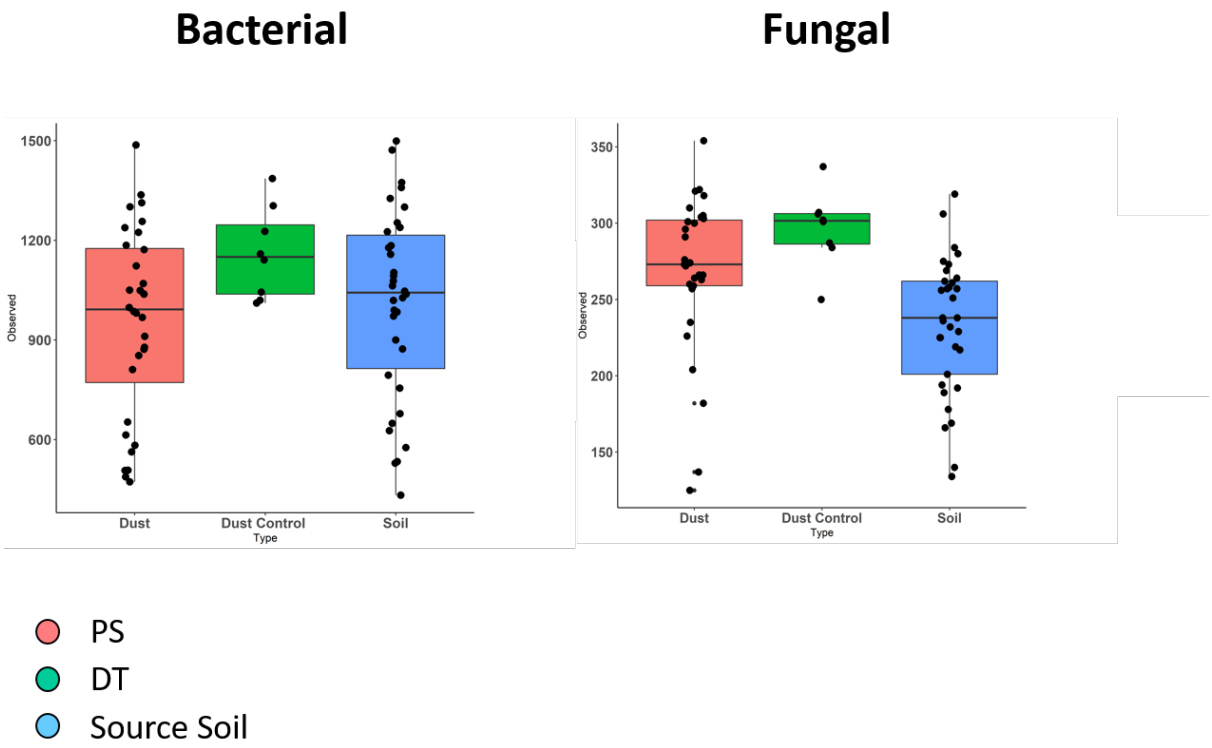

Supplementary Figure 5-2. Bacterial and Fungal taxonomic richness in PS, DT and source soil samples. The richness is expressed as number of unique species per sample group.

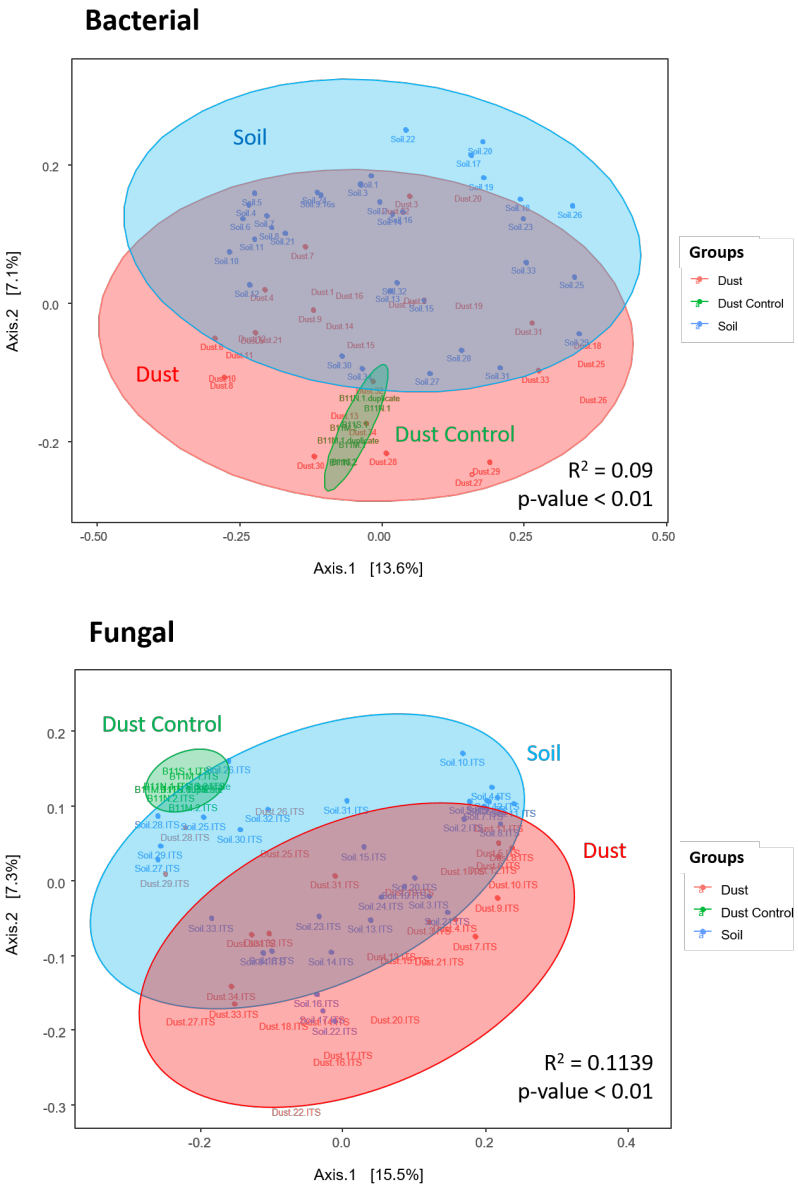

Supplementary Figure 5-3. PCoA plots of the beta-diversity dissimilarities of bacterial and fungal communities, grouped according to type of sample (Dust Control vs Dust vs Soil). Groups are highlighted with ellipses using the following color-code: Dust Control – Green; Dust – Red; Soil – Blue.